NUREG/CP-0064
CSNI Report No. 105
MEA-2313

Proceedings of the

Second CSNI Workshop on Ductile Fracture Test Methods

Held at Paris, France
April 17-19, 1985

Edited by F.J. Loss

Sponsored by
Organization for Economic Co-Operation and Development
U.S. Nuclear Regulatory Commission

Proceedings prepared by
Materials Engineering Associates, Inc.

Available from

Superintendent of Documents
U.S. Government Printing Office
P.O. Box 37082
Washington D.C. 20013-7082

and

National Technical Information Service
Springfield, VA 22161

NUREG/CP-0064
CSNI Report No. 105
MEA-2313
RF, R5

Proceedings of the

Second CSNI Workshop on Ductile Fracture Test Methods

Held at Paris, France
April 17-19, 1985

Manuscript Completed: August 1988
Date Published: August 1988

Edited by F.J. Loss

Sponsored by
Organization for Economic Co-Operation and Development
U.S. Nuclear Regulatory Commission

Proceedings Prepared by
Materials Engineering Associates, Inc.
9700-B Martin Luther King, Jr. Highway
Lanham, MD 20706-1837
NRC FIN B8900

ABSTRACT

This report is a compilation of papers presented at the Second CSNI Workshop on Ductile Fracture Test Methods, held at OECD Headquarters, Paris, France, on April 17-19, 1985.

The contributors addressed advances in test methods to characterize the fracture toughness of structural steels. Sessions were held on new and improved test techniques, standardized J-R curve test procedures, experience and problems with existing techniques, and use of fracture mechanics by the nuclear industry. Summaries of the individual sessions have been prepared by the session chairmen.

The meeting identified progress in test methods since the first workshop was held in 1982. A clear movement to standardize J-R curve tests is now apparent. However, there exists a continuing need to improve elastic-plastic fracture test methods.

PROCEEDINGS OF THE

SECOND CSNI WORKSHOP ON DUCTILE FRACTURE TEST METHODS

April 17-19, 1985

TABLE OF CONTENTS

PREFACE

The Committee on the Safety of Nuclear Installations (CSNI) of the Organization for Economic Cooperation and Development - Nuclear Energy Agency (OECD-NEA) is an international body of scientists and engineers with responsibilities for nuclear safety research and nuclear licensing. The CSNI fosters international cooperation in nuclear safety among OECD member countries. The Second CSNI Workshop on Ductile Fracture Test Methods was undertaken pursuant to an action item by the CSNI Principal Working Group 3 (Primary Circuit Integrity). The meeting was held at OECD Headquarters in Paris, France. The objective of the workshop was to provide a forum for a free exchange of views, based upon informal presentations, covering advances in test methods and techniques for the experimental characterization of ductile fracture toughness. In addition, it was intended to critically assess limitations and problem areas associated with these methods. A workshop on the same topic was held in December 1982. The success of that meeting prompted the organizing of a second such workshop.

The meeting was organized and chaired by F. J. Loss with assistance from Michael Stephens of OECD's Nuclear Energy Agency. A total of 9 countries was represented with 35 persons in attendance, all of whom were invited on the basis of demonstrated expertise in ductile fracture testing. Each participant was asked to prepare a short presentation focused on a particular topic to serve as a basis for discussion. These presentations were to emphasize experimental test procedures as opposed to data trends or theory. A total of 24 presentations was made; these are provided here as the Proceedings of the meeting. Sessions were held on new and improved test techniques, standardized J-R curve test procedures, experience and problems with existing techniques, and use of fracture mechanics by the nuclear industry. Summaries of the individual sessions have been prepared by the session chairmen.

The contribution of all the participants in making this a highly successful meeting is gratefully acknowledged.

F. J. Loss
Chairman

WORKSHOP SUMMARY

In comparison with the first workshop of this type in 1982, the subject meeting reflected progress in the intervening 2.5 years. There was not much discussion on the exact details of conducting J-R curve tests, thereby implying that problems here have been minimized. Instead, focus was on standardization of the J-R curve tests and on measurement of the R curve under extreme conditions such as high temperature, irradiation, water environments, and with small size (e.g., C_v) specimens.

As with the 1982 workshop, the major emphasis was on ductile test methods related to the J-R curve. While the J-R curve methodology was originally developed in the USA, this technology is now fully developed in Europe as well. In contrast, little was said about the COD concept. This probably was due to two fractors: first, a CTOD workshop was scheduled in Geesthacht, FRG, immediately following this workshop and some of the participants were presenting papers on COD-related topics in Geesthacht. Second, the sponsorship of the workshop by a nuclear agency (CSNI) discouraged COD-related papers since the latter concept is not customarily applied in the nuclear industry.There are basically three standardized J-R curve test methods being developed by the USA (ASTM), France, and the European Group on Fracture (EGF). The last is based on a method developed by the CEGB in the UK. However, Schwalbe from FRG has a strong objection to the expression of the blunting behavior proposed by the CEGB method. In addition, the Japanese have developed a method for J_{Ic}. However, no representative from Japan was present at the workshop.

Given the occasional interactions of investigators from the USA and Europe at technical meetings, one could question why the efforts are not focused at the development of a single J-R curve test method. Certainly this would simplify technical exchanges among the various countries. The reason for the present situation appears to be rather simplistic. Test methods are usually developed by relatively small groups of individuals who have evolved their own special way of conducting tests. These groups often have different philosophies on the important features of a test method. Since these groups (especially Europe vs. the USA) do not interact on a regular and formal basis, differences in test procedures can be expected to occur.

A further point to raise is the possibility of resolving the differences among the three candidate procedures to develop a unified approach. This should be possible if more technical interaction can be promoted among investigators from the various countries. Without this interaction, it is conceivable that the ASTM J-R procedure will become the most widely used. However, it will not be used in Europe on a formal (e.g., contractual) basis. This event, by itself, need not be of concern if the differences are only minor, that is, the basic definition of the R curve is the same in all procedures. Given this, one can easily have separate standards which define different validity limits or choose a different position on the R curve as the point of crack initiation since it would be a trivial exercise to transform from one standard to another.

Summarized below are some of the differences among the three methods being developed as standards in the USA, in France and by the EGF (CEGB procedure).

- Blunting Line

  The ASTM uses $J = 2\sigma_f \Delta a$ where σ_f is the flow stress and Δa the crack extension due to blunting. This is a "formal" procedure and does not appear to represent the actual blunting behavior of various metallic materials. Schwalbe (EGF) has proposed a more realistic blunting line that supposedly reflects the material behavior more accurately. On the other hand, the CEGB procedure uses no blunting line at all. The French procedure is preliminary and its description did not address points of disagreement, such as the blunting line. From the partial description of this procedure, it is clear that there would be little problem in combining it with the other procedures (ASTM, EGF).

- Initiation (J_{Ic})

  The ASTM tentative R-curve method does not address J_{Ic} since this quantity is described by ASTM E 813. Nevertheless, it is likely that these two methods will be combined in several years. E 813 is currently undergoing revision because of almost universal dissatisfaction with ASTM approach. In spite of this, clear differences exist between the ASTM and EGF approaches to crack initiation. The EGF method emphasizes the CEGB approach which chooses crack initiation at a fixed value (0.2 mm) of apparent crack extension (blunting plus actual growth). All agree that this does not represent the physical behavior since the proportion of blunting vs. crack extenstion at 0.2 mm of apparent growth is different for different materials. The CEGB philosophy is that 0.2 mm is "good enough" for engineering purposes. It does not propose an equivalence between J_{Ic} and J at 0.2 mm of apparent crack growth.

- Negative Crack Growth

  The disagreement as to the existence of negative crack growth as a physical phenomenon exists as it did during the first workshop in 1982. Some investigators attribute the negative growth to poor mechanical alignment of the test fixture. Nevertheless, the procedure developed by the CEGB admits the existence of negative growth and shifts origin of the J vs. Δa plot to account for this bahavior.

- J Expression

  All countries are using the ASTM expression for J. This expression is published via the ASTM E 24 subcommittee

activities. Unfortunately, this expression changes periodically due to improvements in the theory. Ernst is a leader in promoting these improvements. However, the Europeans would rather forego these changes until proposed improvements have had time to gain more review and acceptance.

Several papers presented the results of J-R curve tests in extreme environments. Two papers described tests at elevated temperature and a third reported on measurements in a high temperature PWR environment. Several papers compared the single-specimen R-curve methods in terms of the compliance procedure vs. the DC-PD procedure. Three papers described the development of the J-R curve with the key-curve approach. A new test procedure, based upon notched tensile specimens for ductile fracture characterization was proposed by Rousselier (France). A paper by Varga described methods to detect crack initiation in precracked C_v specimens. This paper promoted a discussion of interest in the initiation concept which was not as evident during the 1982 CSNI workshop.

Very little theory or analytical modeling was discussed since this was not a topic of the Workshop. However, Ernst presented his work on developing a modified J integral (J_M) whose advantage is the ability to measure uniform R curves from specimens of different geometry to much larger values of crack extension than is possible with the current J expression which is based on deformation theory plasticity. Wallin (Finland) illustrated the advantage of J_M in collapsing the R curve from 1T-CT and C_v-sized specimens to a single R curve. A similar conclusion was reached by McCabe who found that within the CT specimen geometry the J-R curve, in terms of J_M, was independent of plan-view size and relative crack size even when crack growth exceeded 10% of the initial ligament size. A similar unique J_M-R curve was shown for single-edge notch and double-edge notch specimens in comparison with the CT specimen results.

The meeting included a discussion item from CSNI Principal Working Group 3 which was directed to the formation of a J-R curve data bank for reactor primary circuit steels and weldments. It has been proposed that such a data bank be developed in coordination with other types of NEA data stored on computers at Saclay. The NRC is aware of this initiative and has previously informed the CSNI of NRC activities in this direction at Materials Engineering Associates and of a data bank being developed by the Metal Properties Council. Suggestions from several participants regarding the pitfalls of J-R curve data base development were given to Michael Stephens of the CSNI.

In summary, the workshop provided a forum for a valuable exhange of ideas in elastic-plastic test methods among some of the world's leading investigators. The discussions provided a sounding board for new ideas and a means of focus on problem areas within existing methods. The meeting showed an improvement in test procedures in comparison with the first workshop held in 1982. Nevertheless, some the problems and disagreements which evolved in 1982 still exist. On the other hand, there is now a clear movement toward standardization

of the J-R curve methodology in Europe and the USA which was much less apparent in 1982. The meeting showed that while progress has been made, there is need for continuing emphasis on improvements in the field of elastic-plastic test methods. Emphasis should be placed on validation of proper test procedures with respect to a predictive capability for structural performance.

SESSION NO. 1 (PART 1)

New and Improved Test Methods
Chairman: T. Varga

Summary

Session No. 1 was devoted to new and improved test techniques for the measurement of elastic-plastic fracture toughness properties. Crack initiation and growth detection using heat tinting, partial unloading (compliance) acoustic emission, d.c. and a.c. potentail drop was discussed.

Testing conditions have been extended to cover a variety of service loadings: Voss et al. enlarged the temperature range down to 100 (Al-Alloys) and upwards to 1100 K (Incoloy 800 H) into the creep range.

Tjoa et al reported on highly irradiated (to 10^{24} nvt) type 304 stainless steel, tested at 823 K. The effect of radiation embrittlement was such, that ½T-CT specimen seemed to yield valid fracture toughness data.

Balladon and Foucault were successful in applying a d.c. potential drop method on stainless steel 17 Cr 12 Ni for J_i and J-R curve determination at RT. Partial unloading however is less suitable because of excessive blunting. Acoustic emission showed a characteristic change in the cummulative number of events; however, this change did not correlate to initiation.

Gibson performed d.c. potential drop measurements on A 508 class 3 steel at 288 °C (560 K) in air and in PWR-water. Contrary to other experience, he could observe no enhancement or crack growth over time in water compared to air environment.

Loading rates were 5.10^{-4} to 5.10^{-1} mm/min. The potential drop technique did predict final crack extention to within 10 %, except in PWR-water at the lowest loading rate. (Time dependance could begin at that limit.)

Rousselier and Devaux believe in the advantage of initiation and crack growth measurement using notched tensile specimens. Marked compliance change showed crack initiation in a 2 % Cr 1 % Ni rotor steel. The slope of the following section of the curve is related to the ductile resistance of the material.

Since a numerical analysis is recently at our disposal, measured material characteristics of specimens therefore may be transferred to actual structures. An alternate method to ductile fracture mechanics seems therefore to be established, limited to cases where no notch i.e. local stress concentration influence on fracture behaviour has to be taken into account.

During discussion many experimental details have been clarified and procedures and practices compared. The question was also raised whether J-R curves are of overwhelming importance. Contrary to the opinion of many researchers, crack initiation is regarded by governmental agencies and those dealing with the fracture safety assessment of structures as the primary criteria to be used. (First step of a "defence in depth" consideration.) Exact physical definition of initiation (standards) may be applied. Crack propagation has to be regarded only for special well defined cases.

SESSION NO. 2 (PART 2)

New and Improved Test Methods
Chairman: P. Balladon

Summary

The first three presentations were related to the use of the Key Curve method for determining J-R curves with a single specimen.

P. STEENKAMP has obtained accurate single-specimen J-R curves on a ferritic steel for offshore structures, using experimental and finite-element Key Curve functions.

A displacement-based Key Curve method developed by W.R ANDREWS can give J-P curves for several types of materials as accurate as those obtained with the multispecimen method.

Finally, one of the most promising uses of the Key Curve method seems to be determination of J-R curves at high loading rates. Results presented by K. BRUNINGHAUS show that there is a good correlation between predicted and measured crack extension, and make it possible to determine the evolution of J-R curves with loading rates.

The following two presentations were related to the use of precracked Charpy V specimens.

K. WALLIN has shown that, for an A533B steel, J-R curves obtained with precracked Charpy V specimens were similar to those obtained with 1TCT specimens using the single-specimen compliance method, side-grooving, compliance corrections and modified J-integral.

T. VARGA investigated methods for detecting crack initiation in precracked Charpy V specimens in static and dynamic loading. Measurements with ultrasonic tranducers, DC potential drop tests and force-deflection diagrams were made and compared to physical measurement of crack extension.

The two last presentations were related to EPFM testing procedures. A. TANARRO reported on the status of development of J_{IC} testing in Spain. The following discussion concluded that it was possible to use ASTM E399 CT specimens for J-R curve tests.

C. FOSSATI gave results concerning the determination of dynamic J-R curves using precracked Charpy V specimens with a multispecimen method. He gave his point of view on the "negative crack growth" that had been observed in J-R curves determined by unloading compliance methods.

An open discussion on the problem of apparent negative crack growth could not reach any definite conclusions.

SESSION NO. 3

Standardization of J-R Curve Test Procedures
Chairman: K.-H. Schwalbe

Summary

The session dealt with the efforts to revise the present experimental methods for determining a J-R-curve undertaken by ASTM, CEGB (United Kingdom), European Group on Fracture (EGF), French Fracture Group, and German Fracture Group.

Concerning the test pieces, the French Fracture Group recommends the exclusive use of CT specimens whose width can be non-proportional to its thickness. All other groups allow the use of both CT and bend specimens. Non-proportional width is also recommended by ASTM. It is worth noting that the standard E399 CT design is being considered for J evaluation.

Two groups suggest a splitting of the J-integral into a linear elastic and a plastic portion: ASTM uses Ernst's J formulation, which incorporates a crack growth correction, whereas CEGB derived an own expression which will probably also be used by the EGF method.

The multiple specimen method is the reference method chosen by CEGB, EGF, and the French Fracture Group, whereas the ASTM philosophy needs the single specimen method for the crack growth correction of J.

ASTM has a separate method (E813) for the interpretation of a J-R-curve near its origin as a measure of initiation of crack growth. The four activities in Europe are aimed at combining the determination of initiation with the R-curve method. Both the CEGB and the EGF methods take the point on the R-curve at 0.2 mm total crack growth as a "near initiation" value. A value closer to initiation may be obtained by a procedure being discussed in the German Fracture Group which uses a line parallel to and 0.2 mm away from the blunting line the interception of which with the R-curve is taken as a defined initiation point with 0.2 mm ductile tearing. The blunting line accounts for the work-hardening porperties of the material. Similar considerations are reported from ASTM and the French Fracture Group (not presented at this meeting).

It is worth noting that the EGF method will contain both the J-integral and the CTOD evaluation.

SESSION NO. 4

Experience and Problems with Existing Techniques
Chairman: D. E. McCabe

Summary

The blunting line that should be used to identify of the on[illegible] of real slow-stable ductile tearing in R-curve behavior of materials continue[illegible] source of debate. Because personal interpretation on the significance of certain [illegible]s of experimental data is involved, the resolution of the issue may require considerable additional time. In addition to this, the end use for such a toughness number, (real J_{Ic}) if in fact it were identifiable, was a source of further debate. On the positive side of this, we observe that the precision of measurement required to resolve the blunting line issue has properly focused attention on the sharpening of test techniques applied to J_R-curve generation. In this session, abstracts that addressed improved measurement techniques were by; (i) Gordon and Garwood, (ii) Ingham, Morland and Wardle, and (iii) Kramer and Wilkowski.

The issue of geometry dependence versus independence of J_R-curve appears to be heading toward resolution, and in particular for the basic bend geometries. The center cracked tension, CCT, versus bend J_R curve comparisons may need more clarification. The abstract by McCabe showed reasons why the CCT panel is a poor representative of the generalized tension loading case. Conversely, the abstracts by Schwalbe and Cornec point out that the CCT panel proved to be the more powerful geometry from the standpoint of sustaining geometry independent crack growth. In particular, their claim is specific to plane stress constraint.

Studies to demonstrate the compatability between J and CTOD are continuing and understanding is continuously being improved. The presentation of Ernst showed why modified J, J_M, and the δ_5 type CTOD of the Schwalbe-Hellmann method correlate. In appears to be a natural consequence of the properties sought in development of modified J. Correlation is a matter of selection of the appropriate location on a specimen for measurement of COD. McCabe showed R-curves for A533B of various geometries that verify a correlation between J_M and δ_5. Schwalbe showed geometry independence in δ_5 type R-curves on aluminum alloys. Garwood showed the use of CTOD for failure analysis in an R-6 assessment diagram type of format.

New ideas are being generated on how to utilize J_R-curve data, one example of which is the proposed CEGB procedure. The general objective appears to be to seek elimination of known problem areas in defining useable J_R toughness indicies. The abstract by Akhurst discussed potential problem areas in the use of the CEGB proposal, and he cited the directions for future courses of study.

SESSION NO. 5

PANEL DISCUSSION
Use of Fracture Mechanics by the Nuclear Industry
Chairman: S. L. Creswell

Summary

In this fifth, and final session the Use of Fracture Mechanics In The Nuclear Industry was discussed. Three presentations were given which covered the use of fracture mechanics in the Swiss, French and UK Nuclear Industries.

The Swiss Perspective was given by Varga, Houssin gave an overview of the French position and Creswell presented the UK approach.

Several common threads could be drawn from the presentations. In particular the extent to which post initiation (i.e. resistance curve) analysis is considered appropriate and the situations to which it can be applied. It was generally agreed that for nuclear pressure circuit fracture analysis the initiation of stable crack extension should only be exceeded in extreme cases. That is for normal system events all analysis should be based on initiation toughness values and R-curve analysis only considered for use in the rarest - once in a lifetime - events.

Driving force curves for the resistance curve analysis that have been carried out has, up until now, been based on LEFM plus plastic zone correction factors, converted to EPFM via the small scale yielding equivalence formulae. This reliance on small scale yielding equivalence has placed limitations upon the extent of ductile fracture analysis that can be considered valid.

Design resistance curves have been developed for use in these post initiation analysis which are considered to bound the material being considered. These design resistance curves are limited in the amount of ductile tearing incorporated by the need to maintain validity in terms of both the J integral and the small scale equivalence formulae.

SESSION 1 (Part 1): New and Improved Test Methods

CHAIRMAN: T. Varga
HSK, Switzerland

Computer Controlled Measurement and Evaluation of Crack Growth for Temperatures between 100 and 1100 K

B. VOSS, T. HOLLSTEIN, J.G. BLAUEL

Fraunhofer-Institut für Werkstoffmechanik
Wöhlerstrasse 11, D-7800 Freiburg, West Germany

With the growing importance of fracture mechanics concepts to quantify material resistance against crack extension, improved resolution, accuracy, and reproducibility of the crack length measurement procedures and automatic performance are required. IWM Freiburg is using advanced DC and AC potential drop as well as partial unloading compliance methods to conduct ductile and creep crack growth experiments. Possibilities, results and some problems are described when applying these procedures in a temperature range fromm 100 to 1100 K for different materials.

Figure 1 shows the principle of the DC potential drop measurement system. The DC-current is fed through contacts in the plane of the knife edges in the load line. Potential pick ups are positioned on the two opposite side surfaces,normally at W/4 position. The potential drop is partly compensated by a constant DC-voltage, amplified, filtered and recorded together with the force and load line displacement. Initiation of stable crack growth is indicated by a more or less distinct change in slope. For the contact geometry choosen here the final amount of stable crack growth is - in a good approximation - proportional to the difference Ψ_m at the end of the experiment.

Figure 2 shows curves of force and potential drop vs. load line displacement of one experiment of a series of seven specimens tested at 300°C. The J- Δa-curve derived from these measurements is shown in Figure 3 (No 7). All the other specimens were unloaded at different smaller values of load line displacement and of crack growth Δa accordingly. Their final J- Δa points (No 1-6) confirm all the J- Δa-curves derived by interpolation from the potential drop curves of the different specimens.

Figure 4 shows the principle of J-R curve measurement by the partial unloading compliance method as defined in References 1 and 2. This method is realized in a computerized test control and evaluation system (Figure 5) able to control and finish a test automatically according to predefined parameters and conditions. This fully automatic operation of the system is essential for relatively fast tests and for long time tests as creep crack growth tests.

One example of a J-R curve measured at -196°C for a CT-specimen of aluminum alloy weld material is shown in Figure 6. The specimen was cooled by liquid nitrogen. Boiling nitrogen caused oscillations of

the c ip gage totally immersed in the nitrogen and thus some scatter of the Δa-measurements. To avoid any contact of the displacement measurement gage with the hot or cold environment of the specimen a special device (Figure 7) was developed. The load line displacement is transferred to the load line plane on both sides of the clevisses. The centers of these connecting parts are fixed to the same positions where normally razor blades would be fixed, the outer parts are connected by quartz rods to a pair of LVDT's. Core and coils are guided with very low friction by a system of springs. The hysteresis of the system is in the range of 1 µm and even less for a total range of 10 mm. The performance of the system may be demonstrated by the three groups of unloadings (Figure 8) measured at room temperature and at 700°C with two different controlled displacement velocities. Reproducibility and absolute accuracy may be seen in Figure 9: In a creep crack growth test at 600°C at a displacement of V = 1,05 mm there were two unloading cycles (No 13). The two Δa-values are nearly identical (their symbols are overlapping in the Figure). The final value estimated from the last unloading differs by less than 10 % from the fracture surface measurement $\Delta a(BF)$.

In Figure 10 measured data F,V and derived quantities $\Delta a(PE)$ (compliance measurement) and $\Delta a(GP)$ (DCPD measurement, interpolation fixed at initial and final crack length) are plotted versus time. Both Δa-curves are in good agreement, taking into account that the compliance measurements deliver absolute predictions not adjusted for final crack length.

References

1. ASTM E 813-81, Determination of J_{Ic} a measure of fracture toughness, Annual Book of ASTM Standards, Part 10, American Society for Testing and Materials, Philadelphia, 1981.

2. P Albrecht, W.R. Andrews, J.P. Gudas, J.A. Joyce, F.J. Loss, D.E. McGabe, D.W. Schmidt, W.A. VanDerSluys, "Tentative Test Procedure for Determining the Plane Strain J_I-R-Curve, J. Testing and Eval., JTEVA, Vol 10, No. 6, Nov. 1982, pp. 245-251

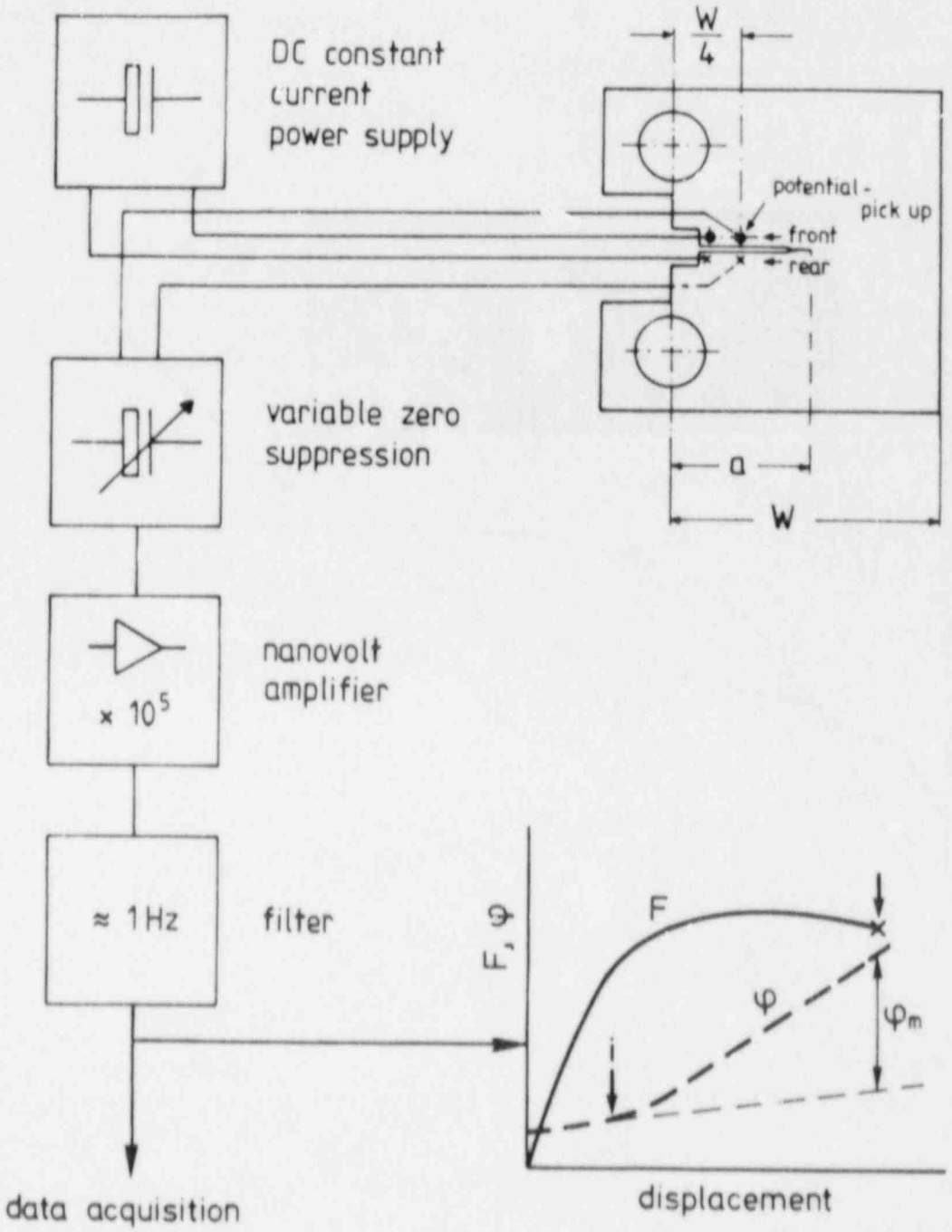

Fig. 1 Principle of DC-potential drop method for initiation detection

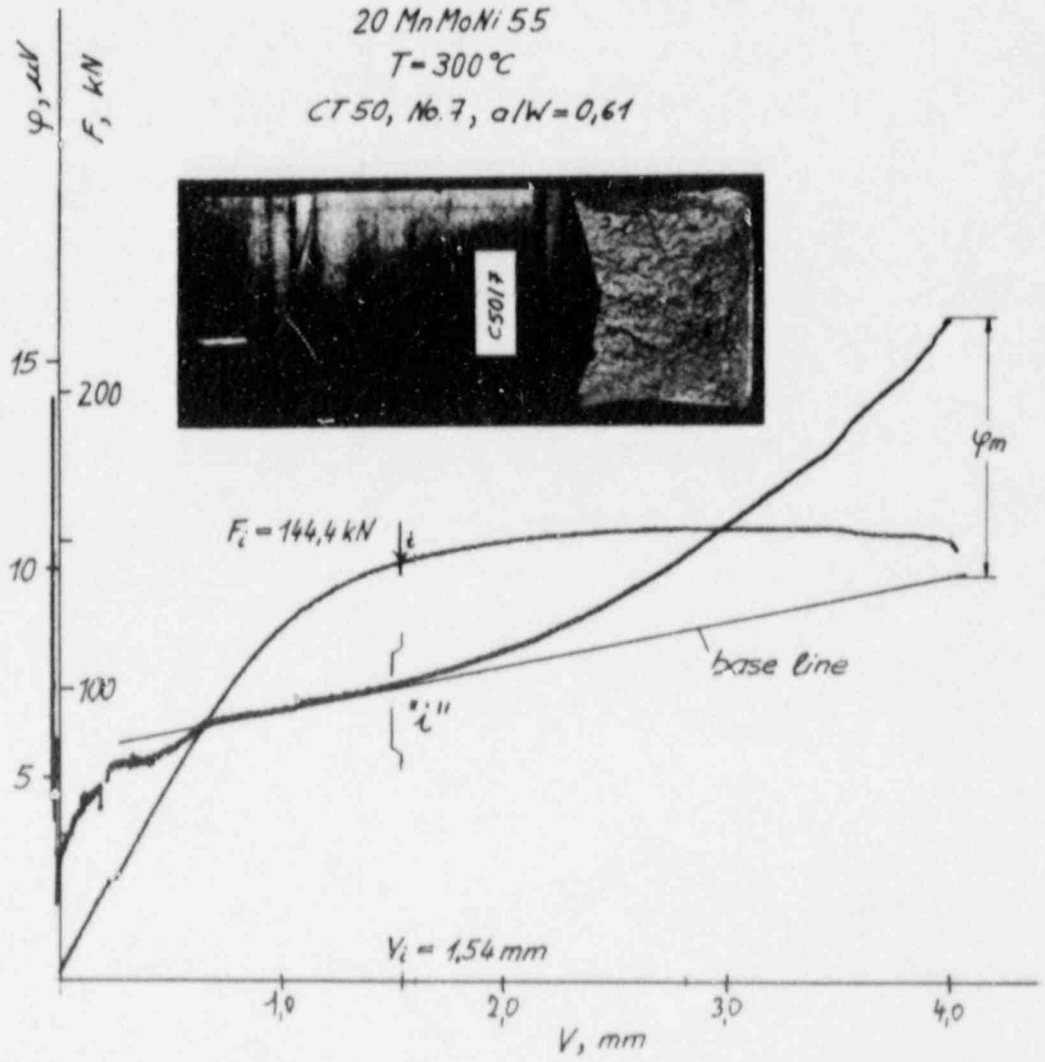

Fig. 2 Example for force-potential-drop vs. displacement with estimated initiation point "i"

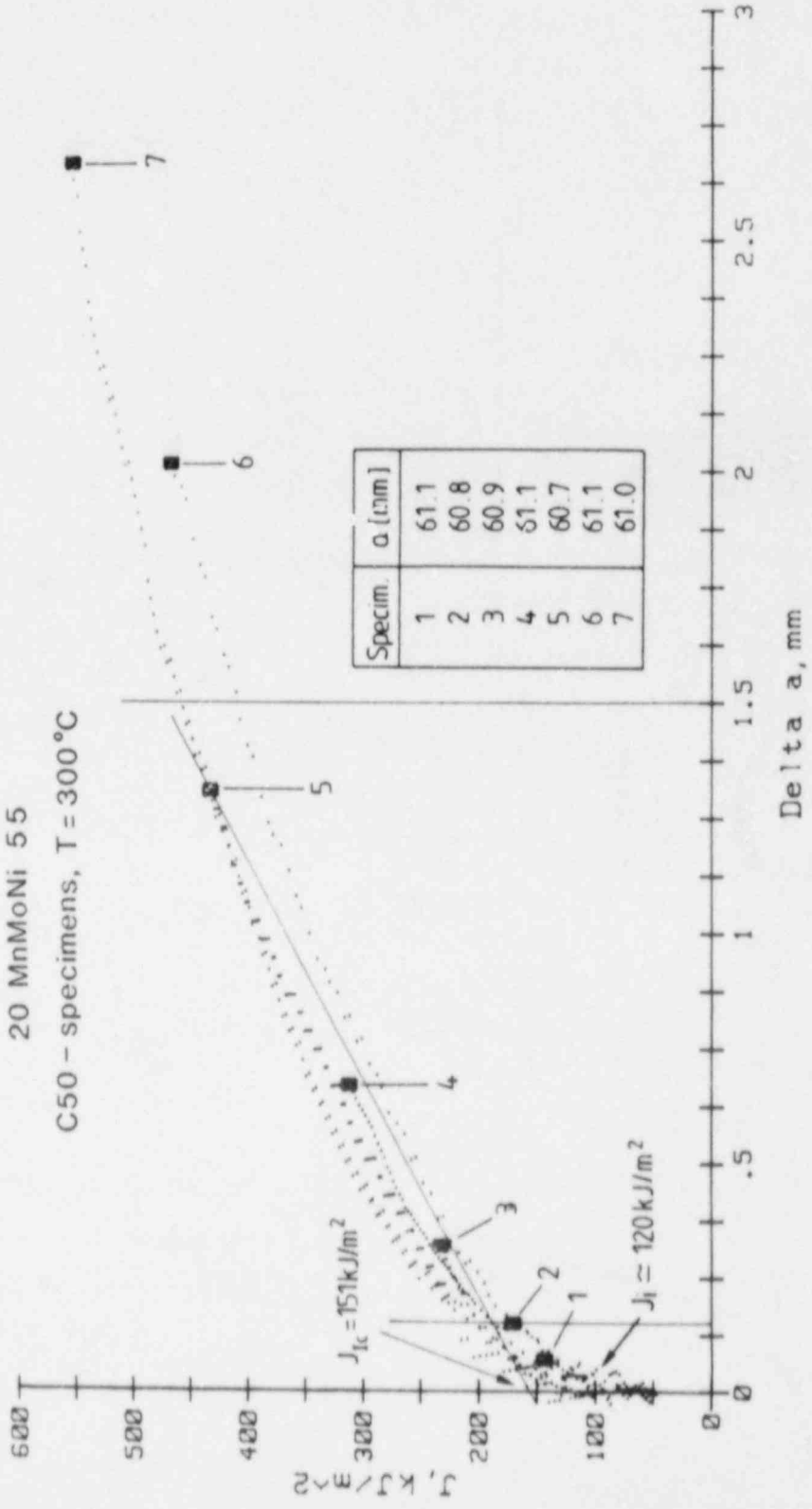

Fig. 3 J-resistance curves of a series of seven specimens. Interrupted load points confirm the J-R-curves derived from DCPD

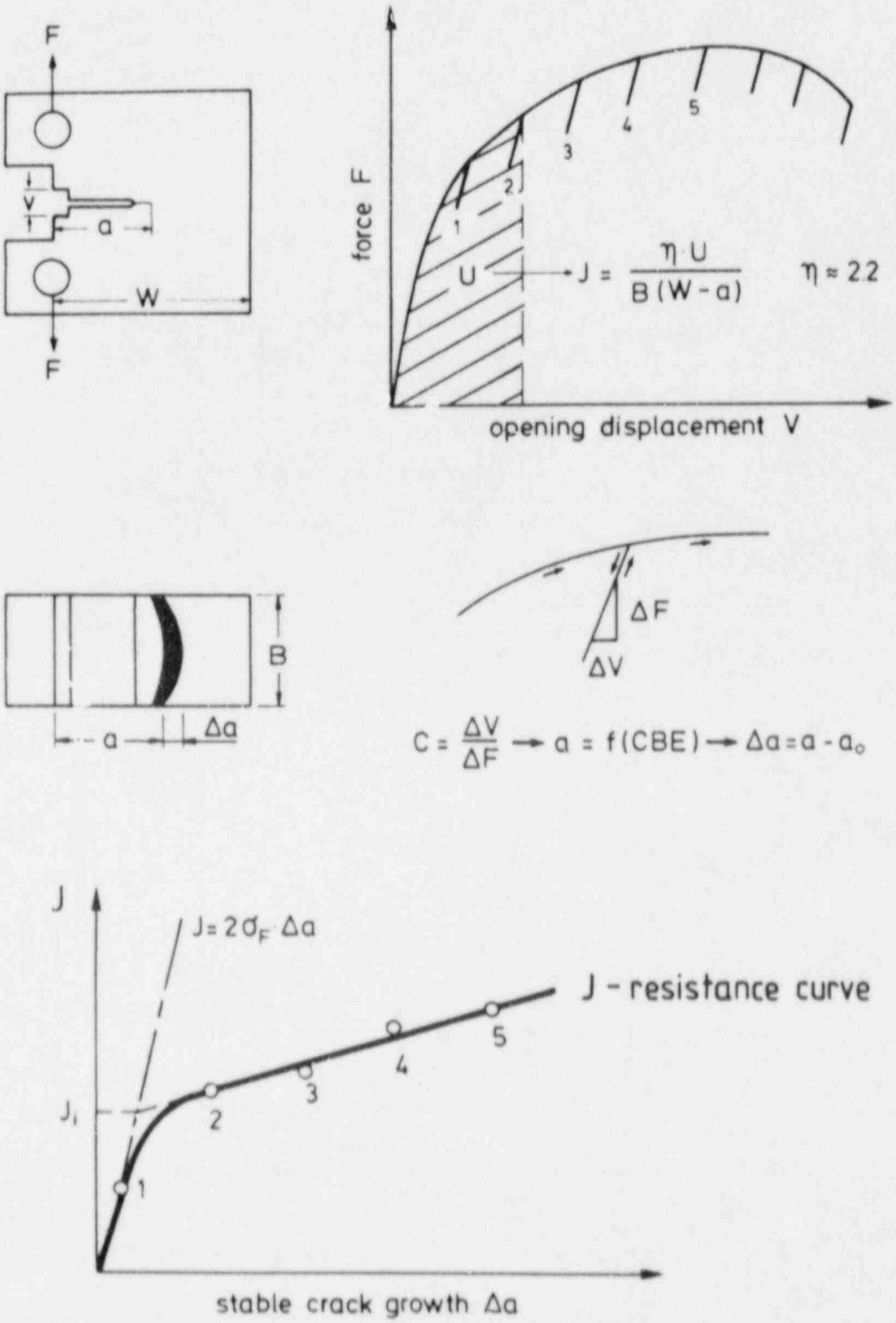

Fig. 4 Principle of J-R-curve measurement by partial unloading compliance technique

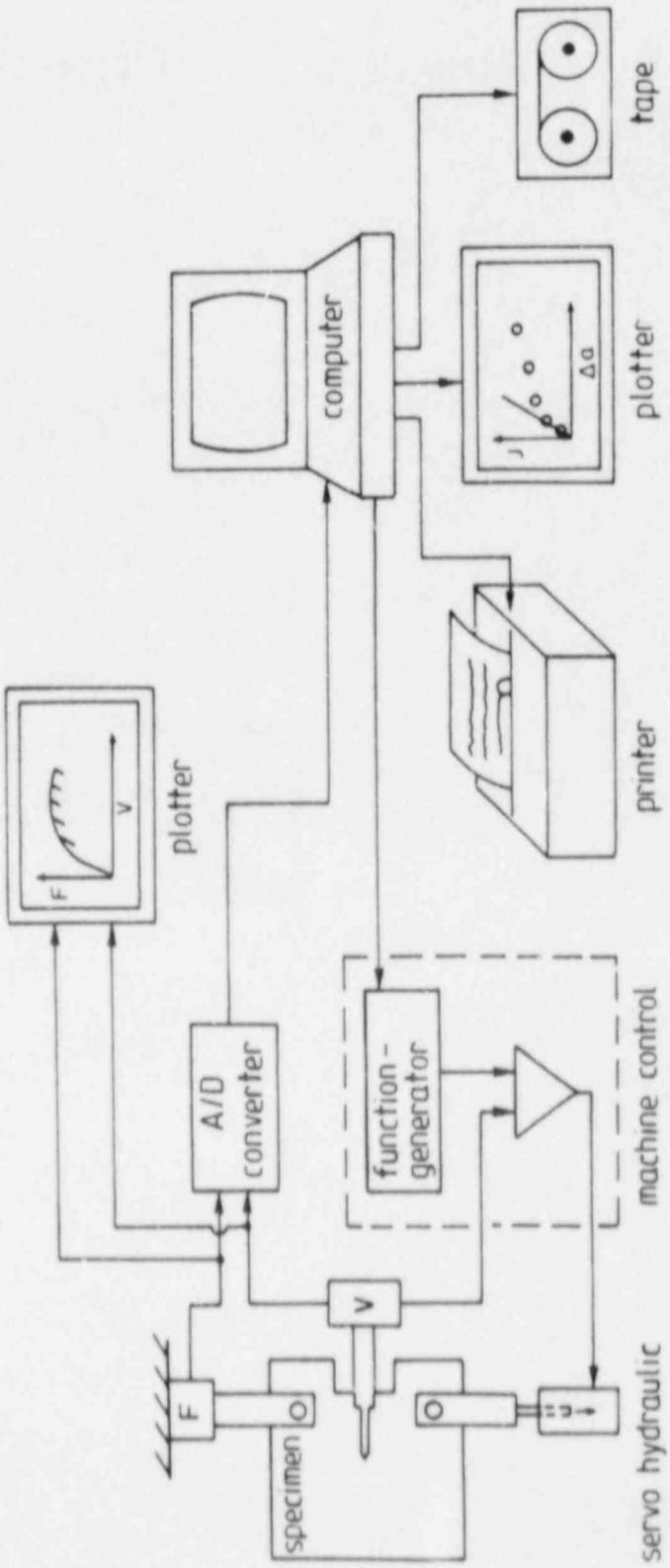

Fig. 5 Schematic of computerized test control and evaluation system

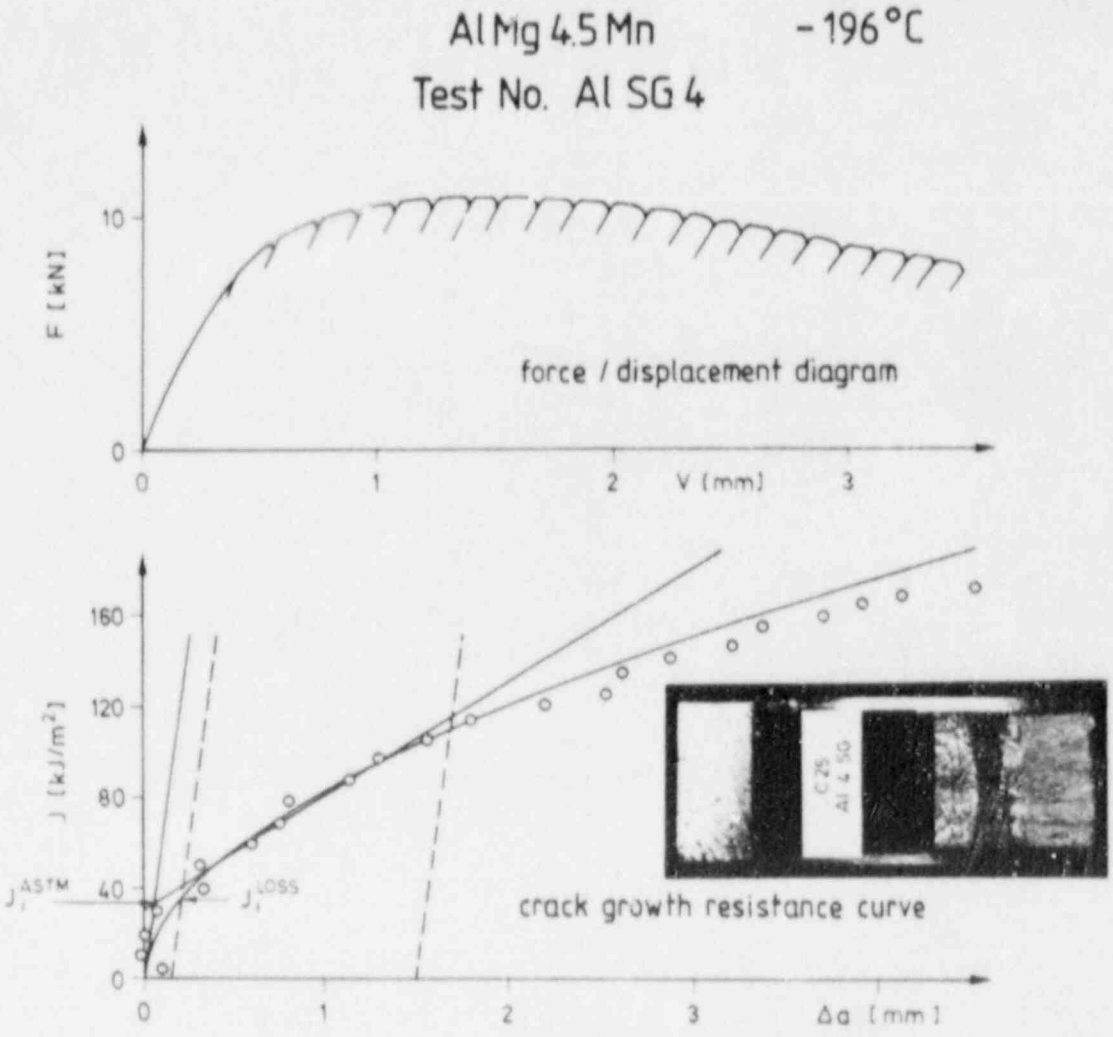

Fig. 6 Example of J-R-curve measured at -196°C for aluminum alloy weld material

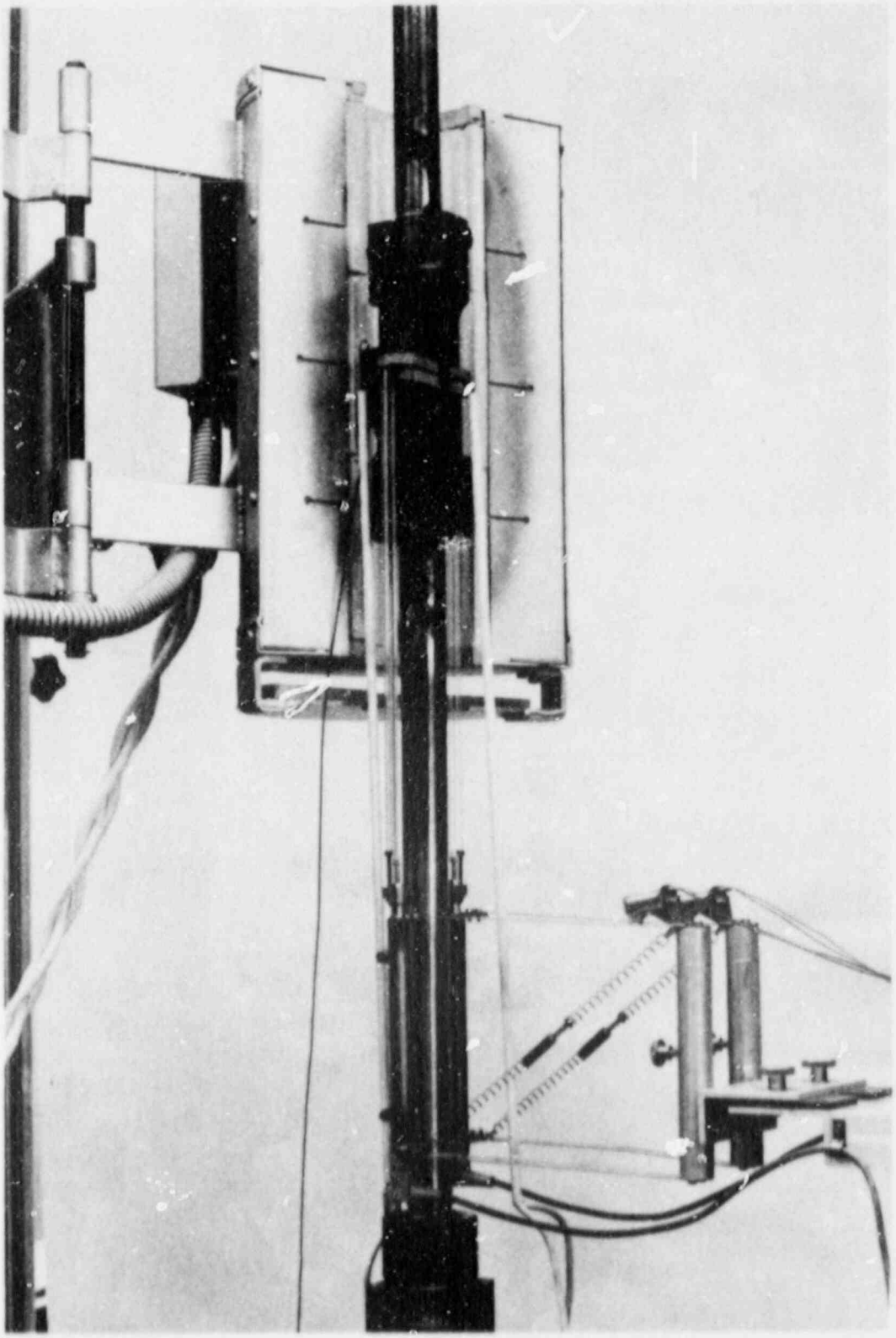

Fig. 7 Test system for CT-specimens for temperatures up to 800°C with special clevisses and load line displacement measurement by LVDT's outside the oven via quartz extension rods

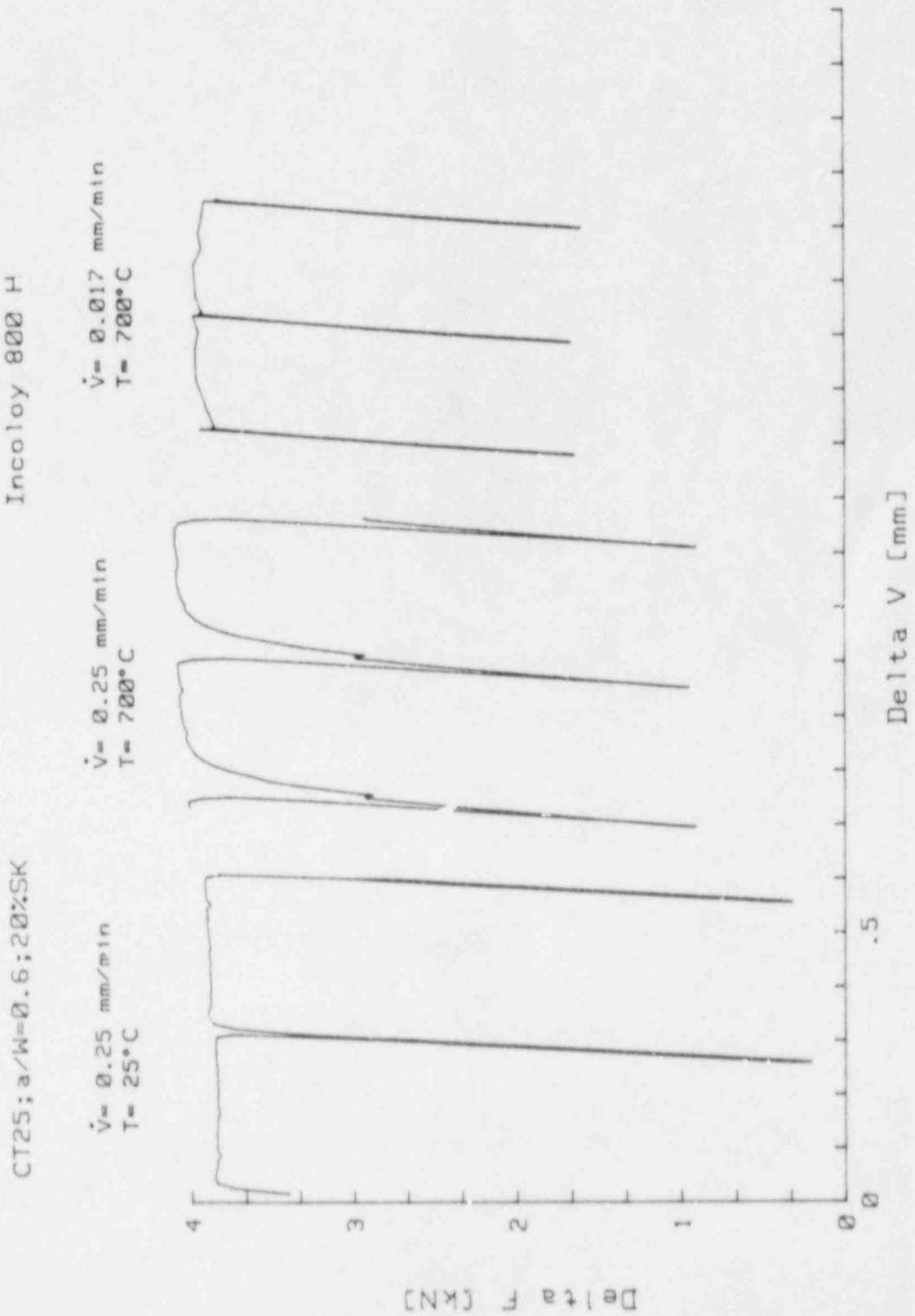

Fig. 8 Enlarged view of partial unloadings at different test temperatures and displacement velocities measured with the system of Fig. 7

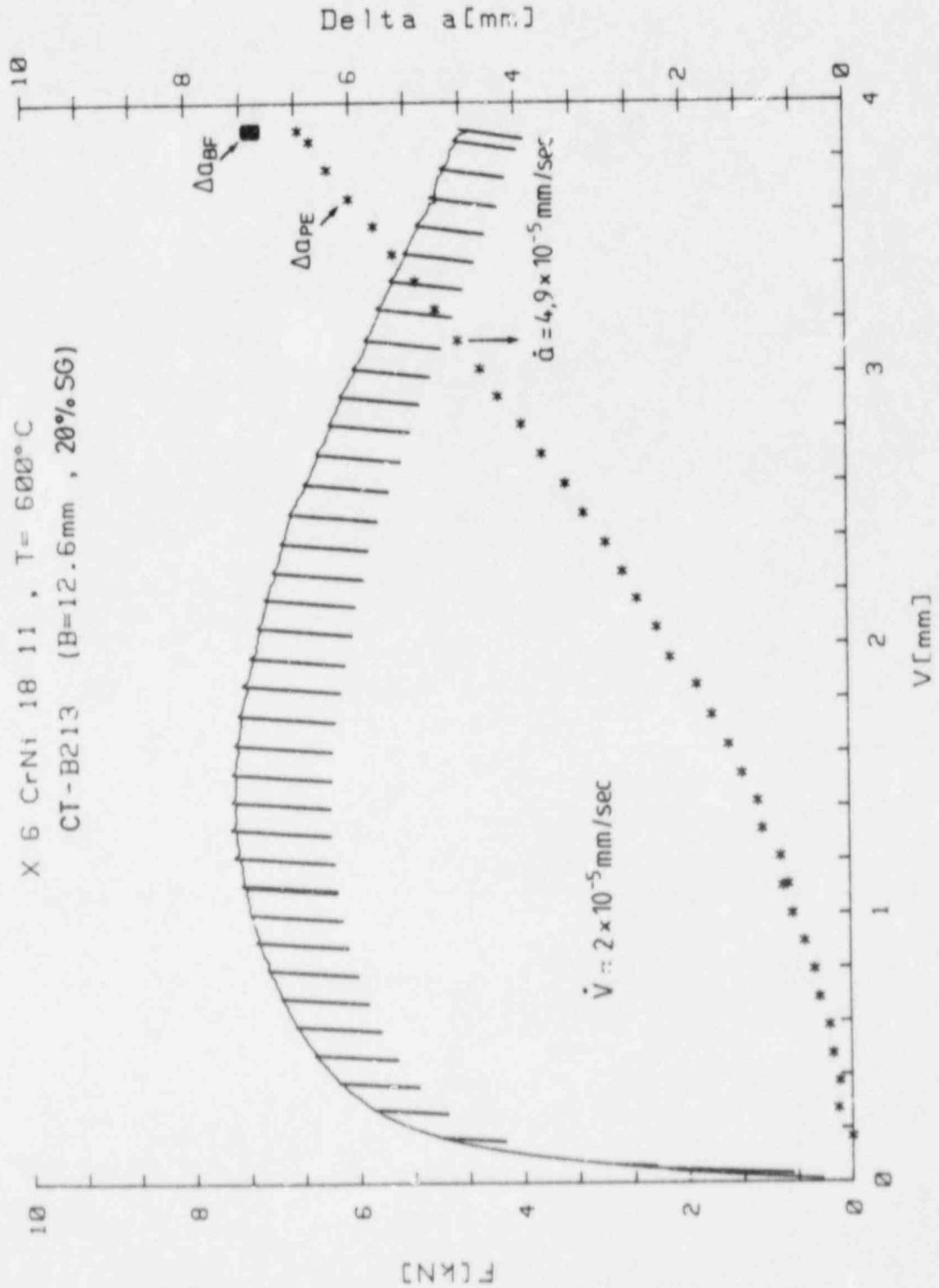

Fig. 9 Force displacement diagram with ▲a derived from partial unloadings showing low scatter and good agreement with final value ▲a(BF)

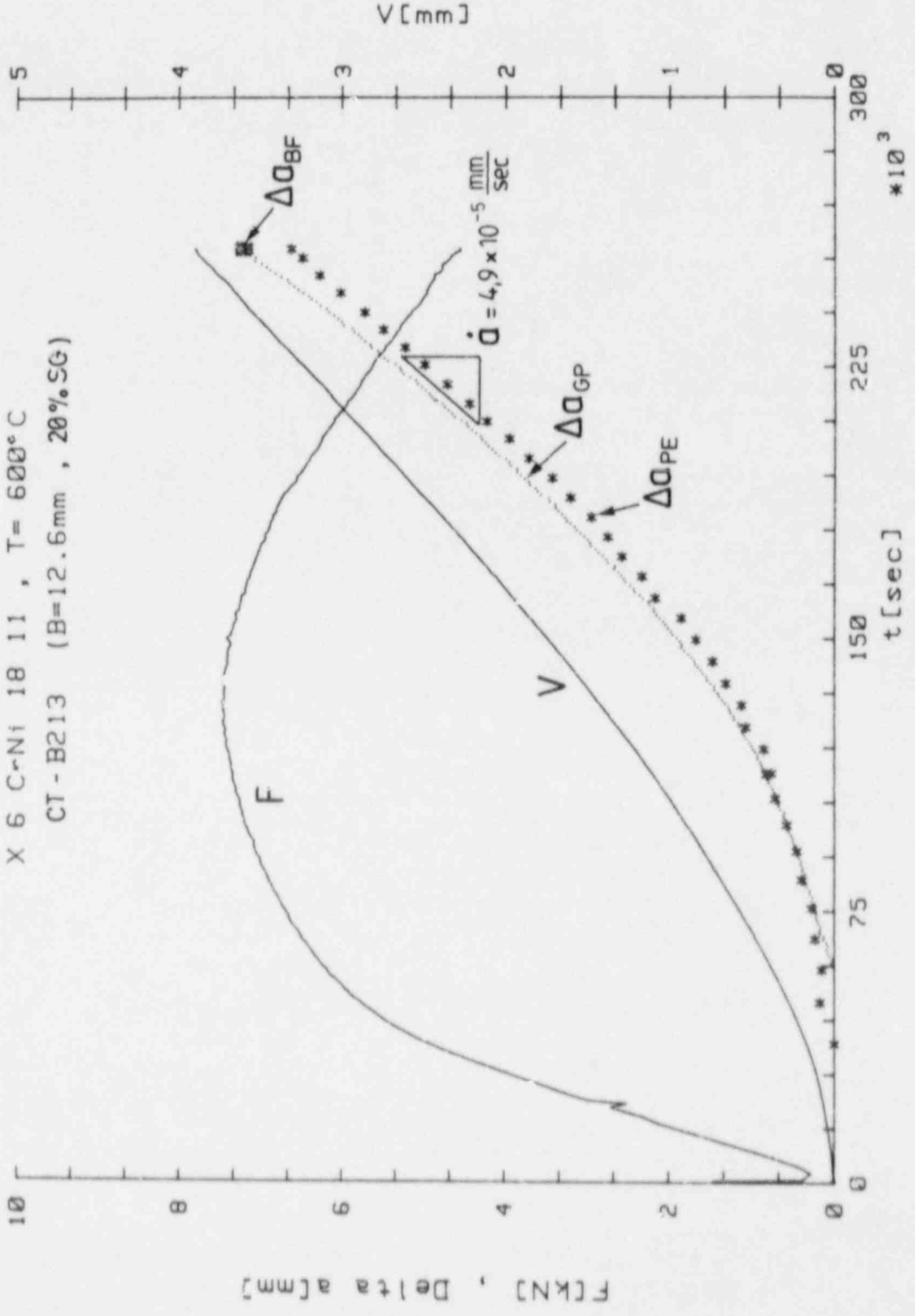

Fig. 10 Creep crack growth measurement comparing results of DCPD measurements ($\Delta a(GP)$) and partial unloadings ($\Delta a(PE)$) with good agreement

EXPERIMENTAL METHOD TO MEASURE THE ELASTIC-PLASTIC FRACTURE TOUGHNESS PROPERTIES OF IRRADIATED STAINLESS STEEL AT ELEVATED TEMPERATURE

M.I. de Vries, G.L. Tjoa, B.A.J. Schaap

NETHERLANDS ENERGY RESEARCH FOUNDATION, ECN
PETTEN, THE NETHERLANDS

ABSTRACT

An experimental test method, based on the combination of the potential drop technique and the interrupted-loading method, has been applied to measure the elastic-plastic fracture toughness properties of irradiated stainless steel at elevated temperatures. The results from this method, with small (½TCT, 30.0-28.8-12.0 mm) compact-tension specimens at 823 K, show small scatter and good reproducibility.

The automatical procedure for data-analysis includes the adjustment of the displacement- and potential drop measurements followed by data-analyses of the crack-growth resistance (J,R-) curve and validation of the results. The significant irradiation effect is quantified by reduction factors ($D_{J,R}$) on the characteristic resistance parameters.

It is concluded that, with this test procedure, valid fracture toughness data can be measured at 823 K with small (½TCT) compact-tension specimens of irradiated Type 304 stainless steel.

INTRODUCTION

Data on the resistance of irradiated stainless steel against crack initiation and crack growth are necessary for the design analyses and the safety assessment of nuclear components of advanced reactors (LMFBR, MFR). These fracture mechanic properties have to be measured by means of non-conventional test methods and new procedures, based on the elastic-plastic (epfm) parameter J-integral.

In this report highly reproducible results are presented from an experimental test procedure at 823 K with small (½TCT) compact-tension specimens of irradiated stainless steel Type 304. This procedure, with small specimens, is demonstrated to be a reliable test method for application in LMFBR-surveillance programmes. Valid fracture toughness data show that the significant irradiation effect can be quantified by reduction factors $D_{J,R}$ on the resistance against crack initiation and crack growth.

EXPERIMENTAL

Method

The experimental test method is based on the combination of the direct-current potential-drop technique and the interrupted-loading method. Multiple tests are performed but the crack extension (Δa) is controlled and continuously measured by the DCPD-technique.

Series of two up to six specimens, depending on the material variability, are tested. The specimens are fatigue-precracked to the a/W-ratio of 0.58. The final fatigue crack length is checked by optical measurements on the fracture surfaces of the broken specimens.

After precracking the specimens are loaded at constant displacement rates to selected crack extension (Δa) levels with discrete intervals ranging between 0.3 and 1.8 mm. Because the data points of the J,R-curve are regularly distributed along the Δa-axis, there is no need for additional conditions on data-grouping.

From the combination of the single-specimen DCPD-technique with the multi-specimen interrupted-loading method, multi J,R-curves are generated. The data points of these resistance curves are distributed with intervals of 0.05 mm along the Δa-axis. The DCPD-signals are calibrated with optical measurements of the final crack length.

Specimens

The dimensions of the specimens for irradiation experiments are usually restricted by the need to accommodate much material within the dimensional limitations of the irradiation facility. Small (½TCT, 30.0-28.8-12.0 mm) compact-tension specimens have been irradiated in the core of the HFR in Petten, The Netherlands, to investigate the applicability for fracture toughness experiments. The advantages and limitations of this specimen for fatigue crack growth experiments have been reported by De Vries and Michel (Ref. 1). Details of the material, specimen geometry and irradiation conditions are shown in Fig. 1.

Equipment

The tests are performed on an Instron servo-hydraulic testing machine, adapted for remote handling. This machine is installed in a lead-cell. The auxiliary equipment consists of electrical-insulated pull-rods with ½TCT-clevises, electrical probes with connections and wirings for DCPD-measurements, a 20 kN load-cell and one ± 5 mm displacement transducer. The specimens are heated in a resistance furnace with two small quartz windows for observation of the crack tip on both sides of the specimen by means of television camera's with microscope-lenses.

The load-line displacement at elevated temperature is indirectly measured from the relative displacement of the clevises. The clevis-displacement is transmitted by an extension rod to the transducer outside the furnace near the bottom of the lower pull-rod. The load-cell is located above the furnace on the top of the upper pull-rod. Load-cell and displacement transducer are temperature conditioned by water-cooling. In Fig. 2 the testing assembly is schematically shown.

The electronics for machine-control, load- and displacement measurements, crack-tip monitoring and DCPD-measurements are installed outside the shielded facility. A block diagram of this equipment is shown in Fig. 3. The details of the equipment, the measuring techniques and the computer programmes have been extensively reported by Van den Broek, Schaap and Tjoa (Refs 2, 3 and 4).

Loading procedure

The specimens are fully automatically tested in one loading sequence, schematically shown in Fig. 4. The complete loading procedure can be divided into three stages:

Fatigue preloading

This stage consists of 4 sequences of 1 mm fatigue crack growth at 823 K under combined load/crack-length control with P_{max} of 4.0, 3.2, 2.6 and 1.8 kN successively. The sequences can be easily observed on the fracture surfaces (markings) due to the scaling at elevated temperature. After the final fatigue cycle the specimen is immediately unloaded to 0.4 kN and the control mode is transferred to combined ram-displacement/crack-length control.

Tensile loading

This is the actual fracture mechanics test. The specimen is loaded at a constant displacement rate (0.002 mm/s) up to a predetermined amount of crack extension, ranging from 0.3 to 1.8 mm. When the final crack extension value has been achieved, the specimen is immediately unloaded to avoid creep crack growth. Then the control mode is changed to load-control and the specimen is cooled to room temperature.

Post-fatigue and fracture

Post-fatigue loading prior to final fracture is applied to separate the specimen without distortion of the crack-tip. After about 5 mm fatigue crack growth at room temperature the specimen is separated under displacement-controlled tensile loading to final fracture. After separation the fracture surfaces are inspected by means of colour photography and the crack-length is optically measured by means of the weighted nine-points averaging method. Selected specimens are prepared for microscopy including SEM and TEM.

RESULTS

Measurements

Two series of data sets, consisting of load-displacement and load-displacement-DCPD values, are automatically measured during the test. The first series is based on displacement intervals of 0.005 mm, to be able to calcul.e accurately the area under the curve. The second series is based on the DCPD-intervals of 3 μV. A combination of load- and DCPD-displacement curves is shown in Fig. 5.

The original displacement data, from the measurements of the relative clevis-displacement, are corrected for additional displacements due to extraneous sources. The correction is calculated from the difference between the slope of the initial linear portion of the original curve and the theoretical specimen compliance for the actual final fatigue crack-length. The correction is validated by comparison with data from system-stiffness measurements. The correction is limited to displacement values for which the area under the corrected curve is less than 95% of the area under the original curve. Corrected curves are shown in Fig. 6.

The advantage of the combination of two test techniques is that the DCPD-signal can be calibrated afterwards from the optical measurements on the fracture surfaces. Such a calibration curve from a series of 6 interrupted loading tests, is shown in Fig. 7. The difference between this calibration curve and the ideal curve for conversion of DCPD-signals into fatigue crack extension values amounts about 18 μV. This is due to the DCPD-contribution from extensive plastic deformation during the initial tensile deformation prior to the real crack extension (Δa). After the conversion of the DCPD-data with this "plasticity correction" the Δa-values are considered to be valid within the Δa-range of the calibration curve.

The corrected values of displacement and crack extension are used in the calculation of the crack growth resistance (J,R-) curve using the incremental J_{i+1}-formula from Reference 5

$$J_{i+1} = [J_i + (\frac{f\ a/W}{b})_i \frac{A_{i,i+1}}{B}] \times \{1 - (\frac{1 + 0.76\ bi/w}{b})_i [(a_p)_{i+1} - (a_p)_i]\} \quad (1)$$

The J,R-curves from the series of 6 irradiated specimens are shown in Fig. 8. The scatter band is small and the results are highly reproducible.

Data analyses

The J,R-data are analysed to determine the values of the characteristic resistance parameters. The procedure consists of the following steps:

- Exclusion of the data outside the validity range of the Δa-correction.
- Exclusion of the data outside the offset values of 0.15 and 1.5 mm parallel to the blunting line. The blunting line is constructed according the estimated formula $J = 4\,\sigma_y$, based on empirical relationships at room temperature (Ref. 2).
- Linear regression analysis of the remaining data (minimum of six data points). The plot of the J,R-data and the regression coefficient for irradiated stainless steel justify the linear regression analysis.
- Determination of J and corresponding Δa-values for the intercept (J_Q) of the blunting line and the regression line.
- Calculation of J at constant Δa-value of 0.3 mm (no offset value!) and comparison with the actual measured $J_{0.3}$. The calculated value is considered to be representative if the difference with the actual measured value is less than 0.15 times the slope of the regression line.
- Calculation of the tearing modulus T.
- Determination of the averaged resistance curve from the collection of the data from all specimens (Fig. 9).
- Validation of J_Q according the criteria from Reference 5:

$$J_Q < \frac{B.\sigma_y}{25} \qquad (2)$$

$$J_Q < \frac{b.\sigma_y}{25} \qquad (3)$$

$$dJ/da < \sigma_y \qquad (4)$$

The values of the resistance parameters for irradiated stainless steel are compared in Table 1 with data for the same unirradiated material. There is a significant reduction due to the irradiation.

We have chosen the parameters $J_{0.3}$ and dJ/da (slope of the regression line) to quantify the irradiation effect on the resistance curve. The $J_{0.3}$ has been chosen because there is a significant difference of a factor 2 between the Δa_Q-values (Δa-values corresponding with J_Q) for unirradiated and irradiated material. Further by using dJ/da instead of T, the σ_y (effect on tensile properties) has not to be taken into account. The reduction factors of the resistance against crack initiation and crack growth are respectively:

$$D_{0.3} = \frac{J_{0.3}\text{ - irr.}}{J_{0.3}\text{ - unirr.}} = 0.63 \qquad (5)$$

$$D_R = \frac{dJ/da\text{ - irr.}}{dJ/da\text{ - unirr.}} = 0.68 \qquad (6)$$

The irradiation effect on the resistance curve is unambiguously characterized by these data.

CONCLUSIONS

A reliable test method is presented for fracture toughness measurements of irradiated stainless steel at elevated temperature.

Highly reproducible $J_i R$-curves are measured at 823 K.

The J_Q-values are valid J_{IC}-data according the criteria of the ASTM-standard E813.

Small ($\frac{1}{2}$TCT, 30.0-28.8-12.0 mm) compact-tension specimens are, in combination with this test procedure, applicable for fracture toughness tests at elevated temperatures in stainless steel irradiation programmes (LMFBR surveillance programmes).

The irradiation effect on the resistance against crack initiation and crack growth can be unambiguously qualified by the parameters $J_{0.3}$ and dJ/da.

REFERENCES

1. M.I. de Vries and D. Michel, "Fatigue Crack Growth in Neutron Irradiated Type 304 and Type 316 Stainless Steel" in Twelfth International Symposium on the Effects of Radiation on Materials, ASTM Symposium, Williamsburg, June 1984.

2. M.I. de Vries and B.A.J. Schaap, "Experimental Observations of Ductile Crack Growth in Type 304 Stainless Steel", in Elastic-Plastic Fracture Toughness Test Methods, ASTM Symposium, Louisville, April 1983.

3. G.L. Tjoa, F.P. van den Broek and J. van Hoepen, "Fatigue Testing of Irradiated Steels at High Temperatures", ECN-135, July 1983.

4. G.L. Tjoa, F.P. van den Broek and B.A.J. Schaap, "Automated Test Methods for Fatigue Crack Growth and Fracture Toughness Tests on Irradiated Steels at High Temperatures", in Automated Test Methods for Fracture and Fatigue Crack Growth, ASTM Symposium, Pittsburgh, November 1983.

5. Standard Test Method for J_{IC}, A Measure of Fracture Toughness, ASTM E813, in Annual Book of ASTM Standards, Volume 03.01 1983.

Table 1 Comparison of the values of the resistance parameters for unirradiated and irradiated stainless steel at 823 K.

		unirradiated	irradiated*
dJ/da**	(kJ/m²)	214	146
C**	(kJ/m²)	215	131
r^2		0.91	0.96
J_Q	(kJ/m²)	267	150
Δa_Q	(mm)	0.26	0.14
$J_{0.3}$	(kJ/m²)	377	175
T		530	360

* 3.10^{24} n.m^{-2} (E > 0.1 MeV)

** linear regression: J = dJ/da Δa + C

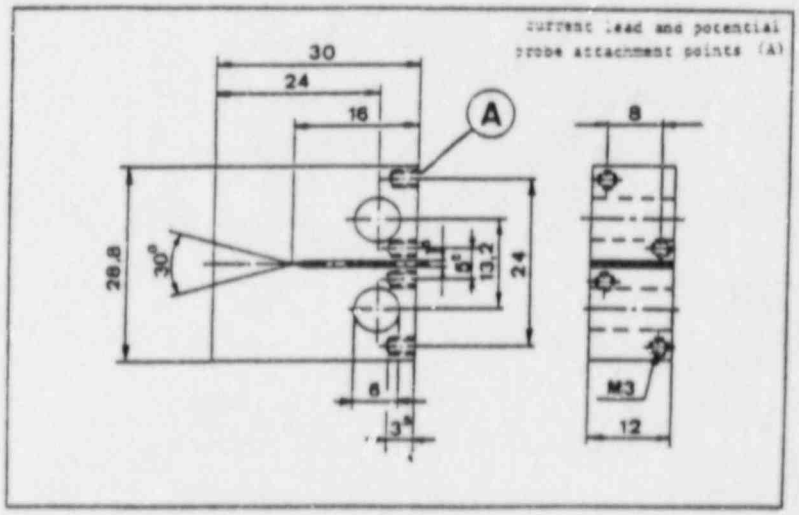

stainless steel Type 304 plate
plate thickness 40mm
½-T CT-specimen with T-L orientation
Irradiation: 3.10^{24} nm^{-2} (E > 0.1 MeV) at 823 K

Fig. 1 Details of test specimen and material conditions.

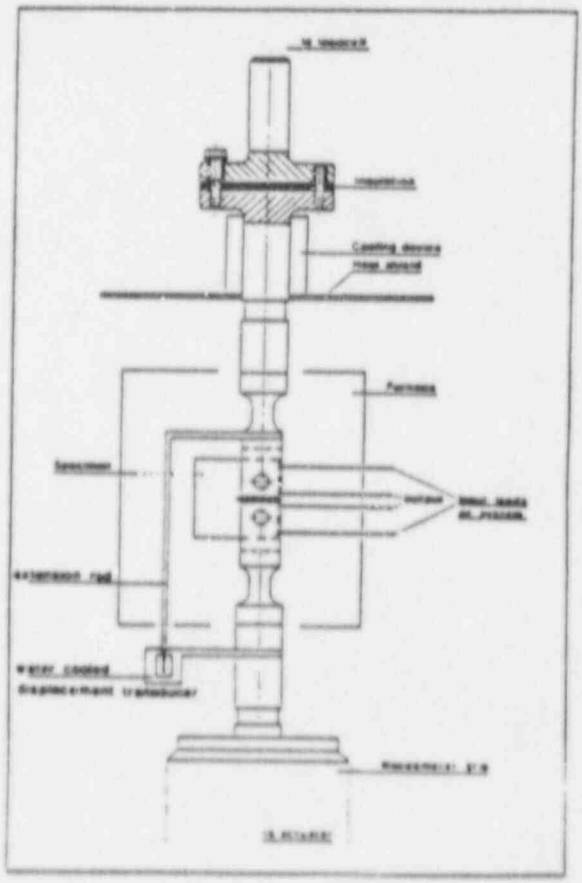

Fig. 2 Testing assembly for fracture toughness tests.

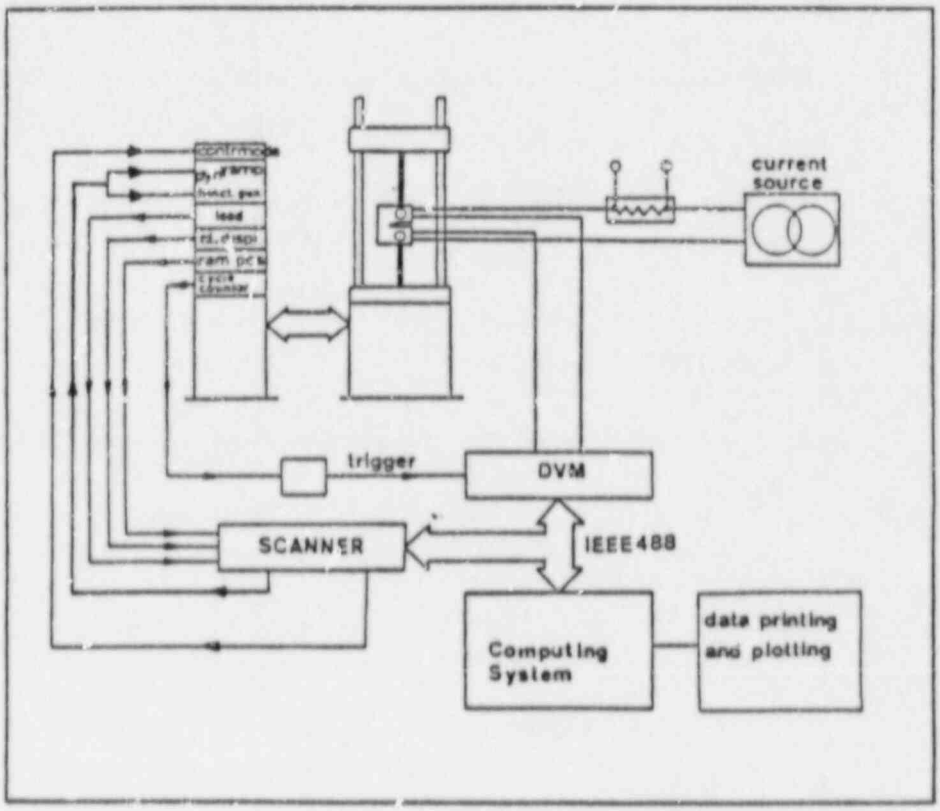

Fig. 3 Block diagram of data-acquisition system for fracture toughness tests.

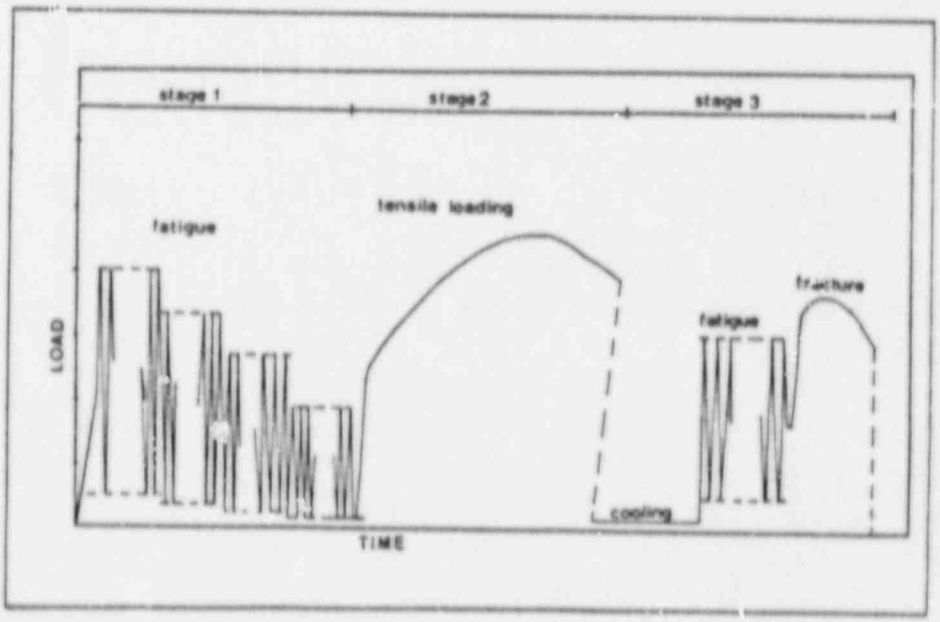

Fig. 4 Scheme of the loading sequence.

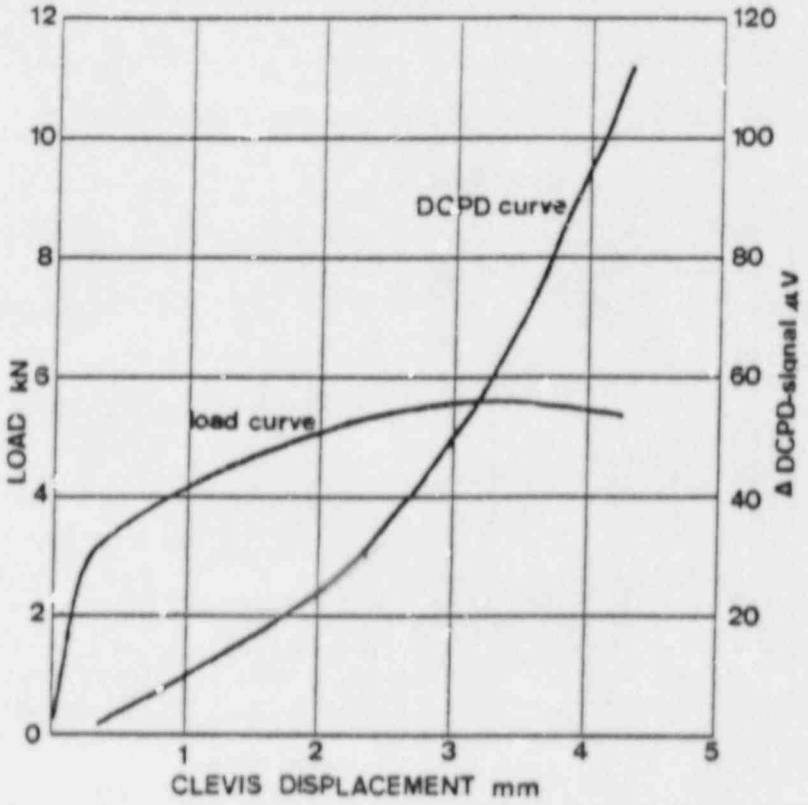

Fig. 5 Combination of load- and DCPD-displacement curves.

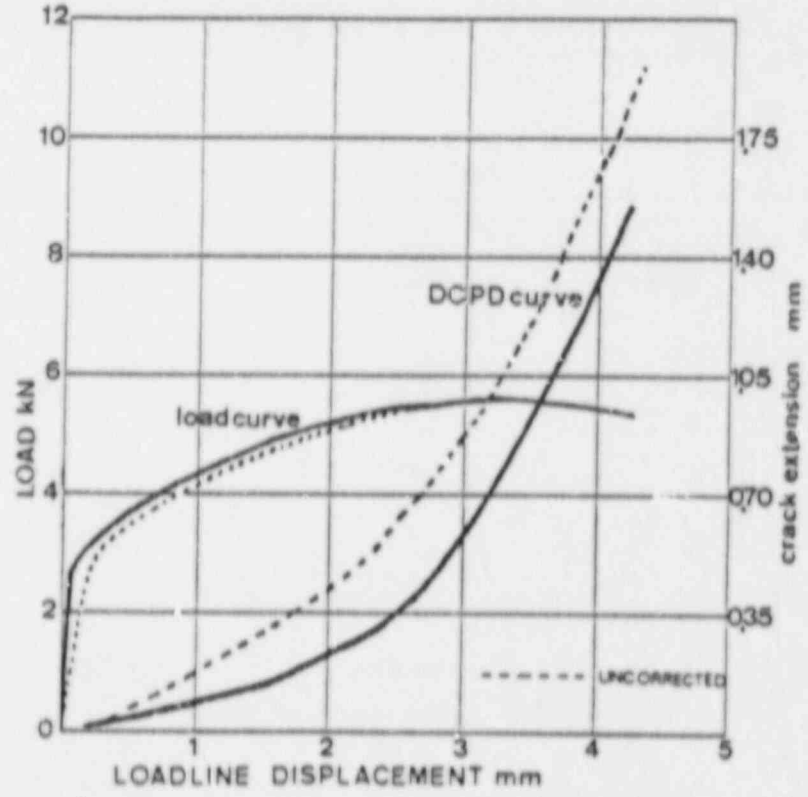

Fig. 6 Load- and crack extension (Δa) curves after correction for extraneous displacement and crack-tip plasticity.

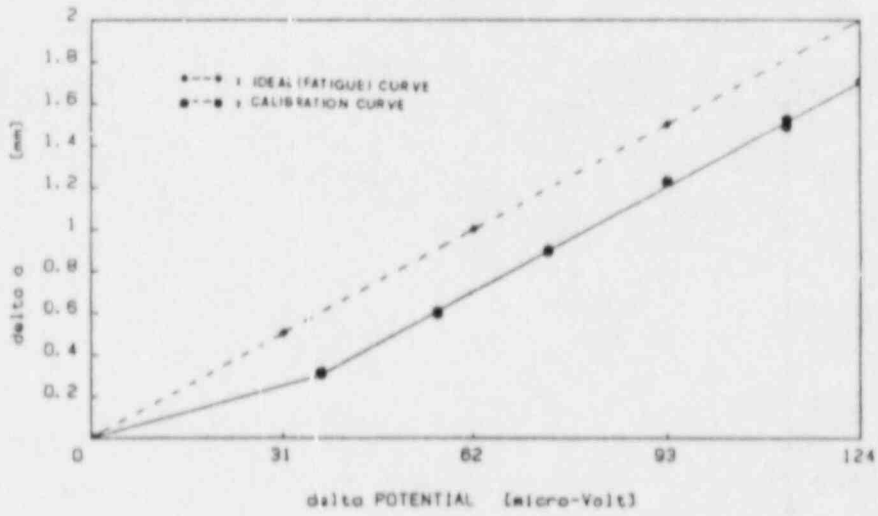

Fig. 7 Calibration curve from optical measurements on the fracture surfaces.

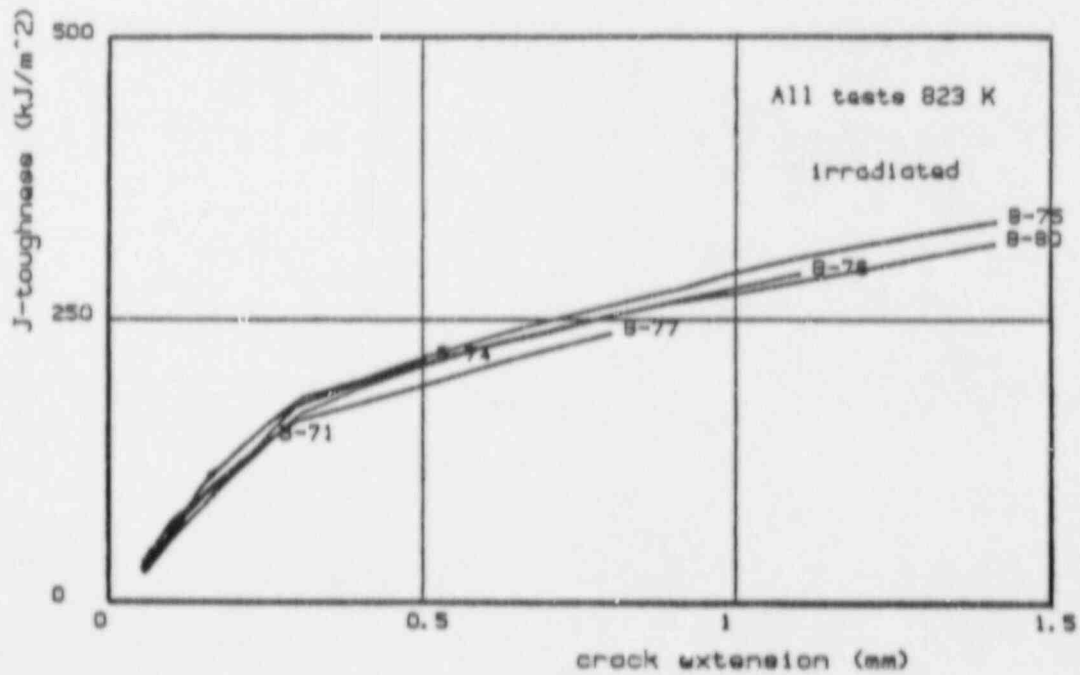

Fig. 8 Combination of the J,R-curves from 6 irradiated specimens.

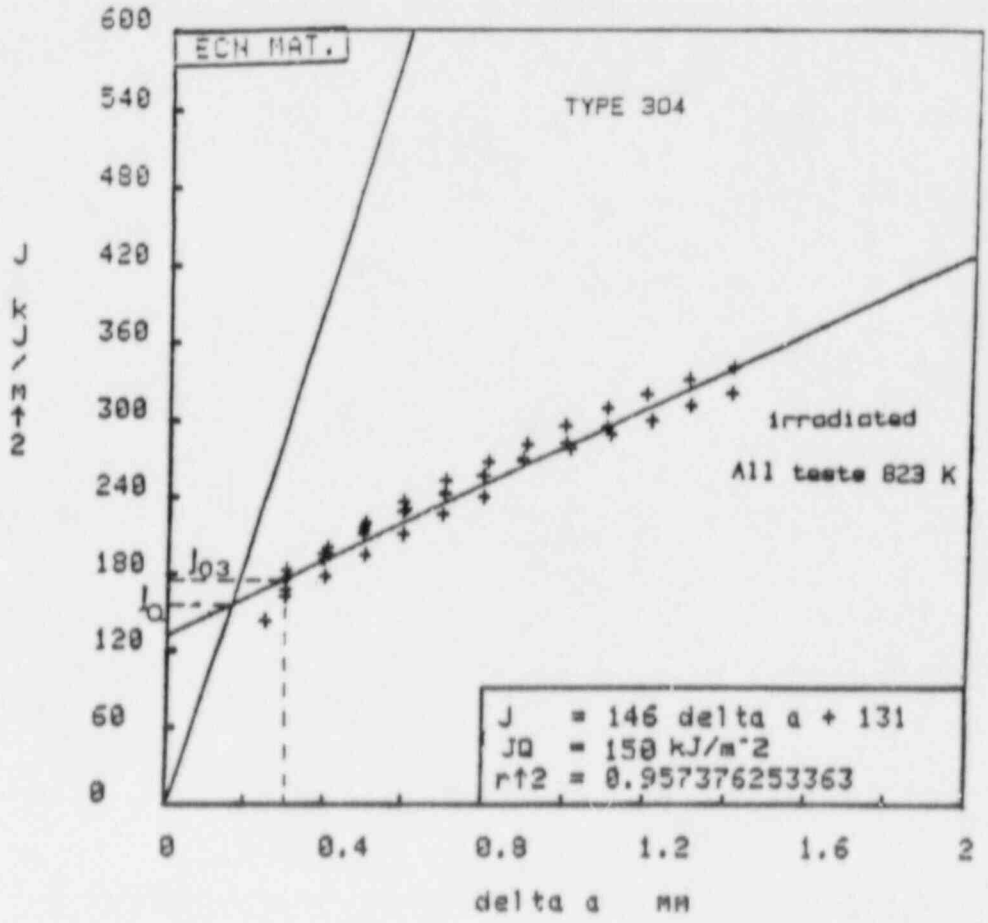

Fig. 9 Data points and averaged resistance curve from all data on irradiated stainless steel.

COMPARISON OF POTENTIAL DROP, ACOUSTIC EMISSION AND PARTIAL UNLOADING METHODS FOR THE EVALUATION OF J-R CURVES OF AUSTENITIC STAINLESS STEELS.

P. BALLADON AND M. FOUCAULT

UNIREC, Centre de Recherches d'Unieux, BP 34
42701 FIRMINY (FRANCE)

INTRODUCTION

Among the single specimen methods to determine J-R curves, one of the widely used is the single specimen compliance (partial unloading) method;

However, results obtained on very tough materials like some austenitic stainless steels show that partial unloading lead to a lack of precision first to determine crack initiation, secondly to determine crack extension due to the large crack opening displacement. Other single specimen methods like potential drop and acoustic emission have been proposed to determine crack initiation and growth.

Aim of this work is to present an attempt to compare J-R curves obtained on an austenitic stainless steel at room temperature using partial unloading, DC potential drop, acoustic emission and interrupted loading (multispecimen) methods.

SUMMARY

Results obtained show that it is possible to use DC potential drop method to determine J-R curve of austenitic stainless steels with a good precision compared to interrupted loading method. This method seems howewer slightly conservative concerning J values for the onset of crack growth. Crack extension can be easily correlated with potential drop using a linear relationship for limited values of crack growth.

Partial unloading method can lead to overestimate J

values for the onset of crack extension due to the lack of precision of compliance measurements in the field of limited crack growth.

Detection of crack initiation by acoustic emission seems to be difficult. Results obtained show that J values corresponding to a change in acoustic emission rate are related to a macroscopic crack extension and that amount of acoustic emission events cannot be directly related to crack extension values. However, further investigations must be done using other signals like cumulative peak amplitudes or cumulative area under peaks.

MATERIAL

17-12 SPH Steel (Type 316L with controlled Nitrogen)

30 mm thick plate 1070 °C water Quenched

C	Mn	Si	S	P	Ni	Cr	Mo	N
0.025	1.81	0.49	0.002	0.027	12.22	17.22	2.38	0.074

chemical analysis

0.2% YS (MPa)	UTS (MPa)	Tot. el. (%)	RA (%)	Charpy U (J/cm^2)
255	584	66.7	81.5	270

Mechanical properties at room. temperature

SPECIMENS

Modified CT25, 20% side-grooved

TL orientation

Precracking according ASTM E 813

before side-grooving - $a/W = 0.5$

TEST METHODS

Single Specimen Compliance (Partial Unloading)

Multiple Specimen (Interrupted Loading)

Potential Drop

DC . Constant amplitude impulses 20 ms

Acoustic Emission

Cumulative number of events

TEST CONDITIONS

Room Temperature

Constant displacement rate 0.8 mm/mn

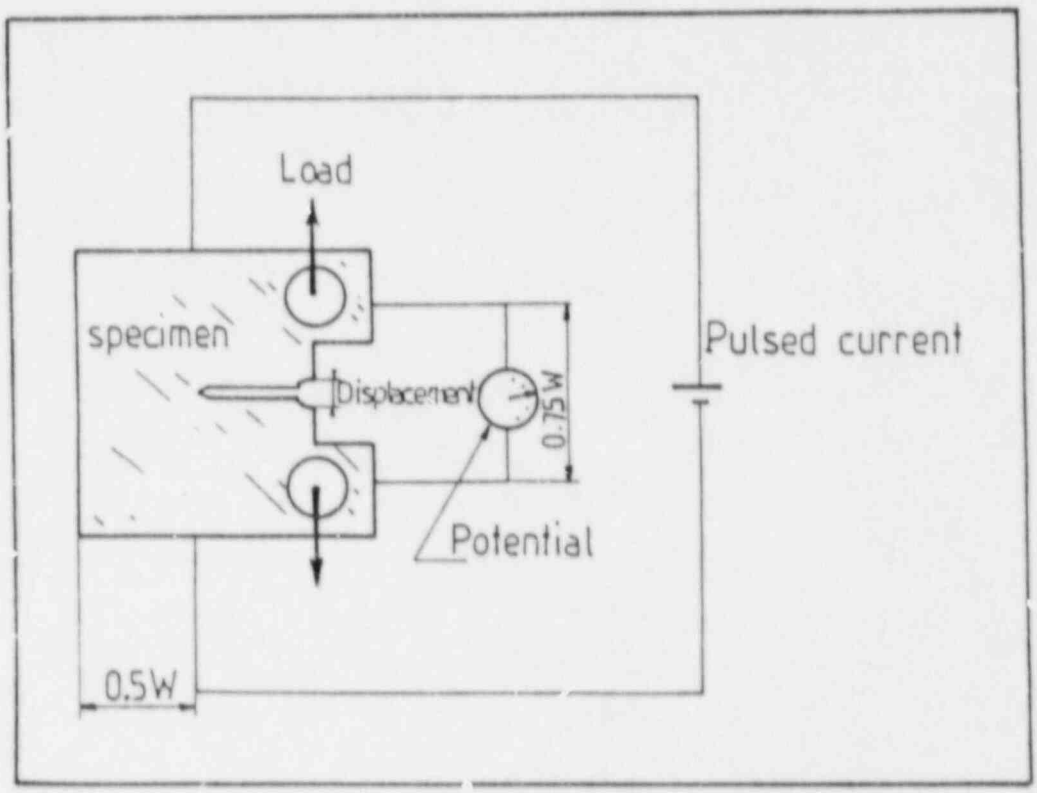

Fig. 1 POTENTIAL DROP METHOD

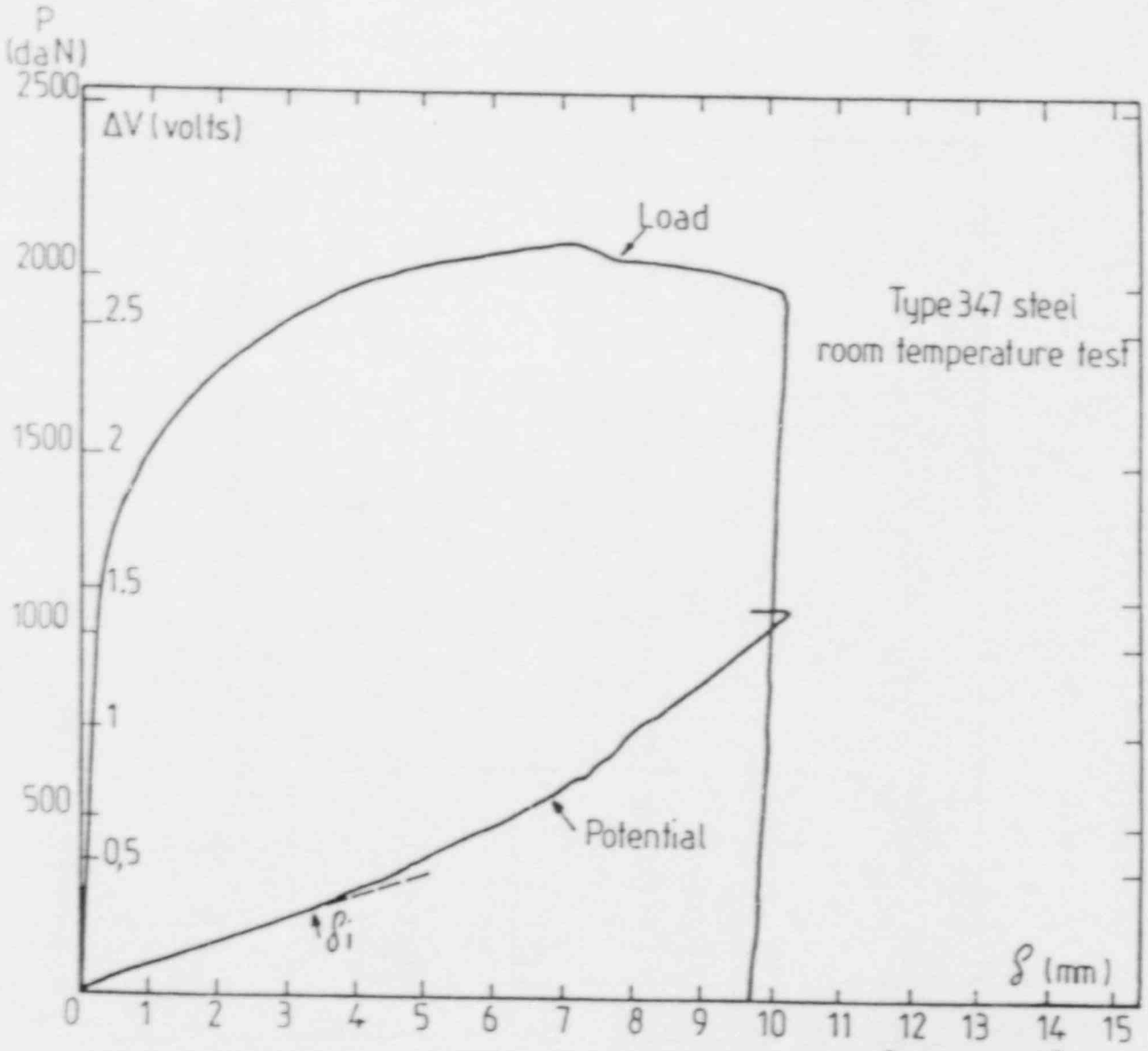

Fig. 2 - EXAMPLE OF P-δ AND ΔV-δ CURVES

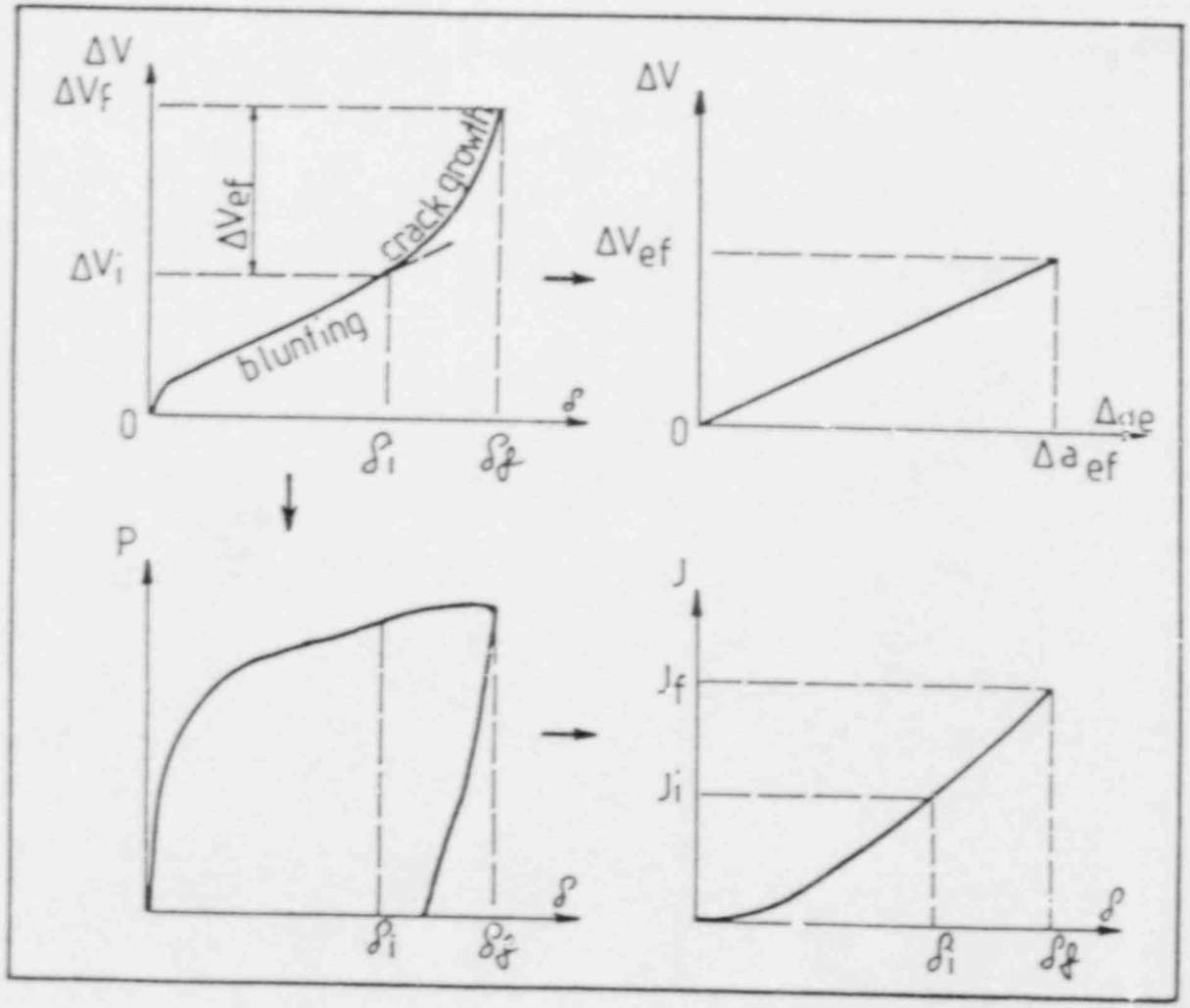

Fig. 3

J-Δa DETERMINATION BY POTENTIAL DROP METHOD

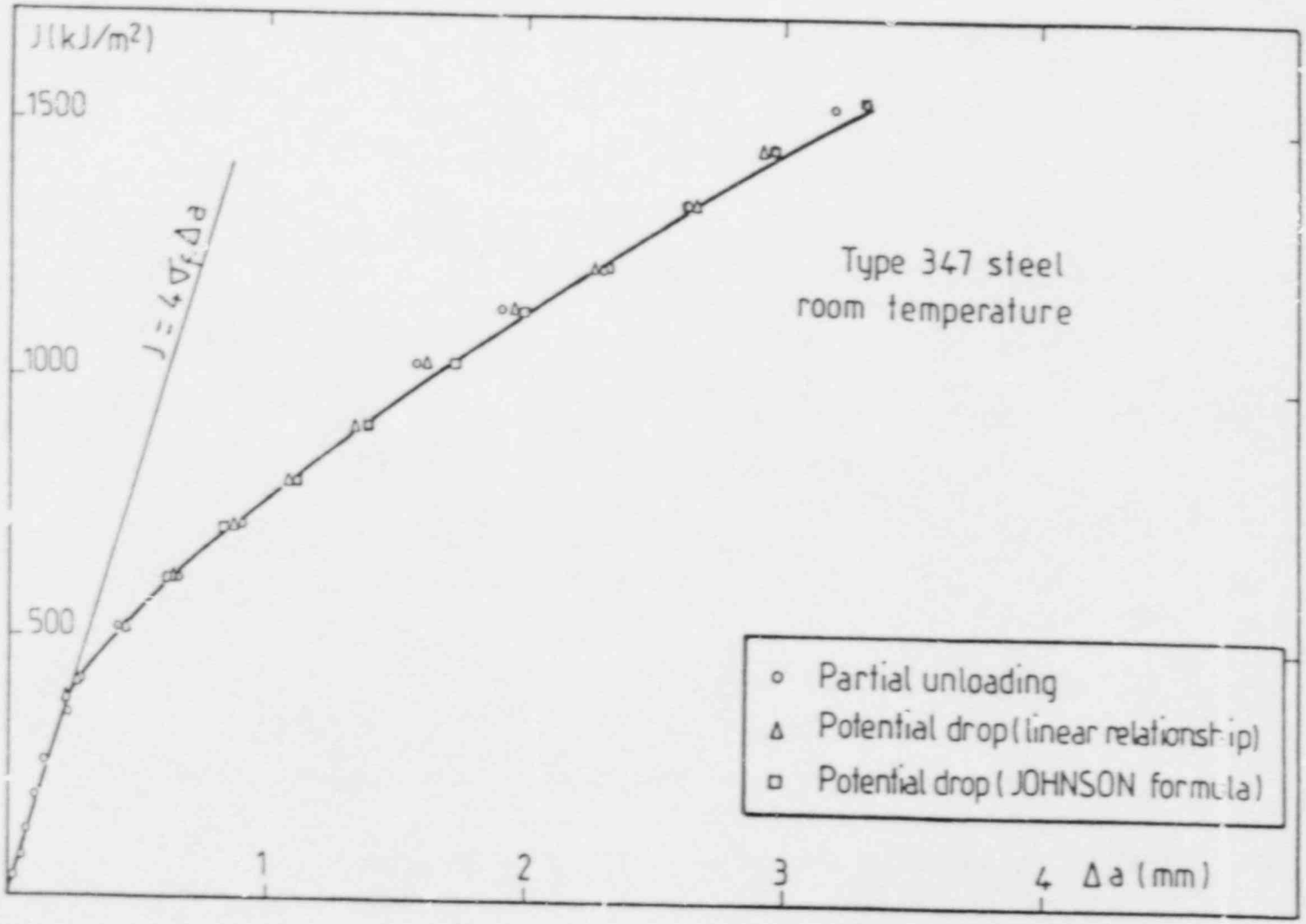

Fig. 4 EXAMPLE OF J-R CURVE

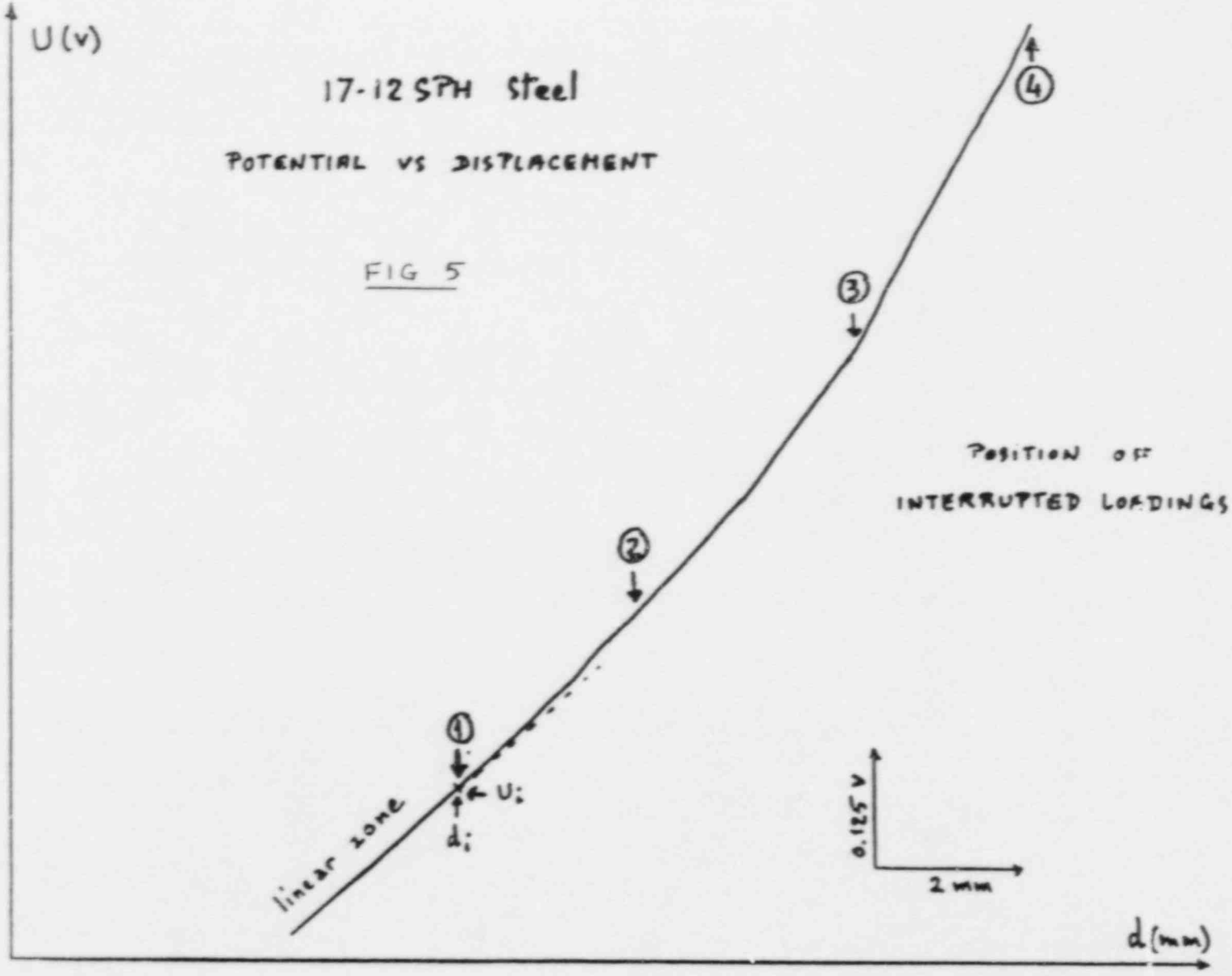
U(v)
17-12 SPH Steel
POTENTIAL VS DISPLACEMENT
FIG 5
POSITION OF
INTERRUPTED LOADINGS
linear zone
U_i
d_i
0.125 V
2 mm
d(mm)

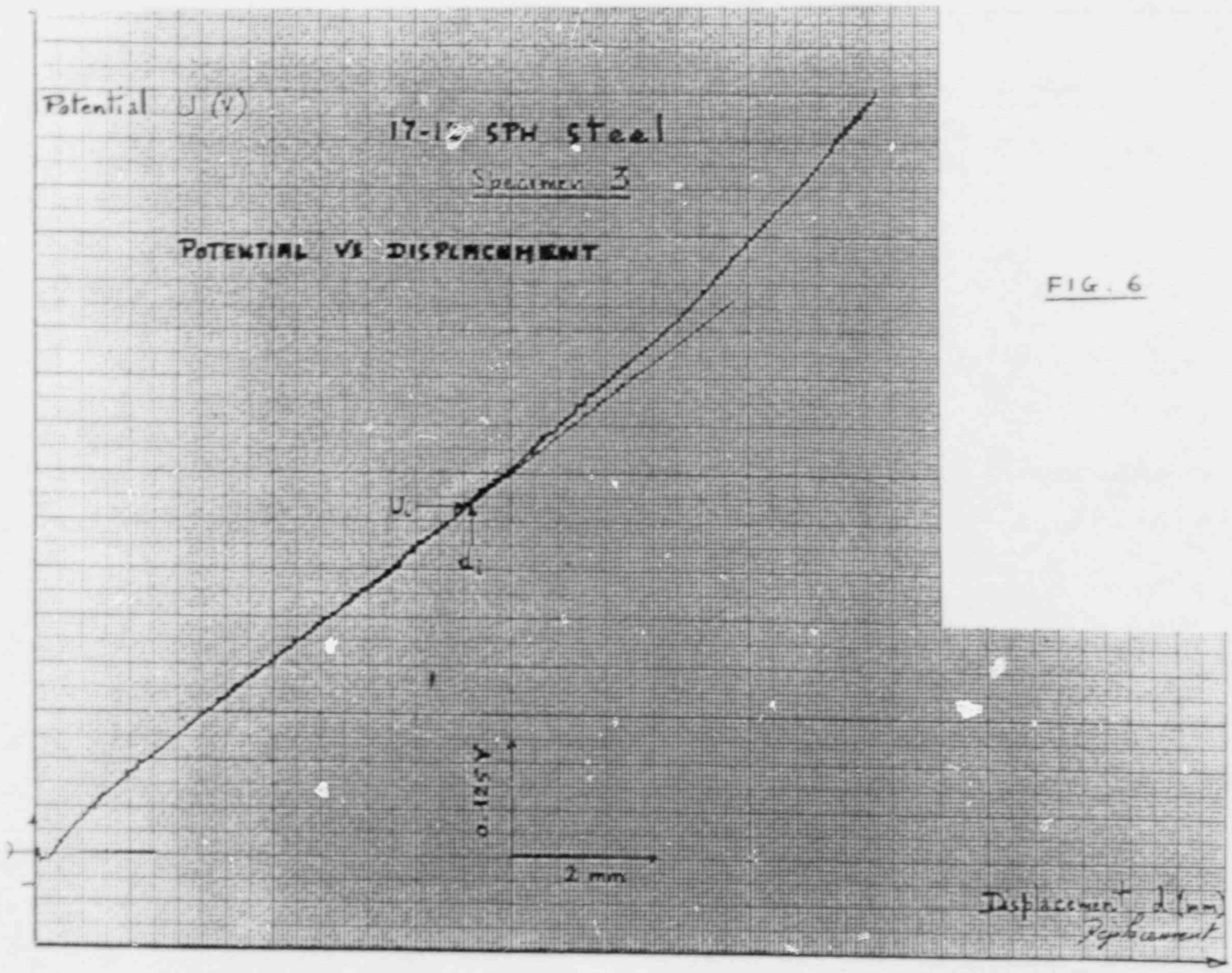
Potential U (V)
17-12 SPH Steel
Specimen 3
POTENTIAL VS DISPLACEMENT
U_i
d_i
0.1 mV
2 mm
Displacement d (mm)

FIG. 6

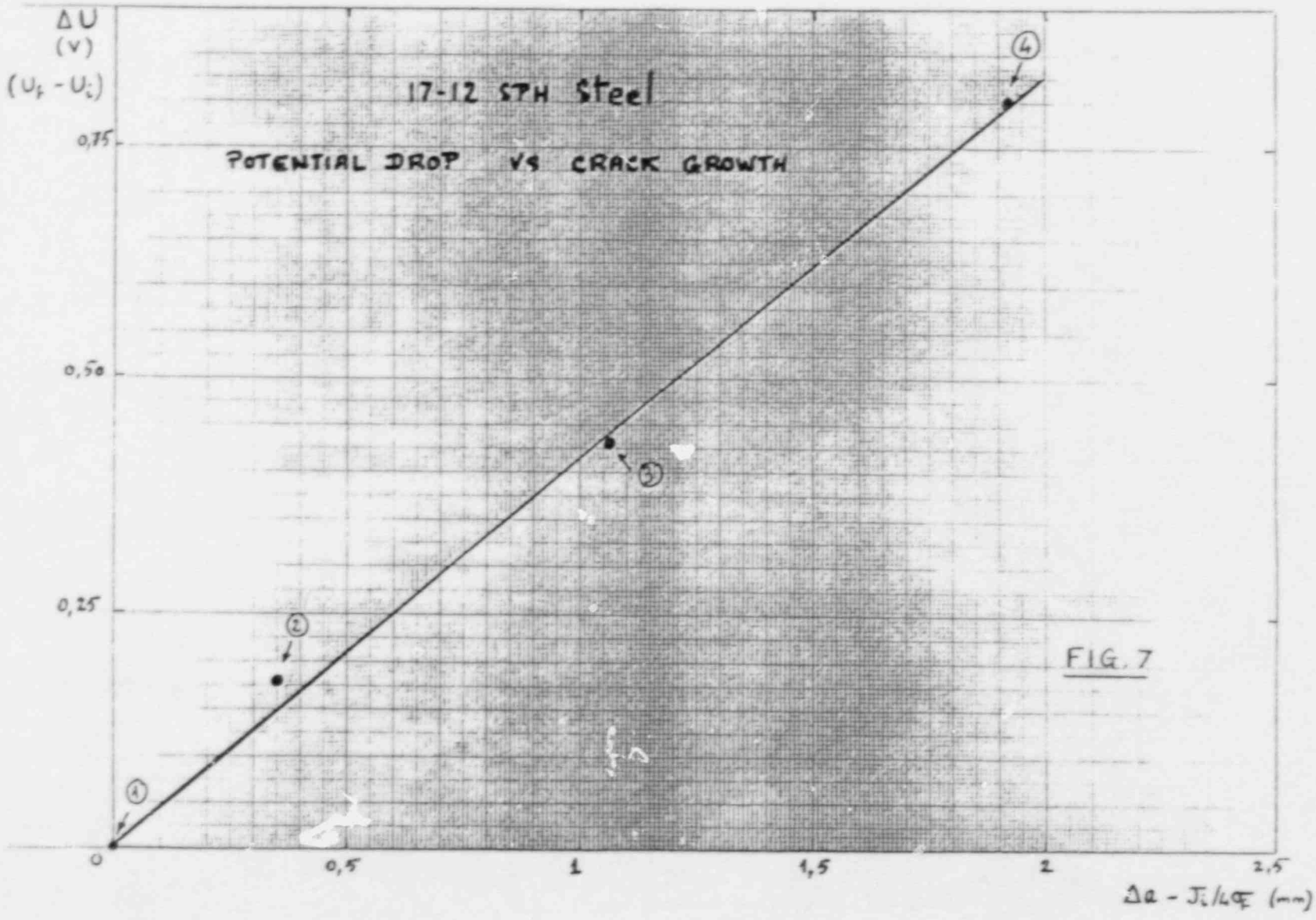
ΔU
(V)
(U_i - U_i)
17-12 STH Steel
POTENTIAL DROP VS CRACK GROWTH
0,75
0,50
0,25
0
0,5
1
1,5
2
2,5
Δa - J_i/2σ_f (mm)
1
2
3
4

FIG. 7

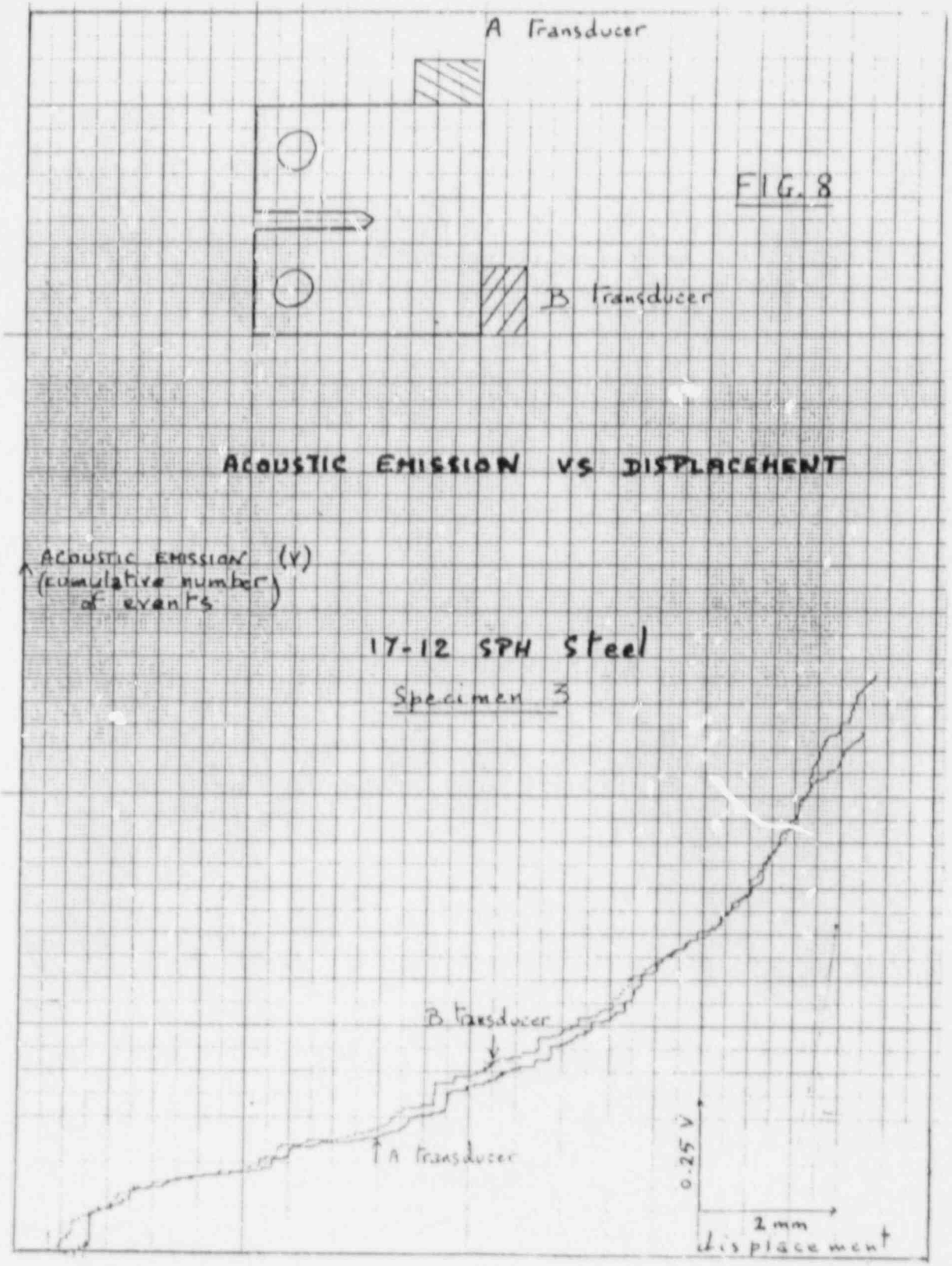
A Transducer
B Transducer
FIG. 8
ACOUSTIC EMISSION VS DISPLACEMENT
ACOUSTIC EMISSION (V)
(cumulative number of events)
17-12 SPH Steel
Specimen 3
B Transducer
A Transducer
0.25 V
2 mm
displacement

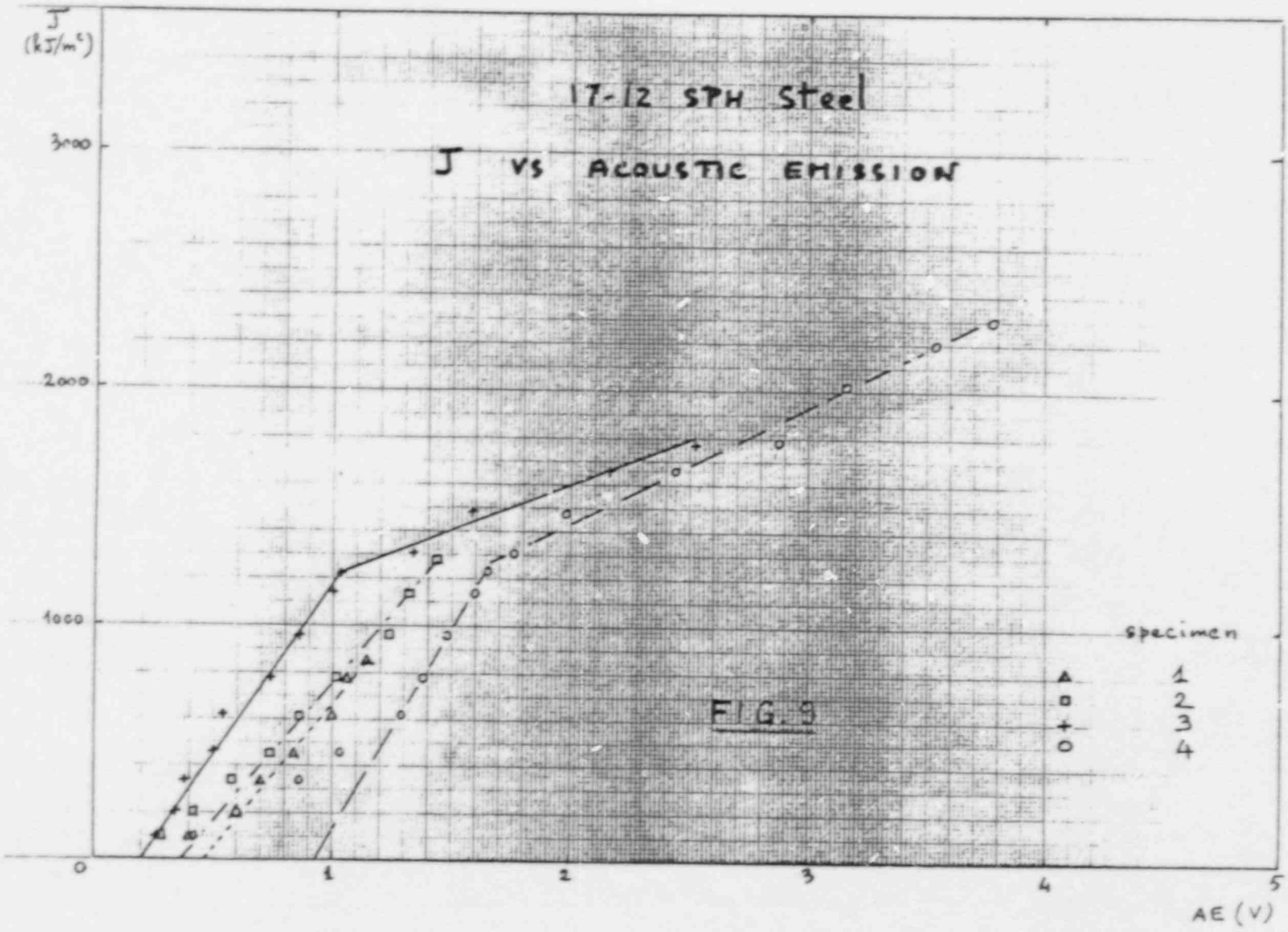
J (kJ/m²)
17-12 SPH Steel
J VS ACOUSTIC EMISSION
3000
2000
1000
0
1
2
3
4
5
AE (V)
specimen
1
2
3
4

FIG. 9

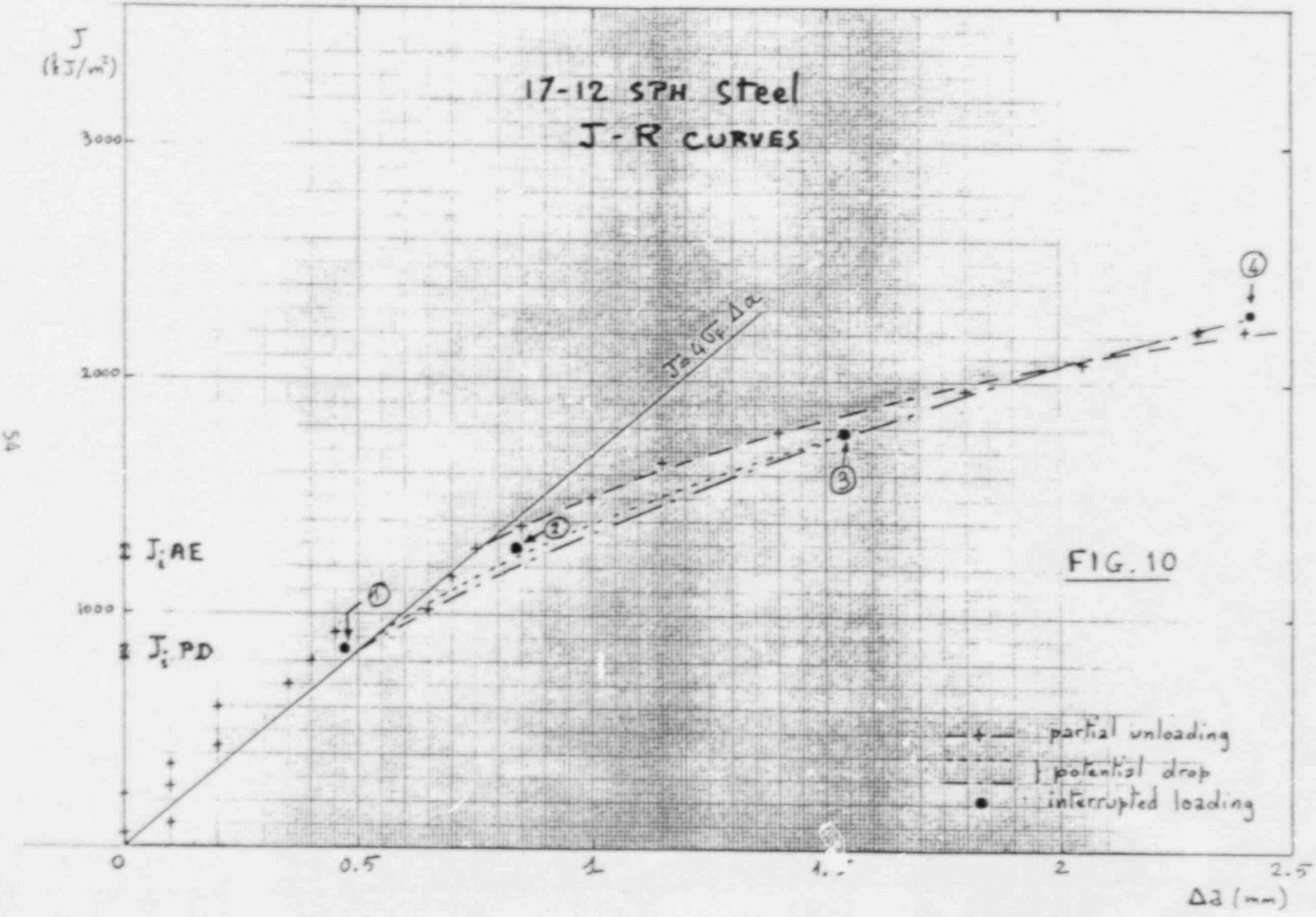
17-12 SPH Steel
J - R CURVES
J (kJ/m²)
3000
2000
1000
0
0.5
1
2
2.5
Δa (mm)
J = 4 σF Δa
J_i AE
J_i PD
partial unloading
potential drop
interrupted loading
1
2
3
4

FIG. 10

USE OF THE DIRECT CURRENT POTENTIAL DROP TECHNIQUE FOR DETERMINING J-R CURVES IN PWR WATER CONDITIONS

G. P. GIBSON

AERE HARWELL, OXON, U. K.

ABSTRACT

An investigation of the DC potential drop technique to determine the amount of crack extension occurring during ductile fracture toughness testing has been carried out. The results show that many factors affect the measured potential drop during loading of a test specimen, although a procedure has been developed to determine the change in potential drop due only to crack extension, which forms the basis of a single specimen method for J-R curve determination. Tests have been carried out on a ASTM A508 class3 material at 288°C, both in air and PWR water conditions, over a range of loading rates($5x10^{-1}$-$5x10^{-4}$mm/minute). The potential drop technique could predict accurately(ie within 10%) the final crack extension in all cases except for tests carried out in PWR water conditions at a loading rate of $5x10^{-4}$mm/minute. The J-R curves determined in air and PWR water conditions were similar and are little affected by loading rate over the range $5x10^{-1}$-$5x10^{-3}$mm/minute, although the J-R curve is higher at a loading rate of $5x10^{-4}$mm/minute.

INTRODUCTION

This report summarises an investigation into the factors which affect the measured potential drop(P.D.), arising from a direct current, during loading of a fracture toughness test specimen; together with the procedure which has been developed to determine the amount of crack extension occurring during the test from the measured P.D.. In addition, the use of the P.D. technique for crack length measurements for tests carried out at 288°C, both in air and PWR water conditions, at various loading rates($5x10^{-1}$ - $5x10^{-4}$mm/minute) is described.

EXPERIMENTAL PROCEDURE

The investigation into the factors which affect the measured P.D. was carried out using compact specimens, manufactured from a plate of a C-Mn steel, BS4360 43A, which were mainly 25mm thick and 50mm wide. The tests were carried out at room temperature at a loading rate of about 1mm/minute.

The procedure used to measure the P.D. across the specimen is briefly described below; further details can be found in reference 1. A constant current of between 25-50 amps, depending on specimen size, is passed through the specimen via electrical leads which are attached either to the front face of the specimen, configuration A, or to the top and bottom surfaces of the specimen, configuration B, see figure 1. The P.D. across the crack mouth is backed off by a known potential and the residual is amplified and recorded on a chart recorder, see figure 2. The load and load-line dislacement are also recorded, from which the J integral is determined according to ASTM E813-81(Ref. 2).

The material used in the rest of the study was an ASTM A508 class3 pressure vessel material from which compact specimens 50mm thick, 100mm wide with 25% sidegrooving were manufactured. The tests were carried out at a temperature of 288±2°C and either in air at a loading rate of $5x10^{-1}$, $5x10^{-2}$, $5x10^{-3}$and $5x10^{-4}$mm/min or in PWR water conditions at a loading rate of $5x10^{-2}$, $5x10^{-3}$and $5x10^{-4}$ mm/min. To take into account possible changes in temperature and current during the test, the current was also passed through a reference specimen, placed close to the specimen being tested and the resulting P.D. was also recorded, except at the loading rate of

5×10^{-1}mm/min when these changes were thought to be negligible.

FACTORS AFFECTING MEASURED P.D.

It was found with current lead configuration A, that there is an increase in P.D. during unloading of the specimen after the test. Figure 3 shows the P.D. and load traces for a 13mm thick 100mm wide specimen for which the increase in P.D. is about 30μV. This increase in P.D. would appear to be a result of current passing through the loading pins when the specimen is loaded. This is illustrated schematically in figure 4 which shows that when the pins form a good electrical contact with the specimen, as a result of loading the specimen, the current can reduce its path length by passing through the pins. Thus when the specimen is unloaded, this "pin effect" results in an increase in P.D., whereas the opposite occurs when the specimen is loaded. It is found by placing an electrically insulating sleeve around each pin that this effect no longer occurs. The P.D. trace obtained during loading can be corrected for this "pin effect" by using the P.D. trace obtained during unloading, as described in reference 1.

Figure 5 shows the P.D. trace, corrected for "pin effect", for a fatigue pre-cracked specimen. This P.D. trace is very similar to that obtained using current lead configuration B, which does not exhibit a "pin effect" because with this configuration the main current paths do not pass around the loading holes. Figure 5 shows that there is an initial rapid increase in P.D. on loading. This does not occur on loading specimens containing notches instead of fatigue cracks, as shown in figure 6, which gives the P.D. trace obtained using current lead configuration A and with electrically insulating sleeves around the pins. A similar trace is obtained using current lead configuration B. This would suggest that the initial rapid increase in P.D. for the fatigue pre-cracked specimens is a result of opening the fatigue crack which had been held closed by fatigue induced crack tip plasticity.

At slightly higher loads there is a hump in the P.D. trace, although this is small for the fatigue pre-cracked specimen, see figures 5 and 6. This would appear to be a result of initial plastic deformation around the crack, for if the notched specimen is cycled a few times up to a load below the previous maximum, the hump in the P.D. trace disappears.

On further loading of either the fatigue pre-cracked or notched specimen, there is a progressive increase in the P.D., see figures 5 and 6. Part of this increase in P.D. for the fatigue pre-cracked specimen will be due to fibrous crack extension, although this is not the case for the notched specimen as no fibrous crack extension occurred in this case. The increase in the P.D. for the notched specimen could be due to opening or advancing of the notch tip by blunting, or remote plastic deformation occurring in the specimen. It would appear that about $\frac{2}{3}$ of the increase is due to opening of the notch tip as this is the factor by which the P.D. decreased when the specimen was compressed back to reobtain the original mouth opening displacement. The rest of the original increase in P.D. can be explained in terms of the advance in the notch tip, which suggests that the P.D. is not affected significantly by remote plastic deformation.

Figure 7 gives a plot of residual P.D. versus J integral for the notched specimen, which shows at higher J values(ie above 0.05MN/M) that the increase in P.D., which arises from notch tip opening and advance due to blunting, is linearly dependent on J. Therefore, the onset of fibrous crack growth can be detected by a deviation from linearity of the P.D. versus J plot. Figure 8 shows a plot of residual P.D. versus J integral for a fatigue pre-cracked specimen, which indeed shows a departure from linearity at higher J values. There is good agreement between the J value at crack initiation(J_i) determined from figure 8 and that determined from stretch zone width(S.Z.W.) measurements taken from the fracture surface. However, it is worth noting that the degree of departure from linearity is not always marked, as in figure 8, which can result in a degree of uncertainty in determining J_i. The residual P.D. obtained by extrapolating the linear region of the P.D. versus J plot to zero J, for the notched specimen, is about zero. Therefore, the residual P.D. obtained in the same manner for the fatigue pre-cracked specimen can be equated approximately to the contribution arising from fatigue crack closure This contribution can be added to the back-off potential to give the P.D. appropriate to the initial crack length(V_o). The amount of crack advance at crack initiation(ie the S.Z.W. at crack initiation, S.Z.W.$_c$) can not be determined from the increase in P.D., above V_o, up to crack initiation, as a significant proportion of this increase is due to crack tip opening. Therefore, the S.Z.W.$_c$ has to be determined either from a J blunting line relationship or from measurements from the fracture surface. However, the increase in P.D. above that at crack initiation can be related directly to the increase in crack extension above the S.Z.W.$_c$, using a previously determined calibration plot of P.D. versus crack length. This is because it is not expected that there is any further increase in P.D. from crack tip opening after crack initiation, as the crack opening at the tip of the growing crack is known to be

independent of crack extension.

J-R TESTS IN AIR AND PWR WATER CONDITIONS

The tests in air and PWR water conditions were carried out using current lead configuration B, to avoid the need for correcting the P.D. traces for the "pin effect". At the test temperature of 288°C, there was a significant P.D., up to 20-30μV, prior to passing a current through the specimen, even when the voltage leads were made of pure iron instead of copper. This is a result of thermal induced emf's. However, the emf varied by less than 1-2μV per day and so it was viable to correct the measured P.D. when the current was passing, for the thermal induced emf's, from measurements taken when the current was off. These measurements were taken before and after the test for the shorter term tests or once a day for the longer term tests. Once the measured P.D. across the specimen and the reference specimen were corrected for thermal induced emf's, the P.D. across the specimen was multiplied by the fractional change in the P.D. across the reference specimen, to take into account slight changes in current and temperature during the test.

There was good agreement between the final crack extension determined from the P.D. traces and that measured from the fracture surfaces (ie within 10%), except for tests carried out at a loading rate of 5×10^{-4}mm/min in PWR water conditions. Under the latter conditions, it would appear that the P.D. increases during crack tip blunting but not after crack initiation, until the crack extension is above about 1.5mm when the P.D. increases again. The reason for this behaviour is not clear, although it may be due to the formation of corrosion products allowing the current to pass across the crack faces. As a result of this behaviour, the amount of crack extension occurring during the test could not be determined from the P.D. trace in these cases.

Figure 9 shows the J-R curves determined in air at the various loading rates, together with the two J-Δa points determined in PWR water conditions at a loading rate of 5×10^{-4}mm/min. There is little effect of loading rate on the J-R curve over the range 5×10^{-1}-5×10^{-3} mm/min, but the J-R curve is higher for the loading rate of 5×10^{-4} mm/min.

It can be seen from figure 9 that the two J-Δa points determined in

PWR water conditions fall very close to the J-R curve determined in air at the same loading rate. This would suggest that PWR water conditions does not enhance the crack growth rate above that determined in air. The same result is obtained at the faster loading rates, for as shown in figure 10 for a loading rate of $5x10^{-3}$mm/min and figure 11 for a loading rate of $5x10^{-2}$mm/min, the J-R curves obtained in air and in PWR water conditions are the same within experimental scatter.

CONCLUSIONS

It has been found that the following factors can alter the measured P.D. across the specimen:thermal induced emf's, fatigue crack closure, initial crack tip plasticity, crack tip opening and advance due to blunting and fibrous crack extension. In addition, with current lead configuration A, electrical conduction through the loading pins also affects the measured P.D..

A procedure has been suggested to determine the amount of crack extension occurring during the test from the P.D. trace.

The final crack extension was determined accurately(ie within 10%) from the P.D. trace for tests carried out at 288°C in air and PWR water conditions over a range of loading rates from $5x10^{-1}$ to $5x10^{-4}$ mm/min, except for tests carried out at the slowest loading rate in PWR water conditions. It has been suggested that the latter is a result of corrosion products allowing current to pass between the crack faces.

The J-R curves determined in air and PWR water conditions were similar for an ASTM A508 class3 material and little affected by loading rate over the range $5x10^{-1}$-$5x10^{-3}$mm/min, but the J-R curve determined at a loading rate of $5x10^{-4}$mm/min was higher.

ACKNOWLEDGMENTS

The author acknowledges the support of Dr S.G. Druce for useful discussions and Dr P.M. Scott, Mr A.E. Truswell and Mr J. Worth for experimental assistance.

REFERENCES

1. G. P. Gibson and S. G. Druce, "Development of the Direct Potential Drop Technique for Determining J-Crack Growth Resistance Curves," AERE Harwell Report AERE-R11443, Oxon, U. K, Sept. 1984.

2. ASTM, 'Standard Test for J_{1c}, A Measure of Fracture Toughness," Testing Standard E813-81.

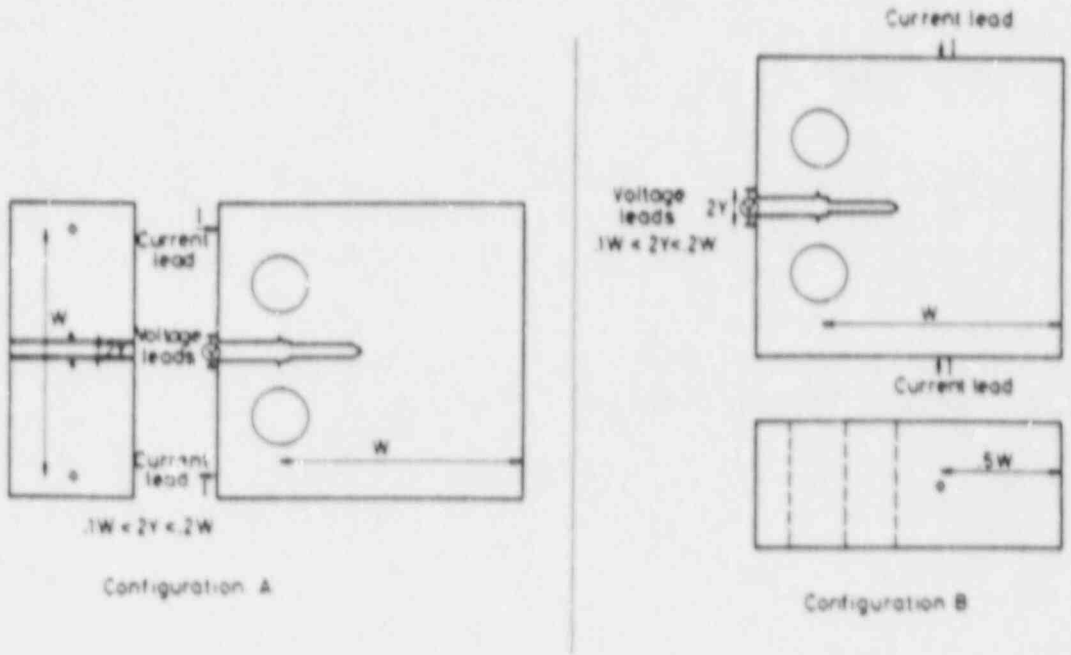

Figure 1 Potential and current lead positions for configurations A and B

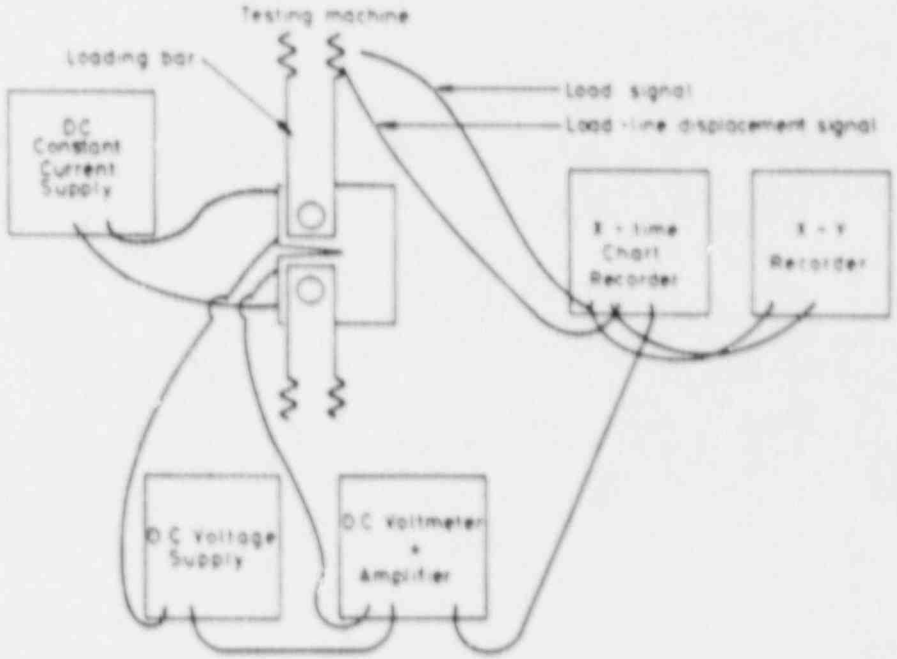

Figure 2 Schematic diagram of potential drop equipment

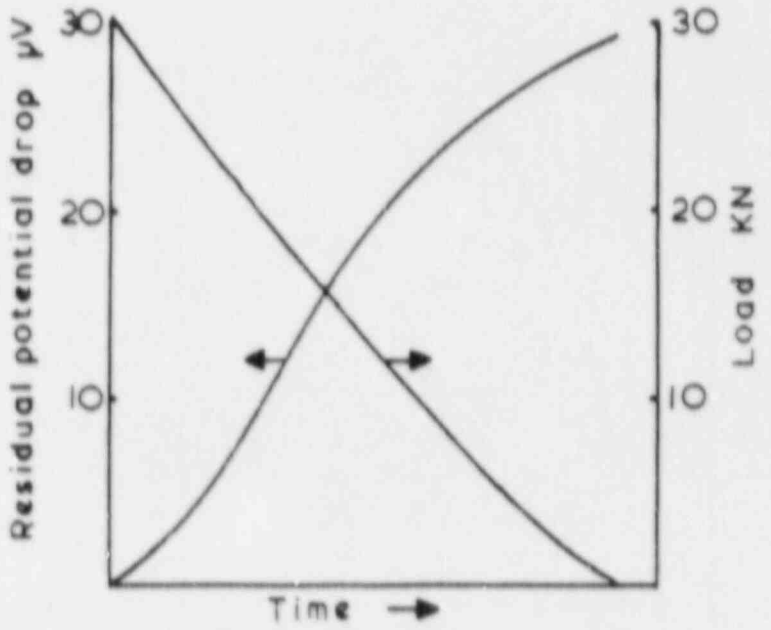

Figure 3 Residual P.D. and load versus time traces on unloading for a specimen, B=13mm, W=100mm

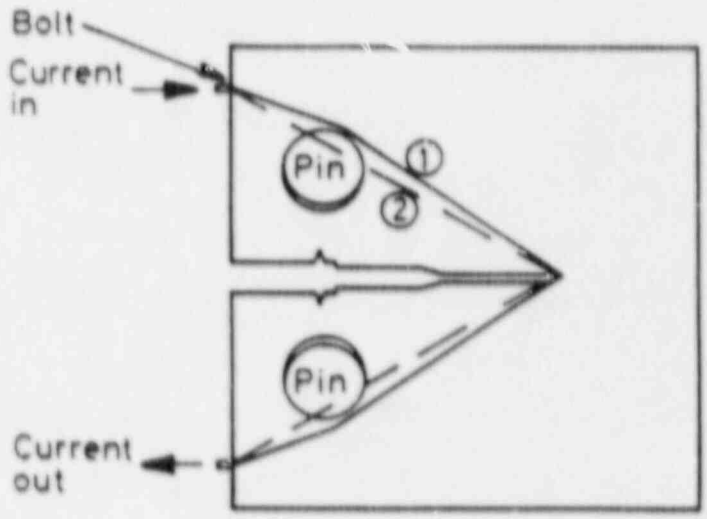

Figure 4 Illustration showing differing current paths before and during loading

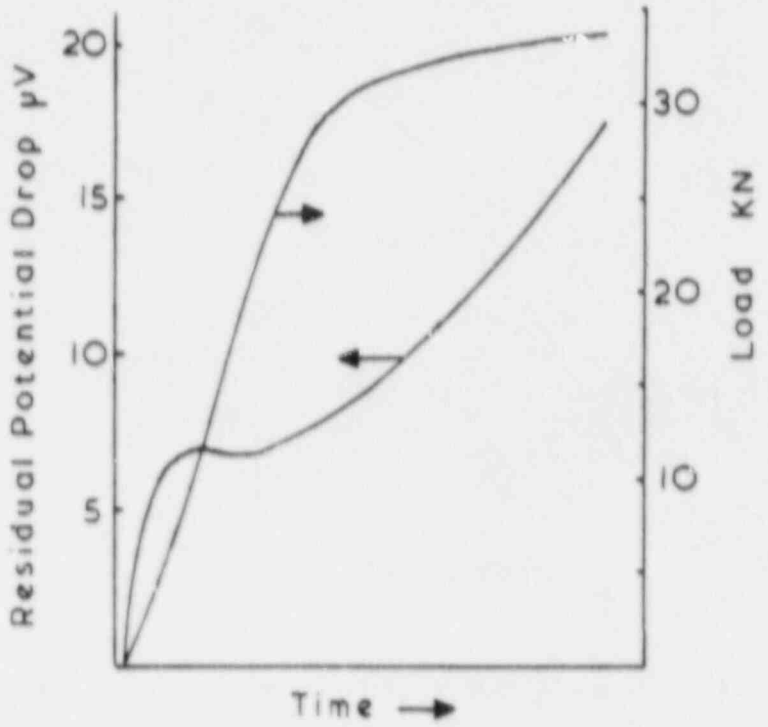

Figure 5 Residual P.D., after correction for pin effect and load versus time traces

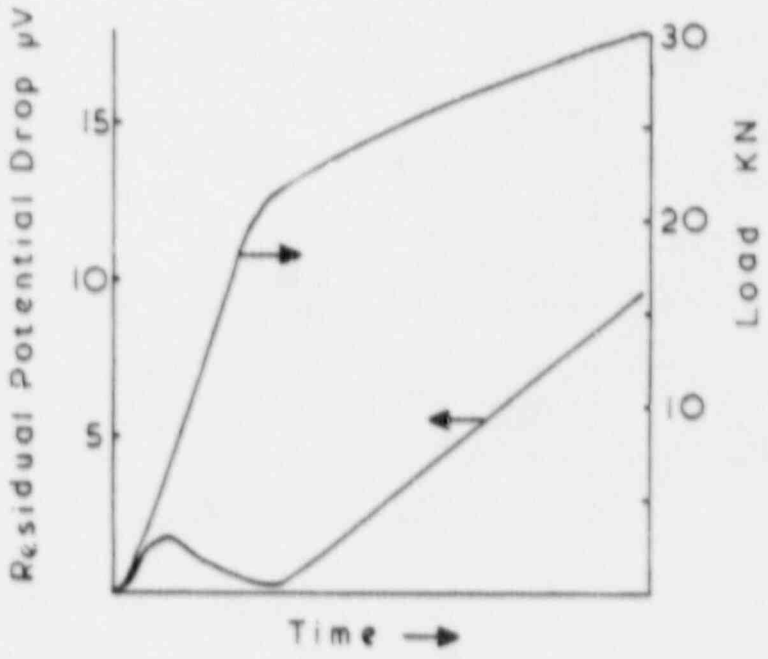

Figure 6 Residual P.D. and load versus time traces for specimen with insulating sleeves and spark cut slot

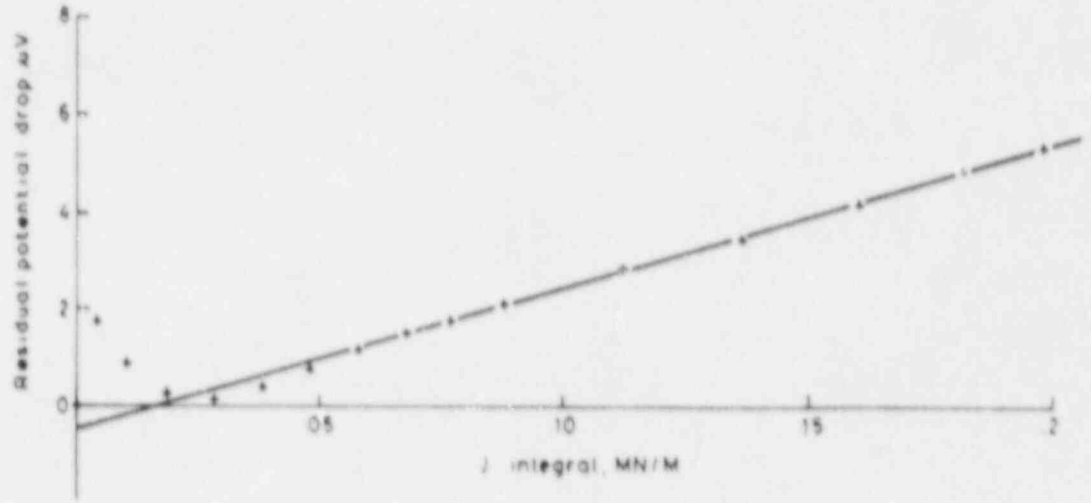

Figure 7 Residual P.D. versus J integral for specimen with insulating sleeves and spark cut slot

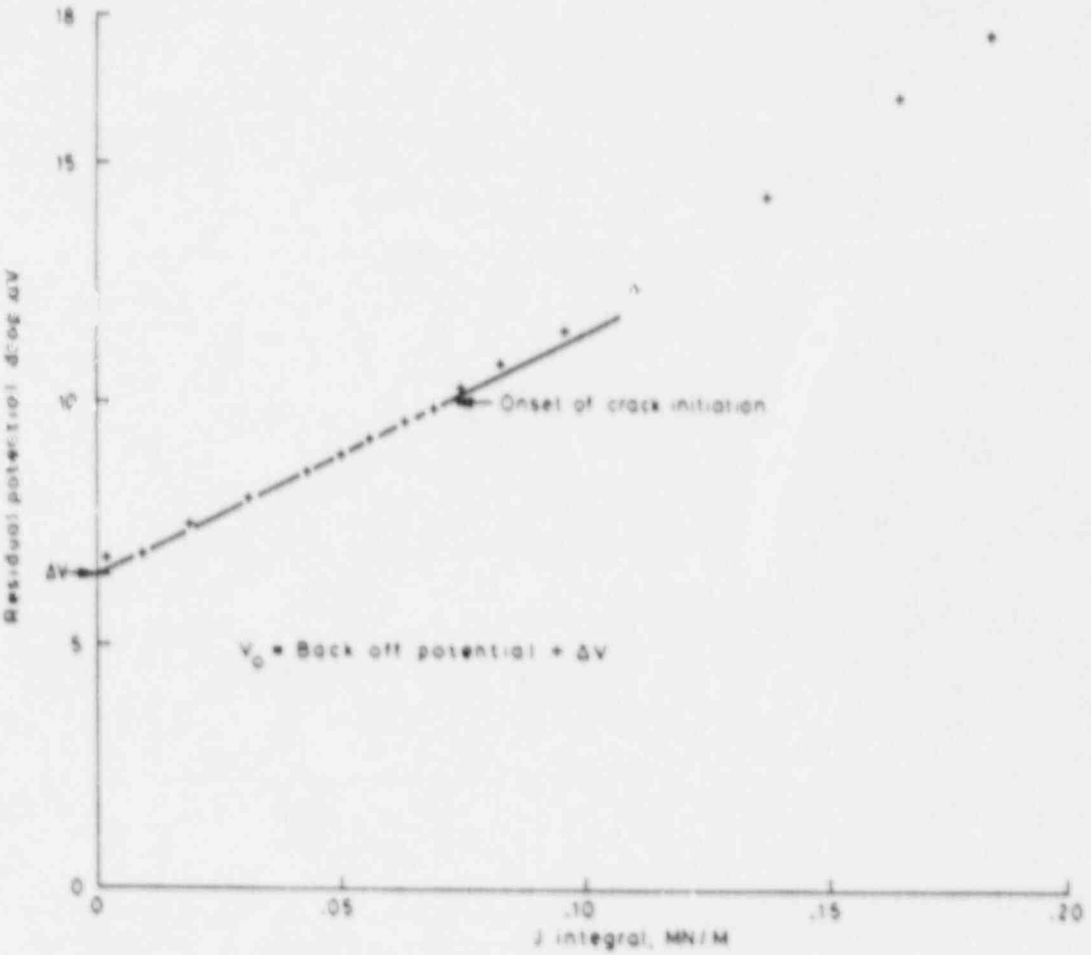

Figure 8 Residual P.D. versus J integral for fatigue pre-cracked specimen

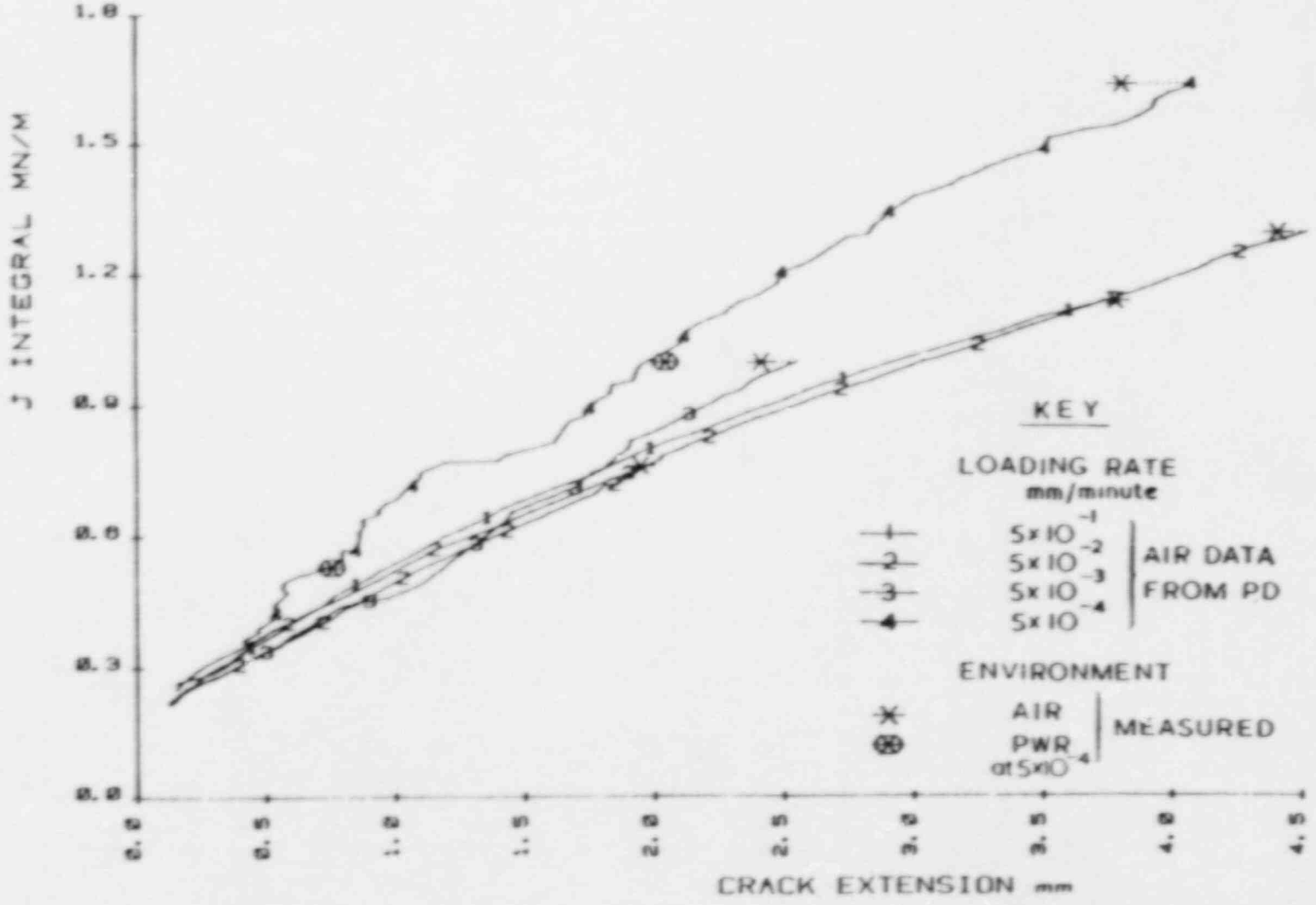

Figure 9 J-R curves determined in air at various loading rates

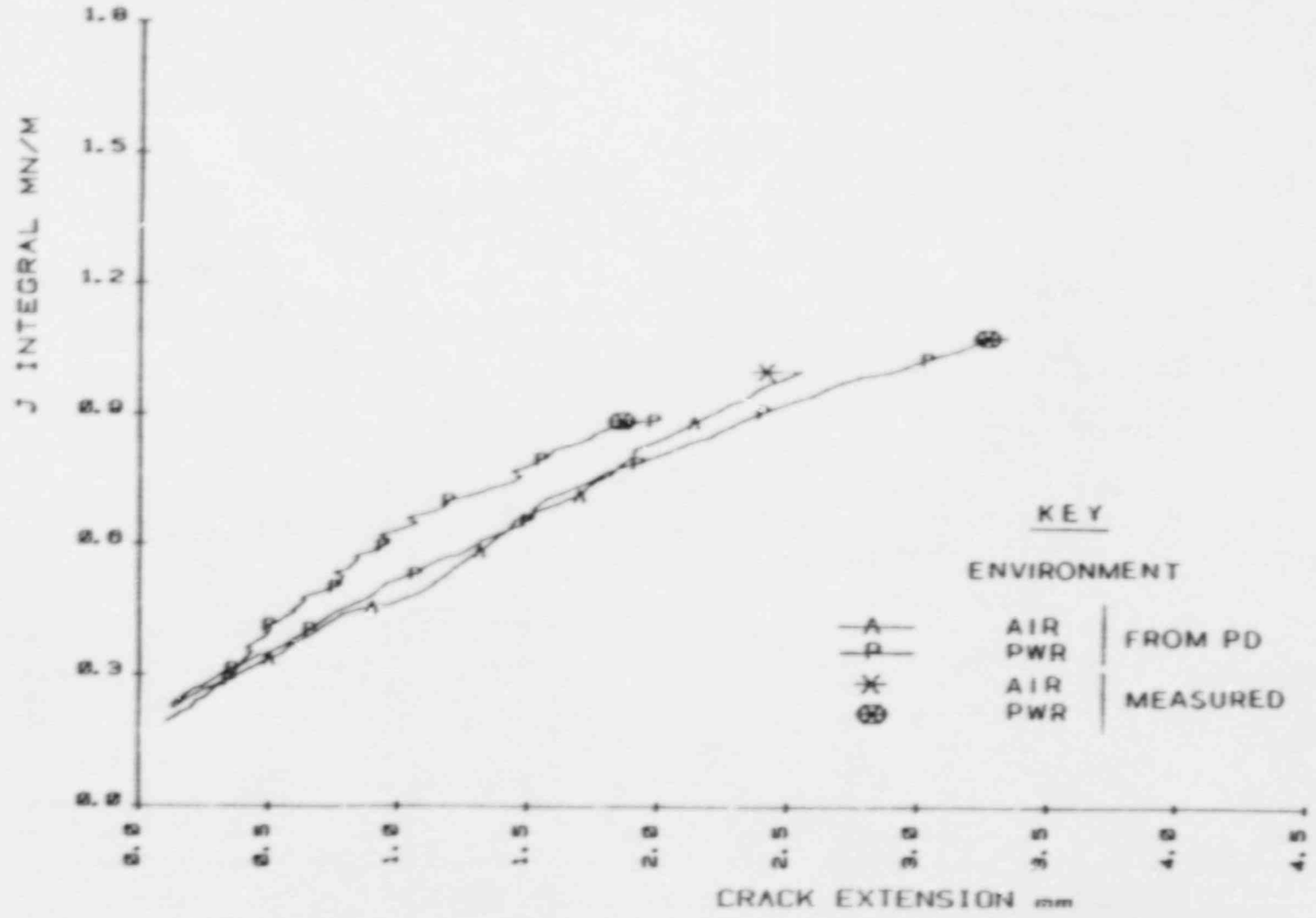

Figure 10 J-R curves obtained at a loading rate or of 5×10^{-3} mm/min

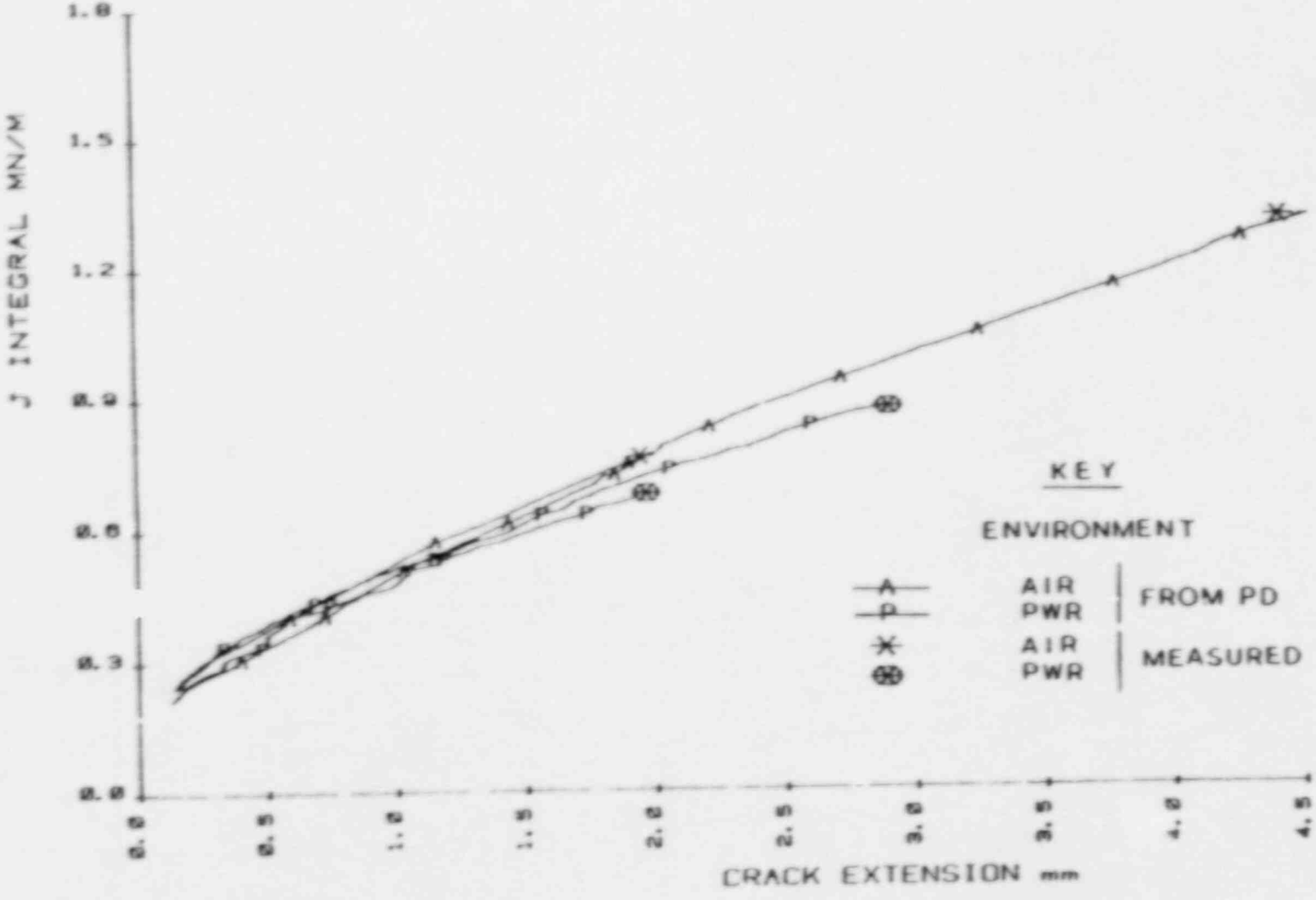

Figure 11 J-R curves obtained at a loading rate of 5×10^{-2} mm/min

DUCTILE FRACTURE MATERIAL CHARACTERIZATION WITH NOTCHED TENSILE SPECIMENS

G. ROUSSELIER[1], J.C. DEVAUX[2]

[1]Electricité de France (EDF), Département Etude des Matériaux,
Les Renardières, 77250 Moret-sur-Loing, France
[2]Framatome, Service Calcul de la Division des Fabrications,
Usine de Chalon-sur-Saône, 71380 Saint-Marcel, France

INTRODUCTION

Ductile fracture test methods aim at :
- fracture initiation determination,
- stable crack growth measurements.

This information is not available from usual load and displacement measurements on precracked specimens. That is why either specimen-consuming or sophisticated methods were developed : interrupted tests, potential drop, partial unloading, etc...

On the other hand, it has been emphasized for a long time (see for instance Reference 1) that both above-mentioned information is available from the load-displacement curve of the simple notched tension test, with no need of sophisticated experimental methods. A numerical analysis of the notched tensile specimen is required to infer the material characteristics from experimental data. Numerical analyses of this specimen, that were incomplete till one year ago, are now close to perfection. It makes the notched tension test a powerful method for ductile fracture material characterization.

THE NOTCHED TENSION TEST

Typical load-displacement curves of round notched specimens are shown in Figs 1 and 2. The notch radii of specimens type AE2, AE4 and AE10 are 2, 4 and 10 mm respectively ; the initial minimum diameter is 10 mm.

At point A (Fig. 1) there is a marked change in the slope of the load-displacement curve. This point coincides with the initiation of a crack in the center of the specimen ; this was demonstrated with interrupted tests before and after point A (Ref. 1) ; the central crack in a 2% Cr 1% Ni steel AE5 specimen is shown in Fig. 3. The slope of the post-initiation curve is related to the ductile tearing resistance of the material. The relation between the crack surface and the diametral contraction is linear, with a precision better than 3% for a crack radius up to 3 mm ; this relation can be calibrated with one interrupted test.

In conclusion, the load-displacement curve of a single notched tensile specimen provides all the information for ductile fracture material characterization.

MATERIAL CHARACTERIZATION

According to Mudry (Ref. 3), values of J_{IC} and dJ/da can be deduced directly from the notched tension test (see for instance Reference 2). However it is more advisable to use this test in a new methodology for ductile fracture analysis, based on damage functions for the growth of voids (Ref. 1, 3 and 4).

In Reference 4, three material parameters are to be calibrated in the ductile fracture model :
- f_O, initial volume fraction of voids,
- ℓ, characteristic length related to spacing between inclusions or voids,
- σ_1, related to the strength of the matrix material.

In ferritic steels f_O is supposed to be equal to the volume fraction of MnS inclusions and can be deduced from the chemical composition of the steel : $f_O = 0.054\ (S\% - 0.001/Mn\%)$. The location of fracture initiation (point A of Fig. 1) depends on f_O and σ_1, but not on ℓ : it is the well-known fact that the ductility depends on the volume fraction of inclusions only (Ref. 5). So, σ_1 is calibrated from the location of point A (Fig. 4), and ℓ from the slope of the post-initiation curve (Fig. 5). Actually only one numerical analysis of the specimen is necessary, with estimated values of σ_1 and ℓ ; the definitive values of σ_1 and ℓ are deduced from this first analysis.

CONCLUSION

The notched tension test is a simple and powerful method for ductile fracture material characterization. It takes place in a new methodology for ductile fracture analysis.

REFERENCES

1. G. Rousselier, «An experimental and analytical study of ductile fracture and stable crack growth», Specialist meeting on elastic-plastic fracture mechanics, Daresbury, 22-24 May 1978, OECD-NEA-CNSI report 32, vol. 2, paper n° 14.

2. P. Petrequin, M.Al Mundheri and P. Soulat, «Elasto-plastic toughness of pressure vessel steels : effect of irradiation, determination from tests on round notched specimens», IAEA Specialist meeting on radiation embrittlement and surveillance of reactor pressure vessel steels, Vienna, 8-10 October 1984.

3. F. Mudry, «Etude de la rupture ductile et de la rupture par clivage d'aciers faiblement alliés», thèse d'État, Université de Technologie de Compiègne, March 1982.

4. G. Rousselier, J.C. Devaux, G. Mottet, «Ductile fracture initiation and crack growth in tensile specimens : application of continuum damage mechanics», Proceedings 8th Int. Conf. on Structural Mechanics in Reactor Technology, Brussels, Belgium, August 1985, paper G 3/5.

5. B.I. Edelson, W.M. Baldwin, «The effect of second phases on the mechanical properties of alloys», Trans. Am. Soc. Metals, vol. 55, 1962, p. 230.

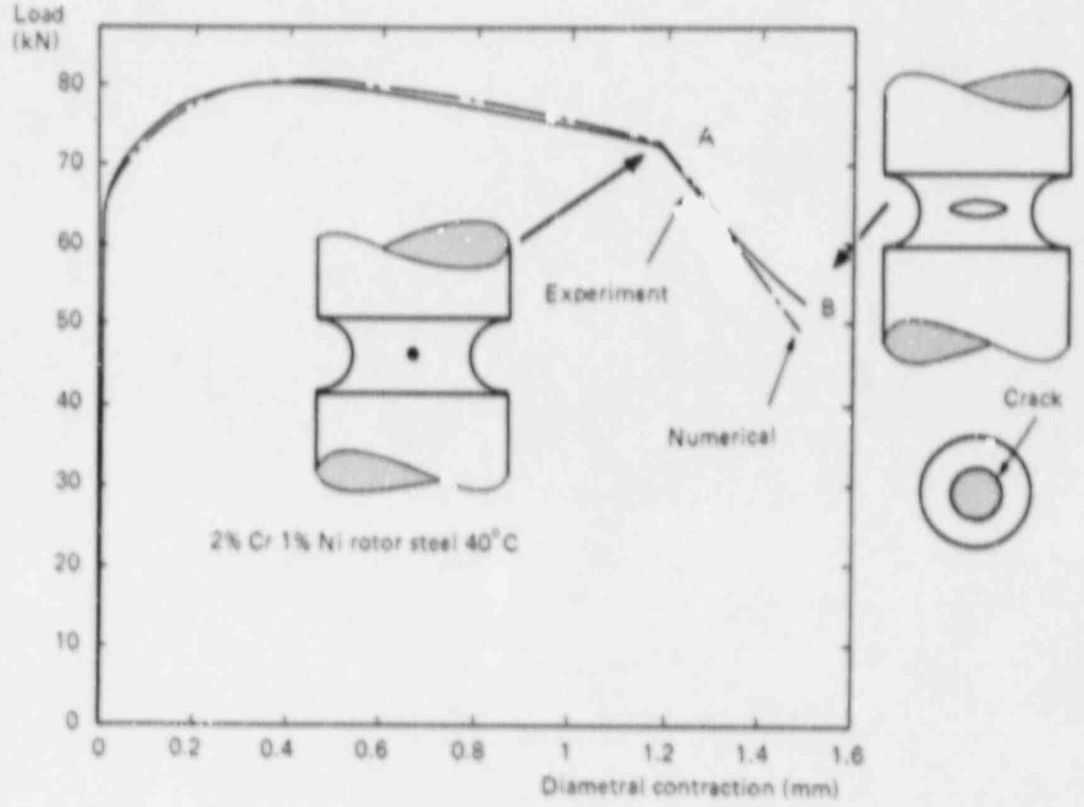

Fig. 1 – Load-contraction curve of a rotor steel specimen type AE5, Φ_0 = 10 m.m (Ref. 1).

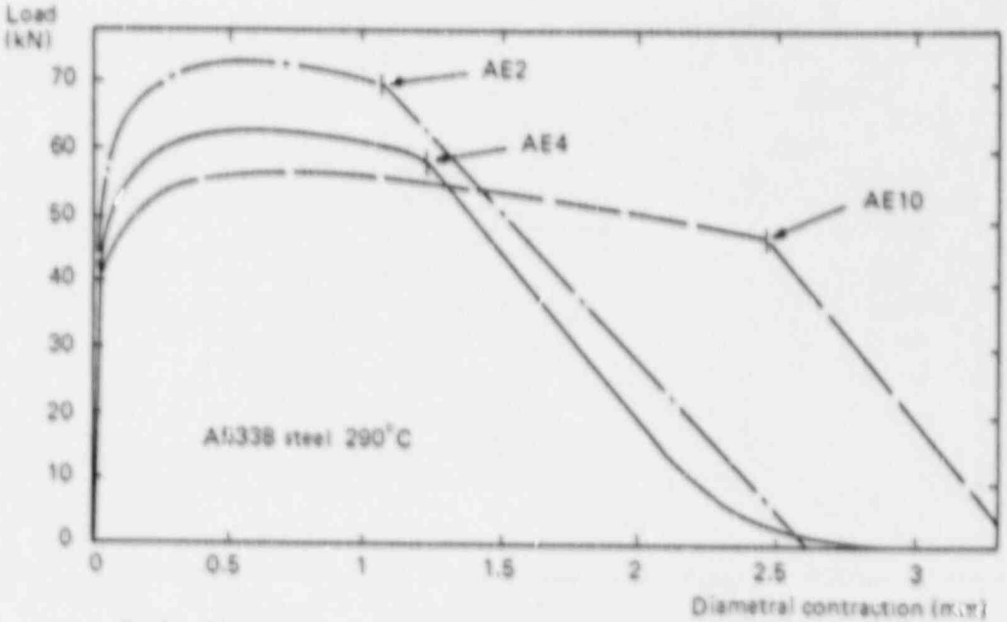

Fig.2 – Typical load-contraction curves on A533B steel at 290°C using specimens type AE2 - AE4 - AE10, Φ_0 = 10 mm (Ref. 2).

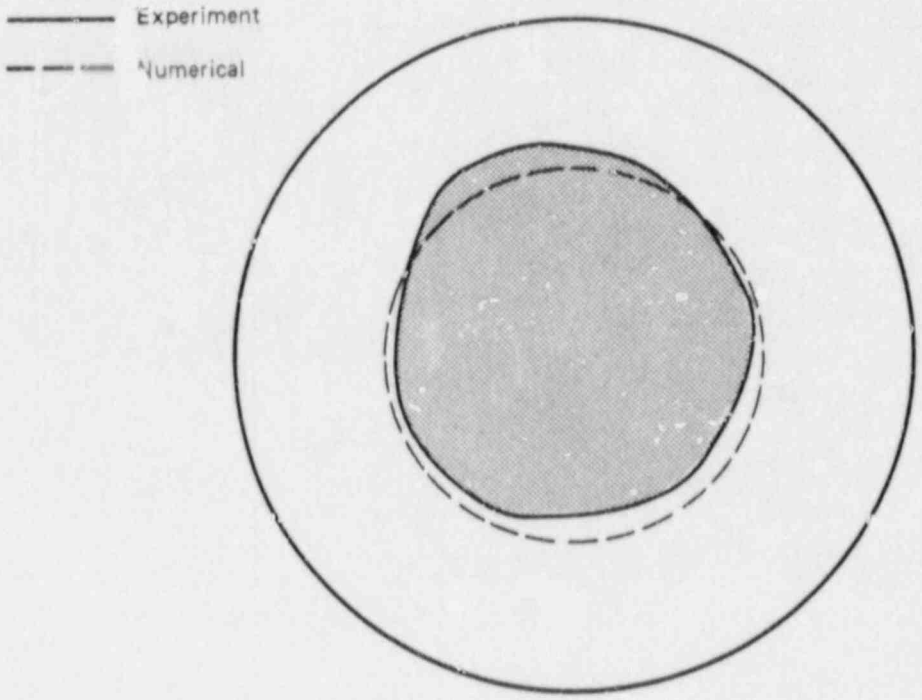

Fig. 3 – Central crack for the interrupted test at point B of Fig. 1.

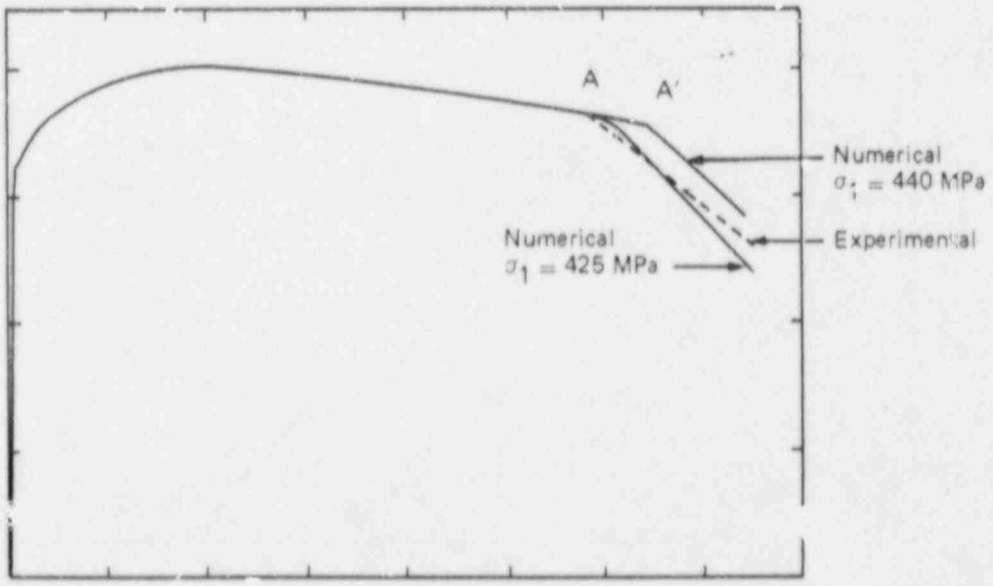

Fig. 4 – Calibration of the material parameter σ_1.

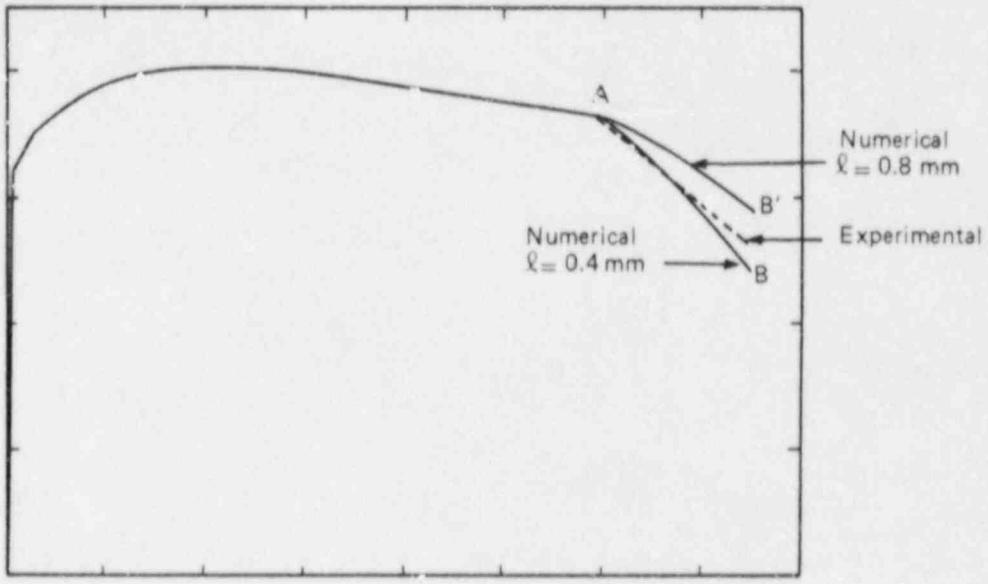

Fig. 5 – Calibration of the material parameter ℓ (with $\sigma_1 = 425$ MPa).

SESSION 2 (Part 2): New and Improved Test Methods

CHAIRMAN: P. Balladon
UNIREC, France

J-R CURVE TESTING BY THE POTENTIAL DROP- AND KEY CURVE METHODS

P.A.J.M. Steenkamp

Delft University of Technology
Laboratory for Thermal Power Engineering
P.O. Box 5055, 2600 GB Delft, The Netherlands

INTRODUCTION

This paper describes two methods for the continuous determination of the amount of stable crack extension during the testing of fracture mechanics specimens, viz. the (DC-) Potential Drop- and Key Curve methods. Single specimens J-R curves obtained by these methods are presented, together with a discussion on their accuracy.

Room temperature tests were performed on plane sided and 20% side grooved SENB- and CNT specimens (dimensions: figure 1) of ferritic steel St.52-3 (equivalent to BS 4360 Grade D), for which the material properties are given in figure 2.

The value for J, corrected for crack growth, is determined from the area under the load-load line displacement test record by (Ref. 1, 2, 3):

$$\text{SENB: } J = 2 \int_{o}^{\Delta} \frac{P}{b} \, d\Delta - \int_{a_o}^{a} \frac{J}{b} \, da \qquad (1)$$

$$\text{CNT: } J = G + 2 \int_{o}^{\Delta_p} \frac{P}{b} \, d\Delta_p - \frac{P\Delta_p}{b} - \int_{a_o}^{a} \frac{J-G}{b} \, da \qquad (2)$$

with Δ_p, P and G as the plastic component of the load line displacement Δ, the load per unit (net-) thickness and per crack tip, and the linear elastic energy release rate, respectively.

A modified definition of J, J_M, was proposed by Ernst (Ref. 4), based on earlier studies by Rice et al. (Ref. 5):

$$J_M = J - \int_{a_o}^{a} \left(\frac{\partial (J-G)}{\partial a}\right)_{\Delta_p} da \qquad (3)$$

which should theoretically yield more consistent J-R curve behaviour. Hence J_M-curves were also determined for the specimens tested.

TEST METHODS

Before presenting actual test results, a brief description of the single specimen test methods, and in particular, the Key Curve method, will be given:

* The DC potential drop method. A crack in a specimen will act as an additional resistance to an electric current flowing through the specimen, resulting in a potential drop over the crack. Needed is a calibration curve relating the potential drop to the crack length, which can be obtained experimentally, numerically or analytically. The present study used the analytical calibration relation by Johnson (Ref. 6).

* The Key Curve method, proposed by Ernst & Paris (Ref. 2). The method is based on the possibility to normalize the load-load line displacement curves of two-dimensional cracked bodies, which permits the determination of Δa at each point of the P-Δ record of a cracking specimen from the P-Δ curve of a geometrically identical specimen with a constant crack length. Such a P-Δ curve can be obtained in three ways:

  - experimentally, by testing subsized and/or blunt notched specimens where crack growth will only initiate at large displacements (Δ) relative to specimen dimensions (W or b),
  - numerically, by finite element computations,
  - numerically, by using the EPRI Elastic-Plastic Handbook solutions (Ref. 7). This handbook contains the tabulated results of finite element computations for a material obeying the Ramberg-Osgood stress-strain law:

$$\frac{\varepsilon}{\varepsilon_o} = \frac{\sigma}{\sigma_o} + \alpha \left(\frac{\sigma}{\sigma_o}\right)^n \qquad (4)$$

  where σ_o and $\varepsilon_o = \sigma_o/E$ are a reference stress and -strain, respectively.

It was demonstrated by Ernst et al. (Ref. 3) for bend specimens and subsequently by Steenkamp (Ref. 1) for tensile specimens that the amount of crack extension Δa can be obtained from the experimental P-Δ record of the cracking specimen by summation of the crack growth increments da, given by:

$$\text{SENB:}\quad da = \frac{b}{2W}\left(\frac{H'}{H} - \frac{W}{P}\frac{dP}{d\Delta}\right) d\Delta \qquad (5)$$

$$\text{CNT:}\quad da = \frac{\frac{F'}{F} - \frac{b}{P}\frac{dP}{d\Delta_p}}{1 - \frac{\Delta_p}{b}\frac{F'}{F}} d\Delta_p \qquad (6)$$

with P, dP, dΔ (or Δ_p and $d\Delta_p$) taken from the actual test record, while the Key Curve functions H'/H and F'/F follow from the (experimentally or numerically obtained) P-Δ record with constant crack length according to:

$$\text{SENB:}\quad \frac{H'}{H} = \frac{H'}{H}\left(\frac{\Delta}{W}\right) = \frac{W}{P}\left(\frac{\partial P}{\partial \Delta}\right)_a \tag{7}$$

$$\text{CNT:}\quad \frac{F'}{F} = \frac{F'}{F}\left(\frac{\Delta_p}{b}\right) = \frac{b}{P}\left(\frac{\partial P}{\partial \Delta_p}\right)_a \tag{8}$$

As an example for SENB specimens of St.52-3, Key Curve functions H'/H as determined in the aforementioned three manners are given in figure 3. The differences between the curves for low Δ-values are caused by the yield plateau in the material's stress-strain curve, figure 2. For each of the SENB and CNT specimens, four J-R curves could thus be derived, viz. one from potential drop measurements and three from the Key Curve concept (using finite element, EPRI and experimental Key Curve functions).

During testing the crack fronts were marked 3 times with dye peretrants (Ref. 8), thus yielding a large number of actual crack extensions against which the accuracy of the various predictions for Δa could be determined; while these beach marks also showed the development of the crack front shape during the testing.

RESULTS

In figure 4, some examples are given of dye penetrant beach marks made during the testing of the specimens. Noteworthy are the longitudinal tears (delaminations) that occurred in this material. The loss of plane strain constraint due to their occurrence is demonstrated by the increasing amount of "double-tunneling" in these specimens as well as by the small shear lips that developed adjacent to the delaminations.

In figure 5, a-d, a comparison is made between the optically measured beach marks and the predicted crack extensions. It is seen that:

* the Key Curve method generally predicted the actual Δa within ± 10%,

* the use of an EPRI Key Curve yielded inaccurate predictions for low values of Δa, which can be explained by the unability of the Ramberg-Osgood power law function, equation (4), to accurately fit the initial part of a stress strain curve exhibiting a yield plateau, figure 2,

* the Potential Drop underestimates the actual Δa by an average of 15%, which is attributed to crack front tunneling and the occurrence of the delaminations in the material.

Due to the differences in predicted Δa, the 4 J-R curves (that can be determined for each specimen tested) will differ as well, as shown in figure 6 for a plane sided and a side grooved SENB specimen. It can be seen that the potential drop J-R curves are to the left of the other curves, while the EPRI J-R curves are shifted to the right for low values of Δa. Both trends are in accordance with the observations stated above with respect to figure 5.

Single specimen J-R curves will be influenced by two main sources of scatter, viz. scatter due to variations in material properties and scatter due to the method employed to determine Δa. In order to separate these two sources, the J-R curves from either the plane sided or the side grooved specimens as obtained by one of the four methods were fitted with a regression function so as to obtain a mean J-R curve with corresponding confidence limits. As an example, J-R curves as obtained from SENB specimens by means of the Key Curve method, using an experimental Key Curve function, are shown in figure 7, while the best-fit mean curve with 90% confidence limits for the plane sided specimens is given in figure 8. The fracture toughness data were found to be best fitted by a power law function (cf. Ref. 9) added by a 4th degree polynomial.

The mean J-R curves for the four methods of Δa-prediction are shown in figure 9. (The 90% confidence limits, which were of comparable size for each method, are omitted for the sake of clarity). The differences between the curves in figure 9 can thus be attributed to the differences in the methods used to determine Δa, while the size of a 90% confidence interval around these regression curves (figure 8) displays the degree of scatter in specimen-to-specimen fracture toughness. It can thus be concluded from figures 8 and 9 that for the material investigated, differences between J-R curves obtained by using an experimental or finite element Key Curve are well within the material scatter. On the other hand, the deviations of using an EPRI Key Curve or the Potential Drop method seem too large to be obscured by the scatter in the material properties.

Trends as described above for SENB specimens were also observed for the CNT specimens tested, (Ref. 1). In figure 10, results for SENB and CNT specimens are compared. Together with figure 7, it confirms two widely noted aspects of geometry dependence in J-R curve testing:

* due to lower constraint at the crack tip, tensile geometries (such as CNT specimens) exhibit significantly higher resistance to crack growth than bending geometries (such as SENB specimens). The discrepancy increases with crack growth (cf. e.g. Ref. 10);

* side grooving significantly lowers the J-R curve by preventing the formation of shear lips at the outer surfaces of the specimen.

The computation of J_M for the J-R curves in figure 10 by equation (3) yields figure 11, and it is seen that the J_M-curves for tensile and bending loads are much closer than in figure 10. Although the use of J_M

thus seems attractive, further investigations are obviously needed to establish its viability for fracture safety assessment purpose.

SUMMARY AND CONCLUSIONS

In this paper, the results of single specimen J-R curve tests performed on SENB and CNT specimens, using the DC Potential Drop and Key Curve methods, were presented. A discussion was given on the accuracy of the thus obtained J-R curves, and a comparison was made between the results for the different geometries.

Based on the results presented above, the following conclusions may be drawn:

* For SENB and CNT specimens made of St.52-3, accurate single specimen J-R curves were obtained by the Key Curve method, using experimental and finite element Key Curve functions.

* Less accurate results were obtained by the DC Potential Drop method and by using an EPRI Key Curve.

* Dye penetrants were successfully used to mark the crack front at several stages during the testing.

* The geometry dependence of the J-R curve (bend vs. tension) remains of concern. Application of the modified J definition dramatically reduced this dependence for the material and specimen dimensions investigated.

REFERENCES

1. P.A.J.M. Steenkamp, Stable Crack Growth and Instability. Delft University of Technology, Laboratory for Thermal Power Engineering, Final report BROS II project, subprogram 6, 1985.

2. H.A. Ernst and P.C. Paris, Techniques of Analysis of Load-Displacement Records by J-Integral Methods. NUREG/CR-1222, 1980.

3. H.A. Ernst, P.C. Paris and J.D. Landes, Estimations on J-Integral and Tearing Modulus T from a Single Specimen Test Record. ASTM-STP 743, pp. 476/502, 1981.

4. H.A. Ernst, Material Resistance and Instability Beyond J-Controlled Crack Growth. ASTM-STP 803, pp I-191/I-213, 1983.

5. J.R. Rice, W.J. Drugan and T.L. Sham, Elastic-Plastic Analysis of Growing Cracks. ASTM-STP 700, pp. 189/221, 1980.

6. H.H. Johnson, Calibration of the Electric Potential Method for Studying Slow Crack Growth. Materials Research and Standards, Vol. 5, pp. 442/445, 1965.

7. V. Kumar, M.D. German and C.F. Shih, An Engineering Approach for Elastic-Plastic Fracture Analysis. General Electric Company, Schenectady (NY), USA. EPRI report NP-1931, 1981.

8. P.A.J.M. Steenkamp and M. Hartevelt, Crack Front Marking by Dye Penetrants. Delft University of Technology, Laboratory for Thermal Power Engineering, report MMPP-232/BROS-84-28, 1984.

9. F.L. Loss, J-R Curve Characterization of Low Upper Shelf Welds. NRC Vessel and Piping Integrity Review, Oak Ridge, Tennessee, 1981.

10. S.J. Garwood, Geometry and Orientation Effects on Ductile Crack Growth Resistance. International Journal of Pressure Vessels and Piping, Vol. 10, pp. 297/319, 1982.

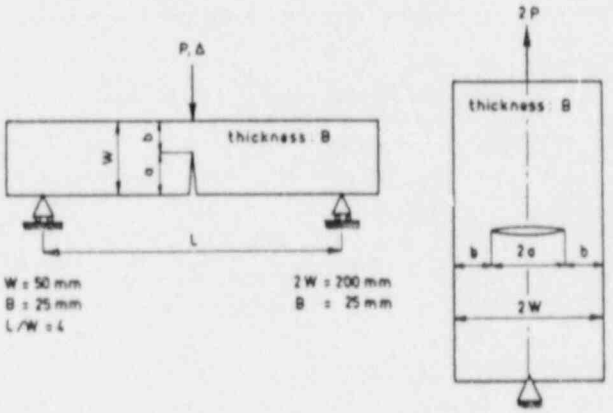

FIGURE 1.
SENB and CNT specimen dimensions. For all specimens, $a_o/W \approx 0.52$. Both plane sided and 20% side grooved specimens were tested.

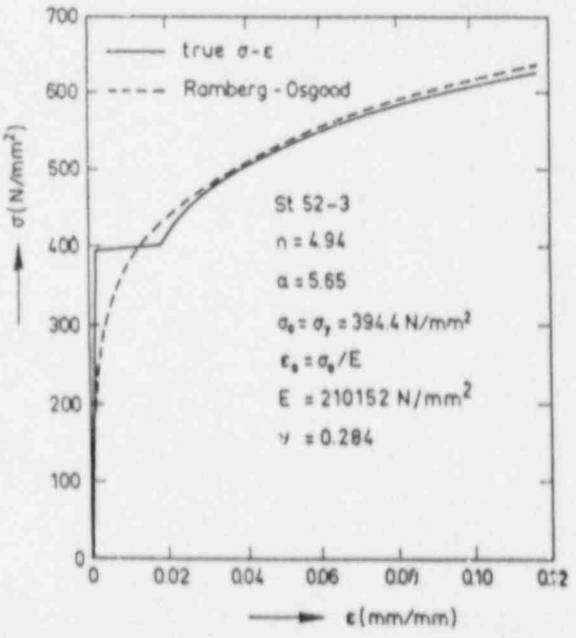

FIGURE 2.
True stress-strain curve for St.52-3, together with a Ramberg-Osgood fit.

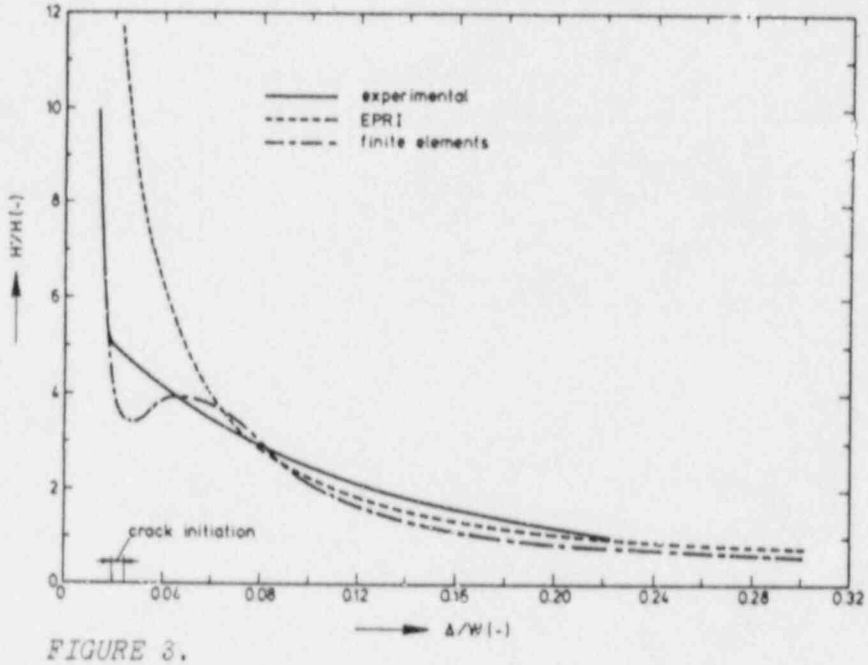

FIGURE 3.

Comparison of H'/H Key Curve functions for SENB specimens, obtained by three different methods.

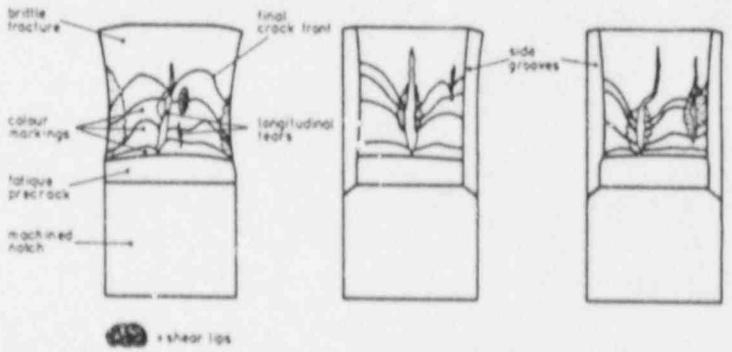

a. SENB

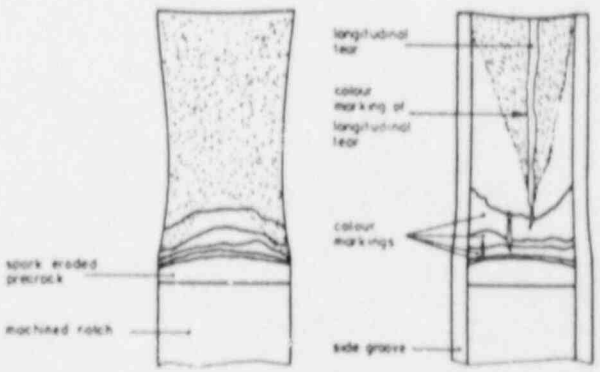

b. CNT

FIGURE 4.

Fracture surfaces of specimens after testing. Indicated are the dye penetrant markings and the extent of shear lip development.

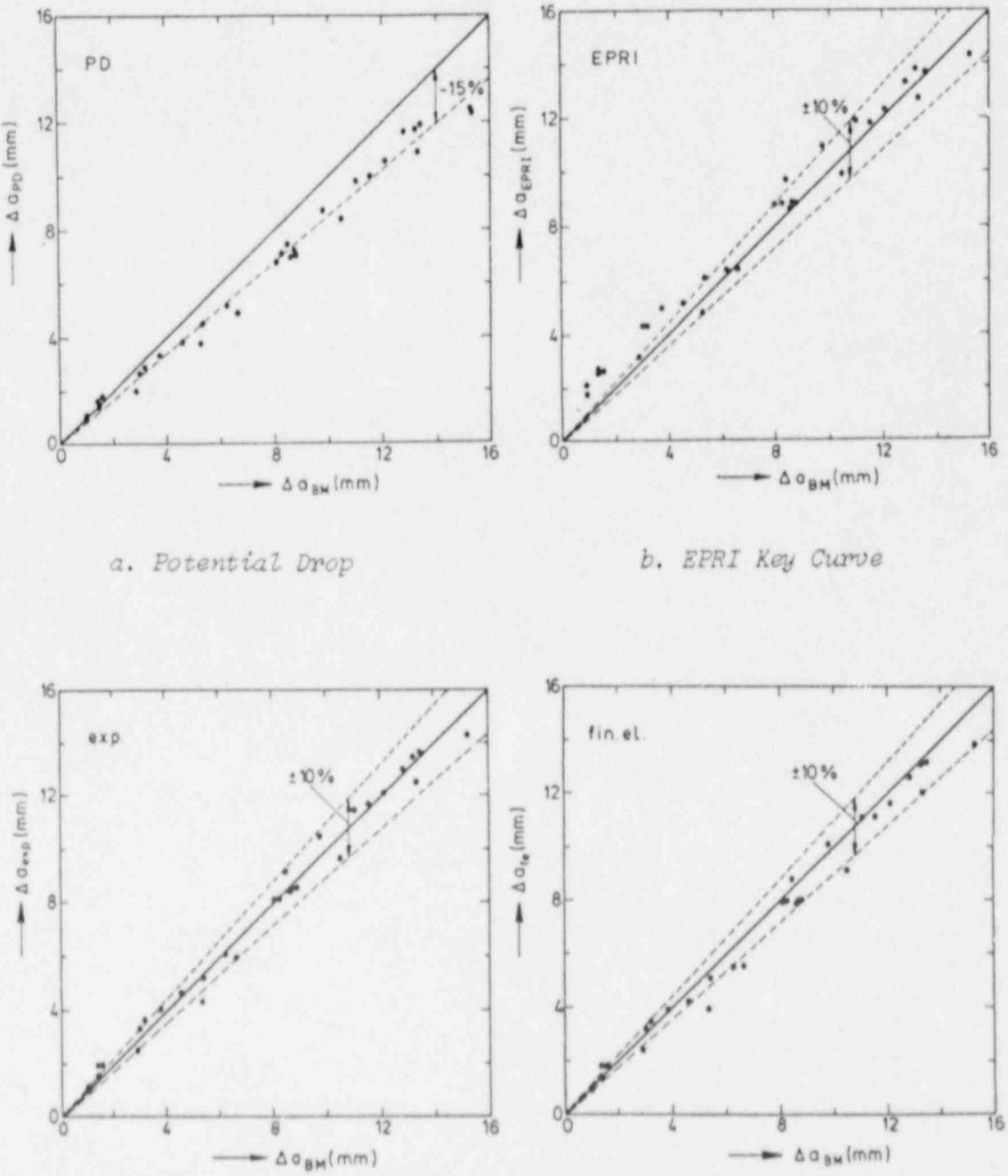

a. Potential Drop

b. EPRI Key Curve

c. Experimental Key Curve

d. Finite elements Key Curve

FIGURE 5.

Comparison between optically measured dye penetrant beach marks (Δa_{BM}), and Δa as predicted by the Potential Drop and Key Curve methods for plane sided and side grooved SENB specimens.

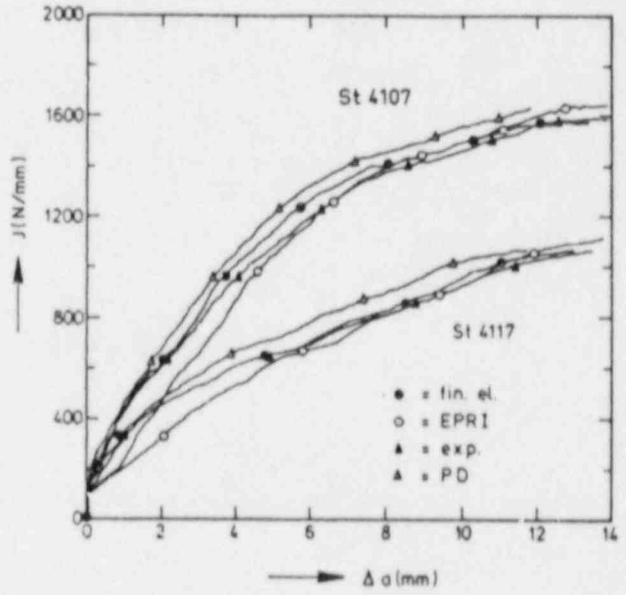

FIGURE 6.

Key Curve- and Potential Drop J_R-curves for a plane sided (St4107) and side grooved (St4117) SENB specimen, using four methods to determine Δa.

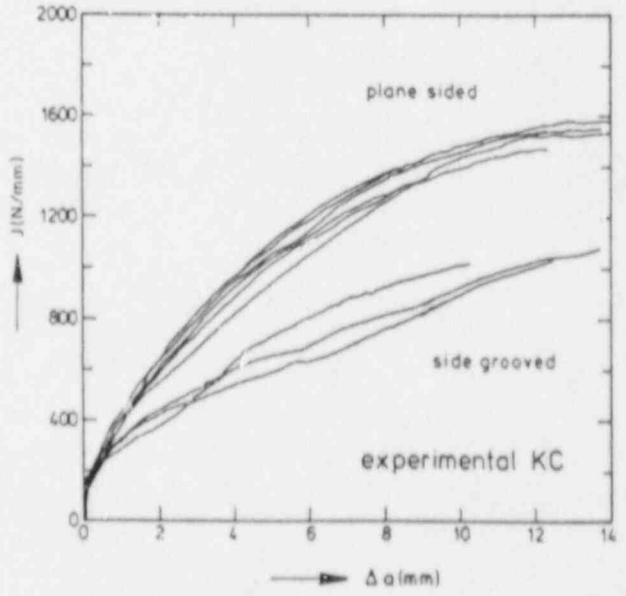

FIGURE 7.

Single specimen J_R-curves (obtained by using an experimental Key Curve) of SENB specimens.

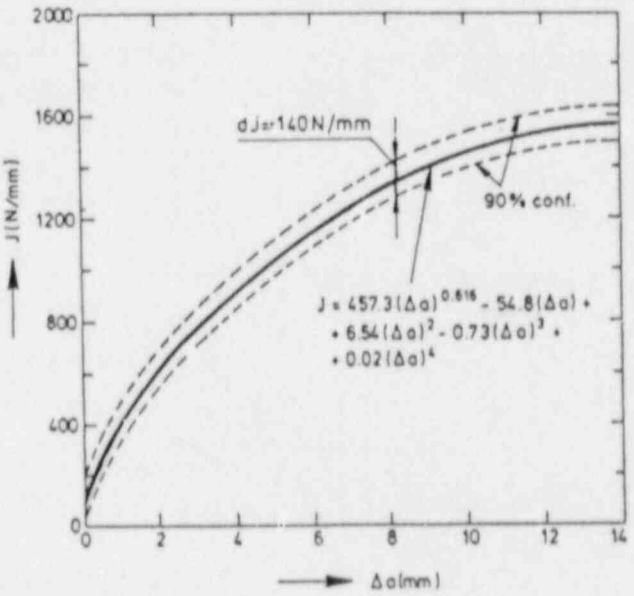

FIGURE 8.

Best-fit mean J_R-curve of the plane sided J_R-curves shown in figure 7. Also shown is the 90% confidence interval around the regression curve, indicating the degree of specimen-to-specimen material variability.

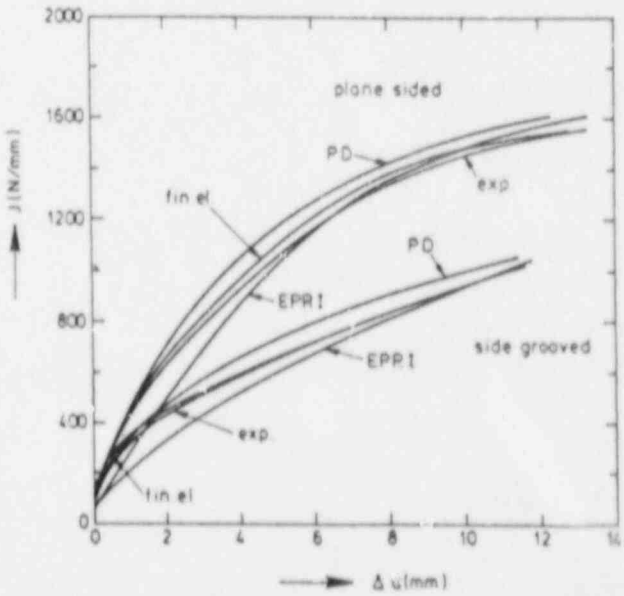

FIGURE 9.

Comparison between the mean J_R-curves for the four methods used. To each curve belongs a confidence interval approximately the size of that in figure 8.

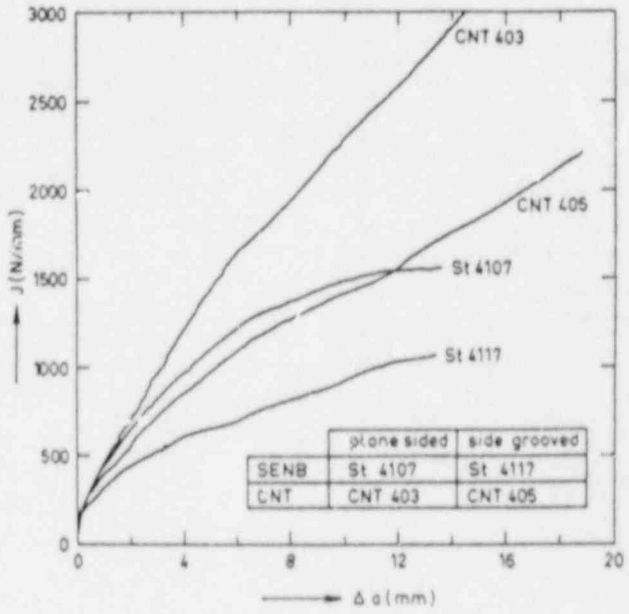

FIGURE 10.
Representative J_R-curves for plane sided and side grooved St.52-3 SENB and CNT specimens.

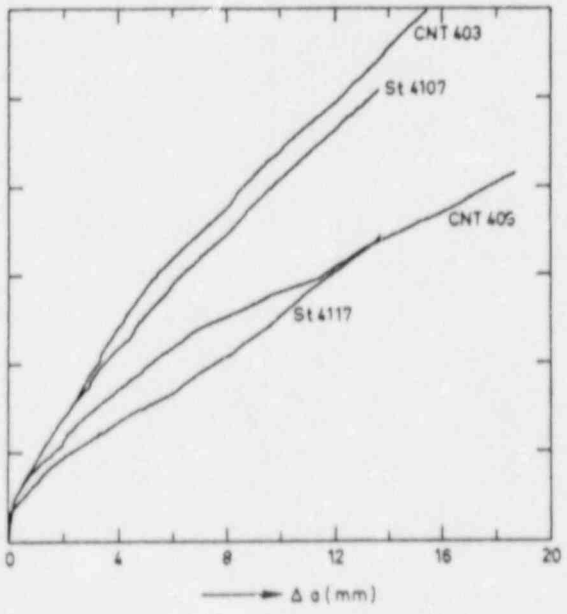

FIGURE 11.
J-modified for the same specimens as in figure 10.

A DISPLACEMENT-BASED KEY CURVE METHOD FOR DETERMINING J-R CURVES

W. R. Andrews

General Electric Co.
Schenectady, NY
USA

INTRODUCTION

An alternative to unloading compliance as a single-specimen method for determining J-R curves is needed due to the complexity and high precision required to obtain good results. The author has developed over the last several years a unique method (Ref. 1) that has the advantages of requiring no unloading and reduced clip gage precision requirement while not sacrificing precision in the crack-length measurements. This paper reviews experience with the method and recommends its extended use.

TEST METHOD

The procedure was developed for use with the compact (C(T)) specimen (Fig. 1). The objective of the adaptation to accomodate two displacement measurements is to obtain measurements at the load line and at the crack tip. Linear interpolation between the positions of the gages accomplishes that objective.

The test procedure calls for loading the specimen monotonically while recording the load P, front displacement V_f, and back displacement V_b with a computer-controlled data logging system.

The completion of a test is indicated by any sign that the crack has extended about 40 percent of the ligament; one such indicator might be a 40 percent drop in the load from maximum load. The specimen is subsequently heat tinted or processed otherwise to mark the crack front. Breaking the specimen and visual measurement of the crack lengths, fatigue precrack and final fracture, allows one to calculate the values of J and physical crack growth delta-a_p. The calculations are made using the equations shown in Fig. 2. Eq. 1 and Eq. 2 give the measured values of load-line displacement V_L and crack-tip opening displacement delta$_T$. Eq. 3, used to calculate crack length, contains two parameters. One of these is the key curve which is given by Eq. 4, and the second is the experimentally determined rho.

The key curve is the crack-tip opening displacement for no crack growth, measured at the mid-thickness of the C(T) specimen. The curve has been normalized by specimen dimensions and material properties as shown in Fig. 3. The independent variable X used in Eq. 4 and Fig. 3 is the normalized function of V_L, initial crack length a_o, Young's modulus E and flow stress sigma$_o$.

The lead term of the key curve (Eq. 4) represents elastic response and the second term represents plastic response. The hyperbolic tangent functions are smoothing functions to join the two terms. Note that the elastic term is a weak function of elastic constants and crack length. The adjustable parameter is determined using the initial elastic loading displacements but must have a value near the mean theoretical of 1.5.

The value of the adjustable parameter rho is accomplished using the final crack length and Eq. 3 rearranged to solve for rho. The order of computation is: first compute the elastic constant for the key curve, second calculate the value of rho.

Once the adjustable parameters are assigned values, the crack extension values may be calculated for each data set recorded during the test using Eq.3. Usual practice is to calculate values for four variables, V_L, CTOD (delta$_T$), J and crack extension delta-a_p.

RESULTS

The results of applying this test method to several materials are illustrated in Figures 4, 5 and 6.

Figures 4 and 5 show results for steels of widely varying strength levels. Fig. 4 is for HY130 steel (0.2% yield 130 ksi). Specimens V502 and V505 were tested using the DBKC method: specimen V503 from the same plate was tested using the unloading compliance by another laboratory. (These tests were part of an ASTM J-R curve round robin.) Fig. 5 shows the results for a structural grade of carbon steel. The four heat tint results indicated were determined using four specimens from the same plate. The results obtained with these two materials are shown to enhance your confidence that the results are reliable.

The test method has been applied to metals having a wide range of properties. Fig. 6 shows R-curve results for three metals, an austenitic nickel base alloy, a ferritic structural steel and an aluminum alloy. These results were all obtained using the DBKC method.

CONCLUSIONS

The experience to date of using the DBKC method for determining R curves indicates that the method is general. The results shown here illustrate that point. The author recommends the extended use of the DBKC method based on it's ease of use and general applicability.

REFERENCES

1. W. R. Andrews, "Determining Crack Extension Using a Displacement Based Key Curve Method," Elastic-Plastic Fracture Test Methods: The User's Experience, ASTM STP 856, E. T. Wessel and F. J. Loss, Eds., ASTM, 1984, pp 308-321

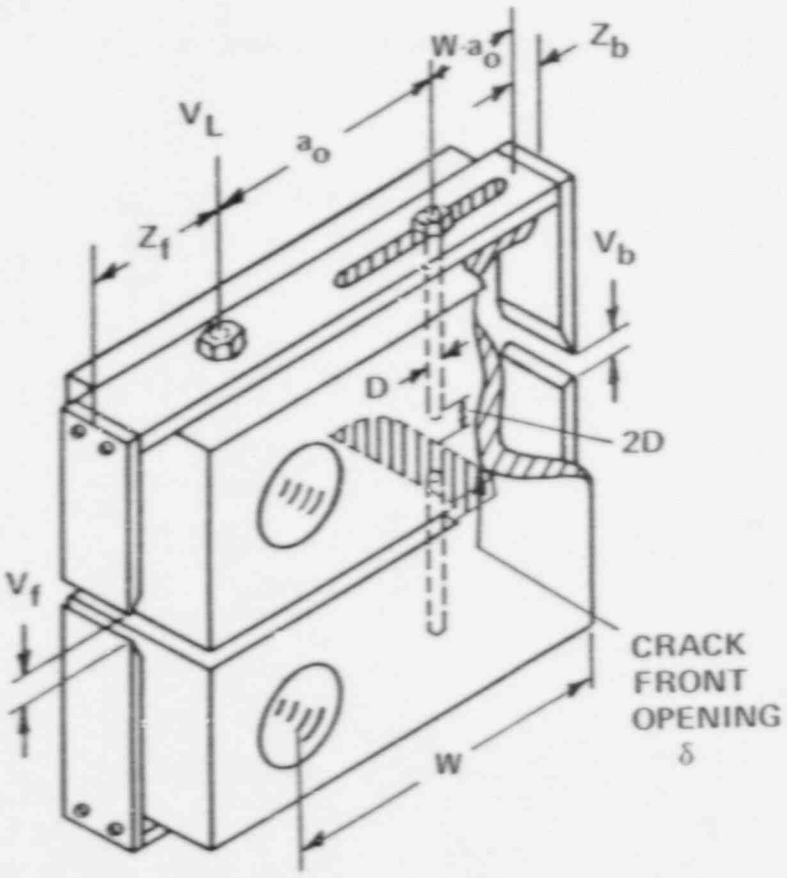

Figure 1. The compact specimen with extensometer fixture.

$$V_L = \frac{V_f (r + a_o)}{(Z_f + a_o + r)} \qquad (1.)$$

$$\delta_o = \frac{V_f \cdot r}{(Z_f + a_o + r)} \qquad (2.)$$

where:

$$r = \frac{Z_b + W - a_o - \left[\frac{V_b}{V_f}(Z_f + a_o)\right]}{\left(\frac{V_b}{V_f} + 1\right)}$$

$$\Delta a = \frac{(\delta_o - \delta_{T|a_o})}{\left(\frac{1}{\rho} + \frac{d\,\delta_r}{da}\right)} \qquad (3.)$$

where ρ = f(material determined at test's end)

$$\frac{\delta_r}{W - a_o} = \frac{\sigma_o}{E}\left\{A\left[X_R \operatorname{Tanh}^{1/n'}\left(\frac{X}{X_R}\right)^{n'}\right] + 3.38\left[X - X_R \operatorname{Tanh}^{1/n'}\left(\frac{X}{X_R}\right)^{n'}\right]\right\} \qquad (4.)$$

where

$$X = \frac{E V_c}{\sigma_o W (2 + \gamma_W)^2}$$

$\sigma_o = (\sigma_{ys} + \sigma_{uts})/2$, $A = f\left(\frac{a_o}{W}\right) \cong 1.5 \pm 1.0$

$X_R = 0.5$, $n' = 1.2$

Figure 2. The formulae for calculating crack extension.

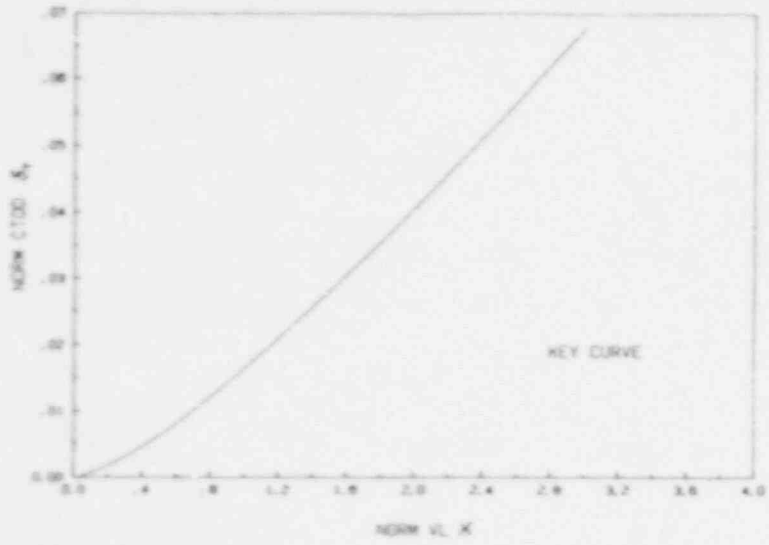

Figure 3. The normalized key curve.

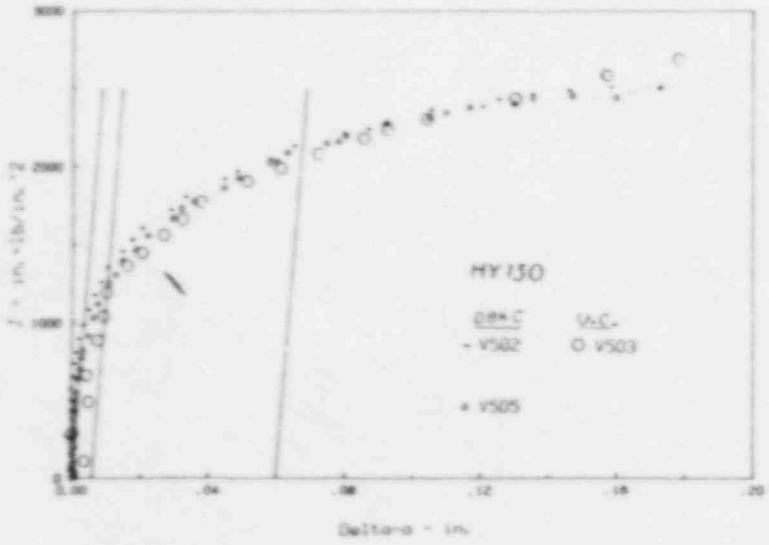

Figure 4. Example J-R curves for HY130 steel.

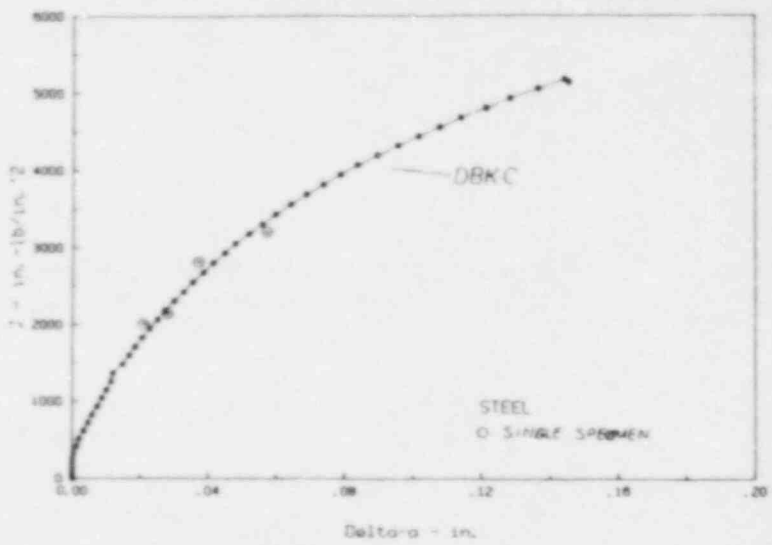

Figure 5. Example J-R curves for structural steel.

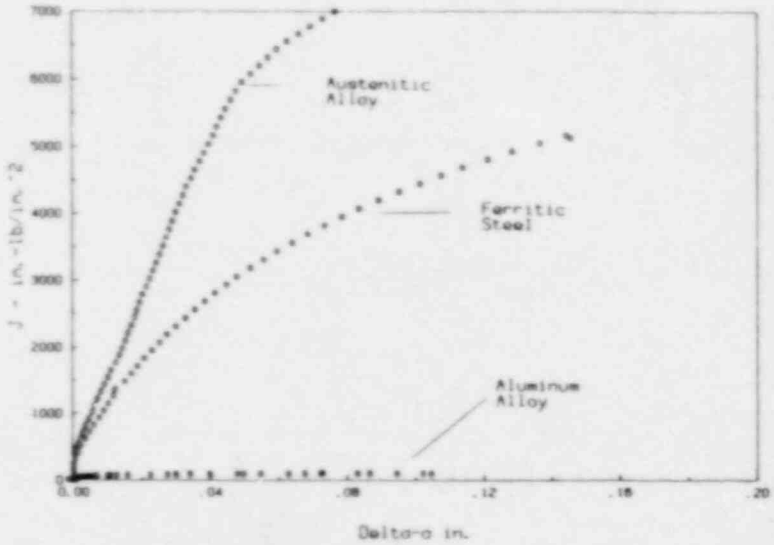

Figure 6. R curves for metals having a wide range of toughness and tested using the DBKC method.

DETERMINATION OF STATIC AND DYNAMIC J-R CURVES USING THE KEY-CURVE METHOD

K. Brüninghaus, W. Hesse, M. Twickler,
R. Twickler and W. Dahl

Institute of Ferrous Metallurgy
Technical University of Aachen

ABSTRACT

The experimental procedure for J_R-curve testing under rapid loading conditions involves problems due to crack length measurement. Usual methods like unloading compliance, potential drop, ultrasonics and multi specimen technique are not suitable for dynamic testing. Thus the key curve method developed by Ernst et al. (Ref. 1), was used to determine J_R-curves for a 20 MnMoNi 5 5 steel at various displacement velocities between 0.01 mm/s and 570 mm/s. At the highest rate of 570 mm/s smooth load displacement records without significant oscillations could be obtained using instrumented specimens. The key curve function was developed by FE-calculations showing some advantages compared with an experimental determination. The key curve function was related to yield strength and converted to the appropriate yield strength corresponding to the strain rate. At the end of each test the stable crack extensions were measured. They show good agreement with values calculated by key curve method. The obtained J_R-curves show increasing tendency with increasing loading rate.

INTRODUCTION

In many cases it is essential for the prediction of failure to know the material behaviour under loading conditions as they occur in components or structures. Not only yielding and work hardening behaviour but also the fracture behaviour characterized by the J_R-curve in the ductile temperature region has to be determined as a function of temperature and loading rate. The experimental procedure for dynamic J_R-curve testing involves problems due to crack length measurement. Usual methods like unloading compliance, potential drop technique, ultrasonics and multi-specimen-technique are not suitable for dynamic testing. Thus the key curve method developed by Ernst et al. (Ref. 1) appears to be a promising alternative for J_R-curve determination, because the crack extension can be obtained directly from the load displacement record if a key curve function is available.

DESCRIPTION OF THE KEY CURVE METHOD DEVELOPED BY ERNST (REF. 1)

Basically unloading compliance and key curve method are similiar. In the first case the crack extension is derived from the elastic compliance whereas in the second case crack extension is obtained from a calibration or key curve function, which represents elastic and plastic specimen behaviour. This calibration function depends on yielding and work hardening behaviour of the material and consequently on strain rate and temperature. Fig. 1 proves that load displacement curves of geometrically similar CT-specimens with constant a/W-ratio are identical, if the load F and the displacement Δ are divided by the proper specimen dimensions. The normalized load value

$$(1) \qquad Fl = \frac{F \cdot W}{B \cdot b^2}$$

W = specimen width
B = specimen thickness
b = ligament length

in the diagram is the tensile stress $F/(W \cdot B)$ divided by the ratio $(b/W)^2$ which implies the dependence of bending stiffness on ligament size. According to Joyce (Ref. 2) Fl becomes therefore independent of a/W for 3-point-bend specimens and the key curve function is given by $Fl\ (\Delta/W)$. In contrary, for CT-specimens the normalized load displacement curve $Fl(\Delta/W)$ additionally depends on the a/W-ratio so that the key curve function is given by the function $Fl(\Delta/W, a/W)$. Ernst has proposed to develop the "key curve" experimentally using subsized specimens, because they can be loaded until higher values of Fl and Δ/W without stable crack growth. In this case the experiment for J_R-curve determination has to be carried out

with a larger geometrically similiar specimen where crack initiation occurs at lower values of Δ/W. Fig. 2 presents the load displacement record of a 1CT-test-specimen with a/W = 0.65 and load displacement curves for 3 a/W-ratios for the same specimen size derived from the calibration function. The point of deviation indicates crack initiation and at the points of intersection the instantanous crack length of the 1CT-specimen is given by the a/W-ratio of the respective load displacement curve. This procedure supposes that the applied load of a specimen at a given combination of Δ/W and a/W is independent of the path in the Δ/W-a/W-field. The expressions for the calculation of crack extension Δa and J-integral are given in Ref. 1.

APPLICATION OF THE KEY CURVE METHOD TO J_R-CURVE DETERMINATION AT HIGH LOADING RATES

In the present work the key curve function was developed by FE-calculations because the experimentally determined one has three principal disadvantages:

1. The scatter of load displacement behaviour causes an uncertain Δa determination especially in the region of crack initiation.

2. Using subsized specimens only a limited region of the key curve function can be obtained as it shows Fig. 3. At a supposed J_{IC}-value of 150 N/mm the crack initiation loads of different geometrically similiar CT-specimens (left diagram) can be transferred in the related load-displacement curve (right diagram). It appears that due to the above supposed J_{IC}-value a calibration function can be only determined with 1/2 CT-specimens until $\Delta/W = 0.035$ because crack growth takes place afterwards.

3. The experimental procedure is very expensive on account of the great number of subsized test specimens.

FE-Calculations

FE-calculations were carried out to determine load displacement curves for CT-specimens with a/W-ratios between 0.5 and 0.75 (6 specimens) under plane strain conditions. The elastic-plastic calculations were performed by the FE-program ABAQUS using the von Mises yield criterion and isotropic strain hardening. The uniaxial stress-strain curve was represented by a multilinear approach. A geometrical nonlinear formulation was used.

As yielding and work hardening behaviour of steel depends on strain rate $\dot{\varepsilon}$, key curve functions corresponding to the displacement rates had to be determined. Yielding

behaviour was investigated as a function of strain rate. For two stress-strain-curves at different strain rates FE-calculations were carried cut to develop a calibration function. Fig. 4 shows stress strain curves and FE-calculations. The calculated load displacement curves are nearly identical, if F1 is related to the lower yield point and Δ/W to the elastic strain at the lower yield point ε_o. Therefore it appears to be more sensible to make only one FE-calculation by converting a related calibration function to the appropriate yield strength with respect to the strain rate, instead of performing FE-calculations for each strain rate. Fig. 5 presents the lower yield strength as a function of the activation energy ΔG. According to Krabiell et al. (Ref. 3) the lower yield strength can be calculated for any required strain rate on the basis of thermally activated yielding. The strain rate near the crack tip was evaluated according to Shoemaker (Ref. 4) at the moment of general yield:

$$\dot{\varepsilon} = \frac{2 \cdot \sqrt{3}\, R_{eL,2}}{E \cdot t_o} \qquad (2)$$

Using this formula time and place dependence of strain rate was neglected and the estimated strain rate was regarded to be characteristic for the specimen behaviour.

Experimental Procedure and Technique

The fracture tests were performed on a high speed servo-hydraulic testing machine at constant displacement velocities between 0.01 mm/s and 570 mm/s. 20% side grooved 1 CT-specimens were tested. They were loaded up to certain displacment values. At velocities up to 100 mm/s the load was measured by a piezoelectric load cell and the displacement by a clip-gage. At higher loading rates calibrated strain gages fixed on both sides of the specimen and a non-contact displacement measuring system were used in order to obtain a smooth load displacement record without significant oscillations. Fig. 6 shows the improvement of the load-time signal with regard to superposed oscillations using strain gages instead of a piezoelectric load cell. Load and displacment were recorded on transient recorders with a capacity of 8 bit x 4000 words and a maximum sample rate of 20 MHZ. Fig. 7 presents the test apparatus for fracture mechanics tests. It shows the clamped CT-specimen in the middle of the figure, the piezoelectric load cell, the traverse of the testing machine, the slack run to enable the piston to achieve the required displacement velocity and additional masses avoiding that the piston slows down at the impact.

The investigated material was a quenched and tempered 20 MnMoNi 5 5 steel. Table 1 presents chemical composition and heat treatment of the steel.

Results and Conclusions

In order to verify the methodology total stable crack extensions were measured after the specimens had been heat tinted and broken at liquid nitrogen temperature. Fig. 8 shows the good agreement between measured and by key curve method obtained crack extensions. The evaluated J_R-curves of different loading rates in terms of $\dot{J}$ are presented in Fig. 9. With the exception of the J_R-curve at $\dot{J} = 3{,}7 \cdot 10^1$ $MNm^{-1}s^{-1}$ crack resistance behaviour increases with loading rate. So a conservative estimation of fracture behaviour can be made by a quasi-static J_R-curve.

REFERENCES

1. H. Ernst, P.C. Paris, M. Rossow and J.W. Hutchnison, "Analysis of Load-Displacement Relationship to Determine J-R Curve and Tearing Instability Material Properties", Fracture Mechanics, ASTM STP 677, 1979, pp. 581-599

2. J.A. Joyce, "Drop Weight J-R Curve Testing Using the Key Curve Method, "Proceedings of a CSNI Workshop on Ducti[illegible] Fracture Test Methods, Nuclear Energy Agency, [illegible]ris, 1982, pp. 517-536

3. A. Kr[illegible] d W. Dahl, "Zum Einfluß von Temperatur und [illegible] indigkeit auf die Streckgrenze von Baustä[illegible] verschiedlicher Festigkeit", Arch. Eisenhü[illegible]., Vol 52, 1981, pp. 429-436

4. [illegible]ker, "Factors Infuencing the Plane-Strain [illegible]nness Values of a Structural Steel", Trans. [illegible], 1969, pp. 506-511

Table 1 Chemical composition and heat treatment of 20 MnMoNi 5 5 steel

C	Si	Mn	P	S	Al	N	Cu	Cr	Ni	Mo	Sn
.19	.24	1.35	.008	.003	.031	0.12	0.10	.16	.72	.48	.005

quenched and tempered: 900°C/40min/oil/650°C/80min/air

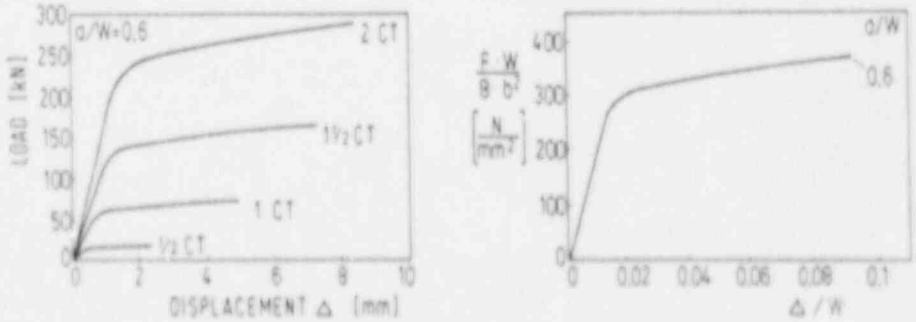

a) b)

Fig. 1 a) Load displacement curves of CT-specimens
b) Normalized load displacement curve

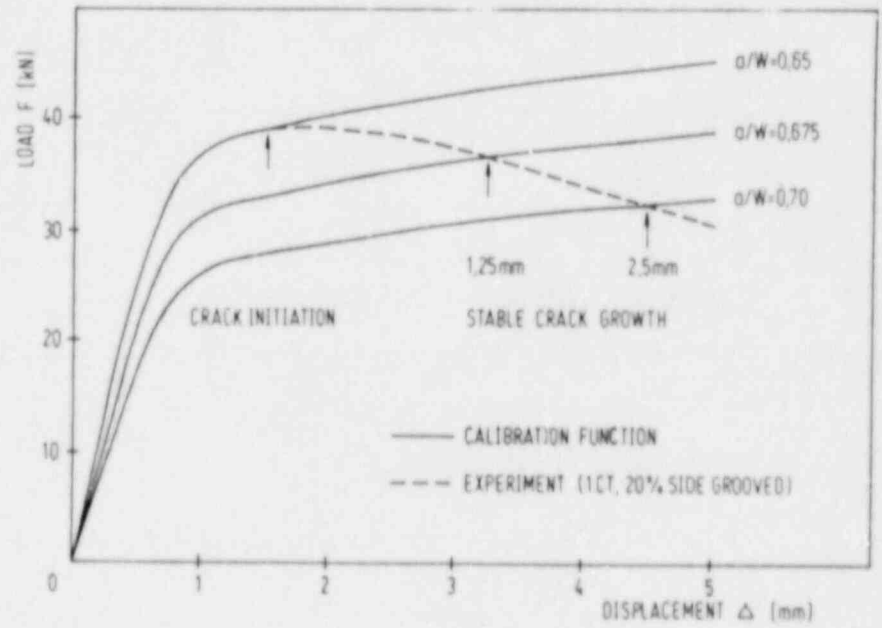

Fig. 2 Comparison of load-displacement curves to determining stable crack growth

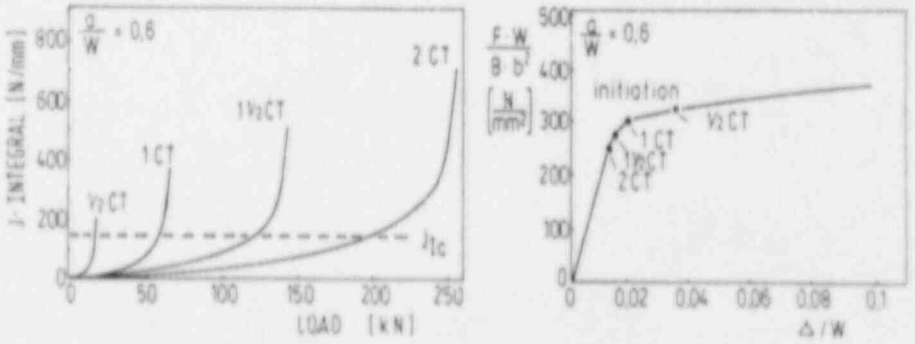

Fig. 3 Signification of CT specimen size for the load displacement point of the initiation of stable crack growth

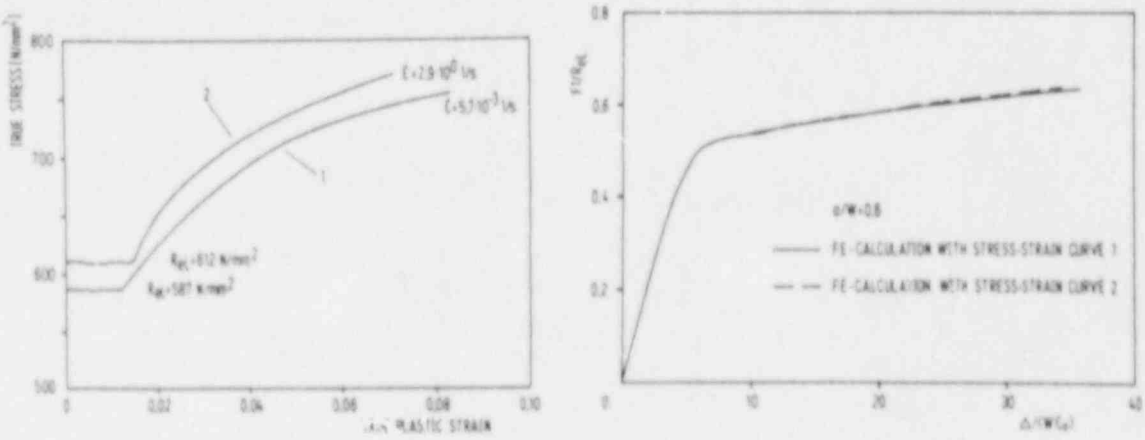

a) b)

Fig. 4 a) True stress strain curve for two different strain rates at room temperature
b) key curve normalized with yield behaviour

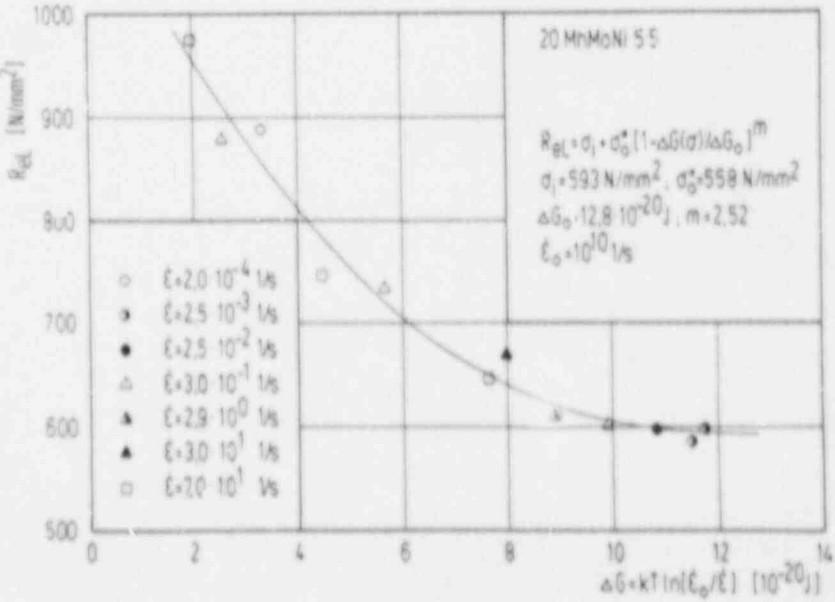

Fig. 5 Yield stress R_{eL} as a function of activation energy

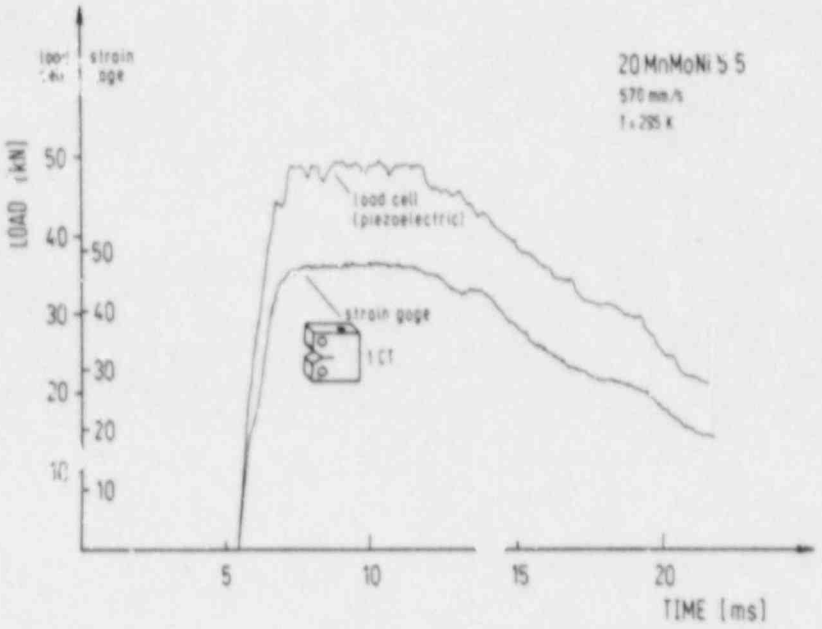

Fig. 6 Comparison of load cell signal with strain gage signal

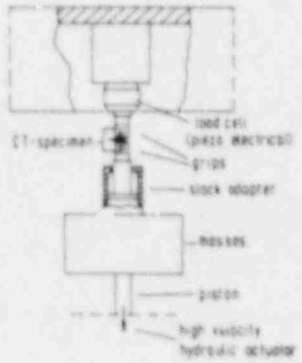

Fig. 7 Test apparatus for fracture mechanics tests at rapid loading rates

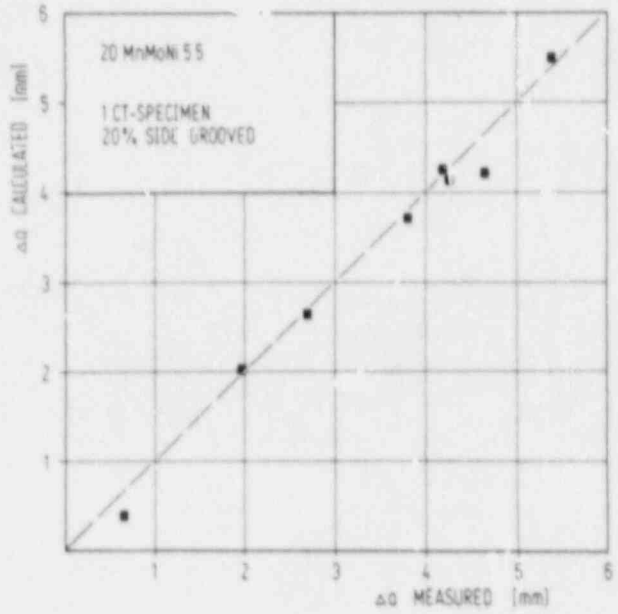

Fig. 8 Comparison of calculated and experimentally observed stable crack growth values

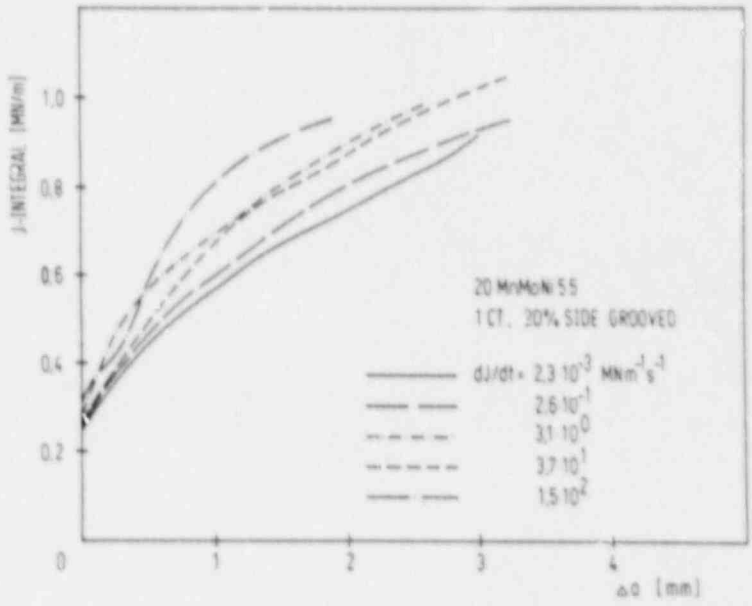

Fig. 9 J_R-Δa-curves as a function of loading rate

FEASIBILITY OF USING CHARPY-SIZE SPECIMENS IN J-R CURVE TESTING

Wallin, K. and Saario, T.

Technical Research Centre of Finland (VTT)
Metals Laboratory, SF-02150 ESPOO 15, Finland

INTRODUCTION

The most commonly used specimen type in nuclear surveillance programs is the Charpy-V-impact specimen. The specimen is small and has a somewhat unpleasant testing geometry. The testing capasity of the Charpy-specimen is also very small. The specimen is, however, much used, and it is therefore important to examine it's suitability for J-R curve testing.

In this work J-R curves obtained with precracked Charpy-specimens are compared with J-R curves obtained from other specimen geometries. Special interest is directed towards the comparison of CVN_{pc}- and 1T CT -specimens.

EXPERIMENTS AND DISCUSSION

The tests were performed with the automatic testing system at VTT, utilizing elastic partial unloading compliance technique (Ref. 1). Four different specimen geometries were tested (3 specimens of each geometry). The geometries were 1T CT, 0.5 T RCT, 15 mm 3PB and CVN_{pc}. The results are presented in Fig. 1a - b. Not much difference is seen in the respective J-R curves, but the calculated crack extensions for the CVN_{pc}-specimens are seen to be much too small.

In order to investigate this error in the calculated crack extension, a compliance curve determination was perfonned for the CVN_{pc}-geometry.

The compliance was measured both at the load line deflection as well as at the crack mouth opening. First a simple geometry correction was used for the crack mouth opening. The results are presented in Fig. 2a - c. Striking in the results are that unbent specimens yielded a different compliance curve than bent specimens. Since the effect was the same both for the crack mouth opening as well as the deflection, the investigation was continued only on the crack mouth opening compliance.

The next step was to perform a real geometric rotation correction on the measured crackmouth opening compliance. The results are presented in Fig. 3a - c. It is seen from Fig. 3c that the geometric rotation correction is sufficient for the unbent specimens. The bent specimens, however, still yield a different compliance.

This bending effect has of course several explanations:
- the loading rolls move causing change in the span width

- the loading rolls indent into the specimen causing uneven loading geometry
- the strongly plastisized unbroken ligament may cause some effect on the compliance.

Because these effects are very difficult to deal with theoretically, an empirical bending correction for the CVN_{pc}-specimen was determined. The results of the final geometry and bending corrected compliance values together with the crack length calculations are presented in Fig. 4a - d. The crack length as well as crack growth results are now excellent.

The final resulting J-R curves are compared with the J-R curves obtained from 1" CT -specimens in Fig. 5a. It is seen that the two specimen geometries yield quite different J-R curves. However, when calculating J_{MOD} as proposed by Ernst (Ref. 2), the two geometries yield essentially identical J_{MOD}-R curves. This is shown in Fig. 5b and c.

SUMMARY AND CONCLUSIONS

In this work J-R curves obtained with precracked Charpy specimens were compared with J-R curves obtained with other specimen geometries.

In conclusion it can be proclaimed that 20 % -side grooved CVN_{pv}-specimens can be used to derive reliable J-R curves. This demands a very rigorous performance of the tests and analysis as well as the use of the so called modified J-integral J_{MOD}.

ACKNOWLEDGEMENTS

This work is a part of the Safety and Reliability of Nuclear Components and Materials Program performed at the Technical Research Centre of Finland (VTT) and financed by the Ministry of Trade and Industry in Finland.

REFERENCES

1. K. Wallin, H. Saarelma, T. Saario and E. Varis, "Automatic Fracture Toughness Testing System at the Technical Research Centre of Finland". Technical Research Centre of Finland, Research Notes 398, 1984, 35 p.

2. H. A. Ernst, "Material Resistance and Instability Beyond J Controlled Crack Growth", presented at the second Int. Symposium on Elastic Plastic Fracture Mechanics, October 1981.

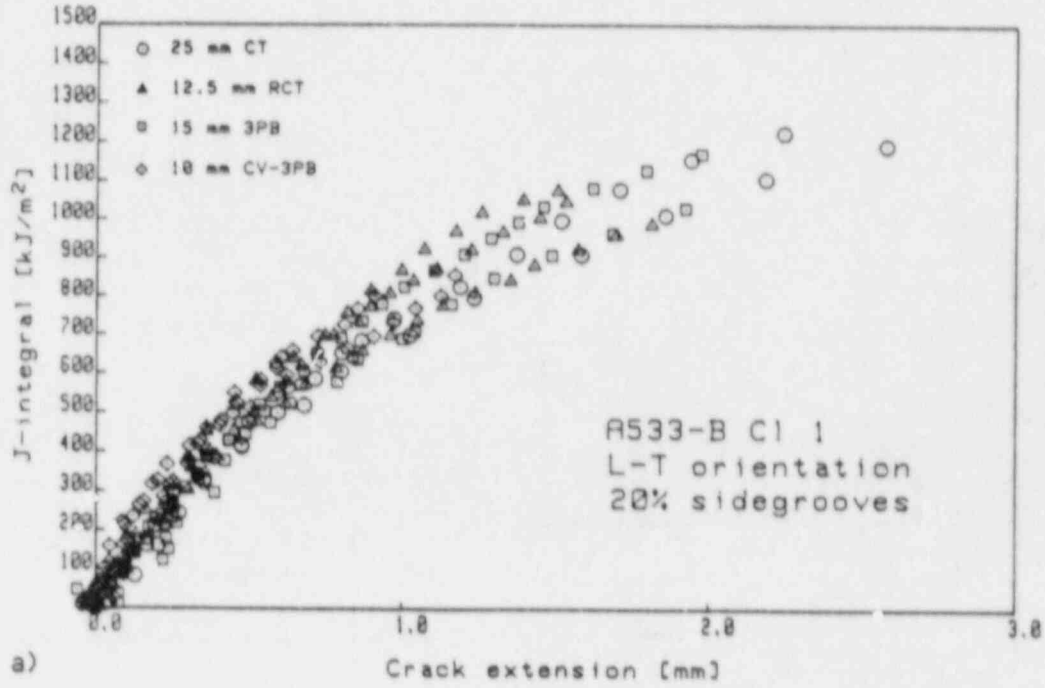

a)

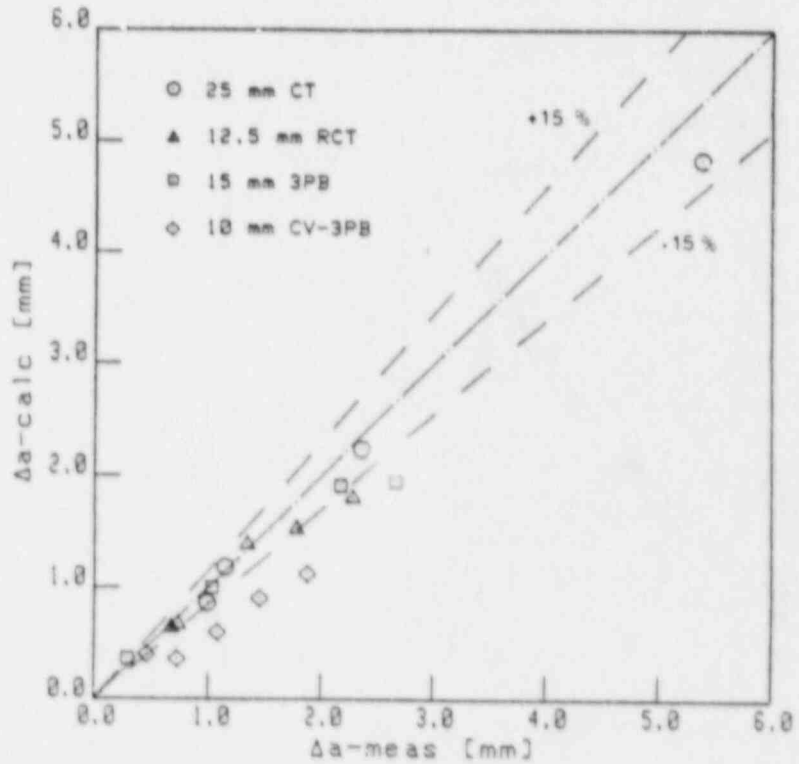

b)

Fig. 1. Results of J-R curve comparison with 4 different specimen geometries.

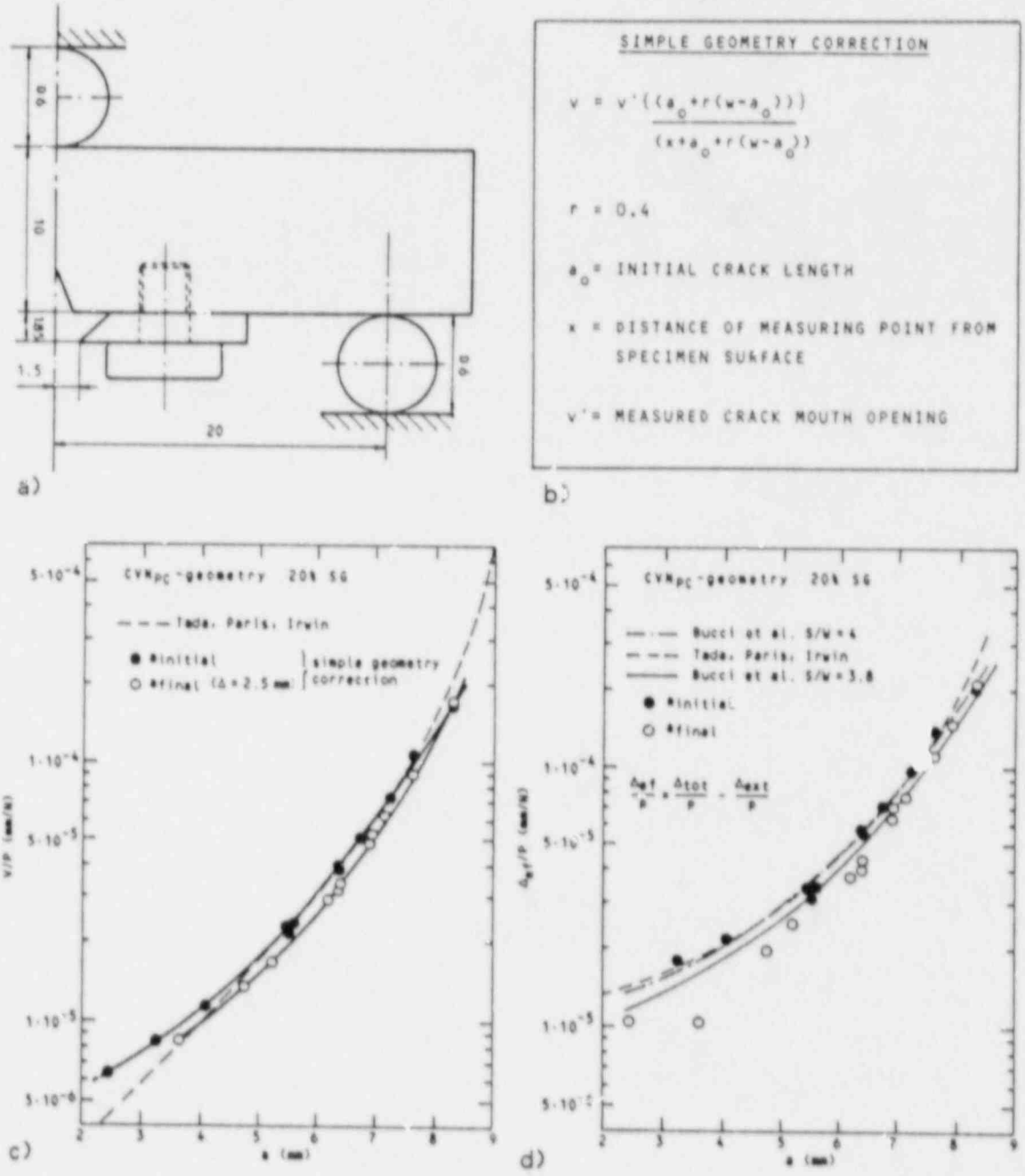

Fig. 7. Results of CVN_{pc}-compliance curve determinations.

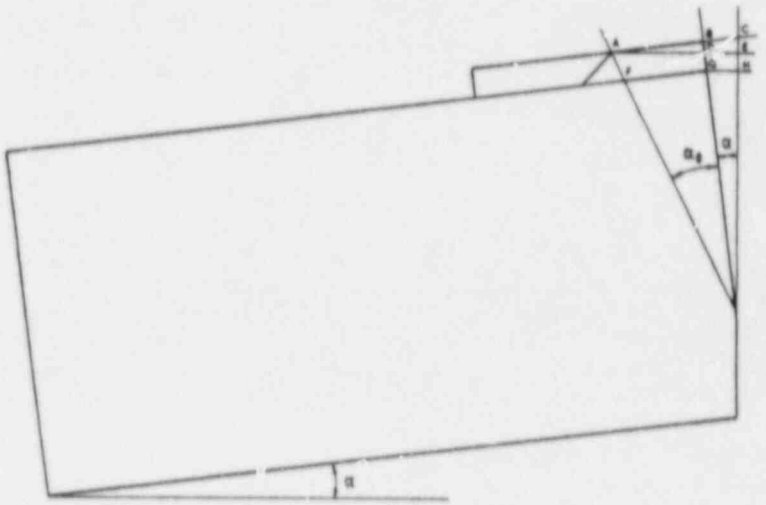

$\frac{V_0}{2}$ = AB ; $\frac{V'}{2}$ = AE - AB ; $\frac{V}{2}$ = GH ; X = BG

a)

GEOMETRIC ROTATION CORRECTION

$$\delta_{(\frac{V}{P})} = \delta_{(\frac{V'}{P})} \cdot \frac{2(a+r(w-a))}{\sqrt{v_0^2-(v'+v_0)^2}} \cdot \frac{\cos(\arcsin((v'+v_0)\cdot\sin(\alpha_0))-\alpha_0)}{v_0}$$

$$\alpha_0 = \arctan \frac{v_0}{2(x+a+r(w-a))}$$

$r = (\frac{\delta}{w})^*$ (ELASTIC ROTATIONAL FACTOR)

a = ACTUAL CRACK LENGTH

x = DISTANCE OF MEASURING POINT FROM SPECIMEN SURFACE

v_0 = MEASURING POINT DISTANCE

$\delta_{(\frac{V'}{P})}$ = MEASURED COMPLIANCE

v' = MEASURED CRACK MOUTH OPENING

b)

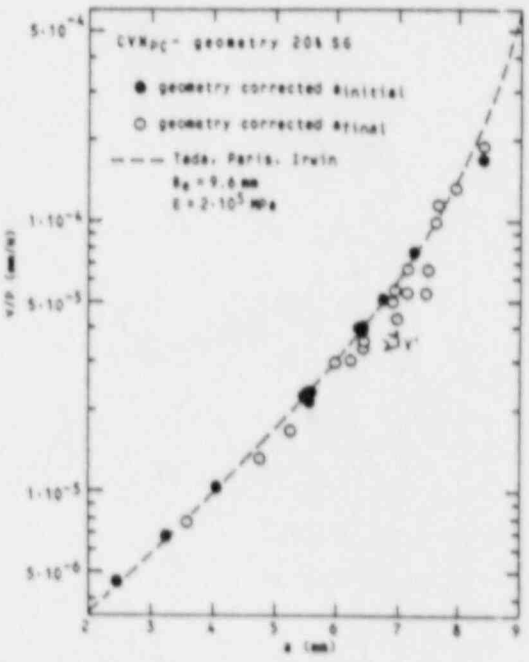

c)

Fig. 3. Effect of geometric rotation correction on CVN_{pc} crack mouth opening compliance curve.

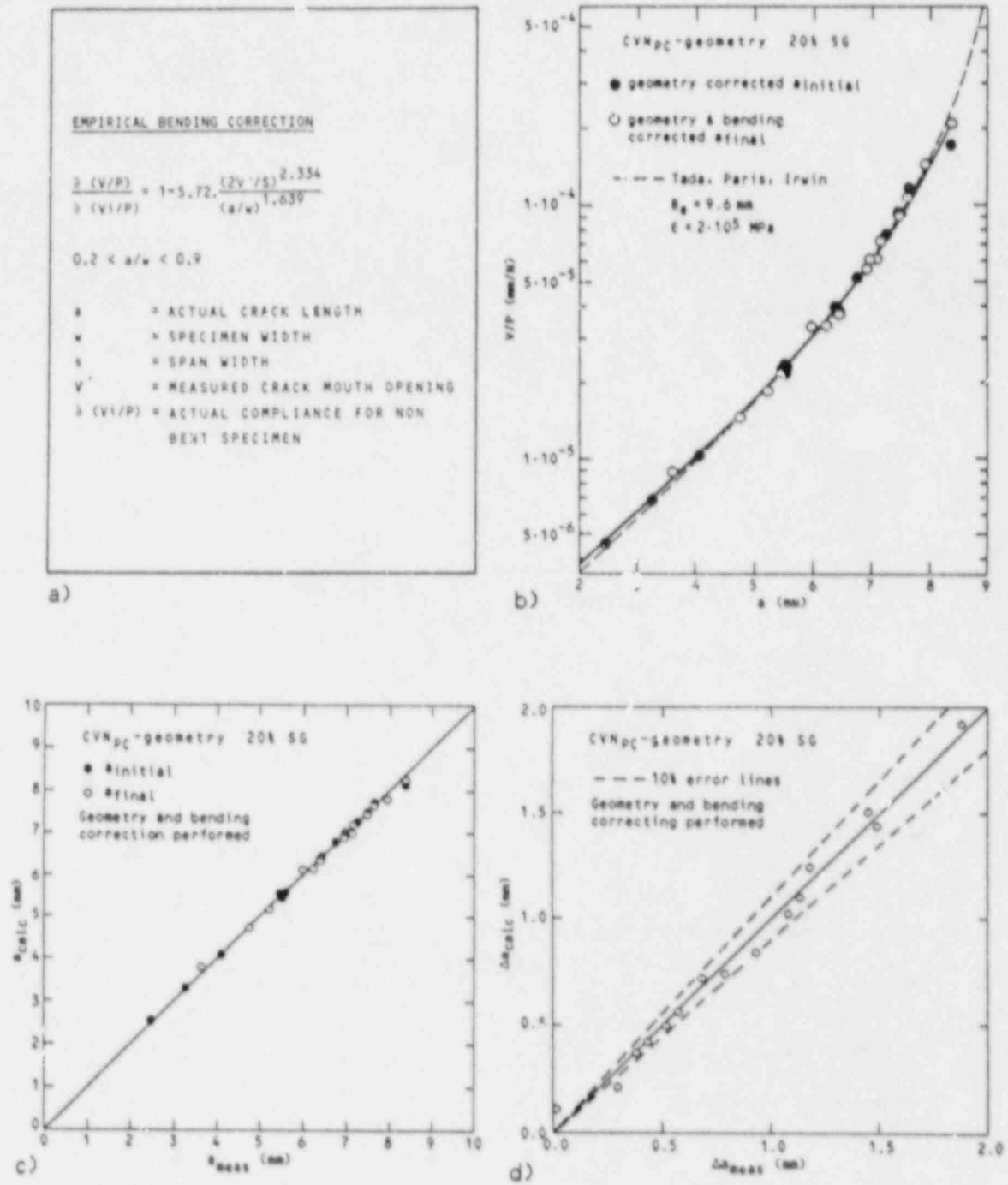

Fig. 4. Geometry & bending corrected compliance and crack length results for the CVN$_{pc}$-specimens.

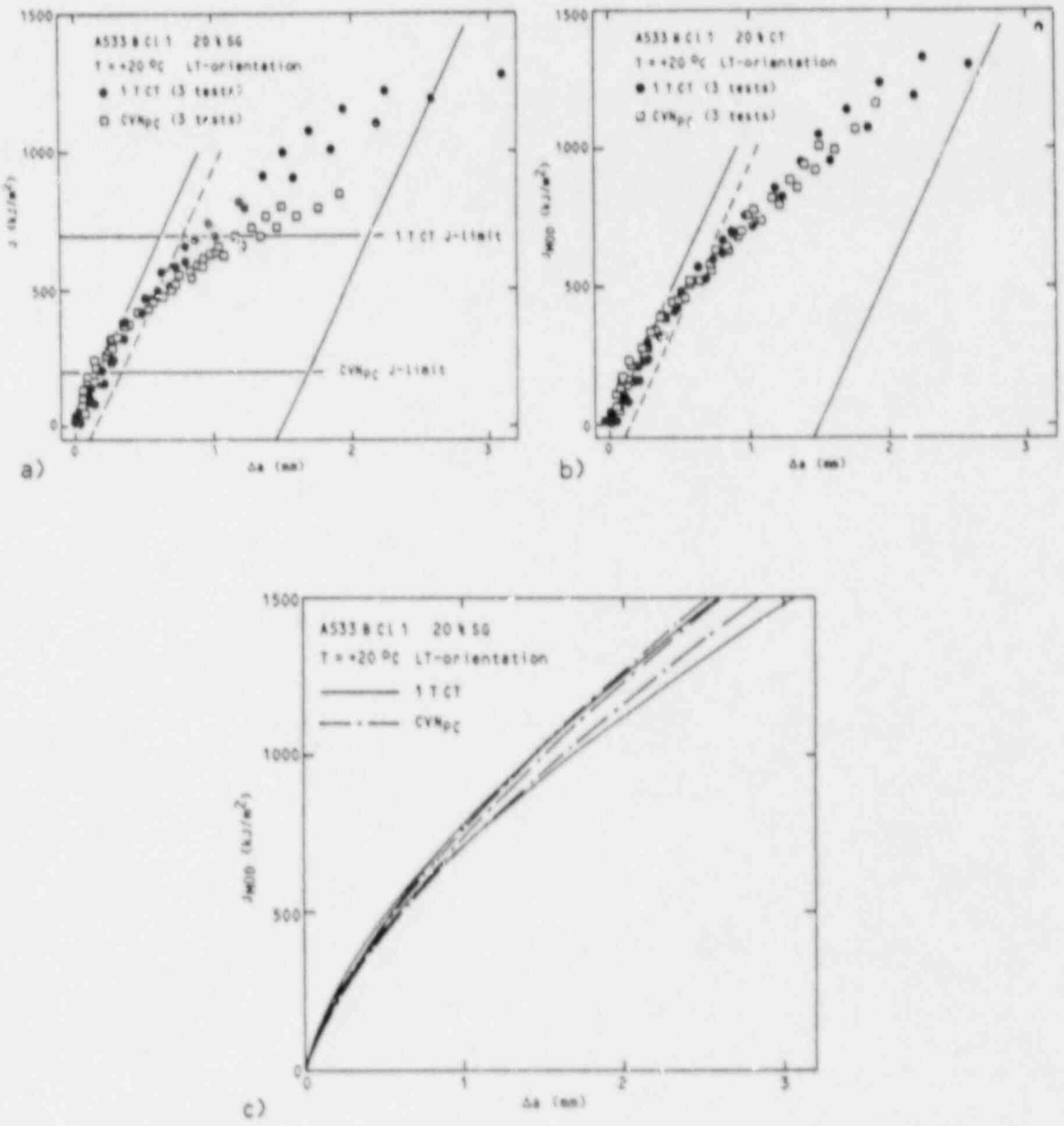

Fig. 5. Final comparison of CVN_{pc}- and 1T CT -geometry J-R curves.

METHODS TO DETECT CRACK INITIATION IN PRECRACKED CHARPY-TYPE SPECIMENS

T. Varga*), F. Loibnegger**), F. Salzmann**)

*) Institute for Testing and Research in Materials Technology (TVFA), Techn. University Vienna, Expert. Div. of Reactor Safety, Swiss Federal Nuclear Safety Inspectorate (HSK)

**) Institute for Testing and Research in Materials Technology (TVFA), Techn. University Vienna, Karlsplatz 13, A-1040 Vienna

Radiation embrittlement of RPV-steel in the core region of Light Water Reactors is usually detected by Charpy-V-specimens. The transition temperature shift at 30 or 50 ftlbs, 52 J/cm² or 86 J/cm² is regarded as the measure necessary to increase the lowest loading temperatures for different pressures; i.e. Porse diagram and its derivations.

Direct measurement of fracture mechanics properties is far more advantageous: quantitative considerations will become feasible instead of arbitrary methods and criteria. For this purpose precracked Charpy-type specimens are included in latest surveillance programs. Additionally, they show significantly smaller transition temperature regions than the original Charpy-V-specimens in general [Ref. 1, 2].

Force-time, or better force-deflection-diagrams are used for the fracture mechanics evaluation. Static loading does not exhibit any difficulties concerning inertia effects; dynamic loading, however, needs special know-how and

properties of the equipment [Ref. 3, 4, 5, 6, 7]. There are some laboratories in Europe and overseas, which can handle this task properly. Up to now the point of maximum load was regarded as critical and led to $J_{Ic\ max}$. Detecting the initiation point represents one of the latest fields of development in dynamic testing of precracked Charpy-size specimens.

Initiation in CT-specimens has been successfully detected by UT, like described in [Ref. 8]. However, Charpy-type specimens need other type of transducers, see Fig. 1; furthermore, according to tests by Salzmann, reflection is less advantageous from the extension of the existing crack. Therefore a higher number of specimens yields no sufficient UT indication of the initiation, see Figs. 2, 3 and 4.

Electrical Potential Methods have been investigated, too. In the Figs. 2,3 and 4 potentials, which were measured with external d.c. electric current feed, are shown. Potential curves were in general of less significance concerning crack initiation, than the UT indications.

Compliance changes, as shown by the force-deflection diagram in Fig. 4, gave on the steels tested, according to tests by Loibnegger, the most reliable indication of crack initiation. (The UT gives more pronounced change in this test). This observation was correct in a similar way in statically or dynamically loaded specimens. The calibration of methods for the detection of initiation is simple for static loading: the test can be stopped at any chosen point of the force-deflection diagram without difficulty. Heat tinting with following low temperature fracture

allows the investigation of the crack face concerning stable crack growth. Crack growth could than be correlated with the indication of the method to be checked and eventually calibrated.

Instead of stopping the pendulum abruptly, the instrumented chisel of the Schnadt Pendulum was limited to an adjustable amount of displacement, see Fig. 5. The loading rate was decreasing during the movement of the chisel to zero: however, the steel behaving in a fully ductile manner under all loading rates, there is no objection possible against the procedure described.

In Fig. 6, 7 und 8 force-deflection and potential-deflection curves are shown. As an own special development due to Loibnegger, no external current was used for the potential measurements. Crack faces show no stable crack growth in Fig. 6, small crack growth in Fig. 7 and considerable crack extension in Fig. 8. The appropriate scanning electron micrographs are given in Fig. 9, 10 a and b resp. in Fig. 11. The local magnification of the force-deflection and potential-deflection curves respectively are depicted in Figs 12 and 13 in a way, as they are prepared for the evaluation of the point of initiation for specimen as in Fig. 11.

REFERENCES

1. D.H. Njo, T. Varga, "Irradiation Surveillance Program as applied in Switzerland," ASTM STP 725 pp. 49-62.

2. Varga T, D.H. Njo, "The Selection of Specimen Types for Irradiation Surveillance Programs,"IAEA IWG RRPC, Special Meeting, 19.-21. Oct. 1981.

3. P.E. McConnel, W.L. Server, "Instrumented Impact Test Prodecures," C.S.N.I. No. 67 Specialist Meeting on Instrumented Precracked Charpy Testing, Palo Alto, 1.-3. Dec. 1980 EPRI NP-2102-LD Project 1757-1, California, USA, 1981, p. 1-1.

4. D.R. Ireland, "A Review of the proposed Standard Method of Test for Impact Testing Precracked Charpy Specimen of Metallic Materials," C.S.N.I. No. 67 Palo Alto, 1.-3. Dec. 1980, EPRI NP-2102-LD Project 1757-1, California, USA, 1981, p. 1-25.

5. T. Varga, D.H. Njo, G. Prantl, "ASK Procedure for Instrumented Precracked Charpy - Type Tests," C.S.N.I. No. 67 Palo Alto 1.-3. Dec. 1980, EPRI NP-2102-LD Project 1757-1, California, USA, 1981, p. 1-65.

6. E.N. Klausnitzer, A. Gerscha, G. Hofer, "KWU Experience with Instrumented Precracked Charpy Testing," C.S.N.I. No. 67 Palo Alto 1.-3. Dec. 1980 EPRI NP-2102-LD Project 1757-1, California, USA, 1981, p. 1-117.

7. W.L. Server, "Linear Elastic and Elastic-Plastic Fracture Toughness Using Instrumented Impact Testing," C.S.N.I. No. 67 Palo Alto 1.-3. Dec. 1980, EPRI Np-2102-LD Project 1757-1, California, USA, 1981, p. 1-131.

8. F. Salzmann, T. Varga, "Ultraschallverfahren zur Bestimmung der Rißinitiation an Kompaktzugproben," Material + Technik 11, (1983) Nr. 3, S. 109.

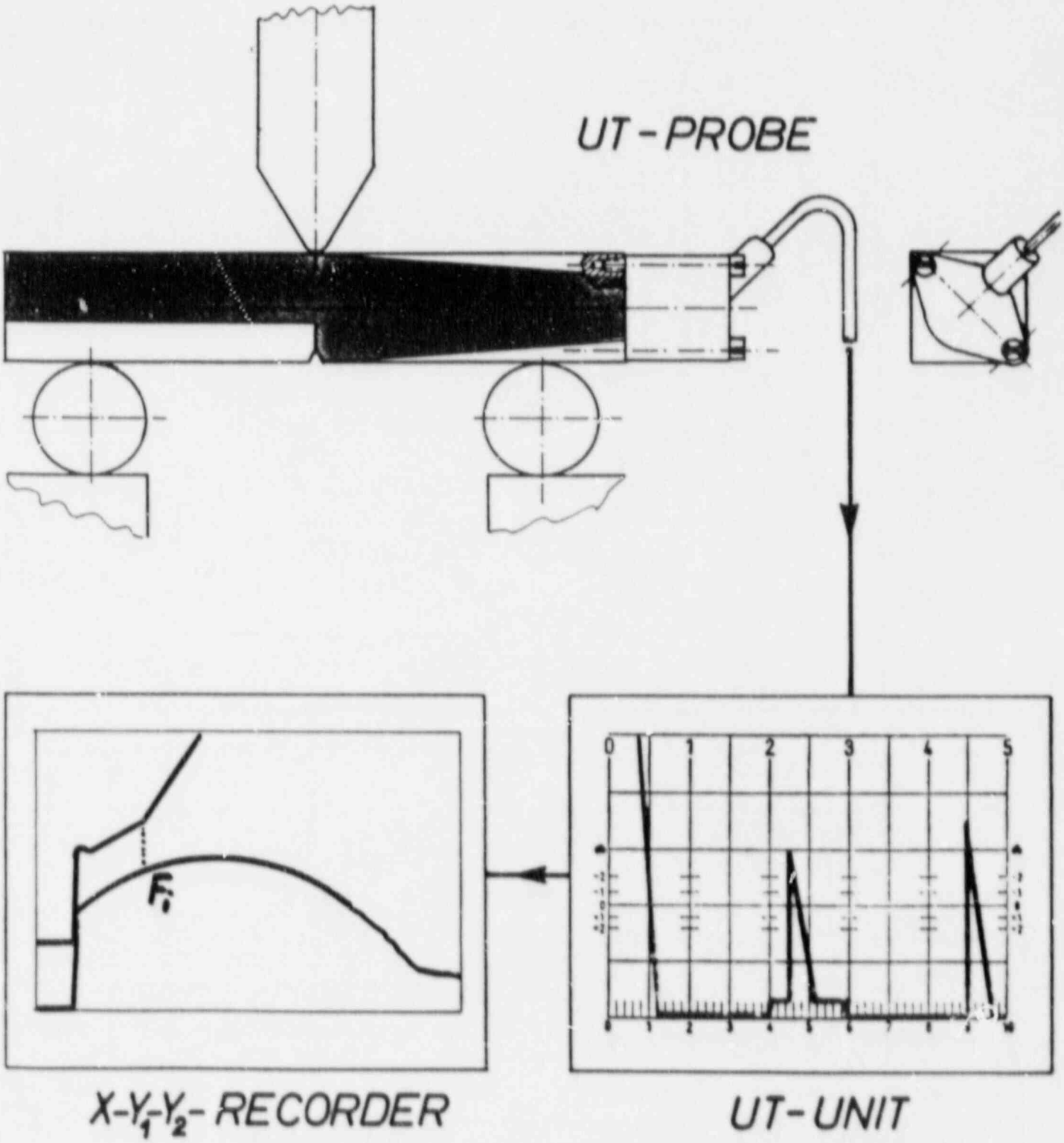

Fig. 1: Experimental arrangement for UT initiation measurement.

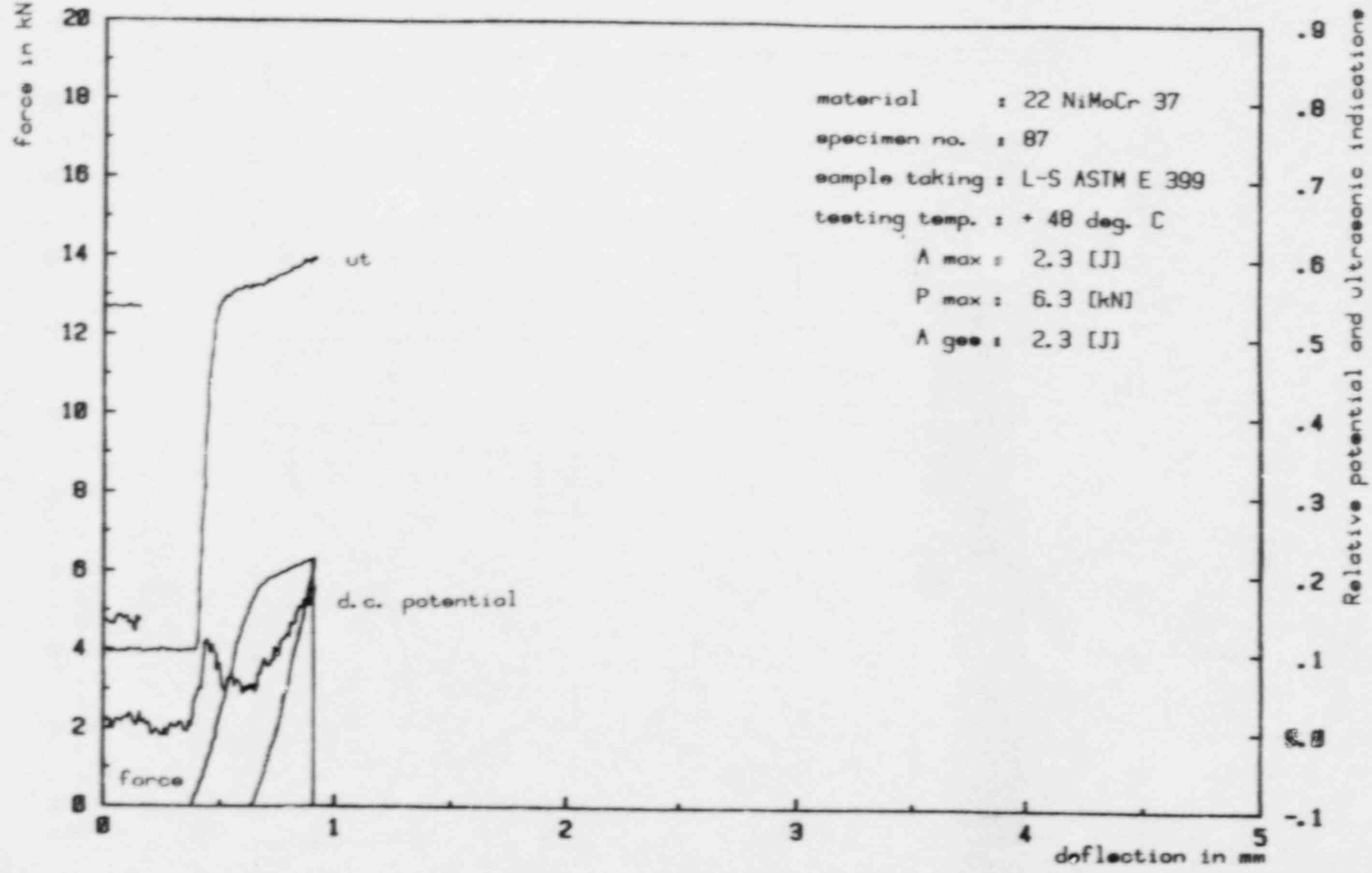

Fig. 2: Force / potential / ut - indications over deflection; instrumented bending test on fatigue precracked charpy - type specimen (d.c. I = 10 Amp).

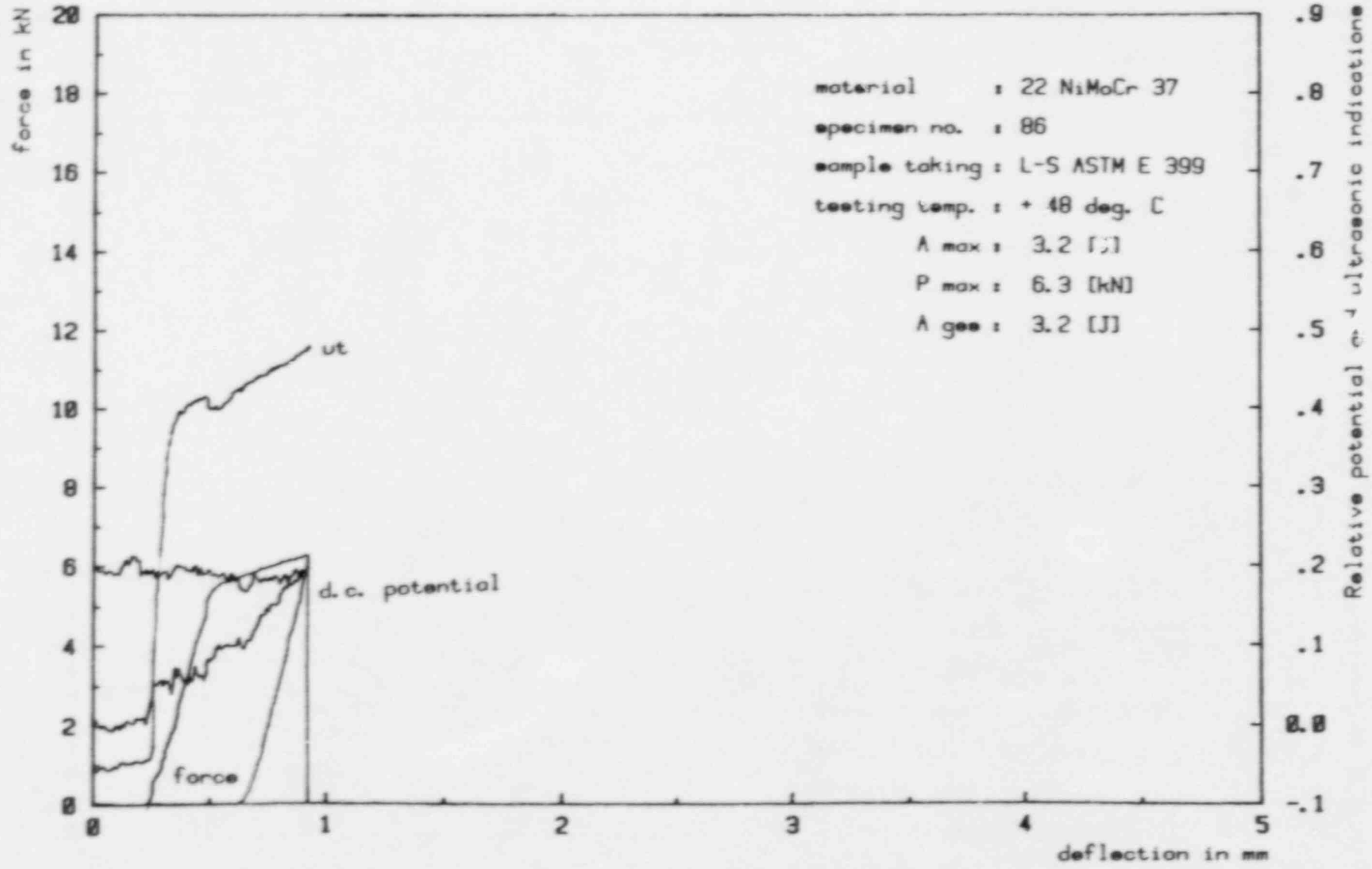

Fig. 3: Force / potential / ut - indications over deflection; instrumented bending test on fatigue precracked charpy - type specimen (d.c. I = 10 Amp).

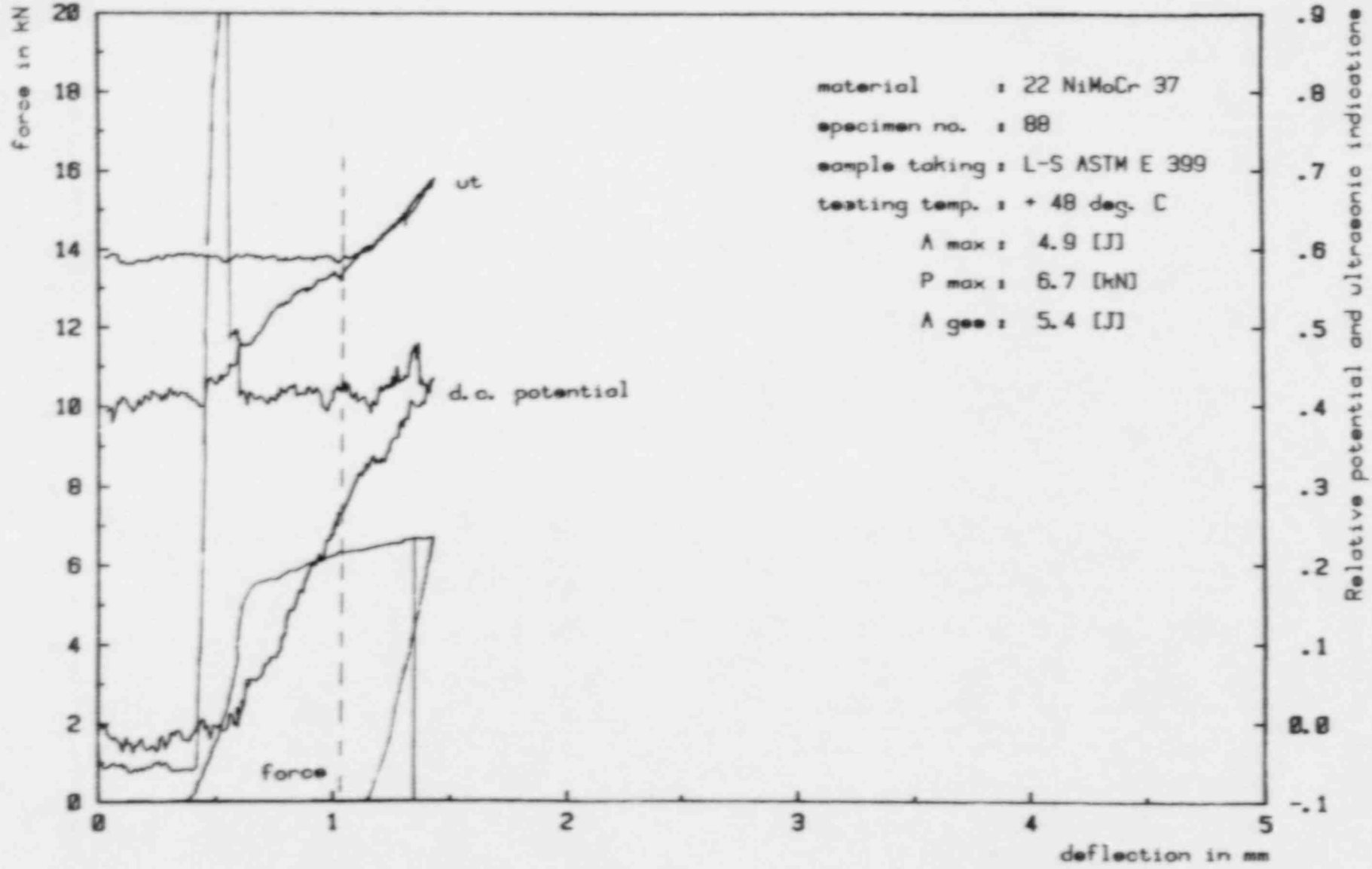

Fig. 4: Force / potential / ut - indications over deflection; instrumented bending test on fatigue precracked charpy - type specimen (d.c. I = 10 Amp).

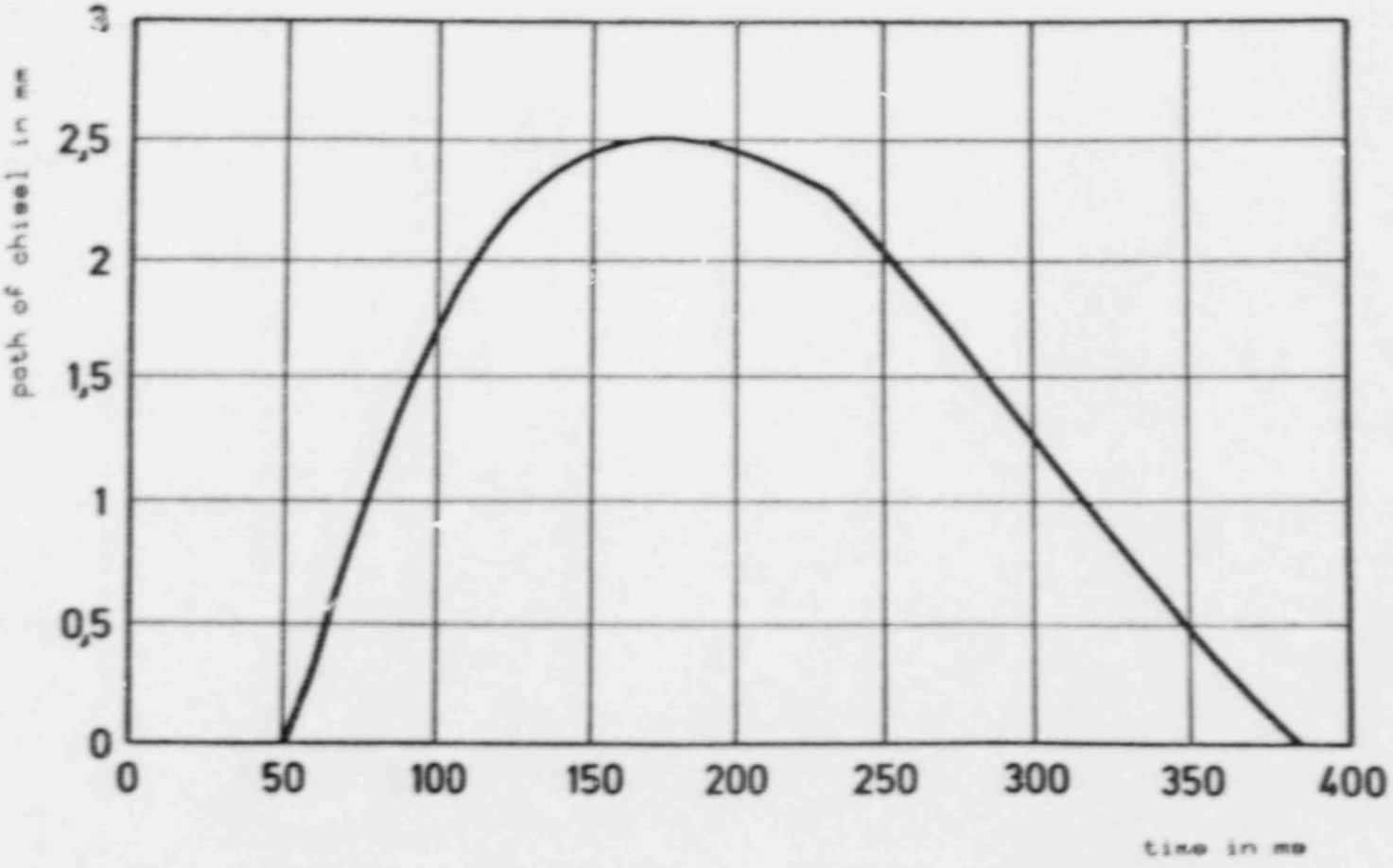

Fig. 5: Path of chisel over time.

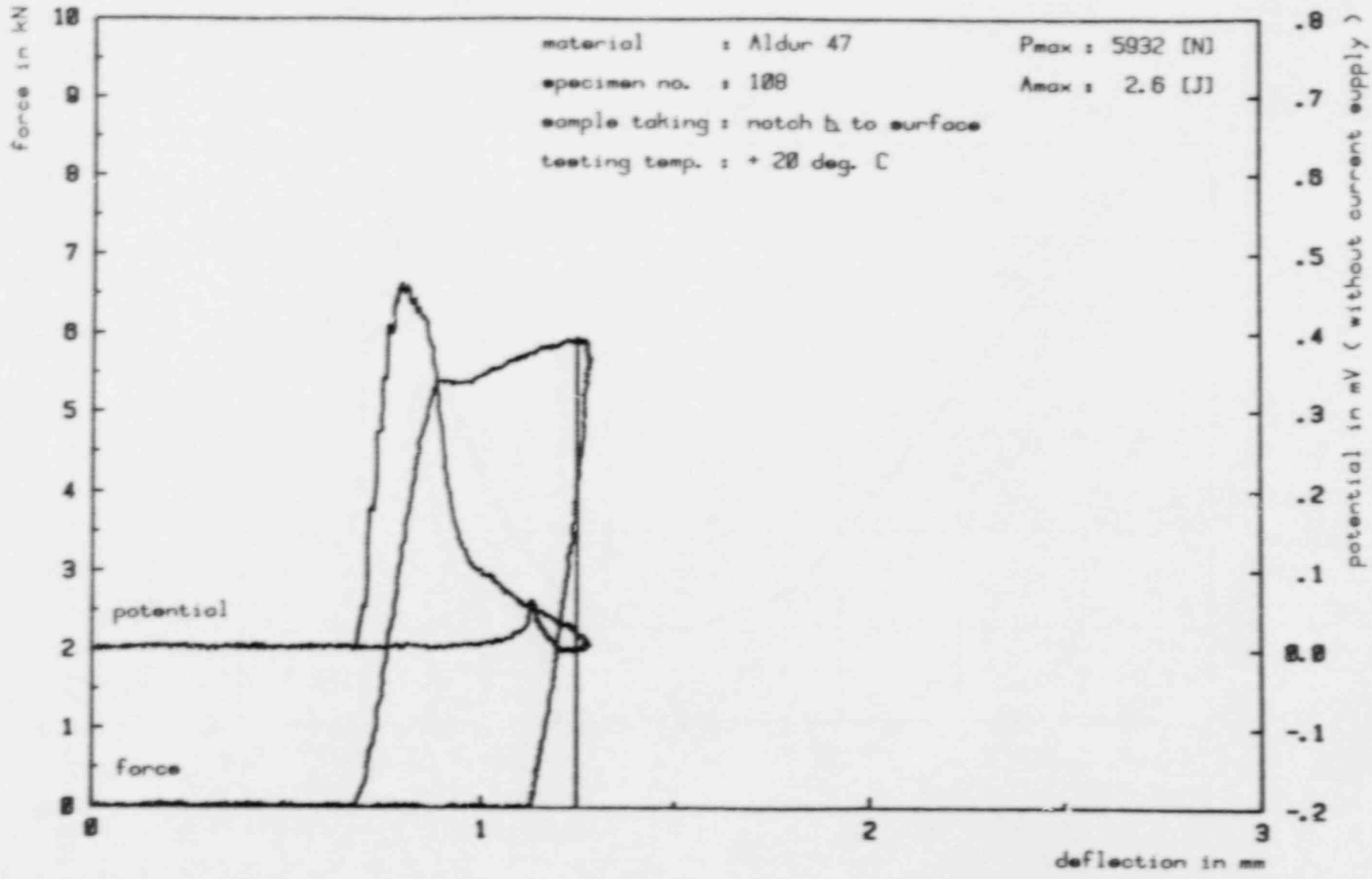

Fig. 6: Force and potential over deflection; increase and decrease of potential and force during an instrumented notched bar impact test on a fatigue precracked specimen; limited deflection.

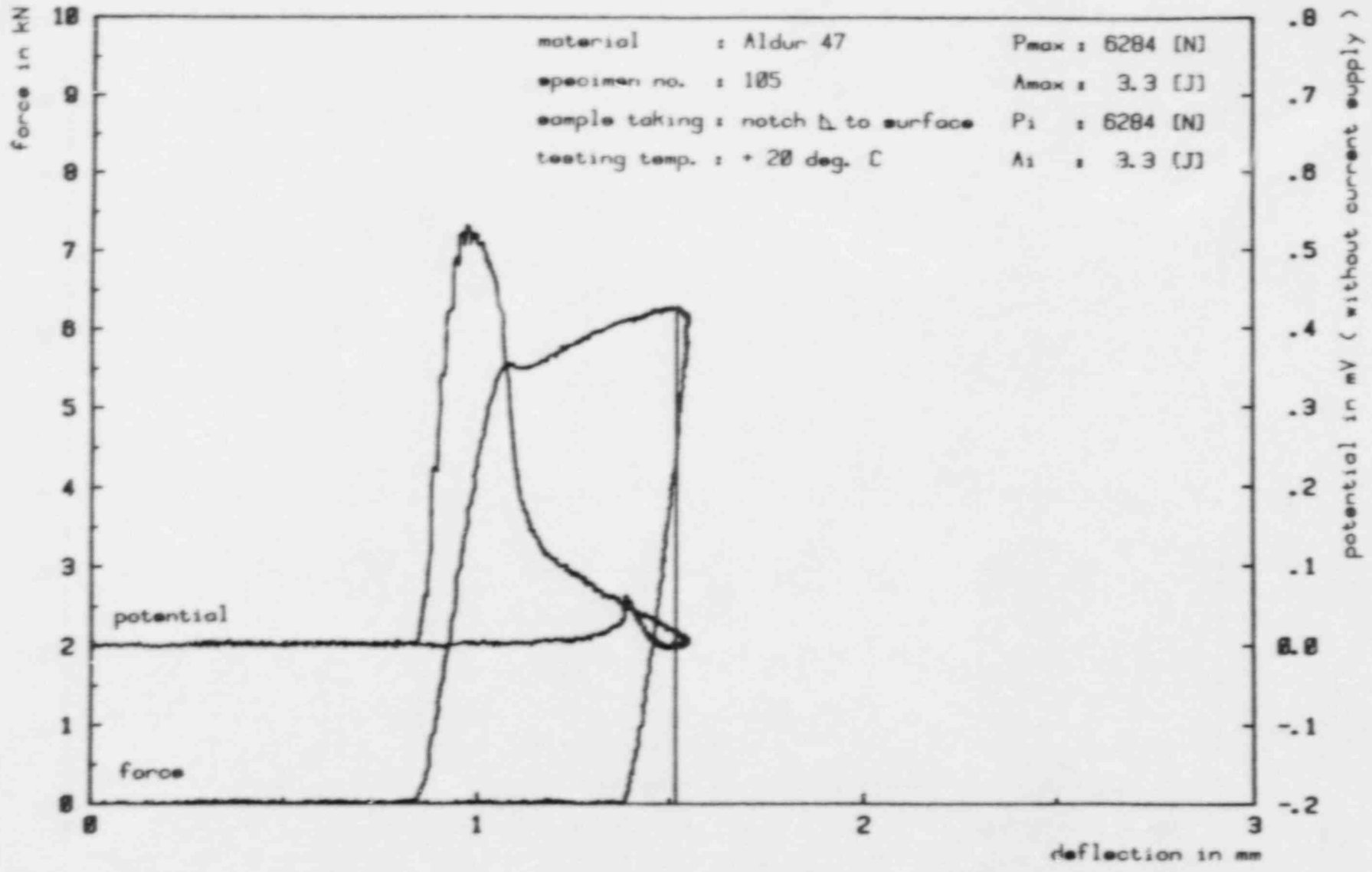

Fig. 7: Force and potential over deflection: increase and decrease of potential and force during an instrumented notched bar impact test on a fatigue precracked specimen: limited deflection.

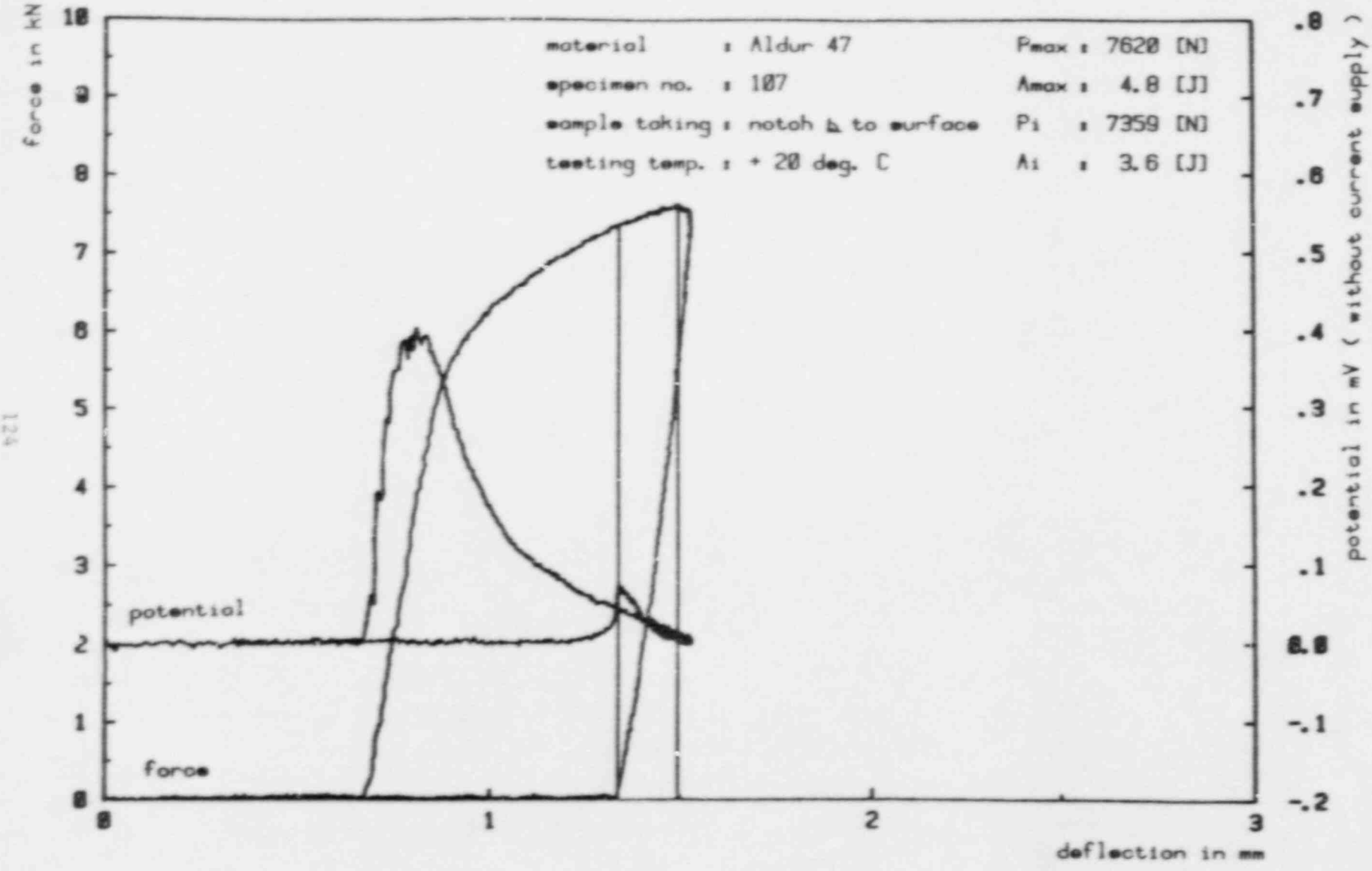

Fig. 8: Force and potential over deflection: increase and decrease of potential and force during an instrumented notched bar impact test on a fatigue precracked specimen: limited deflection.

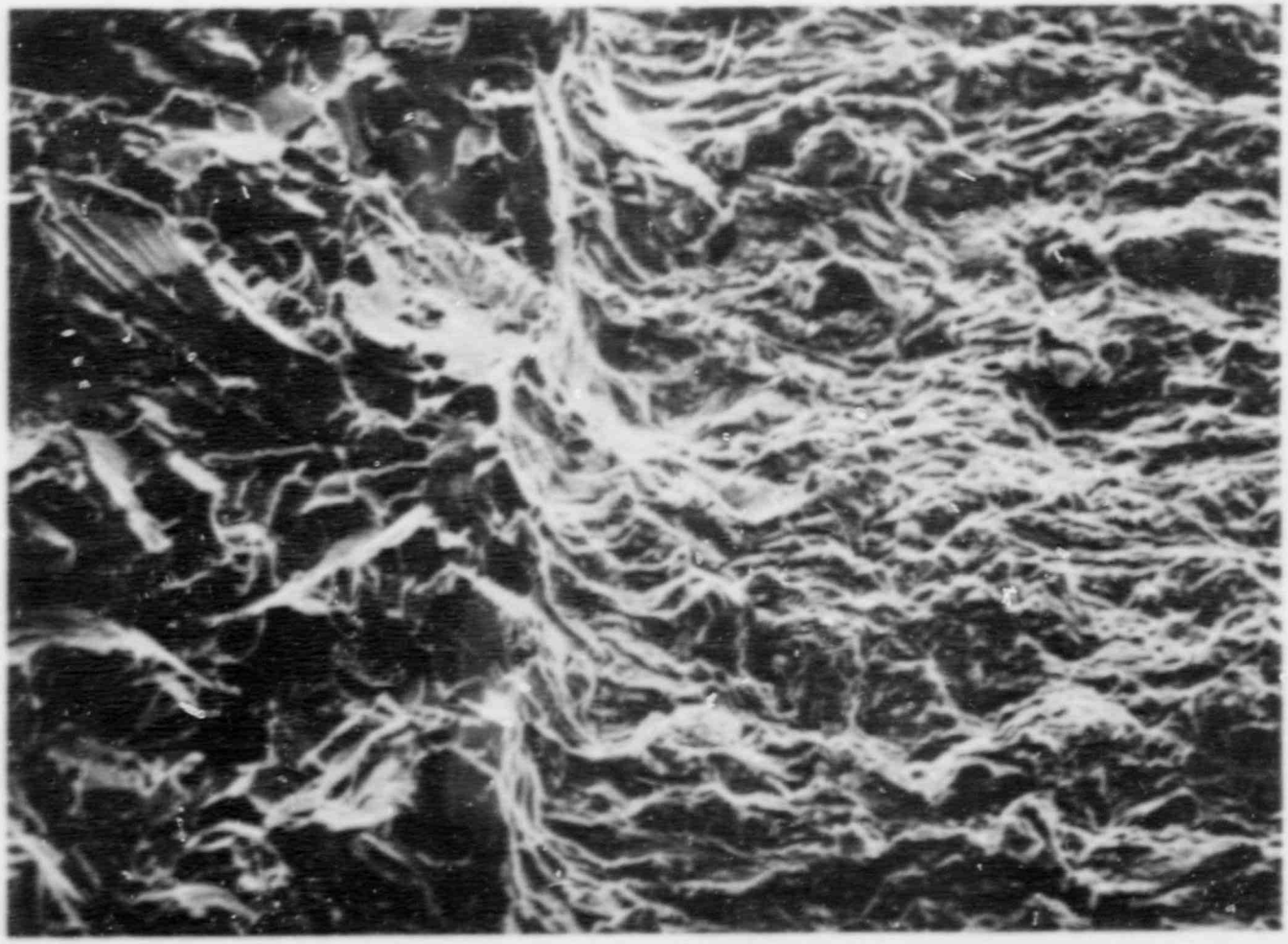

Fig. 9: Scanning elektron micrograph appropriate to diagram fig. 6 (specimen no. 108); enlargement 310 : 1.

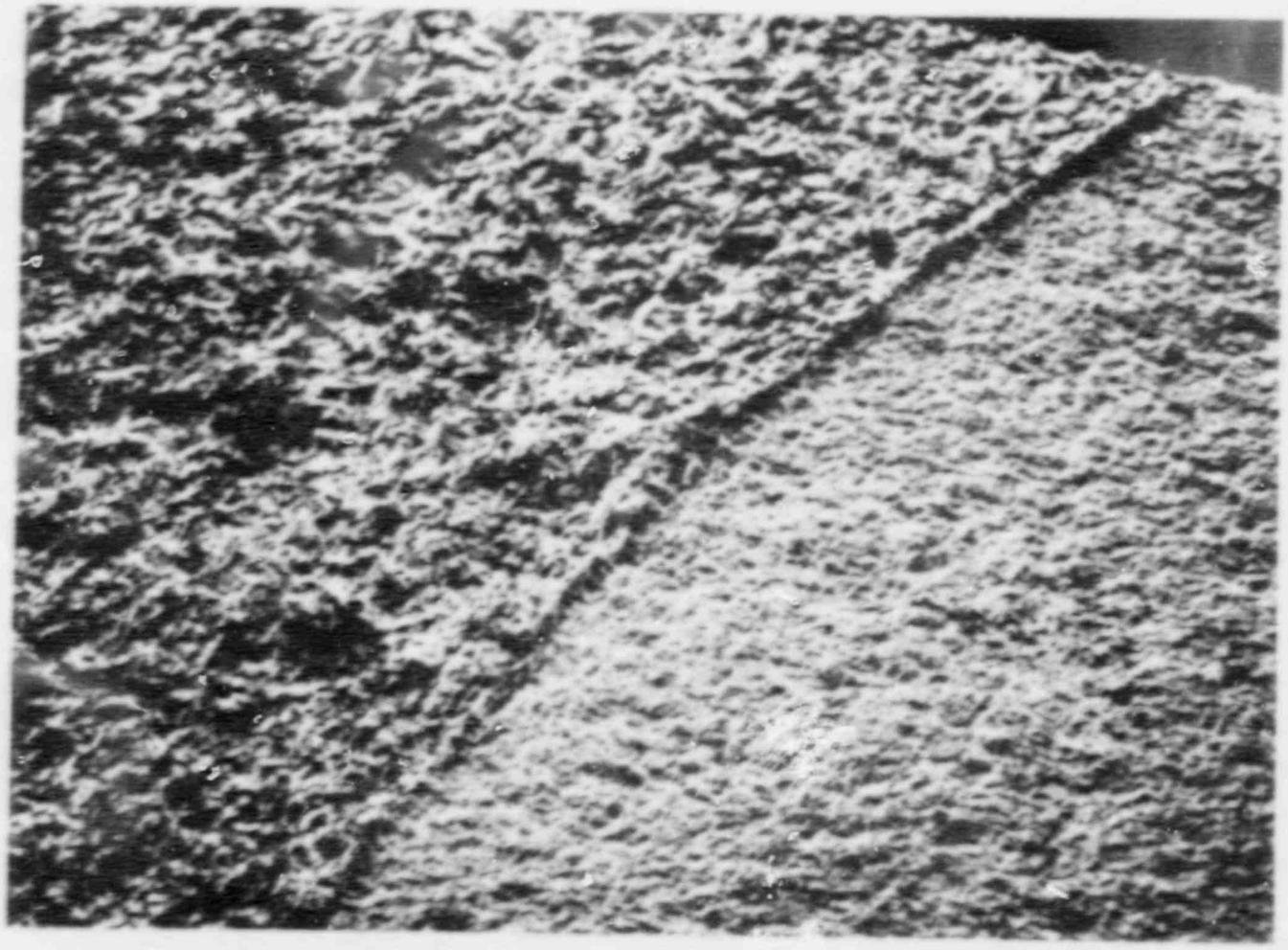

Fig. 18a Scanning elektron micrograph appropriate to diagram fig. 7
(specimen no. 185); enlargement 31.5 : 1.

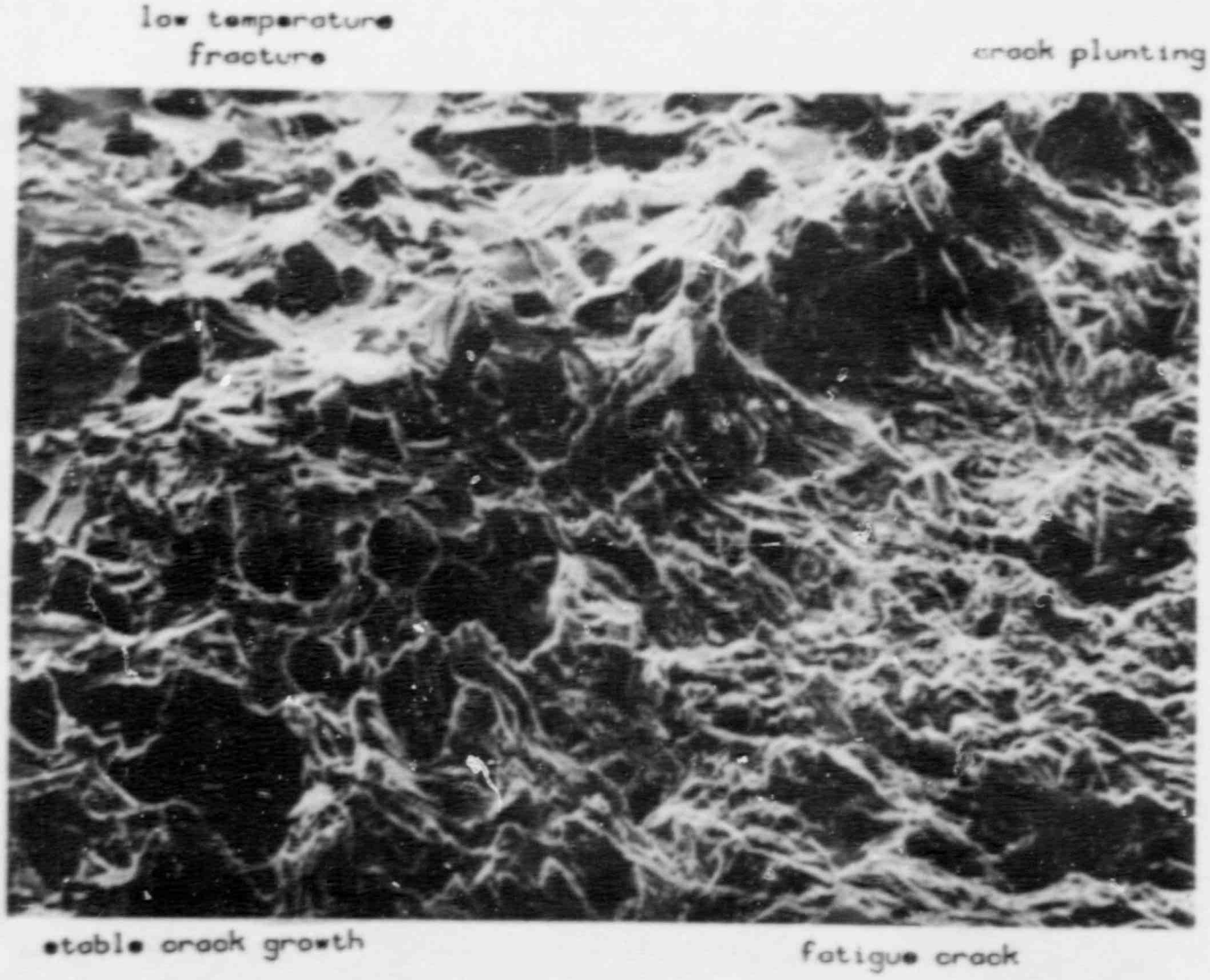

Fig. 10b: Scanning elektron micrograph appropriate to diagram fig. 7
(specimen no. 105); enlargement 261 : 1.

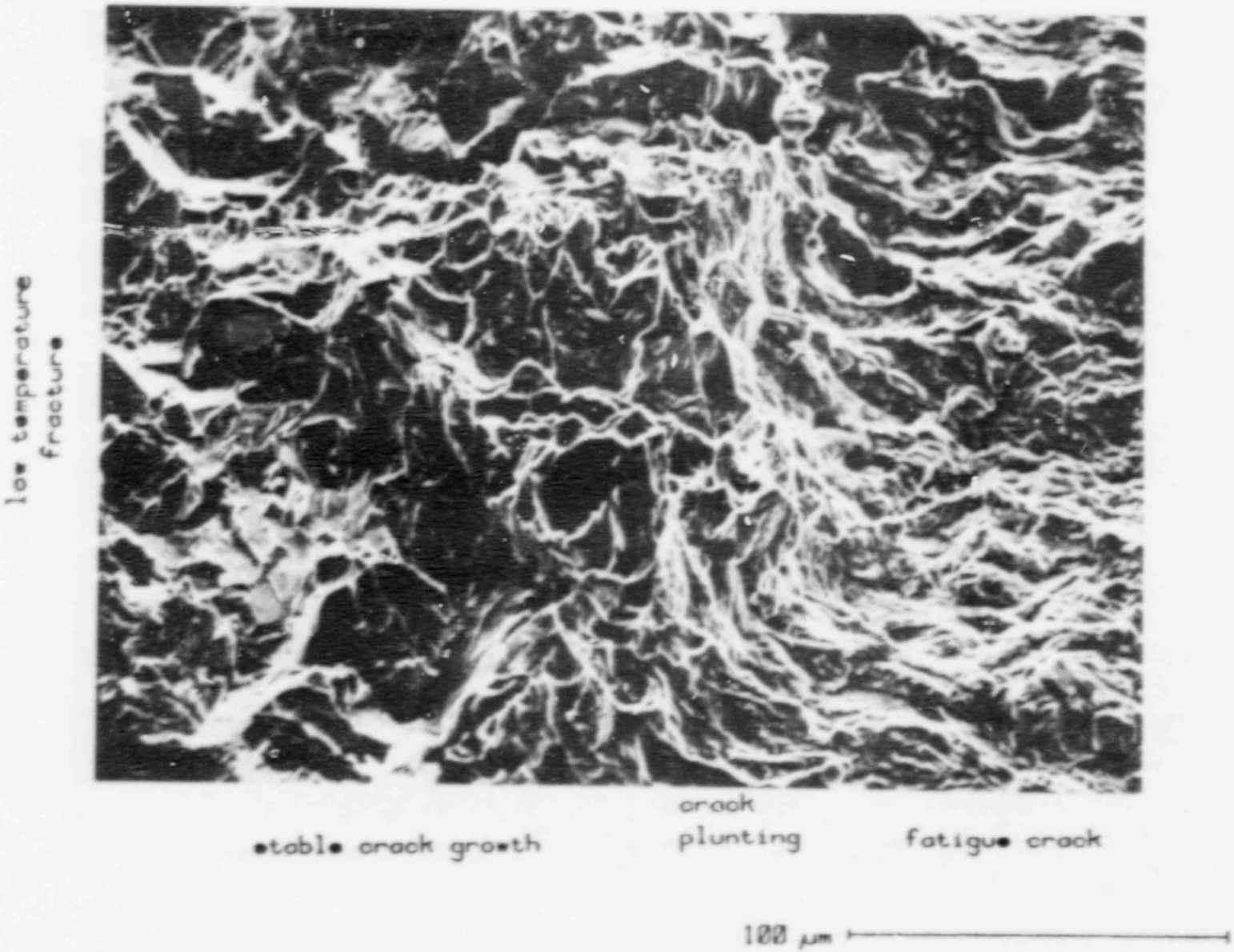

Fig. 11: Scanning elektron micrograph appropriate to diagram fig. 8
(specimen no. 107); enlargement 294 : 1.

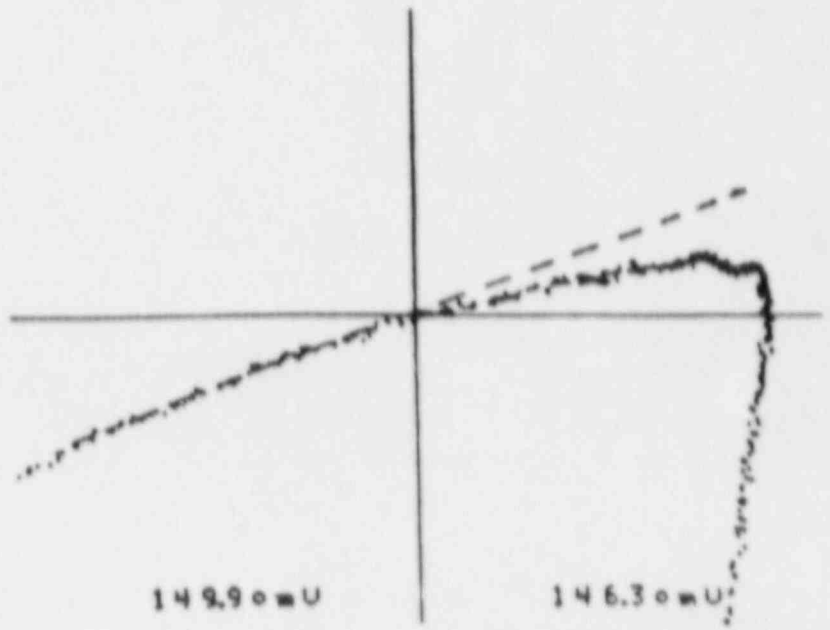

Fig. 12: Enlarged force over deflection diagram of specimen no. 107.

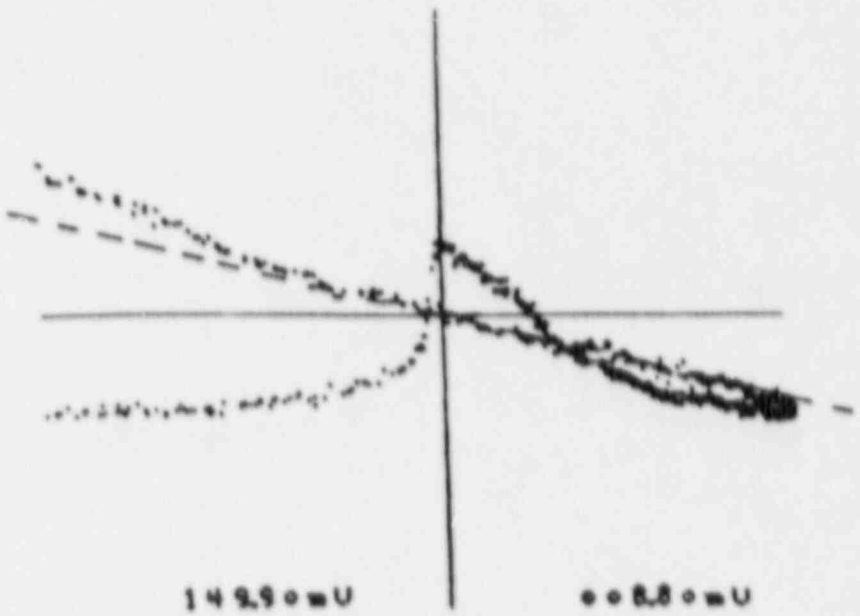

Fig. 13: Enlarged potential over deflection diagram of specimen no. 107.

OECD/CSNI - Workshop on Ductile Fracture Test Methods
Paris - April 17:19, 1985

C. Fossati - CISE, Segrate, Milan
S. Ragazzoni - ENEL-CRTN, Milan

EPFM TEST METHODS FOR PRESSURE VESSEL STEELS CHARACTERIZATION

Use of elastic-plastic fracture mechanics for the integrity assessment of nuclear structural components, which generally exhibit ductile upper shelf behavior under operating conditions, is now entering the common engineering practice. Structural integrity criteria, based upon EPFM concepts, have recently been developed [1,2], which should result in a more realistic prediction of the fracture behavior of flawed structures somewhat alleviating the high degree of conservatism currently included in design.

Defect stability analyses rely upon the measure of parameters characterizing the material fracture resistance. Many experimental techniques have been proposed: it is however fairly well recognised that further developments are required in order to come to a well established and standardized procedure for assessing the fracture resistance of ductile structural materials.

Research and Development Division of ENEL started a research project on "Structural materials integrity and stability" [3] focused on primary pressure boundary system components, with particular reference to the pressure vessel and the primary circuit piping. The program is developed jointly with CISE, where overall of the experimental work is carried out.

In the frame of this project some main topics are being addressed i.e. fracture mechanics, environmental fatigue and intergranular stress corrosion cracking.

In the fracture mechanics area, the program is focused on ductile fracture test methods development and on the characterization of structural materials of plant components. Fracture toughness

properties under static as well as dynamic loading conditions are measured for the components and weldments of the primary circuit system [4]. An extensive structural material characterization is indeed felt to be necessary in view of the high safety and reliability requirements of nuclear plants [3,5].

Measured mechanical properties are being included in a Data Base of plant materials, to be used as a reference for in-service inspection and surveillance programs.

The test methods for pressure vessel steels ductile fracture resistance characterization, used in the frame of the aforementioned program, are hereafter shortly outlined, together with some related problems.

- Initiation fracture toughness and ductile tearing resistance

The single specimen unloading compliance (U.C.) test method is used. Tests are performed following ASTM E813 standard [6] on 20% side grooved CT specimens, usually 1" thick. The specimen geometry, Fig. 1, slightly differs from the recommended one in that the pin holes spacing has been reduced (according to E399 [7] geometry) to avoid plasticity problems in the specimen arms. Standard E813 flat bottom holes are used for clevises. J_{IC} value is determined using a linear fit to data points between 0.15 and 1.5 mm exclusion lines and the theroretical blunting line with slope $2\sigma_{flow}$, as per E813 procedure, Fig. 2.

In the initial blunting stage, U.C. test method often yields J-Δa points which do not fall on the $2\sigma_f$ blunting line, resulting in no-apparent crack growth or in an apparent "negative" growth, Fig. 3. Rotation, friction and indentation effects have been suggested as possible causes of this behavior [8].

Different technicalities and/or data reduction methods are used at present to handle this problem; in our testing procedure, to avoid negative crack growth values, data reduction includes a shift of the Δa axis origin. On the other hand, experimental results of specific tests [9] on different specimen geometries (CT, CCT) seem to indicate that, during initial loading, crack length doesn't increase up to initiation.

The need of further investigation for a better understanding and description of the blunting stage, in order to obtain a re- determination of the onset of crack growth and initiation is, is now being widely recognized.
Following this, both experimental and theoretical work on this is under way at CISE.

Initiation J value is not the only useful parameter in EPFM, since design against initiation may be overconservative for structural components which, in the operating temperature range, behave in a fully ductile manner and can accomodate, by plastic deformation, even large crack growth. In such instances, the use of the J-resistance curve concept, and associated parameters like the tearing modulus, can allow a more realistic approach to the stability assessment.

The influence of specimen size, testing technique and data reduction method on these parameters,has not yet been well assessed. Use of small size specimens for J-R curve determination only allows small amounts of crack growth. The need may however arise in structural assessment of accounting for large crack growths: if this is the case, the validity of J-R curves obtained on small size specimens has to be checked beyond the limits of a J controlled growth.

Specimen size effect on the fracture resistance behavior, namely on initiation and J-R curve, is now being investigated at CISE by testing CT specimens from 1" to full plate thickness.

A specimen size effect is indeed recognized. Plain 4" thick CT specimens of A533B Cl 1 steel tested at room temperature underwent cleavage instability after a small amount of stable tearing, whereas side grooved 1" specimens behaved at the same temperature in a fully ductile manner.

Some concern may so arise in the use of fracture toughness data obtained on small size specimens: in the transition region an increase in the crack tip constraint may cause a change of the fracture mechanism, leading to a shift towards higher temperatures of measured transition range.

A correction has been proposed [10] to properly account for this effect.

J-R curves are determined by means of the U.C. testing method. A power law function is used to fit experimental J-Δa points, Fig. 4. Deformation J is being used, but attention will also be devoted to the modified J parameter developed by Ernst [11], use of which should overcome the inaccuracies due to growth, yielding an effective indipendence from crack growth and specimen geometry.

- Dymamic fracture toughness

The need of accounting also for dynamic loading conditions in defects assessment is well established: the LEFM approach of ASME code [12] includes dynamic toughness data to draw the reference K_{IR} curve. Such an approach should be pursued in the elastic-plastic regime as well: not only initiation values but also dynamic resistance curves should characterize material fracture behavior.

Dynamic toughness characterization of pressure vessel steels has therefore been included in the "Structural materials integrity and stability" program.

Precracked Charpy-V specimens (PCC_V) are impact tested in an instrumented pendulum; CISE testing procedure substantially follows ASTM [13] and EPRI [14] proposals. Upper shelf dynamic initiation toughness is evaluated as J_{ID} at maximum load: the assumption is therefore made of no subcritical growth before maximum load, which has been proved at least for A533B steel [15].

A special testing technique (Very Low Blow, VLB) has been developed [15] for dynamic resistance curve determination.

The technique again makes use of PCC_V specimens impact tested on the instrumented pendulum: different blow angles of the hammer yield different crack extensions which can be easily marked by heat tinting. A multispecimen dynamic J-Δa curve is so obtained. Data reduction is performed in a quite similar way as for static tests (following ASTM E813 recommendations), Fig. 5, except for the blunting line which is experimentally determined.

Again specimen size effects should be carefully considered. The fairly limited amount of crack extension (less than .5 mm) allowed within the limits of a J controlled growth suggests the use of the modified J parameter.

- Final remarks

· A direct measurement of the fracture resistance properties, under both static and dynamic loading conditions, is to be pursued for primary pressure boundary structural materials.

· In the ductile regime, material behavior up to initiation and in particular the real consistancy of the blunting stage are to be better clarified.

· Application to actual structures may require J-R curves with large Δa values not influenced by specimen geometry and size. Geometry, size, and also loading mode effects are important items still to be addressed in R&D programs.

· Dynamic resistance curves should be included in a full material characterization in the elastic-plastic regime.

REFERENCES

(1) Kumar V. et al. "An Engineering Approach for Elastic--Plastic Fracture Analysis", EPRI NP 1931, 1981.

(2) Milne I. "Failure Analysis in the Presence of Ductile Crack Growth", Mat. Scienc. and Eng., 39, 1979.

(3) Borgese D., Pascali R., Regis V. "ENEL's R&D Programme on Material and Water Chemistry for PWR and BWR Power Plants", US-NRC SURRY Programme, TAG Meeting, Rome, 24 Sept. 1984.

(4) Barbesino F., Fossati C., Ragazzoni S. "Static and Dynamic Fracture Toughness Characterization on SA508 Forging and SA533 Welded Plate" 5th ICPVT Conference, S. Francisco, 9-14 September 1984.

(5) UKAEA, "An Assessment of the Integrity of PWR Pressure Vessels", Second report by a study group under the Chairmanship of Dr. W. Marshall, C.B.E., F.R.S. 1982.

(6) ASTM, "Standard Test Method for J_{IC}, a Measure of Fracture Toughness", E813-81, 1982.

(7) ASTM, "Standard Test Method for Plane-Strain Fracture Toughness of Metallic Materials", E 399-81, 1982.

(8) Voss B., and Mayville R.A., "On the Use of Partial Unloading Compliance Method for the Determination of J-R Curves and J_{IC}", Symposium on User's Experience with Elastic--Plastic Fracture Toughness Test Methods, 20-22 April 1983, Louisville, Kentuchy.

(9) Angelino G. and Fossati C., "J_{IC} and J-R Curve Determination on High Toughness Materials and on Different Test Geometries" 5th European Conference on Fracture, Lisbon 17-21 September 1984.

(10) Merkle J.G. "An Examination of the Size Effects and Data Scatter Observed in Small-Specimen Cleavage Fracture Toughness Testing" NUREG/CR-3672 (ORNL/NUREG/TM-9088), Oak Ridge National Laboratory, Oak Ridge, Tenn., April 1984.

(11) H.A. Ernst, "Material Resistance and Instability Beyond J Controlled Crack Growth", presented at the second Int. Symposium on Elastic Plastic Fracture Mechanics, October 1981.

(12) ASME, Boiler and Pressure Vessel Code - Section III, 1977.

(13) ASTM, "Proposed Standard Method of Test for Instrumented Impact Testing of Precracked Charpy Specimens of Metallic Materials", E 24.03.03, 1980.

(14) Server, W.L. "Verification of the EPRI Dynamic Fracture Toughness Testing Procedures", ETI TR 75-42, 1975.

(15) Angelino G., Fossati C. "Dynamic Elastic-Plastic Characterization of Nuclear Pressure Vessel Material", 5th International Conference on Fracture, Cannes, 1981.

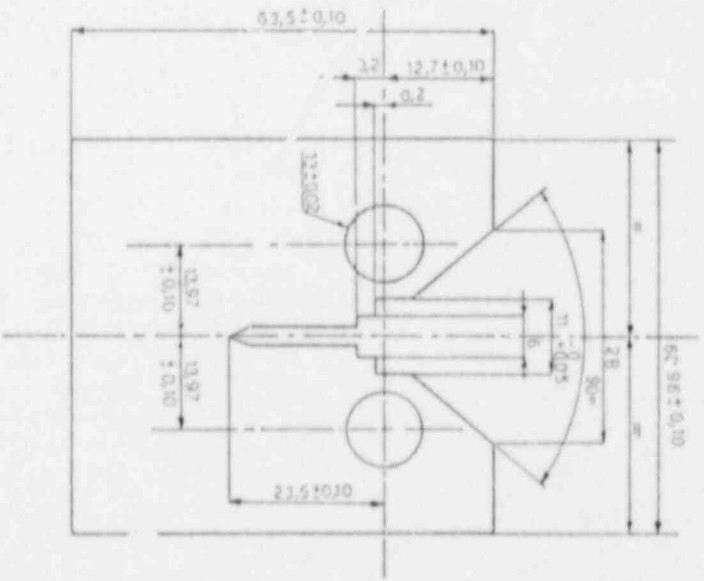

Fig. 1 - CT specimen geometry (1")

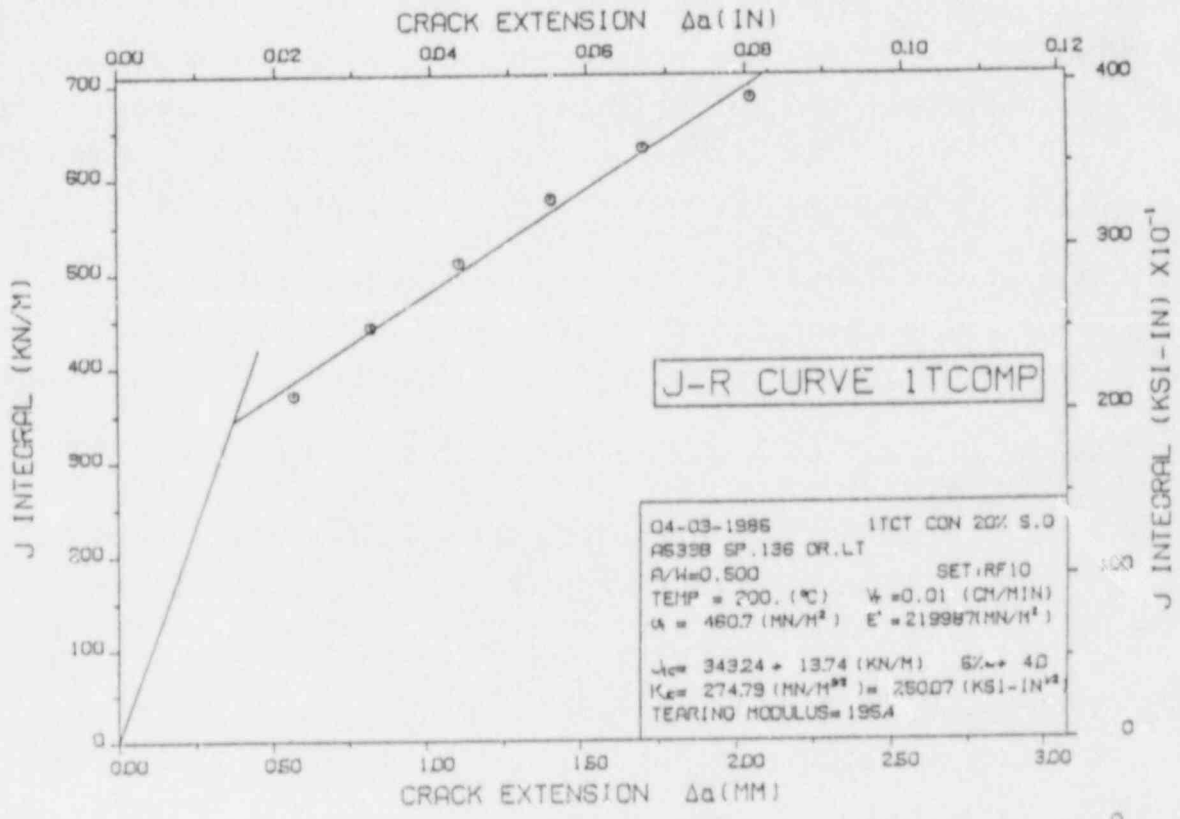

Fig. 2 - J_{IC} determination according to ASTM E813 - A533 B steel at 200 °C.

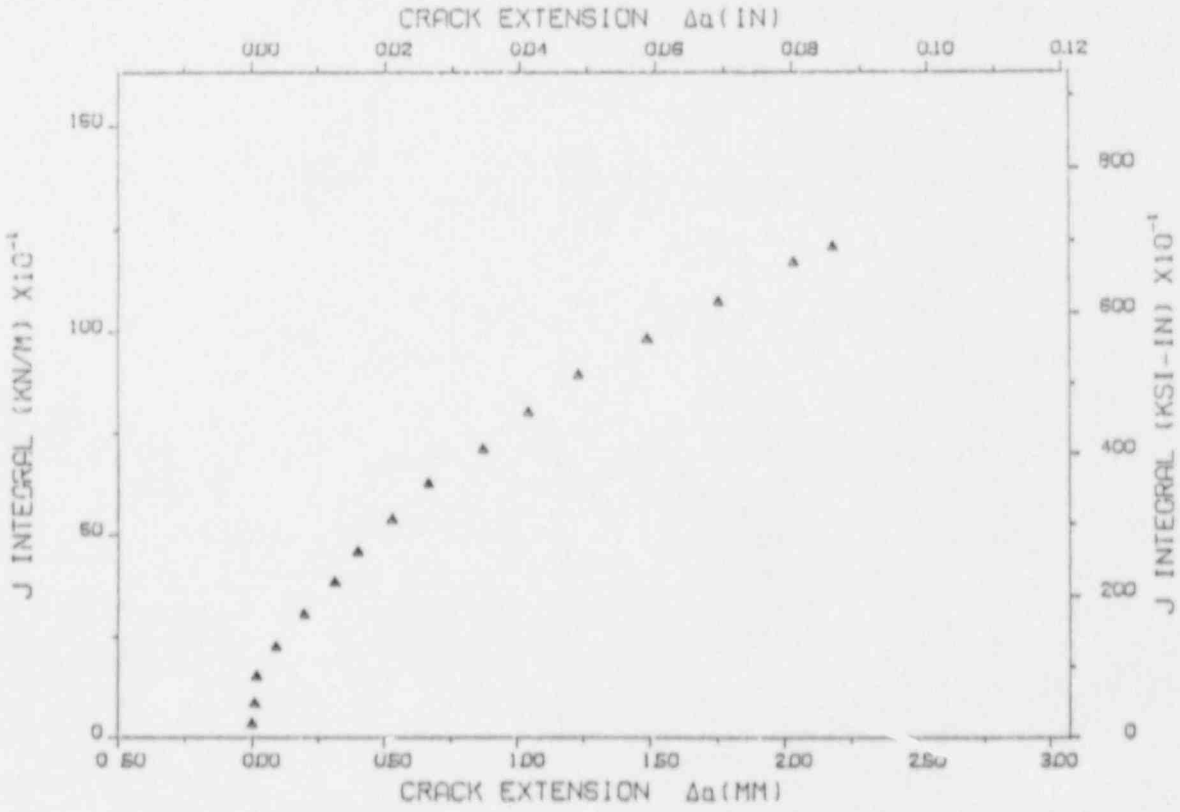

Fig. 3 - J-R curve obtained via U.C. method - AISI 304 stainless steel at 288 °C.

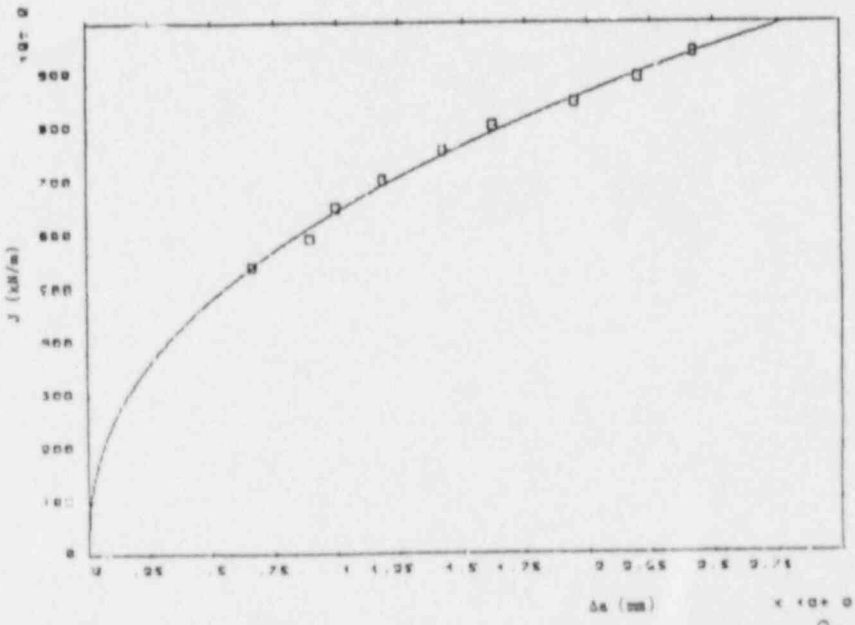

Fig. 4 - Power law fitting of J-R curve - A533 B steel at 20 °C.

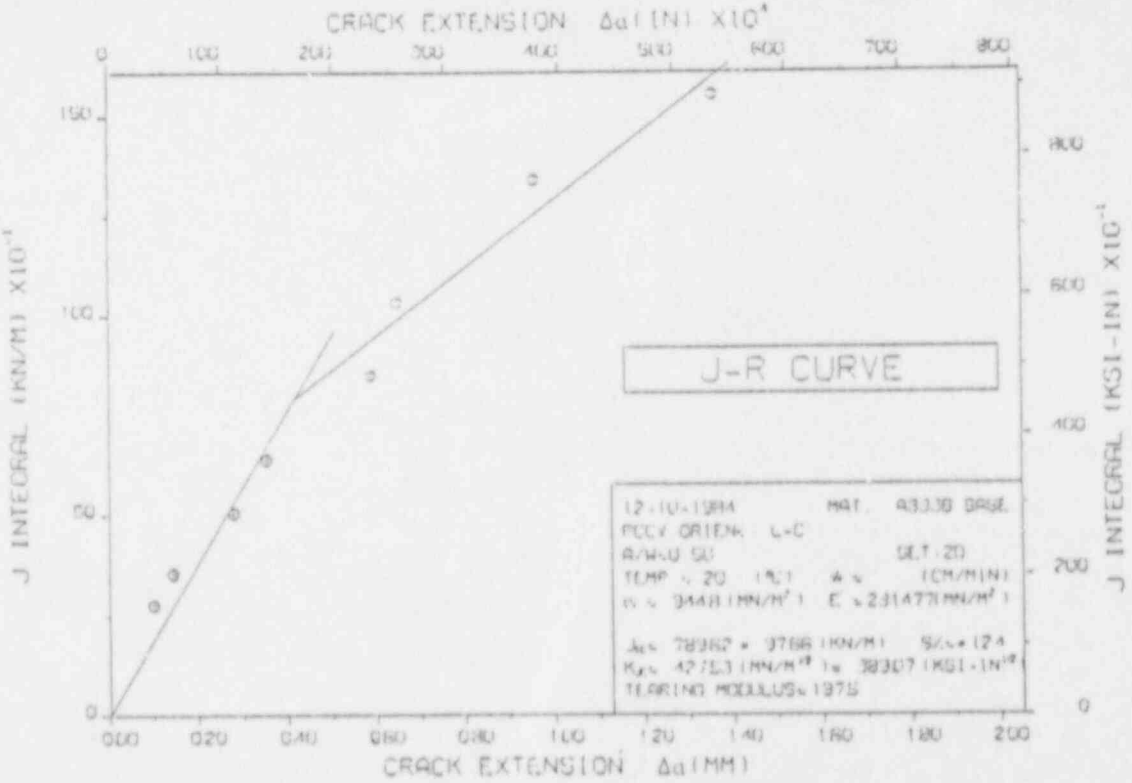

Fig. 5 - Dynamic J-R curve determined via VLB technique - A333 B steel at 20 °C.

STATUS OF SPAIN IN IRRADIATED SPECIMENS J_{IC} TEST DEVELOPMENT

Antonio Tanarro Aparicio

TECNATOM, S.A. Km 19 CNI. Madrid-Irún
San Sebastian de los Reyes, Madrid, Spain

INTRODUCTION

This report summarises the conditions under which, TECNATOM decided to develop a testing procedure for determining the plane strain J_I-R curve.

The procedure will be finished before the end of this year.

SUMMARY

In Spain there are four Nuclear Power Plants with Westinghouse reactor vessel surveillance program and early there will be another one. Their surveillance capsules contains ½ T-CT (compact tension) and TPB (three point bend) fracture mechanics specimens. These specimens were machined and fatigue precracked according to ASTM E 399 "Standard test Method for Plane-Strain Fracture Toughness of Metallic Materials" (fig 1).

In light of current requirements of 10CFR, Part 50 and NUREG 0744 "Resolution of the Reactor Vessel Materials Toughness Safety Issue", TECNATOM decided to develop a testing procedure according to ASTM E 813 "Standard Test for J_{IC}, A Measure of Fracture Toughness" by unloading compliance method for determinig the plane strain J_I-R curve taking into account recent issues about this theme (ref. 1).

The need for the engineering method proposed in the mentioned NUREG (ref. 2) is dictated by the fact that some materials (primarily weld metals) used in RPVs will have Charpy V-notch (Cv) impact test upper shelf energy (U.S.E.) levels of less than 68 J. before the end of their design life. When RPV steel exhibits a Cv U.S.E. level of less than 68 J., the requirements of Title 10 of the Code of Federal Regulations (10 CFR 50) are not being met, and a safety analysis must be performed to ensure continued safe operation of the reactor.

The former analysis needed an experimental procedure to obtain material fracture parameters in a form compatible with theoretical concepts. The single specimen unloading compliance method was proposed and recommended in the mentioned paper.

Current test procedures recommend a compact specimen configuration similar as described in ASTM E 399 (fig 1), but modified to permit load-line displacement measurement (fig 2). This measurement is needed by procedures presented in ASTM E 813 (ref. 3) and ref. 1 though it is not possible to do it in specimens with geometry according to ASTM E 399. This is why we intend to measure the displacement at the front face of the specimen and, after that, to apply the elastic compliance expressions formulated by Saxena and Hudak in reference 4.

The major problems with the partial unloading compliance method which we have found, were the requirements of a very high accuracy, stability, and linearity of all components of the measurement and data adquisition system and of a low friction loading device.

Also we have found an apparent negative crack growth, which we think is induced by local plastic deformations and friction in the region of the loading bolts.

At this moment we have not finished the procedure although we are developing a computer program taking into account the computer interactive unloading compliance method proposed by Joyce and Gudas in ref. 5.

This testing procedure will be very useful for some current research programs in Spain about radiation embrittlement and fracture analysis.

REFERENCES

1. Albrecht, P, Andrews, W.R., Gudas, J.P., Joyce, J.A., Loss, F.J., Mc Cabe, D.E., Schmidt, D.W., and Van Der Sluys, W.A., "Tentative Test Procedure for Determinig the Plane Strain J_I-R Curve" Journal of testing and Evaluation. JTEVA, Vol. 10. No. 6, Nov. 1982, pp. 245-251

2. R.E. Johnson and others. "Resolution of the Reactor Vessel Materials Thoughness Safety Issue". NUREG - 0744 Division of Safety Technology Office of Nuclear Reactor Regulation U.S. Nuclear Regulatory Commission. Washington D.C. 20555

3. "Standard Test for J_{IC}, A Measure of Fracture Toughness" ASTM E813-81

4. Ashok Saxena and S.J. Hudak, Jr. "Review and extension of compliance information for common crack growth specimens" International Journal of Fracture, Vol. 14, No. 5, October 1978.

5. Joyce, J.A. and Gudas, J.P., "Computer Interactive J_{IC} Testing of Navy Alloys", Elastic-Plastic Fracture, ASTM STP 688, J.D. Landes J.A. Begley, and G.A. Clarke, Eds., American Society for Testing and Materials, 1979, pp. 451-468.

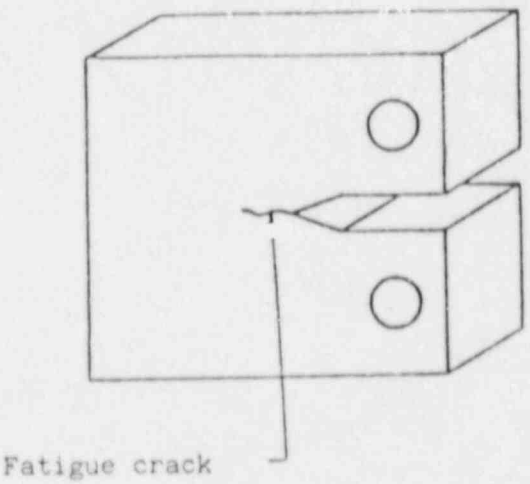

FIG. 1 COMPACT SPECIMEN ACCORDING TO ASTM E399

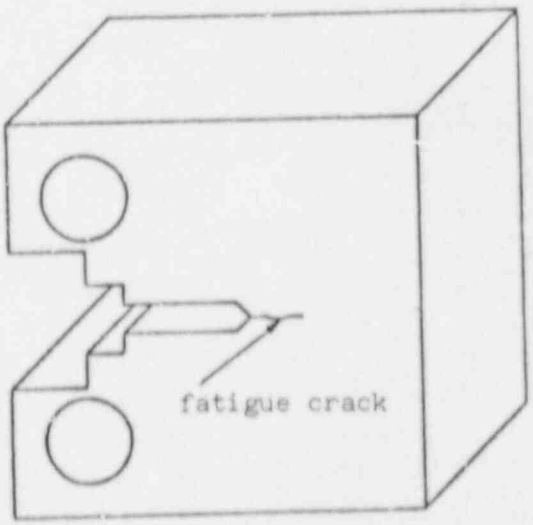

FIG. 2 COMPACT SPECIMEN ACCORDING TO ASTM E813

SESSION 3: Standardization of J-R Curve Test Procedures

CHAIRMAN: K.-H. Schwalbe
GKSS, FRG

PRESENTATION OF A FRENCH TENTATIVE TEST PROCEDURE FOR THE DETERMINATION OF THE FRACTURE RESISTANCE OF DUCTILE STEELS

M. BETHMONT

Electricité de France (EDF), Département Etude des Matériaux,
Les Renardières, 77250 Moret-sur-Loing, France

ABSTRACT

This tentative procedure has been drawn up by the task-group «J-Δa» of the French Group on Fracture (the list of members is given in Appendix).

INTRODUCTION

This paper deals with the project of a French test procedure for the determination of the fracture resistance of ductile steels which has been written recently. The discussion is still open about it in France.

The presentation is limited to the first part of this procedure in which an effort has been made to detail the experimental aspects of the single specimen elastic compliance method which is usually developed in French laboratories. This experimental part has been written with the intention of unifying the testing procedures of different laboratories and to permit direct comparisons of results with the assumption that the scatter from one laboratory to another would be significantly reduced.

COMMENTS ON THE PROJECT (see appendix)

Contents

The contents of this procedure is typical of French standards. This paper is limited to the comment of chapters 5 and 6 and annexes 1, 2 and 3 in which some experimental procedures are detailed.

Specimens

1 - In the objective of unifying the experimental procedures, it seemed better to recommend the sole use of Compact Tension specimens (appendix § 5.1). A new procedure would be necessary with bend specimens.
2 - With the same intention of unifying the specimen geometry, only one side-groove geometry is proposed.
3 - The remark about distance between the pin-holes (appendix § 5.3) comes from observations on specimens in austenitic stainless steel 316 L, for example ; for such a material, the model B is more appropriate.
4 - Only one condition is recommended for the pre-cracking of the specimens : the maximum load should never exceed 0.4 P_L (appendix § 5.4). In ductile fracture resistance measurements, the test is carried out on a material which fails in the ductile mode and there is no reason to limit the range of ΔK during pre-cracking.

Equipment

1 - The clevis geometry recommended in AFNOR French Standards is the same as in ASTM Standards (appendix § 5.1). It was calculated that with the standard clevis, the pins are free of friction if the load line opening is approximatively less than 7 mm, for a CT25 specimen. In the case of the austenitic stainless steels, the opening may reach 15 mm. It is the reason why a different clevis is proposed with a larger flat part in the pin-holes. In addition, the angle of the clevis in contact with the pin is rounded in order to minimize the plasticity and consequently the friction at this point.

2 - Again with the intention to keep pins free of friction as long as possible during the test, it is recommended to center properly the pins on flat parts. Unfortunately, it is not possible to quantify simply this recommendation.
3 - In annex 2, methods of fixture alignment control are proposed. For example in A.2.3., it is proposed to utilize a CT specimen fitted with a deformation gage which makes possible to quantify the misalignment of the fixture.
4 - The calibration of load or displacement transducers is a very important point especially if compliance method is used.
In case of multiple specimens method, the requirements, which are similar for load or displacement transducers, are concerning only the accuracy and the reproducibility.
But if single specimen elastic compliance method is used, it could be necessary to take account of the curvature of the calibration curves of the transducers. The criteria which is used to determine the analytical form of the calibration curve is based on statistical analysis of measurements. It is expressed by the following relationship (see annex 3) : $2\sigma/\Delta u \leqslant 0{,}1\%$.

APPENDIX

TENTATIVE TEST PROCEDURE FOR THE DETERMINATION OF THE FRACTURE RESISTANCE OF DUCTILE STEELS

Members :

M.	BALLADON	(UNIREC)
M.	BETHMONT	(EDF)
M.	CHAVAILLARD	(FRAMATOME)
Mlle	MAAS	(IRSID)
M.	MILOCEVIC	(University of Compiègne)
M.	NICOLINO	(CEA)
M.	PLUVINAGE	(University of Metz)
M.	PONSOT	(Creusot-Loire Industries)
M.	ROUSSELIER	(EDF)
M.	SOULAT	(CEA)

- Contents
- Chapter 5 : Specimens
- Chapter 6 : Equipment
- Annex 1 : Clevis model
- Annex 2 : Fixture alignment control
- Annex 3 : Transducer calibration procedures

CONTENTS

5 - SPECIMENS

5.1 - The specimens used are the Compact Tension specimens (CT). Reference geometries are CT 25 and CT 50 specimens.

If necessary other geometries may be used, such as :
- CT 12.5, CT 75 and CT 100
- or reduced thickness CT 12.5/B, CT 25/B, CT 50/B, CT 75/B or CT 100/B.

In these latter cases, the first number is the nominal specimen dimension (0.5 W) and B, the thickness.

5.2 - Following the fatigue pre-cracking stage, the specimens are side-grooved on a total depth equal to 20% of thickness (Charpy V type notch : $d = 45°$, $\rho = 0{,}25 \pm 0{,}025$).

The thickness in specimen notch plane is designated by B_N.

In some cases, for example for heterogeneous materials, it may be helpful to cut shallower side grooves, prior to pre-cracking. These grooves provide a fatigue crack growth in the plane of the notch with a straigth crack front. The thickness in the notch plane of this specimen is designated by B_f.

5.3 - For measurements of load line opening, the knife edges permitting the attachment of a clip gage are either machined in the specimen or inserted. Before each test, knife edge sharpness and edge parallelism should be checked.

Specimen machining may eventually be adapted to other types of transducers so that measurement be carried out on load line.

For information, specimen models are shown on Figure 1.

With ductile and very tough steels, care should be taken to limite the distance between the pinholes in order to prevent plasticity in the arms of the specimens.

5.4 - Specimen fatigue pre-craking. Specimen pre-cracking is carried out until the relative depth of the crack reaches 0.60 ± 0.05. The length of fatigue crack f should be greater than 5% of a_0 and at least equal to 1.3 mm.

Maximum load of pre-cracking should never exceed value $0.4\ P_L$ where :

$$P_L = \frac{B_f (W - h - f)^2 R_{ec}}{2W + h + f}$$

Fatigue crack propagation is most often monitored by compliance, resistivity or optical techniques, however, any other method providing an equivalent precision may be utilized.

A chevron shape at the tip of the machined notch is suggested if crack initiation is a problem.

It is advisable to use the lowest ratio $R = P^f_{min} / P^f_{max}$ as possible (as a rule 0.1) to minimize cracking procedure duration.

Fatigue pre-cracking should preferably be carried out with the material in the same metallurgical condition in which the material is to be tested.

6 - EQUIPMENT

6.1 - The recommended clevis geometry is identical to that indicated in AFNOR A 03-180 standard (figure 2).

For information, another geometry is proposed in Annex 1 for single specimen compliance method.

It is advisable to ascertain that the selected geometry allows a friction-less rotation of the pins up to the maximal specimen opening.

6.2 - Check of fixture alignment. Prior to each test, it should be made sure that the pins are properly centered on clevis holes flat parts.

A periodical check is performed regarding proper machine and clevis system aligment. An alignment checking method is proposed in Annex 2.

6.3 - Calibration of Load and Displacement Transducers.

- Load Transducer :

Load transducer should be class 1 to AFNOR NFA 03-501 standard.

- Displacement Transducer :

Accuracy error and reproducibility (Cf. NFA 03-501) should be at the most 1% of measured value, or at the most 0.2% of transducer range, only the highest of these two values being selected.

- Specification for Single Specimen Elastic Compliance Method :

Load and displacement transducer calibration curves are expressed under linear or polynomial analytical form (Cf. Annex 3).

An analytical expression is acceptable, if the following inequality is verified : $2\sigma/\Delta u \leqslant 0.1\%$ where σ is the measurement standard deviation and Δu measurement range.

This checking procedure applies to the whole multiple instrument measurement assembly.

6.4 - Temperature Measurements

It is recommended to measure specimen temperature 5 mm away from fatigue crack plane and tip or in such a way as to know the temperature in the propagation zone through a prior calibration.

Temperature should remain stable in said zone at $\pm$ 3°C ; also prior to the test it should remain stable for a period such that :
$t \geqslant B \times 1$ min/mm.

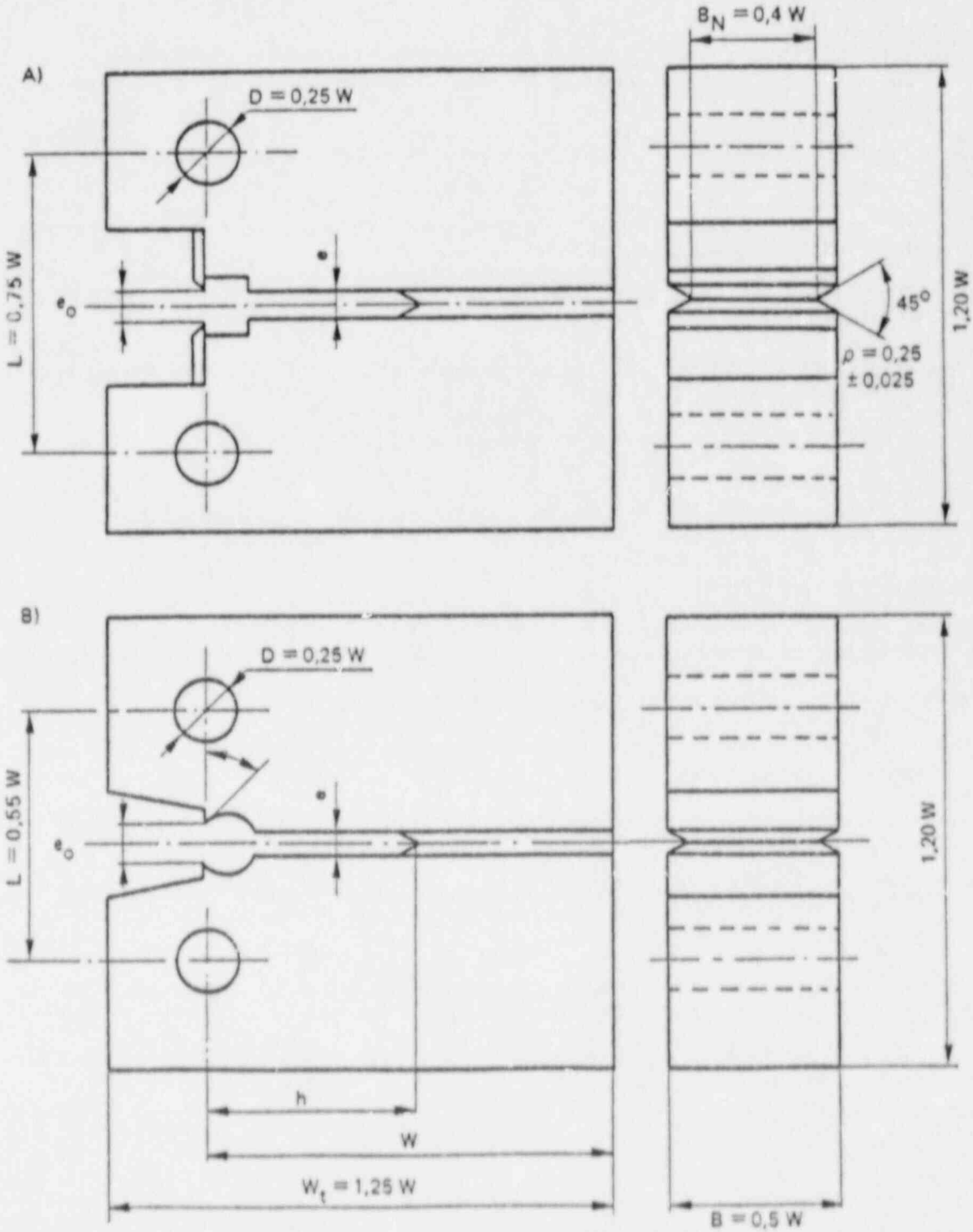

General tolerances ± 0.001 W.
Surface roughness R_a = 0.4 µm.

Figure 1 - CT specimen models

A - Inserted knifeedges
B - Knifeedges machined into the specimen

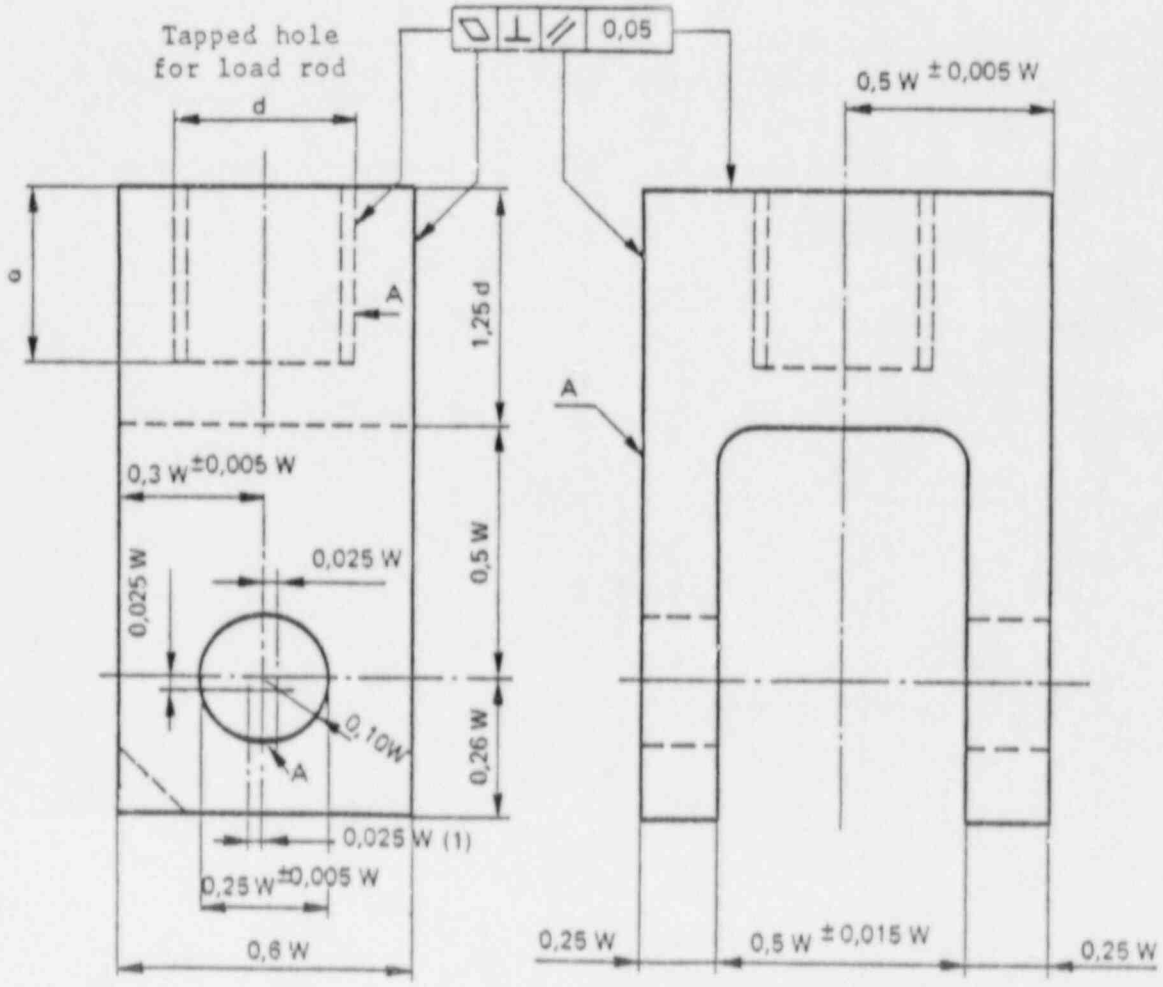

"A" surfaces should be plane, parallel and at right angle with one another within ± 0.05 mm.

(1) This dimension may be increased for the application of the partial unloading method (cf. 6.1 and 6.2).

Figure 2 - Clevis for compact specimens (after AFNOR A 03-180 standard)

ANNEX 1

CLEVIS MODEL
(single specimen compliance method)

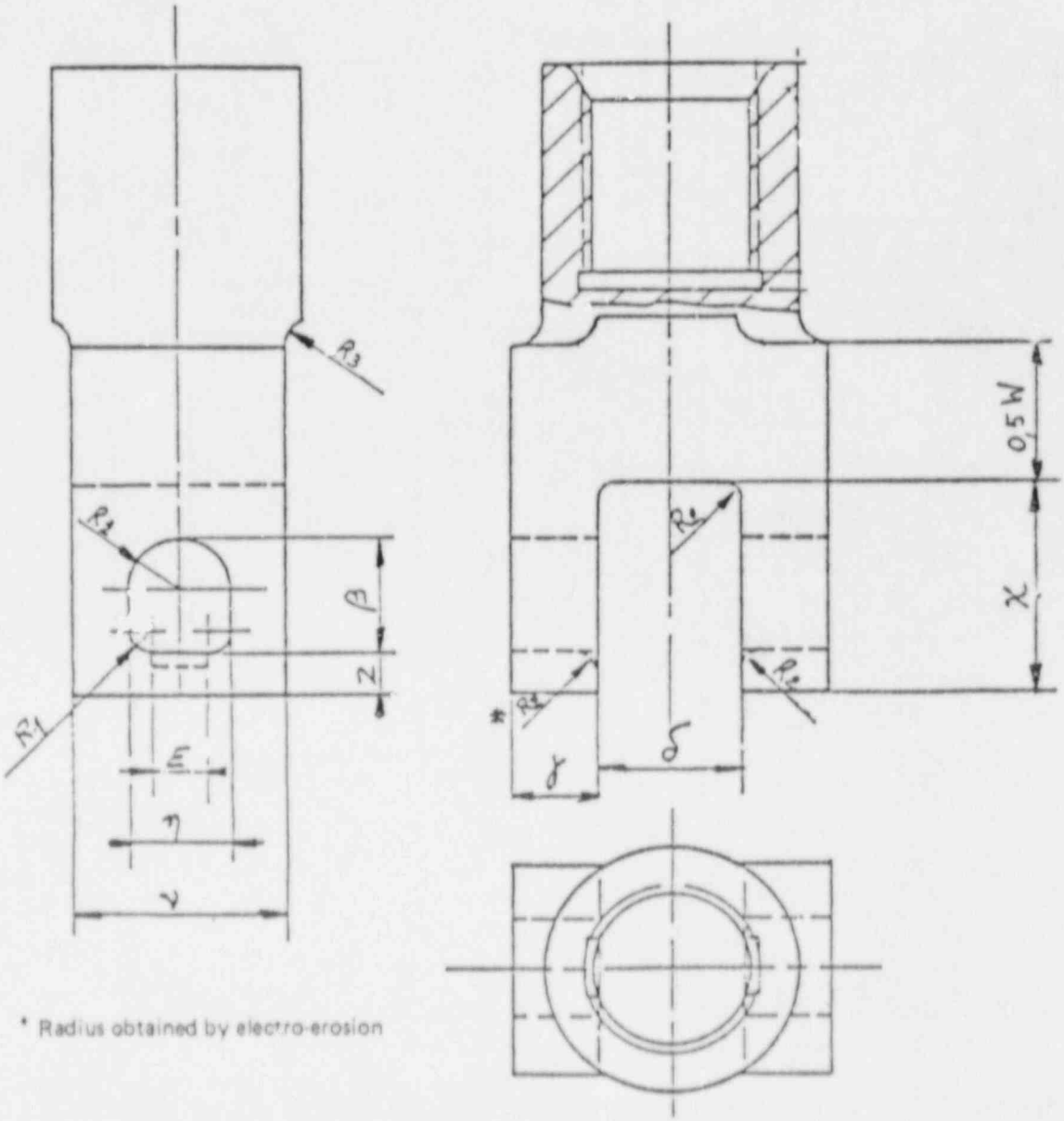

* Radius obtained by electro-erosion

β = 0,4 W	χ = 0,75 W
δ = 0,5 W + 0,015 W	Z = 0,14 W
E = 0,2 W	R_1 = 0,075 W
γ = 0,3 W	R_2 = 0,05 W
η = 0,35 W	R_3 = 0,1 W
ν = 0,75 W	

ANNEX 2

FIXTURE ALIGNMENT CONTROL

A.2.1 - Tensile Calibration Bar

Gages glued on this bar are utilized to display the parasite bending : for a given tensile load, the electric signal emitted by each gage varies as the bar revolves around its own axis.

A.2.2 - Utilization of a Comparator

The measurement principle is sketched on figure A2.1 : the comparator, while leaning against a reference cylindrical surface integral with fixture top, is made to turn around lower fixture axis. The maximal deviation between measurement values read on the comparator should not exceed 0.05 mm.

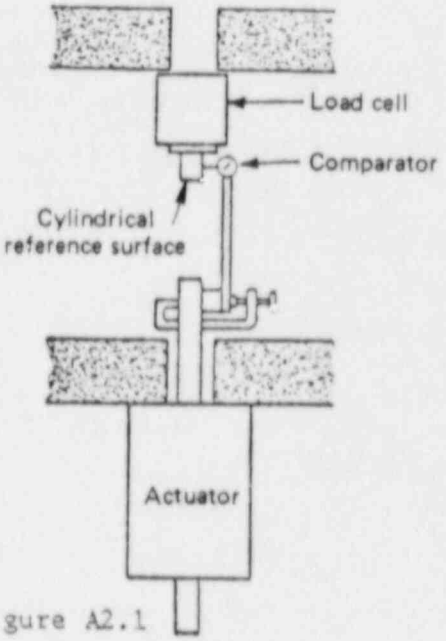

Figure A2.1 - *Fixture alignment control by means of a comparator.*

A.2.3 - Utilization of a Crack Specimen (fig. A2.2)

A CT specimen, fitted with a deformation gage on one of its faces, at a 1.5 mm distance from notch tip, is utilized. It should be made sure the gage is placed away from the plastic zone at the crack tip, by verifying that the emitted signal returns to zero with the load after a few cycles.

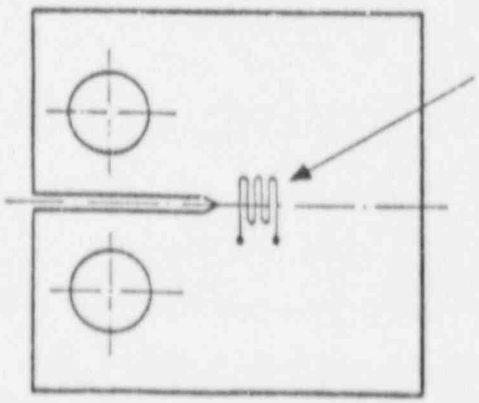

Figure A2.2 - *Uncracked CT specimen fitted with gages for the purpose of checking clevis alignment.*

Then the specimen is stressed up to a load corresponding approximately to 0.4 P_L. The load vs. deformation diagram is recorded. After the specimen has been turned end for end, the same load application is carried out and a second load vs. deformation diagram is recorded. The alignment is considered satisfactory when the deviation between the readings on the gage for the same maximal load does not exceed 2%.

ANNEX 3

TRANSDUCER CALIBRATION PROCEDURES

A.3.1 - Transducer Linearity Control

The calibration range of the transducer is divided into a minimum of 10 equal intervals. Three series of measurements are carried out in each of the subdivision points.

The measurements are carried out at the end of a multiple instrument measurement assembly (plotting table or computer). Following the reproducibility control (Cf. § 6.3), the correlation factor $r = \sqrt{p\ p'}$ is calculated (p and p' are the slopes of the two linear regressions, obtained through the least square method).

The transducer may be considered linear if linkage probability A is such that :

$A = 1 - \sqrt{1 - r^2} > 0.998$

This limit corresponds approximately to the result obtained for a series of points with a $\pm\ 10^{-3}$ amplitude random rectangular distribution around a theoretical linear linkage $y = x$ within the [0, 1] interval.

Therefore, this limit is equivalent to :

$2\ \sigma/\Delta u \leqslant 0.1\%$ where σ is the measurement standard deviation and Δu the measurement range.

Otherwise, calibration procedure proceeds as described below.

A.3.2 - Calibration of Transducers non-Linear According to A.3.1

1st Method On the basis of preceding data, a polynomial of a degree not exceeding 4 is established as follows :

$$Y = \sum_{j=1}^{m} B_j\ X^{j-1}$$

with $3 \leqslant m \leqslant 5$.

Y is the physical magnitude and X the measured information. Coefficients B_j are determined by the least square method i.e., if no specific constraints are imposed, by the resolution of the system :

$$[A_{ij}]\ [B_j] = [C_i] \qquad \text{with : } A_{ij} = \sum_{k=1}^{N} X_k^{i+j-2} \quad \text{and} \quad C_i = \sum_{k=1}^{N} Y_k\ \ X_k^{i-1}$$

Other fittings with adapted calculations permitting an analytical formulation may be used. In all cases :

- the condition of accuracy according to scatter index should be : $2\sigma/\Delta u \leqslant 0.1\%$.
- the compatibility between the adjustment function derivative and the local evaluations should be verified.

2nd Method In the vicinity of each point in the calibration range subdivisions, a local calibration is performed on a range corresponding to a partial unloading (for instance 0.1 mm for the displacement). It is necessary to carry out a minimum of 10 evenly spaced apart measurements. The local slopes ($\delta Y/\delta X$) are determined by linear fitting according to the least square method.

a/ Test Carried out in Analogic Mode

It shall be possible to use the transducer only if the local slope evolution, throughout the measurement range, may be linearized with a scatter band 4 σ less than 2% of the average slope and if the overall variation does not exceed 4% of said average slope.

If these conditions are met, together with those of accuracy and reproducibility (cf. § 6.3), the transducer may be assumed to be linear, as an initial evaluation. The compliance measurements should be corrected by taking into account the local slope/average slope ratio at the middle point where the partial unloading is carried out.

b/ Test Carried out with Digital Acquisition

The preceding procedure applies with the same reservations about validity.

More generally, the evolution of the reciprocal of the measured local slope is expressed in function of the measured mean signal by a polynomial of a degree less or equal to 3, through the least square method.

i.e. : $Y' = \sum_{j=1}^{m'} B'_j X^{j-1}$ with $2 \leqslant m' \leqslant 4$

Then, the calibration polynomial is determined by :

$$Y = \sum_{j=1}^{m} B_j X^{j-1} \quad \text{with} \quad m = m' + 1$$

$$\text{with} \quad B_j = \frac{B'_j - 1}{j - 1} \qquad \text{for } 2 \leqslant j \leqslant m$$

$$\text{and} \quad B_1 = \frac{\sum_{k=1}^{N} \left[Y_R - \sum_{k=2}^{m} B_j X_R^{j-1} \right]}{N}$$

B_1 is the integration constant optimized on the basis of the initial data obtained as described in A.3.1.

The accuracy condition according to the scatter index still is : $2\sigma/\Delta u \leqslant 0{,}1\%$.

THE DETERMINATION OF THE FRACTURE RESISTANCE OF DUCTILE STEELS

B.K. Neale

Central Electricity Generating Board
Berkeley Nuclear Laboratories
Berkeley
Glos
GL13 9PB

APPROACH

In order to fully assess the integrity of a structure, it is necessary to know the fracture properties of the component steels. The CEGB Procedure (Ref 1) provides a method for determining the fracture properties of ferritic steels by measuring the variation in fracture resistance J with crack growth Δa. Typical J-Δa behaviour for a steel is shown in Figure 1. The initial behaviour is associated with crack tip blunting followed by crack initiation and crack growth as J attains some limiting value. Crack initiation occurs at a value of J usually designated J_i.

For assessment purposes, J values which do not characterise the fracture behaviour are unimportant. Consequently, the objectives of the CEGB Procedure are to measure J_i and determine the limit to the J-Δa behaviour beyond which J - controlled behaviour can no longer be assured. In practice, it is difficult to determine the precise location of J_i. An alternative approach used in the CEGB Procedure is to determine the value of J at 0.2mm crack growth. $J_{0.2}$ can then be used as an engineering approximation to J_i.

METHODOLOGY

In the CEGB Procedure, the J-Δa behaviour of a steel can be measured using either the single edge notch bend specimen shown in Figure 2 or the compact tension specimens shown in Figure 3. A modified compact tension specimen can be used which incorporates wider pin hole spacing than the standard specimen so that a clip gauge can be inserted on the load line. Using these specimens typical load displacement behaviour shown in Figure 4 is measured. The behaviour is usually characterised by a linear region followed by crack initiation and crack growth as a limit load is reached and collapse of the specimen occurs.

Both single specimen and multiple specimen methods can be used for measuring crack growth. With the multiple specimen method the crack growth Δa is measured directly from the fracture surfaces while the fracture resistance J is determined from the area under the load displacement record.

The single specimen method is based on the unloading compliance technique and details are given in the Procedure for both performing the

test and analysing the data. Typical J versus crack length behaviour is shown in Figure 5. The minimum crack length is used to estimate the initial crack length a_o. The unloading compliance at the end of the test is used to estimate the final crack length. Providing the estimated initial and final crack lengths and the crack growth meet specified accuracy requirements, a_o can be subtracted from the crack length data to provide the J-Δa behaviour.

J-Δa VALIDITY REQUIREMENTS

Validity limits are applied to the J-Δa data to ensure that J characterises the stress fields ahead of the growing crack, Figure 6. It is assumed that data satisfying these limits are a material property independent of test specimen size and can be used to derive fracture parameters suitable for the assessment of structural integrity.

INTERPRETATION OF J-Δa DATA

The derivation of fracture parameters from J-Δa data used in the Procedure is dependent upon the extent of the valid crack growth range, Δa_{max}. If Δa_{max} is less than 2 mm then a straight line is drawn through the data remaining between a 0.2mm exclusion line and Δa_{max}, as shown in Figure 7. The intercept of this line with the 0.2mm and Δa_{max} exclusion lines defines $J_{0.2}$ and J_{max}, respectively. The slope of the line is dJ/da. If Δa_{max} is greater than 2mm, a power law fit is drawn through the data remaining between the exclusion lines in order to avoid overestimating $J_{0.2}$ and J_{max} at large crack growths. For this case the J-Δa data is described by $J^g_{0.2}$, J_g and the equation of the power law.

SIGNIFICANCE OF FRACTURE PARAMETERS

For many steels, $J_{0.2}$ can be regarded as an engineering approximation to the initiation fracture resistance. The value of J_g represents the maximum fracture resistance that can be measured from a given test specimen for J-controlled crack growth. In writing the Procedure, it should be noted that $J_{0.2}$ was considered less important than J_g which attempts to exploit the increase in fracture resistance with crack growth.

CONCLUDING REMARKS

This note briefly describes the essential features of the CEGB Procedure for the determination of the fracture resistance of ductile steels.

The advantages of the CEGB Procedure are:

1. It permits the use of single edge notch bend and compact tension specimens.

2. It incorporates multiple and single specimen methods.

3. It avoids the use of a blunting line construction.

4. It does not attempt to measure J at crack initiation.

5. It describes a valid crack growth fracture resistance curve in terms of suitable chracterising parameters.

For a more thorough treatment, the reader is referred to Reference 1 and to the accompanying explanatory background notes to the Procedure given in Reference 2.

ACKNOWLEDGEMENTS

The author acknowledges the support of his co-authors in writing the CEGB Procedure. The paper is published by permission of the Central Electricity Generating Board.

REFERENCES

1. B.K. Neale, D.A. Curry, G. Green, J.R. Haigh and K.N. Akhurst, "A Procedure for the Determination of the Fracture Resistance of Ductile Steels", CEGB Report TPRD/B/0495/R84.

2. K.N. Akhurst, G. Green, J.R. Haigh and B.K. Neale, "Explanatory Background Notes to A Procedure for the Determination of the Fracture Resistance of Ductile Steels", CEGB Report TPRD/B/0496/N84.

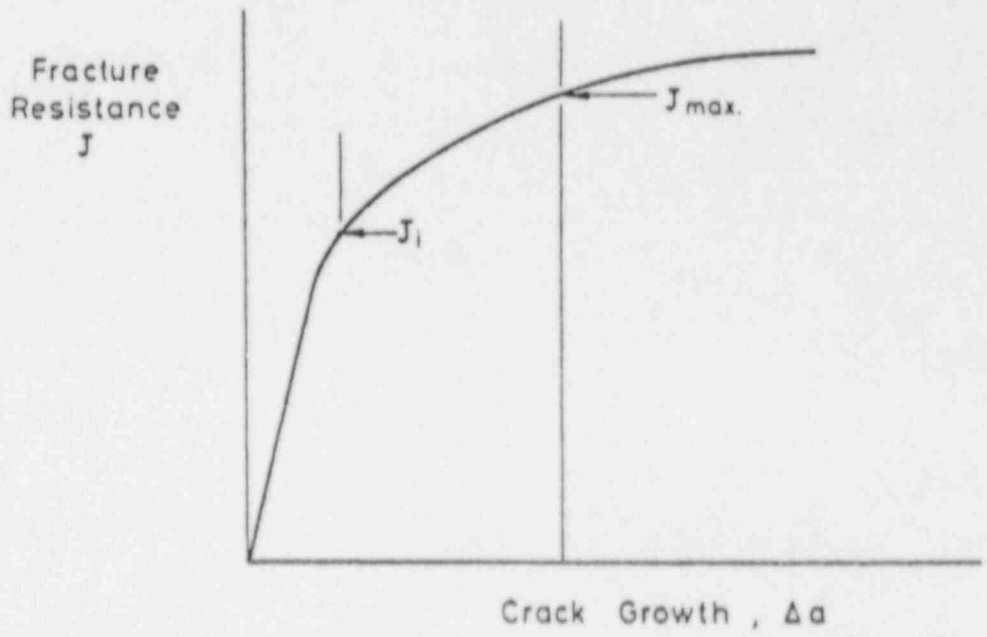

Figure 1. Typical Crack Growth Fracture Resistance Behaviour of a Ferritic Steel

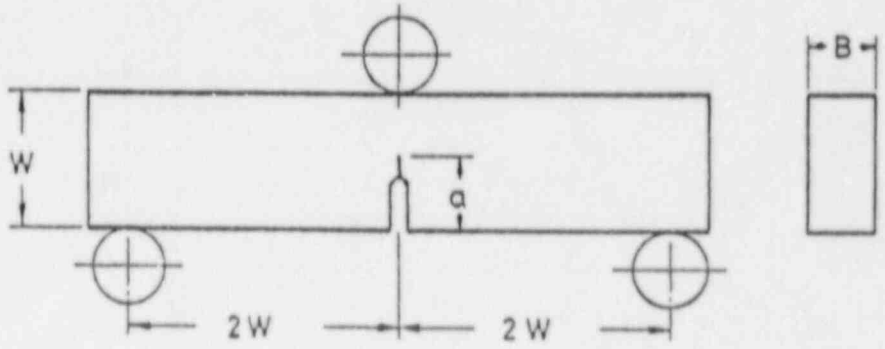

Width = W
Thickness = B usually 0.5W

Figure 2. Single Edge Notch Bend Specimen

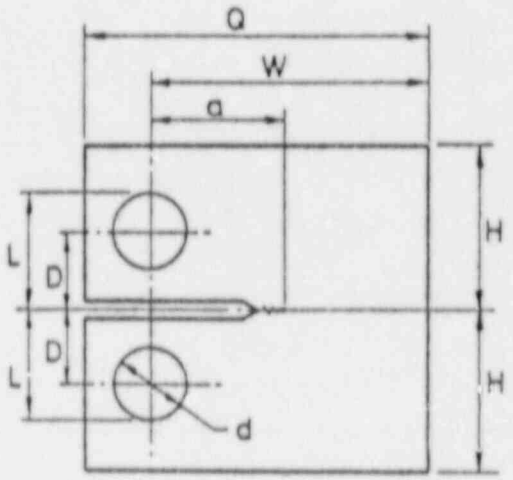

Where Q = 1.25W For standard specimen
H = 0.6 W D = 0.275W L = 0.4 W
d = 0.25 W For modified specimen
D = 0.375W L = 0.5 W

Figure 3 Compact Tension Specimens

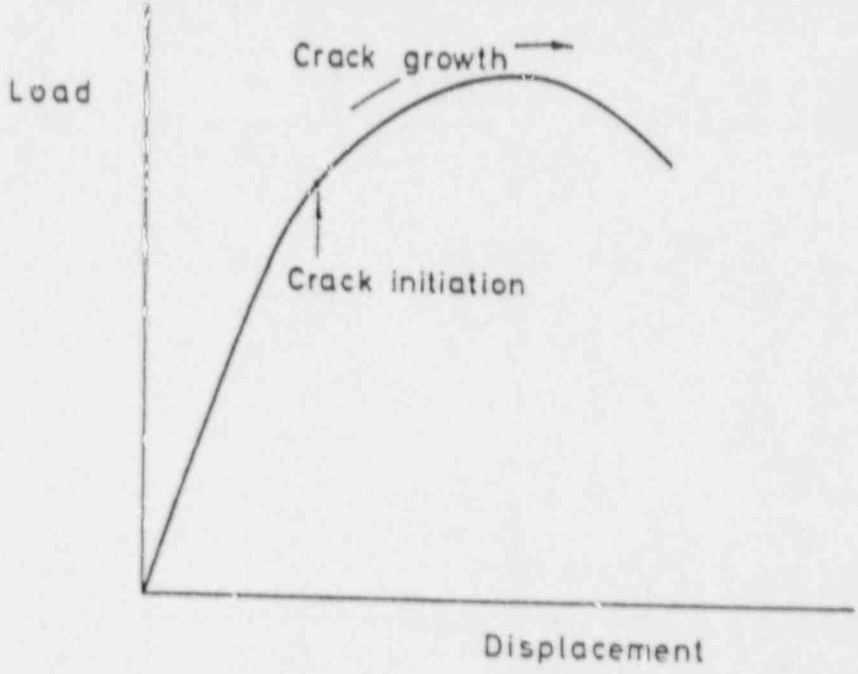

Figure 4 Typical Load-Displacement Behaviour of a Test Specimen

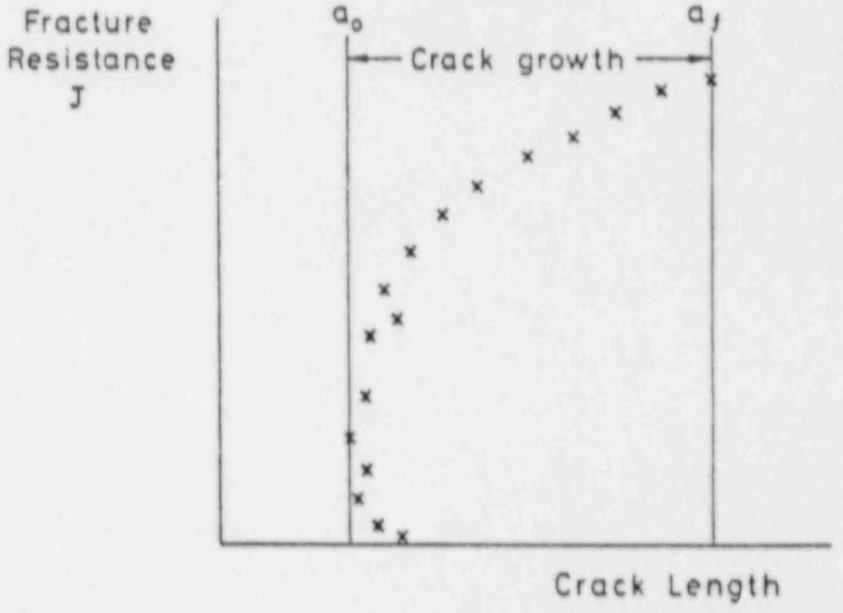

Figure 5 Fracture Resistance versus Crack Length Behaviour

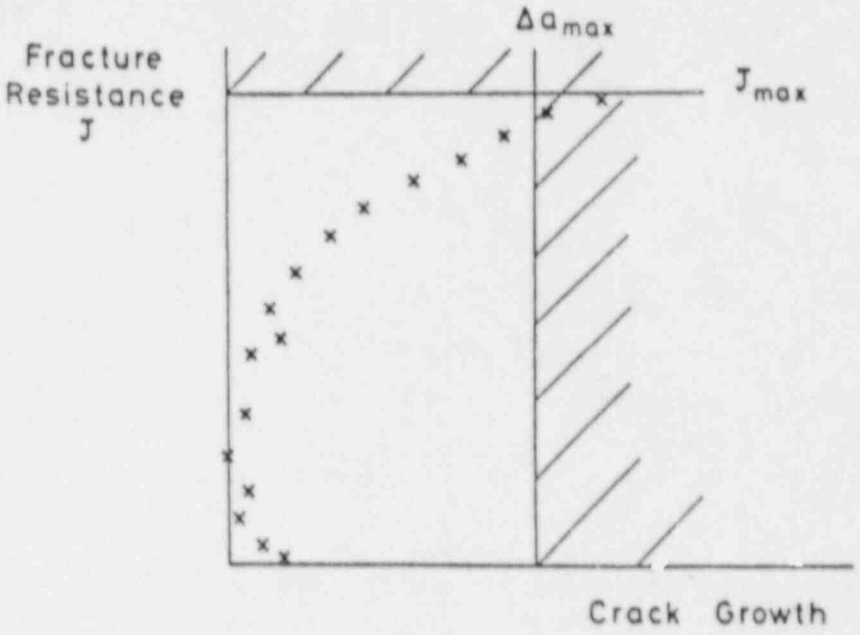

J_{max} is the lower of $(W-a_o)\ \frac{\sigma_f}{25}$ or $B\ \frac{\sigma_f}{25}$

$$\Delta a_{max} = 0.06\,(W-a_o) + 0.2$$

$$\left(\frac{W-a_o}{J}\right)\frac{dJ}{da} > 10$$

Figure 6 Data Validity Requirements

For $\Delta a_{max} \leq 2mm$

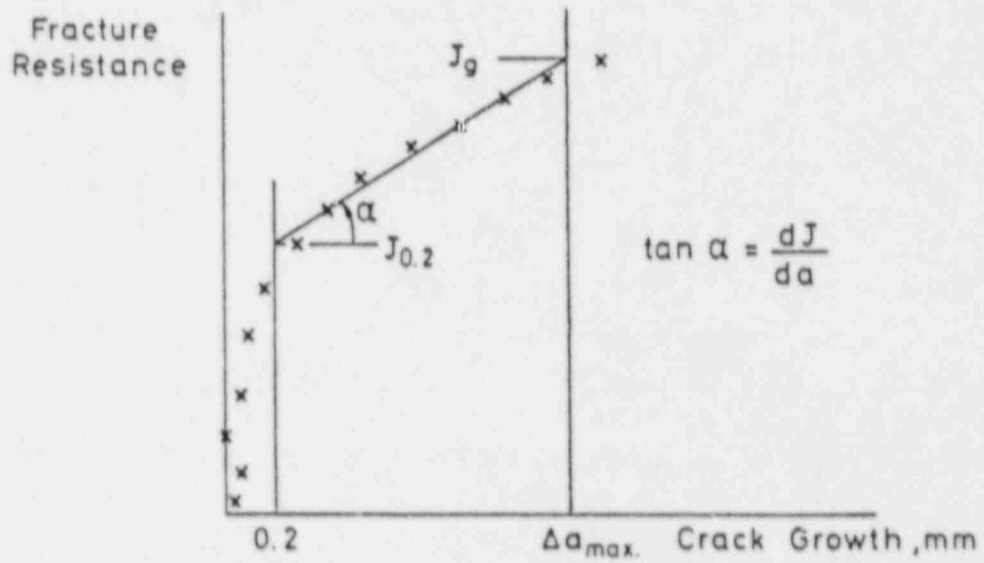

Figure 7 Interpretation of Crack Growth Fracture Resistance Behaviour, $\Delta a_{max} \leq 2mm$

For $\Delta a_{max.} > 2mm$

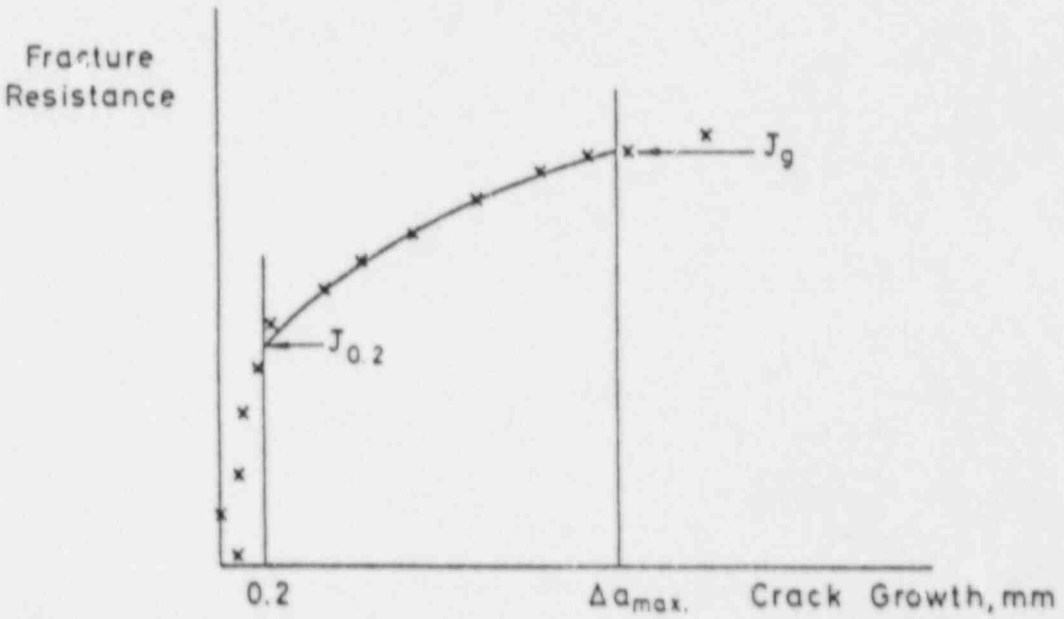

Figure 8 Interpretation of Crack Growth Fracture Resistance Behaviour, $\Delta a_{max} > 2mm$

PROGRESS REPORT ON THE ASTM R-CURVE STANDARD

D. E. McCabe

Westinghouse R&D
1310 Beulah Road
Pittsburgh, PA 15235

The method is now in its 10th draft, and as of November 1984, the method has been approved for submittal to subcommittee ballot. The 10th draft has several substantive changes from the earlier draft that had been reported in the Journal of Testing and Evaluation, November 1982. These are:

1. Title and Scope
   [Old] Tentative Test Procedure for Determining the Plane Strain J_I-R-Curve.
   [New] Test Procedure for Determining J-R-Curve.

2. Specimen Design
   [Old] David Taylor Specimen [0.188W pins]
   [New] Westinghouse Design [0.25W pins]
   David Taylor Design [0.188W pins]
   Ratio H/W must be maintained. Thickness is nominally 0.5W but any thickness can be used so long as the size criteria of section 9 can be met. When the component structure being evaluated has a thickness too small to meet the size requirement of section 9, the J_R-Curve may be determined for that thickness so long as the planar size requirements are met. ($J_{max} = b\sigma_Y/20$). In that case, the J_R-Curve may not be geometry independent but will give toughness that is appropriate for the component thickness being evaluated.

3. New Equations for J_D

[Old] $$J_{i+1} = \left[J_i + \left(\frac{\eta}{b}\right)_i \frac{A_{i,\,i+1}}{B_N}\right] \left[1 - \left(\frac{\gamma}{b}\right)_i (a_{i+1}-a_i)\right]$$

[New] $$J_{i+1} = \frac{(K_{i+1})^2}{E} + (J_p)_{i+1}$$

$$(J_p)_{i+1} = \left[(J_p)_i + \left(\frac{\eta}{b}\right)_i \left(\frac{(A_p)_{i,\,i+1}}{B_N}\right)\right] \left[1 - \left(\frac{\gamma}{b}\right)_i (a_{i+1}-a_i)\right]$$

$$(A_p)_{i+1} = \left[(\delta_p)_{i+1} - (\delta_p)_i\right] \left[\frac{P_{i+1} + P_i}{2}\right]$$

$$(\delta_p)_i = \delta_i - P_i C_i$$

4. Effective Modulus Adjustment for Compatability Between a_o and Initial Elastic Slope

$$E_M = \frac{1}{C_o B_e} \left(\frac{W + a_o}{W - a_o}\right)^2 \cdot f\left(\frac{a_o}{W}\right)$$

where: C_o = initial compliance

$$B_e = B-(B-B_N)^2/B$$

$$\text{then:} \quad U_{LL} = \frac{1}{[E_M B_e C]^{1/2} + 1}$$

$$a/W = f\ (U_{LL})$$

5. Rotation Correction to Unloading Compliance

$$C_c = C_m \frac{1}{[(H/R)\sin\theta-\cos\theta]\ [(D/R)\sin\theta-\cos\theta]}$$

C_m = measured elastic compliance (load line)

C_c = corrected compliance

Issues

Specimen type effects on J-R-Curve (bend Bar-Compact)
Seen in round robin on HY130
Seen in round robin on A710
J. Newman results suggest no geometry effects
To subcommittee ballot Mar-Nov 1985.

Dwg. 4274B42

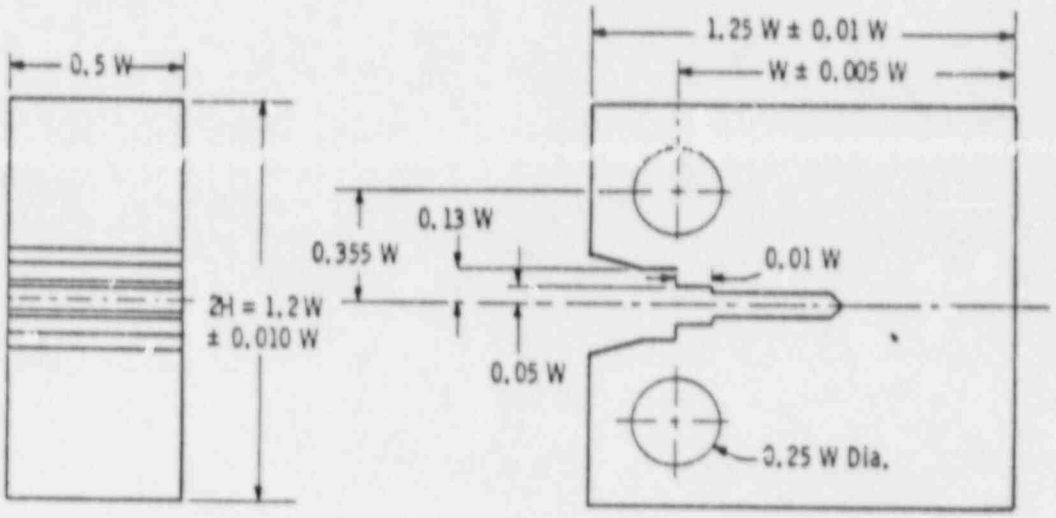

Compact Test Specimen for Pin of 0.24 W (+ 0.000 W/− 0.005 W) Diameter

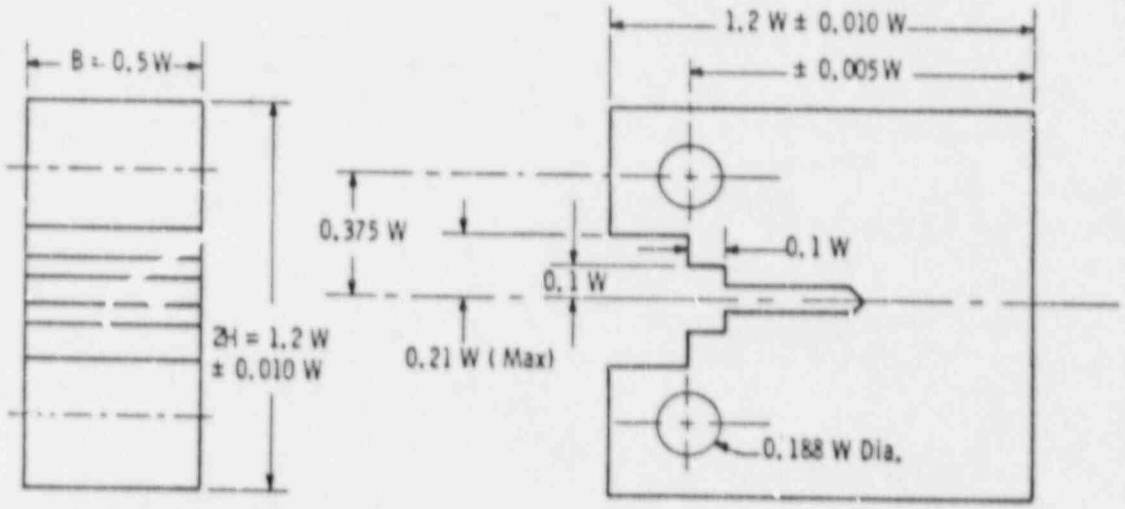

Compact Test Specimen for Pin of 0.1875 W (+ 0.000 W/- 0.001 W) Diameter

Two compact specimen designs that have been proposed in the R-Curve test procedure

EXPRESSIONS FOR J AND J_M FOR GROWING CRACKS

Hugo Ernst[1]

TECHNINT Argentina
Buenos Aires

Since the introduction of the multispecimen method to determine J, by Begley and Landes, significant effort was devoted to decrease the number of specimens needed for its determination. Expressions for J were then developed based on single specimen behavior following the original work of Rice, Paris and Merkle [1]. In general J can be expressed as

$$J = \frac{\eta}{bB} \int P d\delta \qquad (1)$$

where η: is a function of the crack length and material properties, but not on the level of deformation.

b: is the remaining ligament.

B: is the specimen thickness.

P: is the applied load.

δ: is the load-point displacement.

As discussed extensively in Reference 2, the existence of η as a function of a, but independent of the level of deformation is related to the possibility of variable separation in the expression of load as a function of crack length and displacement.

$$P = A(a)\, D(\delta) \qquad (2)$$

The value of η is related to the scaling properties of the above expression, in terms of crack length. More precisely, η is given by

$$\eta = \frac{\partial P}{\partial b} \frac{b}{P} \qquad (3)$$

[1]Mailing address: TECHNINT SA, 708 Third Ave., NY, NY 10017.

As was noted in Reference 2, there are some cases for which the scaling properties of the P-δ relationships are not the same in the linear elastic regime and in the fully plastic one. Thus giving the two values the elastic, η_{el}, and the plastic one, η_{pl}. Consequently, J is expressed as:

$$J = \frac{\eta_{el}}{Bb} \int P d\delta_{el} + \frac{\eta_{pl}}{Bb} \int P d\delta_{pl} \qquad (4)$$

where δ_{el} and δ_{pl} are the linear elastic and the plastic part of the displacement, respectively. Only for cases where $\eta_{el} \approx \eta_{pl}$, an expression like Equation (1) is expected to give correct results.

Growing Cracks

For the case of growing cracks, the meaning of J is not clear, since unloading occurs in some portions of the body and the irreversibility of the process becomes apparent. This fact can be ignored, as a first approximation, and strict deformation theory of plasticity interpretation of J can be followed. That is, consider the material as nonlinear elastic, and J is history independent in the P-δ plane. The value of J at a point, can be obtained following any path getting to that point in the P-δ plane.

The expression of Equations (1) and (2) could then be used, provided the areas were taken under the corresponding calibration or nongrowing crack curve, passing through the point of interest. Usually, this is not a very practical way of calculating J since nongrowing crack curves are not always available. Instead, Equation (1) and (2) can be differentiated and reintegrated to give the value of J based on the actual test record. This procedure was followed by several investigators using different estimation techniques to give formulas for J for growing cracks. Among these, Ernst [3] proposed an incremental formula for J given by:

$$J_i = (J_{i-1} + (\frac{\eta}{Bb})_{i-1} A_{i-1,i})(1 - (\frac{\gamma}{b})_{i-1}(a_i - a_{i-1})) \qquad (5)$$

with $a_{i-1,i}$ as the area under the load displacement record between these two steps

$\eta = 2$ SENB

$\eta = (2 + 0.522\ b/w)$ CT

$\gamma = 1$ SENB

$\gamma = (1 + 0.76\ b/W)$ CT

Recent and more detailed studies [4] seem to show that the value of η given above tends to overestimate the η_{el} for the SENB, whereas it tends to underestimate the η_{el} for the CT. As a result it seems more convenient to use an expression of the type of Equation (2), using for the first term on the right hand side $J_{el} = K^2/E'$,

$$J = J_{el} + J_{pl} \tag{6}$$

Following the preceeding discussion, J_{pl} is given, for growing cracks,

$$J_{pl} = \int_{a_o}^{a} \frac{\partial J_{pl}}{B\,\partial a}\, da + \int_{o}^{\delta_{pl}} \frac{\partial J_{pl}}{B\partial \delta_{pl}}\, d\delta_{pl}$$

$$= - \int_{a_o}^{a} \gamma \frac{J_{pl}}{b}\, da + \int_{o}^{\delta_{pl}} \eta_{pl} \frac{P}{b}\, d\delta_{pl} \tag{7}$$

with $\eta_{pl} = 2$ SENB

$= (2 + 0.522\ b/W)$ CT

$\gamma = 1$ SENB

$\gamma = 1 + 0.76\ b/W$ CT

To numerically evaluate this expression, different estimation techniques can be followed. One, is to simply use Equation (5) applied to the plastic area, that is

$$J_{pl_i} = \left(J_{pl_{i-1}} + \left(\frac{\eta}{Bb}\right)_{i-1} A_{pl_{i-1,i}}\right)\left(1 - \left(\frac{\gamma}{b}\right)_{i-1}(a_i - a_{i-1})\right) \tag{9}$$

Another method, specially suited for situations where values of a are obtained at very close intervals (continuously monitored, for example), uses a trapezoidal rule for evaluating the integrals to give

$$J_{pl} = \left\{\left[J_{pl_{i-1}}\left(1 - \left(\frac{\gamma}{b}\right)_{i-1}\frac{(a_i - a_{i-1})}{2}\right)\right] + \left[\left(\frac{\eta P}{b}\right)_i + \left(\frac{\eta P}{b}\right)_{i-1}\right]\left[\frac{\delta_{pl_i} - \delta_{pl_{i-1}}}{2B}\right]\right\}$$

$$\left\{\frac{1}{\left[1 + \left(\frac{\gamma}{b}\right)_i \frac{(a_i - a_{i-1})}{2}\right]}\right\} \qquad (10)$$

The Modified J_M

Recently a modified version of J, J_M, has been introduced [5], as a parameter believed to give a better description of the process of deformation and growth. It has been defined as

$$J_M = J - \int_{a_o}^{a} \frac{\partial J_{pl}}{\partial a}\bigg|_{\delta_{pl}} da \qquad (11)$$

It can be shown [6], that this expression is completely equivalent to:

$$J_M = G + \int_{o}^{\delta_{pl}} \frac{\partial J_{pl}}{\partial \delta_{pl}}\bigg|_{a} d\delta_{pl} =$$

$$= G + \int_{o}^{\delta_{pl}} \frac{\partial P}{B\partial b}\bigg|_{\delta_{pl}} d\delta_{pl} \qquad (12)$$

In particular for the SENB and CT, these expressions give:

$$J_M = J - \int_{a_o}^{a} \gamma \frac{J_{pl}}{Bb}\, da$$

$$J_M = G + \int_{o}^{\delta_{pl}} \frac{\eta P}{Bb}\, d\delta_{pl} \qquad (13)$$

with γ and n as defined in Equation (8). Correspondingly, incremental expressions for J_M can be produced using the above equations together with either, Equations (6) and (7) or Equations (6) and (8), depending on the size of step between crack length determinations. As mentioned before, the former would best express J_M for the case of the larger steps, whereas the latter would be better for cases of continuously monitored crack length.

In particular for this last case, J_M can be expressed as:

$$J_M = G + J_{M_{pl}} \tag{14}$$

$$J_{M_{pli}} = J_{M_{pli-1}} + \left[\left(\frac{\eta P}{b}\right)_i + \left(\frac{\eta P}{b}\right)_{i-1}\right]\left[\frac{\delta_{pli} - \delta_{pli-1}}{2B}\right]$$

It is emphasized that two different parameters are defined here. J and J_M. The different formulaes appearing above, for each of them, should be regarded as different numerical techniques to evaluate the integrals, depending on the size step of crack length determinations.

References

1. Rice, J. R., Paris, P. C. and Merkle, J in "Progress in Flaw Growth and Toughness Testing", ASTM STP 536, American Society for Testing and Materials, 1973, pp. 231-244.
2. Paris, P. C., Ernst, H. A. and Turner, C. E. in "Fracture Mechanics: Twelfth Conference", ASTM STP 700, American Society for Testing and Materials, 1980, pp. 338-351.
3. Ernst, H. A., Paris, P. C. and Landes, J. D., in "Fracture Mechanics: Thirteenth Conference", ASTM STP 743, American Society for Testing and Materials, 1981, pp. 476-502.
4. Shih, C. F. and Hutchinson, J. W., "Combined Loading of a Fully Plastic Ligament Ahead of an Edge Crack", Report MECH-65, Division of Applied Sciences, Harvard University, April 1985.

5. Ernst, H. A., "Material Resistance and Instability Beyond J-Controlled Crack Growth", ASTM STP 803, American Society for Testing and Materials, 1983, Vol. I, pp. I-191-J-213.
6. Ernst, H. A., "Further Developments on the Modified J, J_M", to be published in the International Journal of Fracture, 1986.

SESSION 4: Experience and Problems with Existing Techniques

CHAIRMAN: D. E. McCabe
Westinghouse R&D, USA

THE MEASUREMENT, INTERPRETATION AND USE OF CRACK GROWTH RESISTANCE CURVES

J.R. Gordon and S.J. Garwood

The Welding Institute,
Abington Hall,
Abington, Cambridge,
CB1 6AL

SUMMARY

In the first section of the report various aspects concerned with the measurement of crack growth resistance (R) curves are discussed:

* use of compliance formulae
* transducer sensitivity requirements
* variation of Young's Modulus
* data spacing
* comparison of bend and CT test geometries.

The second part of the report covers recommendations with regard to the interpretation of fracture toughness data (CTOD and J) from R curves for fracture assessments.

Finally a fracture assessment procedure for using CTOD R curves and maximum load toughness is presented.

INTRODUCTION

The Welding Institute has been actively involved with the measurement of material resistance (R) curves using single and multiple specimen methods using J and CTOD methods for the past ten years. More recently studies have been extended to incorporate R curves into fracture assessment procedures. This paper is divided into three sections indicating the latest developments concerning the measurement, interpretation and use of R curves.

MEASUREMENT OF R-CURVES

A procedure for the determination of the fracture resistance of fully ductile metals has recently been produced at The Welding Institute (1). This document covers both the multiple specimen method and single specimen unloading compliance technique. Particular areas of interest include:

Calculation of Crack Tip Opening Displacement (CTOD)

The formula advocated in BS5762 (2) to calculate CTOD is:

$$\delta = \frac{K^2 (1-\nu^2)}{2\sigma_{YS} E} + \frac{0.4 (W-a_o) V_p}{0.4W + 0.6a_o + z} \quad (1)$$

The first term in this formula represents the elastic component of CTOD which is expressed as a function of the stress intensity factor. An additive plastic component of CTOD is then calculated from the plastic component of clip gauge displacement (V_p). The general method of determining V_p involves measuring the slope of the load versus clip gauge displacement line in the elastic regime so that the elastic component of clip gauge displacement at failure may be deducted from the total displacement. (This method is demonstrated schematically in Fig. 1). However since it is not always easy to define the slope of the elastic loading line this method can result in substantial errors in the estimation of V_p. With this in mind an alternative method of calculating V_p which is based on elastic compliance relationships has been developed (1). In this method the plastic component of clip gauge displacement V_p is determined by subtracting the elastic component of clip gauge displacement calculated from elastic compliance relationships (based on the applied load at the point of interest and the measured initial fatigue crack length) from the total clip gauge displacement. The relevant equations for single edge notch bend and compact tension specimens are:

a) SENB specimens

$$V_e = \frac{24P (1-\nu^2)(1 + 1.7\, z/W)}{EB} \frac{a_o}{W} \left[0.76 - 2.28 \left(\frac{a_o}{W}\right) + 3.87 \left(a_o/W\right)^2 - 2.04 \left(a_o/W\right)^3 + \frac{0.66}{(1 - a_o/W)^2}\right] \quad (2)$$

b) Compact tension specimens

$$V_e = \frac{P (1 + 1.7\, z/W)}{BE} \left(\frac{1 + a_o/W}{1 - a_o/W}\right)^2 \left[2.163 + 12.219 \left(a_o/W\right) - 20.065 \left(a_o/W\right)^2 - 0.9925 \left(a_o/W\right)^3 + 20.609 \left(a_o/W\right)^4 - 9.9314 \left(a_o/W\right)^5\right] \quad (3)$$

For sidegrooved specimens B should be replaced by B_e in both the above equations.

E is Young's Modulus at test temperature.

The compliance relationships used in the single edge notch bend and compact tension specimen expressions were originally proposed by Tada et al. (3), and Saxena and Hudak (4) respectively. However both equations have subsequently been modified by including the term (1 + 1.7 z/W) to take account of the effect of knife edge height (5). This correction term is based on the results of a finite element study (6) to assess the influence of knife edge height on elastic compliance relationships.

A graph showing the error in converting the compliance measured at a knife edge height z to the compliance measured at the specimen surface (SENB) or load line (CTS) using the (1 + 1.7 z/W) conversion factor is shown in Fig. 2. It is evident that the ratio z/W should be kept as small as possible.

Resolution Requirements for the Unloading Compliance Method

If the load and displacement signals are converted to digital form for subsequent computer processing the resolution of the digital signals for the unloading compliance method should be such that the following values of load and displacement can be resolved.

$$\text{Displacement} \quad \frac{W \sigma_{YS}}{500\ E} \tag{4}$$

$$\text{Load} \quad \frac{BW}{15000}\ \sigma_{YS} \tag{5}$$

It should be noted that the resolution requirements are dependent on the specimen size becoming more stringent the smaller the test piece. The above requirements can be applied to either compact tension or SENB specimens provided the a/W ratio is at least 0.5.

These requirements ensure that the resolution of the load and displacement channels are less than 0.5% of the load and displacement ranges produced by a 15% unloading at general yield conditions.

Alternatively these requirements can be expressed as the maximum transducer range a data acquisition system can handle. For an n bit data acquisition system with a resolution of λ the range (R) is given by:

$$R = 2^{n-1}\ \lambda \tag{6}$$

Substituting the resolution requirements for λ therefore gives the

maximum transducer range that a data acquisition system can handle yet still provide the required resolution. Figs. 3 and 4 show the maximum load and displacement transducer ranges for a 12 bit and a 16 bit data acquisition systems as a function of specimen size for a typical nuclear A533B type steel. ie:

($\sigma_{YS} \sim 500 N/mm^2$ $E = 207 \times 10^3 N/mm^2$)

Variation of Young's Modulus with Temperature

If the single specimen unloading compliance method is used to estimate crack lengths then the material's Young's Modulus must be known at the temperature of interest.

Graphs showing the variation of Young's Modulus with temperature for ferritic steels, austenitic steels, and aluminium are presented in Figs. 5 and 6. (This information is from BS5500 (7). In addition Table 1 lists values and ranges of E for different materials (8).

Data Spacing

To ensure that the R-curve is sufficiently well defined over the crack growth range of interest the following requirements on data spacing have been proposed. (Note these requirements should only really apply to multiple specimen data).

i) Ideally at least four data points (all associated with evidence of tearing) should be evenly spaced between:

$\Delta a = 0$ and $\Delta a = 2mm$ or $\Delta a = 5\% (W-a)$

whichever is the largest.

ii) Furthermore if the total crack extension up to the maximum exclusion limit is divided into four equal regions and numbered 1,2,3 and 4 in order of increasing Δa, as shown in Fig. 7 then at least one point should lie within each of the regions 2,3 and 4. A fourth point should lie within regions 1 to 4.

CT vs SENB R-curves

Figs. 8 and 9 relate the R-curve behaviour of 50mm thick CT and SENB specimens. The material employed was 50mm thick A533B Class I plate in the L-T orientation with a yield stress of $471 N/mm^2$ and an ultimate of $591 N/mm^2$.

The SENB specimens were manufactured to BS5762 procedures with $W = 100mm$ and $a/W = 0.4$. The CT specimens were of the modified geometry in ASTM E813 also with $W = 100mm$ but $a/W = 0.55$.

The figures show five datum points for each geometry obtained by interrupting the loading at +70°C on five separate specimens, heat tinting and breaking open cold. Load point displacement measurements were obtained using the double clip gauge method for SENB, and from a clip gauge on the load line position in the notch for the CT geometry.

J estimates were made using E813 procedures, whilst CTOD measurements (δ_o) were derived using the formula in BS5762 for SENB and the ASTM E24.08.04 draft procedure for the CT geometry.

Fig. 8 indicates a slight tendency for the SENB data to be grouped above the CT.

These specimens are non sidegrooved and it appears that the SENB specimens tend to show less crack growth at the surface of the specimens although crack extension measurements over the central 70% of the width are similar for the two geometries. Fig. 9, which illustrates the CTOD R-curve shows good agreement between SENB and CT results due to the use of Δa measurements to BS5762 Appendix A.

INTERPRETATION OF R-CURVES

Whilst the Welding Institute Procedure (1) sets out a method of estimating the initial crack length in the event of apparent negative crack growth, recent modifications to the Welding Institute unloading compliance system have, to a large extent, removed the phenomenon of negative crack growth. These modifications include:

1. a new servo electric test machine.

2. computer control of test machine.

3. tests performed under clip gauge control.

4. continual monitoring of the unloading rate observed during the hold periods (ie. constant clip gauge opening) before an unloading. The subsequent unloading sequence does not commence until the load relaxation rate is less than 0.5% of the elastic loading rate measured in the elastic regime.

Typical J and CTOD R-curves produced by the present system are shown in Figs. 10, and 11 respectively.

It is evident from Figs. 8 and 10, that the ASTM J_{Ic} estimation procedure is unrealistic for this material as the R-curve has an initial slope which is similar to the [illegible] line. It is therefore

Welding Institute policy to express the value of toughness (either J or CTOD) corresponding to 0.2mm ductile crack length extension. The procedure used to determine $J_{0.2}$ or $CTOD_{0.2}$ is to draw a best fit line or curve through the data between the upper exclusion limit (Δa = 2mm or 5% (W-a)) and a line corresponding to 0.2mm ductile crack growth. The value of toughness at 0.2mm is defined as the point of intersection between the best fit curve and the line constructed at 0.2mm ductile crack growth

THE USE OF R CURVES IN A FRACTURE ASSESSMENT

Part of BS PD6493 is based on an approximate version of The Welding Institute's present CTOD design curve approach. In its current form BS PD 6493 suffers from four major deficiencies:

i) The present CTOD design curve is partly empirical and validated only for ferritic steels. For other materials an LEFM based approach is adopted.

ii) A variable safety factor is inherent in the approach making probablistic studies and critical analyses difficult.

iii) There is no mechanism for incorporating a material's resistance curve.

iv) Plastic collapse solutions are not an integral part of the analysis.

To address these drawbacks, a collapse modified strip yield model of the form:

$$\delta = \frac{8(\sigma_{pc})^2 \bar{a}}{\pi E \sigma_{YS}} \ln \sec \left(\frac{\pi \sigma}{2\sigma_{pc}}\right) \qquad (7)$$

is examined in reference (9). This model does not incorporate a safety factor and is also relevent to materials other than ferritic steels.

The model can also be written in the form of the ratio of applied CTOD to critical CTOD, δ_r ($= \delta_{app}/\delta_c$)

$$\text{i.e. } \delta_r = \frac{\pi^2}{8} S_r \left(\ln \sec \frac{\pi}{2} S_r\right)^{-1} \qquad (8)$$

where S_r $\left(= \frac{\sigma}{\sigma_{pc}}\right)$ is the stress ratio.

This relationship can be plotted as a CTOD Failure Assessment Diagram equivalent to the CEGB R6 approach, see Fig. 12.

A material's CTOD resistance curve describes the variation of crack tip opening displacement, δ_o, with incremental crack extension, Δa_p. Rewriting equation (7) in the form:

$$\sigma = \frac{2\sigma_{pc}}{\pi} \cos^{-1} \left[\exp \left(- \frac{\pi E \sigma_{YS} \delta_o}{8(\sigma_{pc})^2 \bar{a}} \right) \right] \qquad (9)$$

allows input of δ_o values to determine the locus of applied stress, σ, with incremental crack extension, as in Fig. 13. In this way, the maximum applied stress and crack extension at that stress, can be determined for a particular cracked component. By plotting this curve with the predicted collapse behaviour, the mechanism of failure (ie. whether dominated by collapse or fracture) can also be assessed. The maximum applied stress is the instability condition under load controlled conditions; however, in a less compliant loading system, stable tearing will continue beyond maximum stress.

The effectiveness of this procedure was assessed in Ref. (9) by predicting the behaviour of wide plates and burst tests in API 5LX56 and A533B Class I ferritic parent steels and of wide plate tension tests in stainless steel plate and weldments. The predictions were then compared with physical data obtained from the tests.

Reasonable predictions of maximum applied stress were achieved. However, the accuracy was very dependent on the plastic collapse estimations. This was particularly true for the high work hardening stainless steel plate where, to avoid an overestimate of collapse, an effective flow stress was assumed equal to the stress at 3% strain in a uniaxial tensile test.

The accuracy of the crack growth prediction at maximum applied stress varied from very good for the API 5LX56 steel, to a severe underestimate for the stainless steel plate. For accurate predictions of the behaviour of a high work hardening material it was necessary to adopt a more complex assessment incorporating the material's stress-strain curve as discussed in Ref. (10).

The use of maximum load CTOD, δ_m, with the collapse modified strip yield model was also considered in Ref. (9). Using this approach, conservative predictions of the maximum applied stress were obtained for the tests analysed. These results were also compared with predictions using δ_m and the CTOD design curve. More accurate and more consistent predictions were obtained with the strip yield model.

Finally the use of the CTOD at initiation of tearing, δ_i, as input to the assessment procedures was evaluated. In general, this procedure gives unacceptable levels of conservatism and misleading indications of the controlling mechanism of failure.

The geometry dependence of resistance curves and the inaccuracy of the strip yield model for high work hardening materials means that the cost of producing an R curve and the extra analysis time would not generally be repaid by significant improvements in the accuracy of the predictions.

Thus for general assessments of ductile materials, the use is recommended of maximum load toughness with the collapse modified strip yield model or, for ferritic steels, of the CTOD design curve. The complexity of more sophisticated approaches is not generally warranted where input data are variable or uncertain. However, for very specific assessments and particularly when analysing laboratory tests, a more accurate and complex approach (eg. see Ref. (10)) is necessary.

REFERENCES

1. J.R. Gordon, 'The Welding Institute Procedure for the determination of the fracture resistance of fully ductile metals'. Welding Inst. Report 1985 (To be published).

2. BS5762: 1979 'Methods for crack opening displacement (COD) testing'. British Standards Institution 1979.

3. H. Tada, H. P.C. Paris, and G.R., Irwin 'The stress analysis of cracks'. Handbook Del. Research Corporation.

4. A. Saxena, and S.J. Hudak, 'Review and extension of compliance information for common crack growth specimens'. Int. Journal of Fracture, Vol. 14, No. 5, 1978, pp 453-468.

5. S.J. Garwood and A.A. Willoughby, 'Fracture toughness measurements on materials exhibiting stable ductile crack extension'. Presented at the International Conference' Fracture Toughness Testing - Methods, Interpretation, and Application', London 1982.

6. A.A. Willoughby, 'On the unloading compliance method of deriving single specimen R-curves in three point beinding'. Welding Institute Report, 153/1981.

7. BS5500, 'Specification for unfired fusion welded welded pressure vessels'. British Standards Institution, 1982.

8. M.F. Ashby and D.R.H. Jones 'Engineering materials, an introduction to their properties and applications'. Pergamon Press.

9. S.J. Garwood, 'A crack tip opening displacement (CTOD) method for the analysis of ductile materials'. Welding Institute Members Report 1985.

10. T.L. Anderson, 'Elastic-plastic fracture assessments based on CTOD'. Welding Institute Members Report 1985.

Table 1 Data for Youngs Modulus at 20°C

Material	E (GN/M^2)
Nickel	214
Nickel Alloys	130 - 234
Iron	196
Ferritic steels, low alloy steels	200 - 207
Stainless, austenitic steels	190 - 200
Cast Irons	170 - 190
Copper	124
Copper alloys	120 - 150
Vanadium	130
Titanium	116
Titanium alloys	80 - 130
Zirconium and alloys	96
Aluminium	69
Aluminium alloys	69 - 79

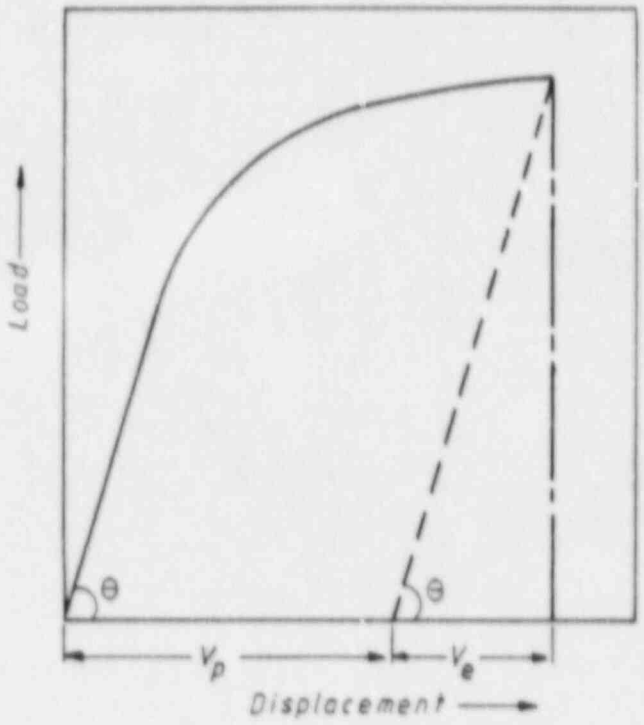

Fig.1. Graphical determination of V_p

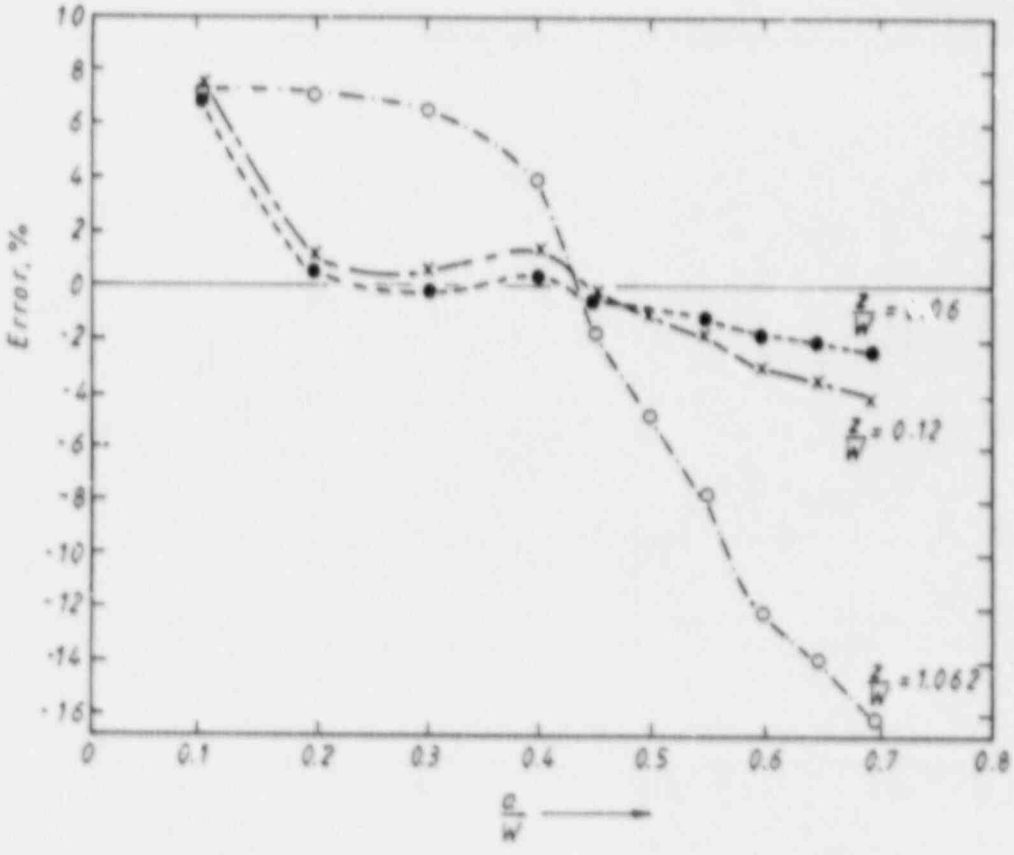

Fig.2. Percentage error in compliance using the knife edge height correction formula.

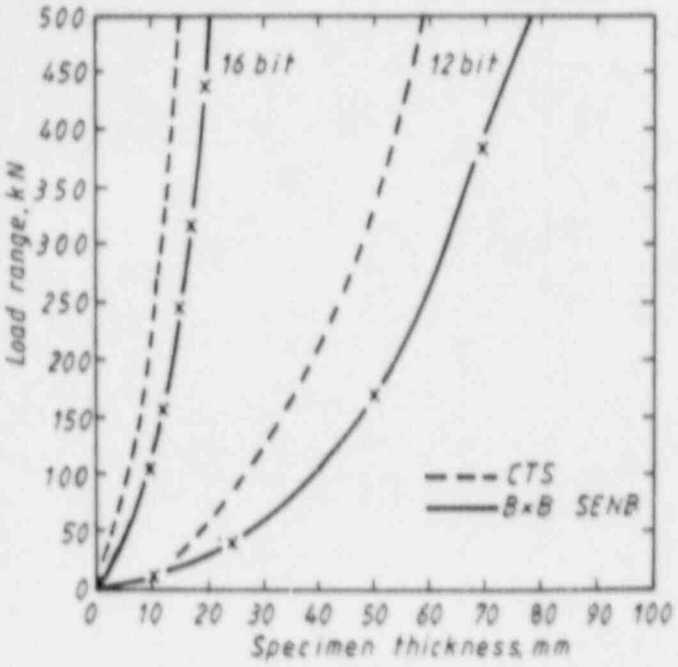

Fig.3. Load range v. specimen thickness.

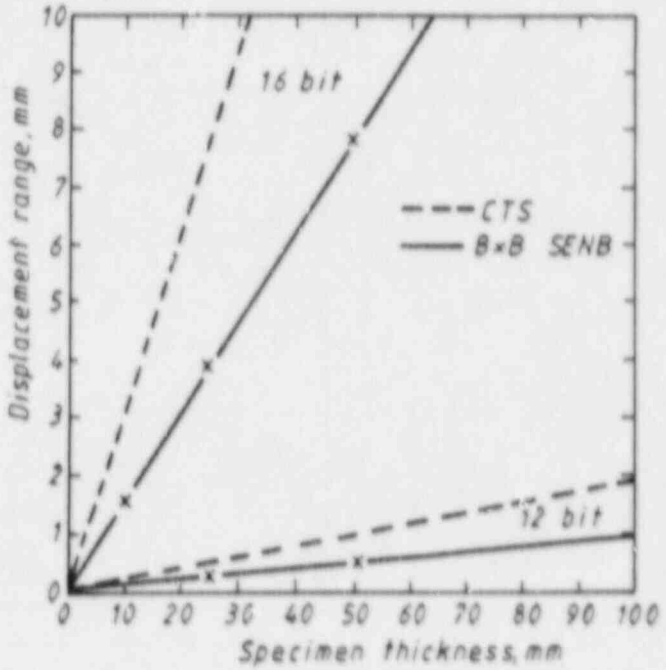

Fig.4. Displacement range v. specimen thickness.

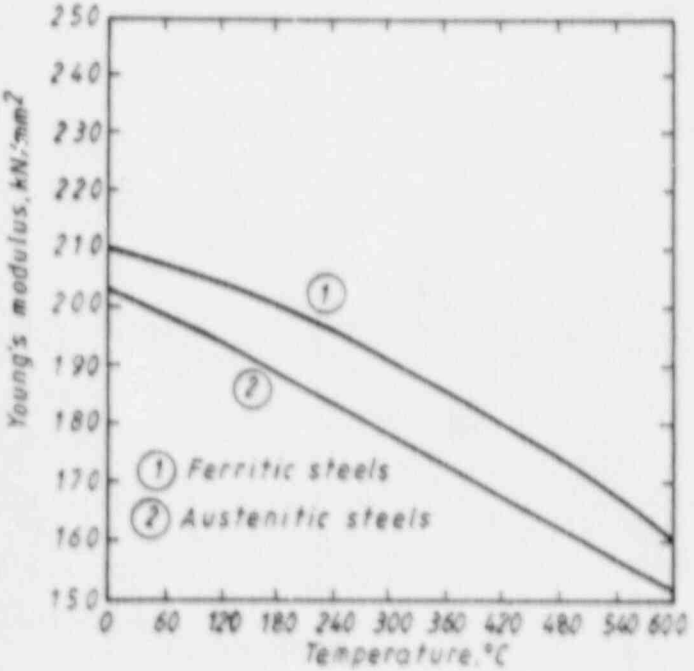

Fig.5. Variation in Young's modulus with temperature (ferritic steels and austenitic steels).

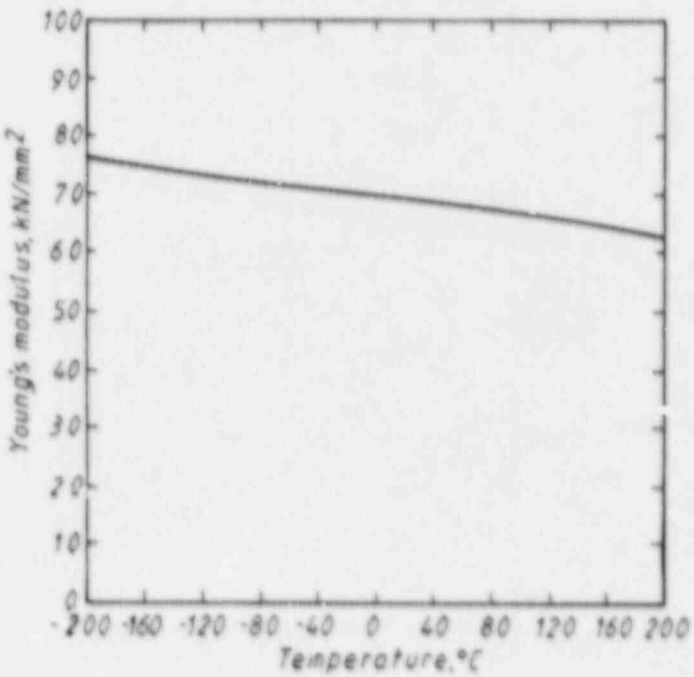

Fig.6. Variation in Young's modulus with temperature (aluminium).

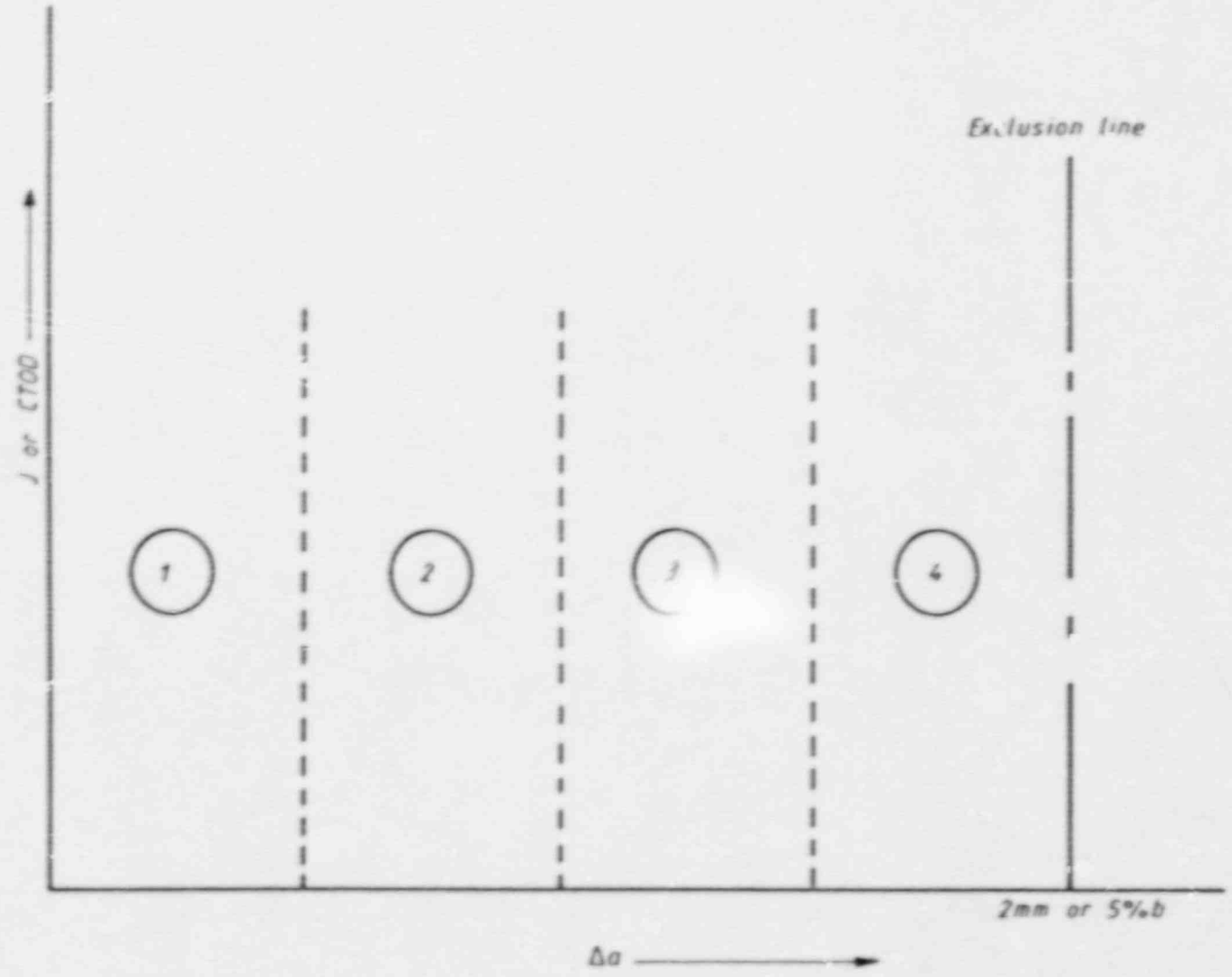

Fig. 7. Regions 1-4 for data spacing requirements.

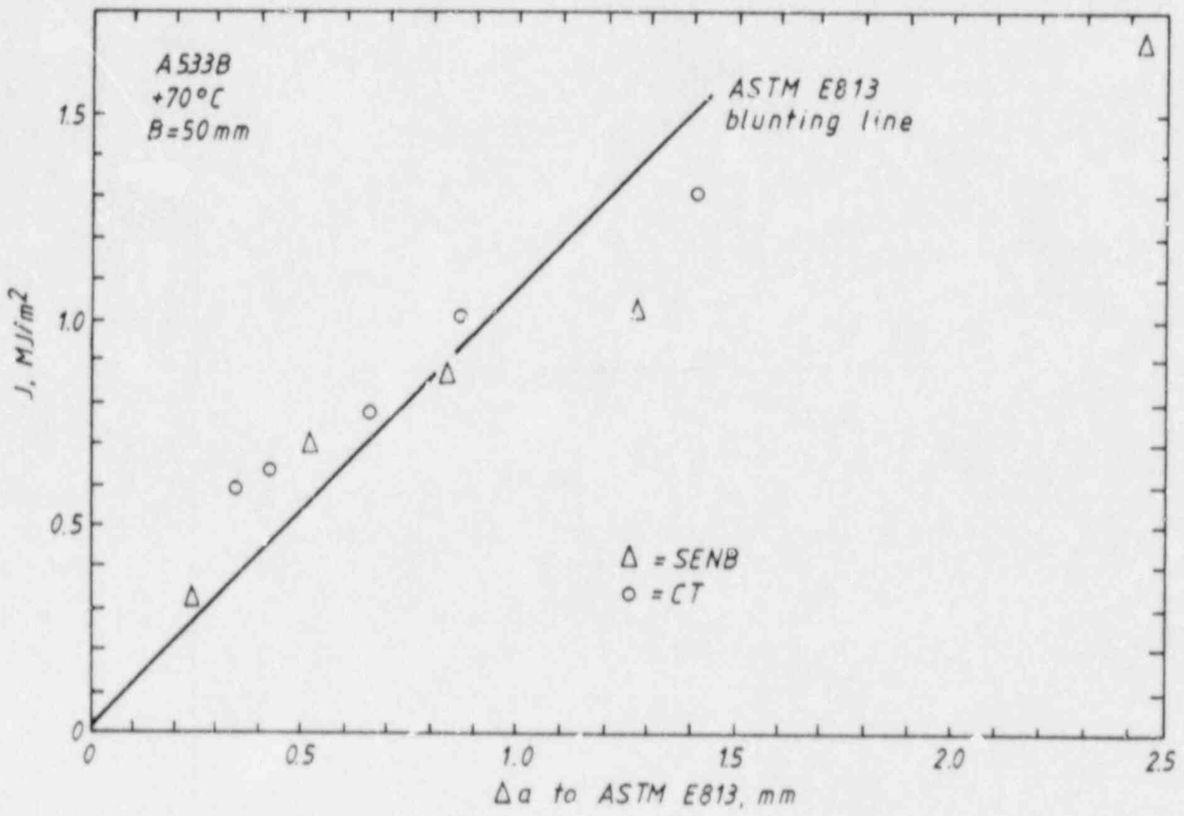

Fig.8. J R-curve (with Δa including stretch zone width).

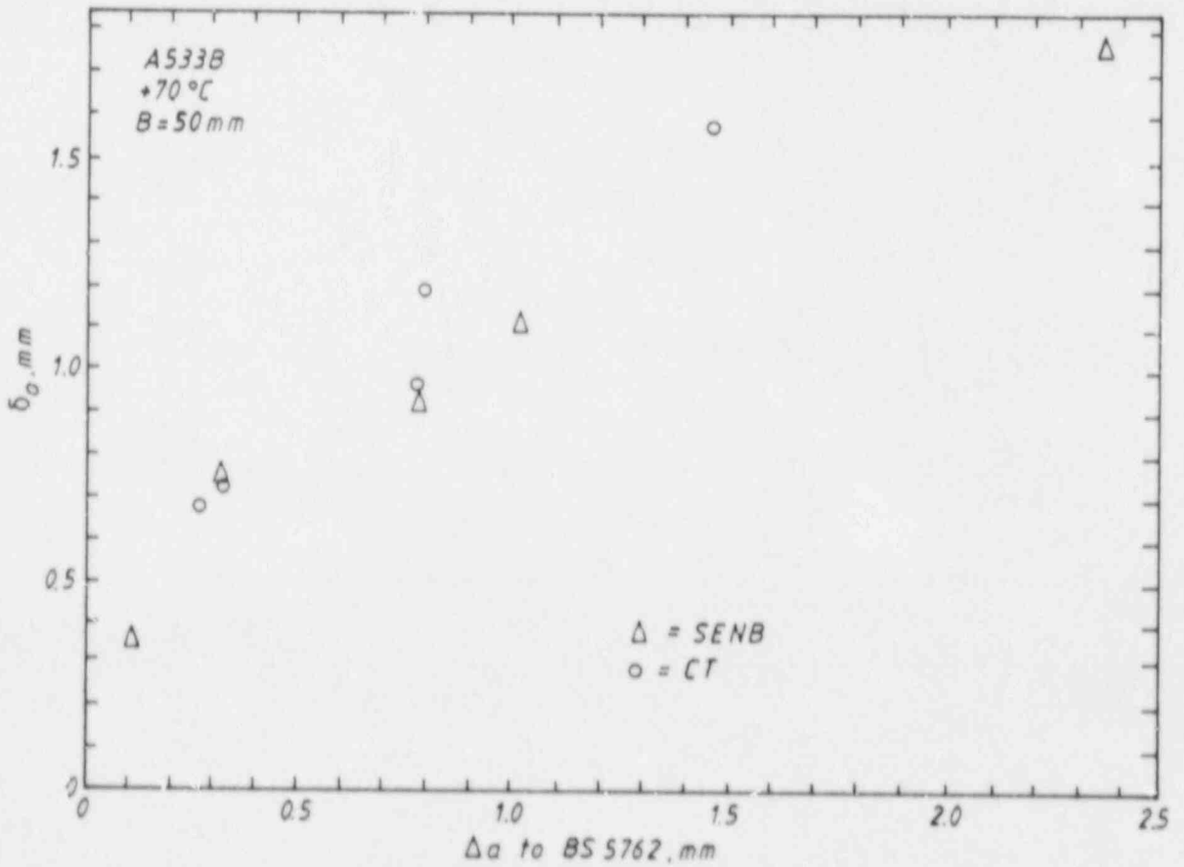

Fig.9. CTOD R-curve to BS 5762.

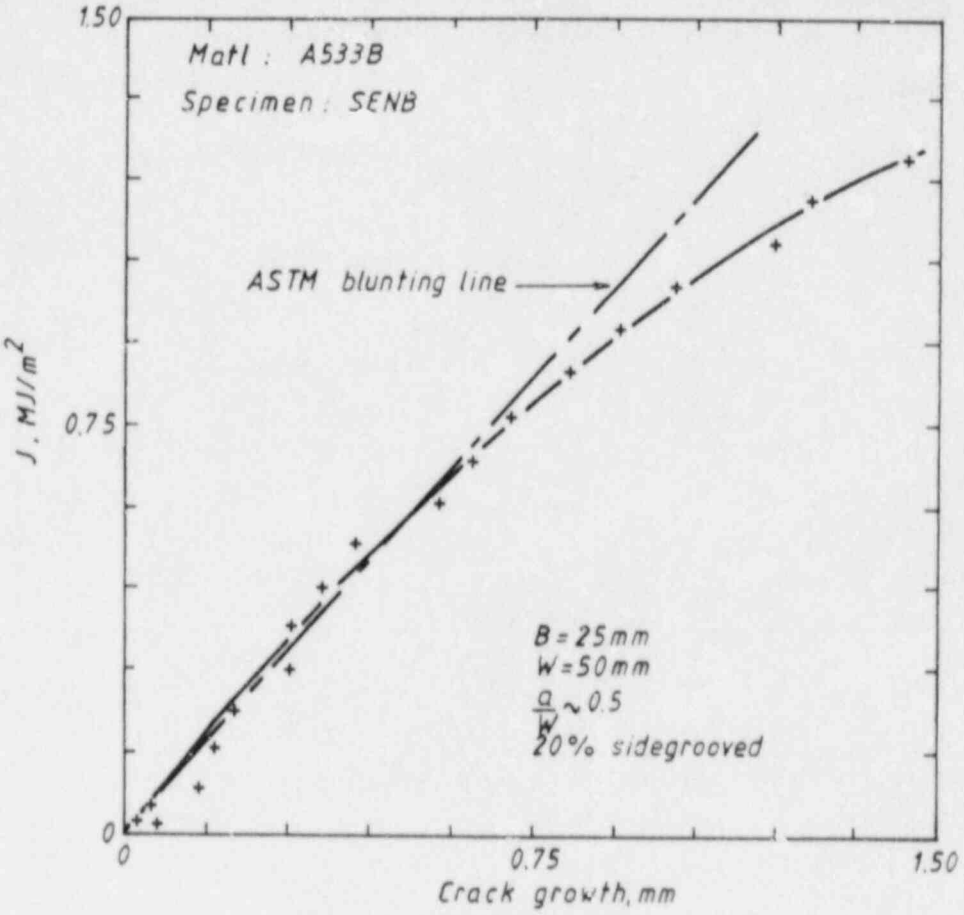

Fig.10. J R-curve.

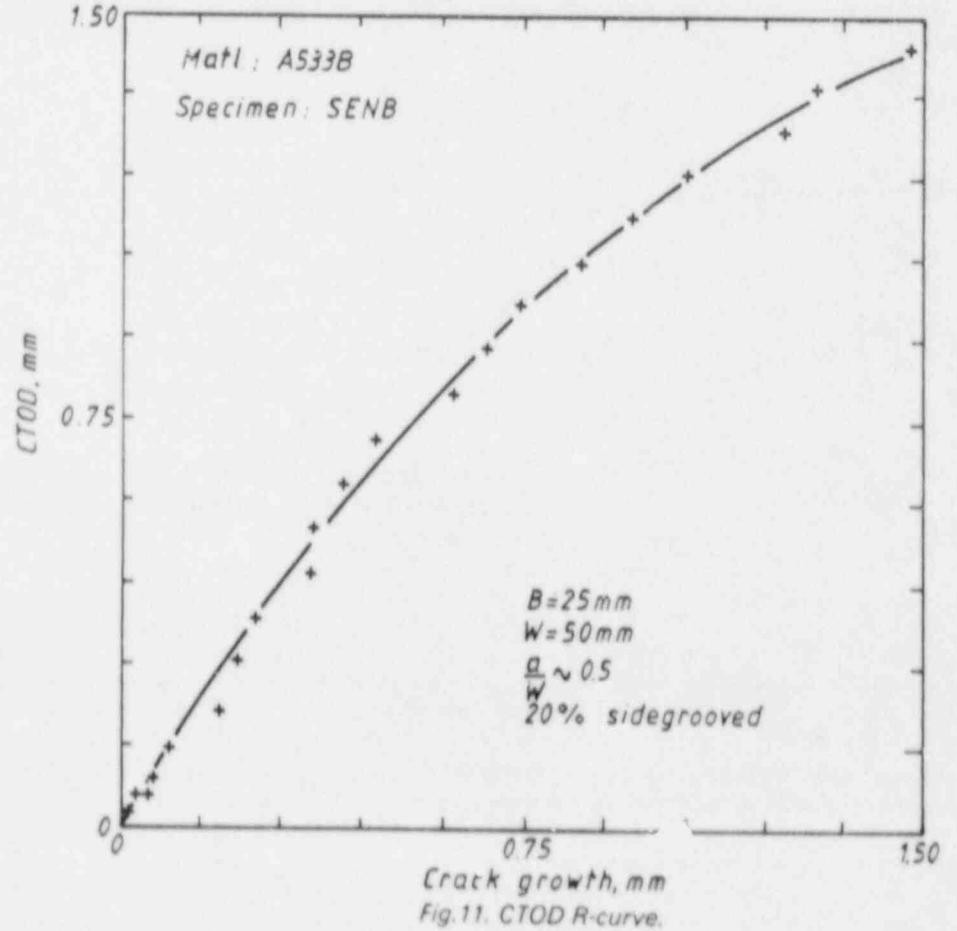

Fig.11. CTOD R-curve.

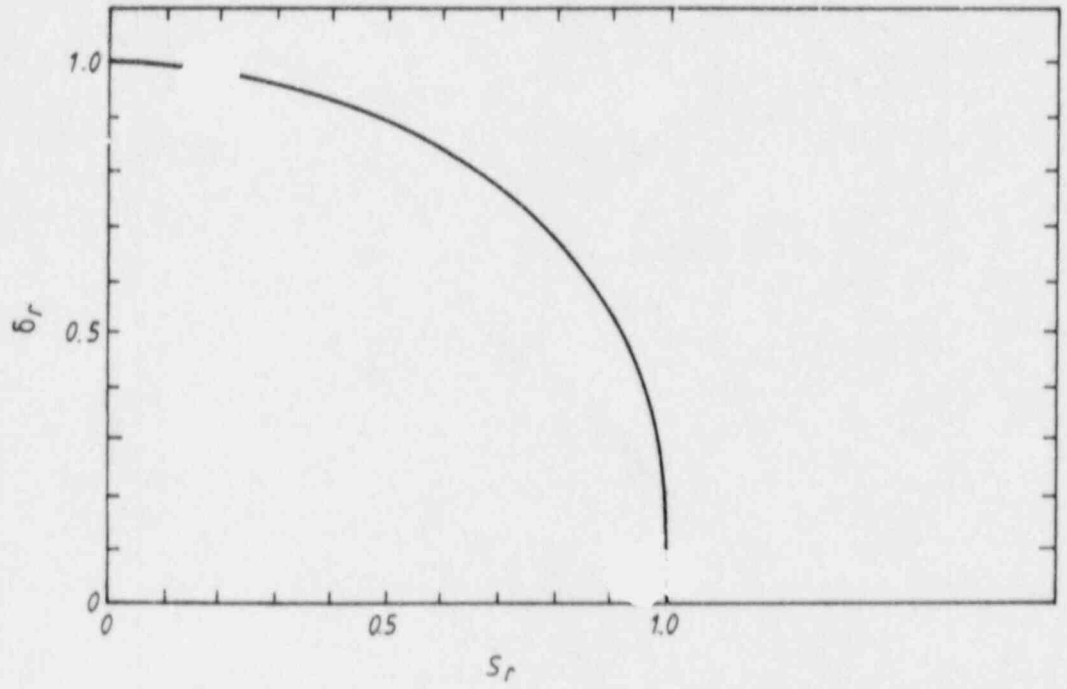

Fig.12. CTOD failure analysis diagram derived using the strip yield model.

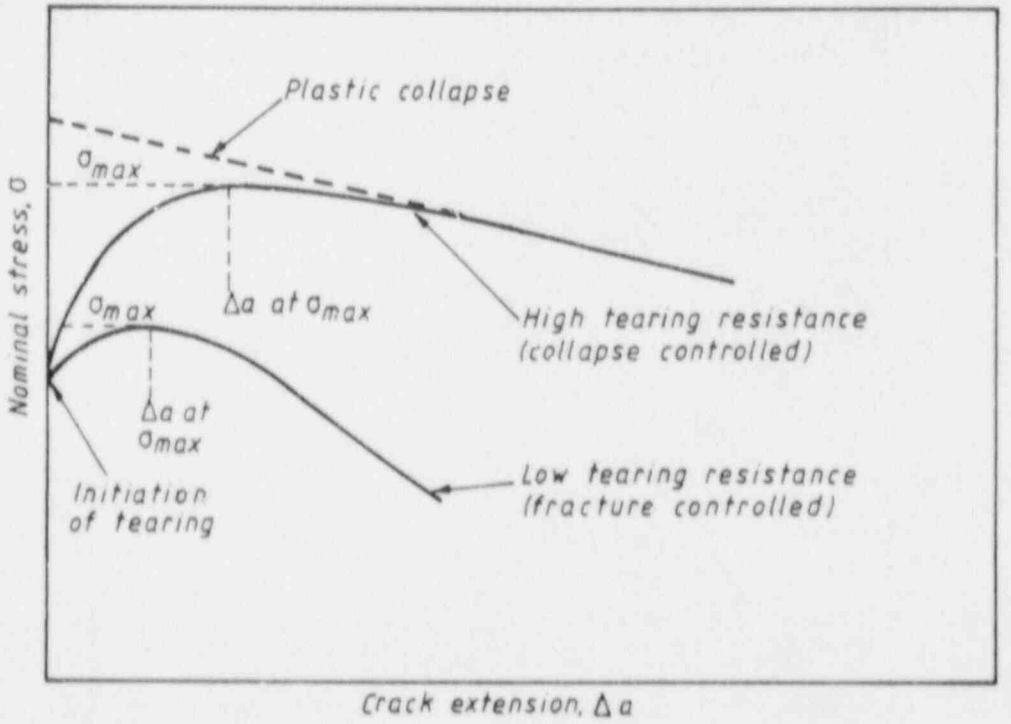

Fig.13. Maximum stress assessment derived from the locus of the predicted nominal stress with increasing crack extension.

DETERMINATION OF J_{Ic} USING NEW BLUNTING LINE CONSTRUCTION

J. Heerens, A. Cornec, K.-H. Schwalbe
GKSS-Forschungszentrum Geesthacht GmbH
Institut für Werkstofftechnologie
Max-Planck-Str.
D-2054 Geesthacht, FRG.

ABSTRACT

A modification to the present J_{Ic} test standard ASTM E813-81 [1] is proposed, which is currently being discussed by the german working group "Kennwertermittlung und Anwendung der Bruchmechanik".

In the Propcsed procedure J_{Ic} is defined at a certain amount of ductile tearing, Δa = 0.2 mm. J_{Ic} is determined by the intersection between the J-Δa curve and an intercept line which is a line parallel to, and 0.2 mm off the blunting line.

In addition, requirements for the data point distribution, the data point fitting and crack growth measurement accuracy are proposed.

For the calculation of the stretch zone development during the blunting phase, an improved blunting line equation $J = \Delta a \sigma_o / 0.4\ d_n$ is derived, which is based on the HRR-field theory. This improved blunting line equation gives good agreement with the experimental stretch zone width measurements, whereas the recommended ASTM blunting line equation $J = 2\sigma_f \cdot \Delta a$ overestimates the stretch zone width in all materials tested.

Proposed J_{Ic}-Procedure

J_{Ic}-procedure being discussed by the german working group "Kennwertermittlung und Anwendung der Bruchmechanik" is shown in Fig. 1.

For the determination of a J_{Ic}-value the following requirements must be satisfied:

- At least five data points must be within the exclusion lines E1 and E4.
- At least one data point must be between E1 and E2, E2 and E3, E3 and E4 respectively.

The data points between E1 and E4 should be fitted using the power law $J = A \Delta a^{\beta}$. The J_{Ic}-value is determined by the intersection of the power law and the 0.2 mm offset line, see Fig. 1

Using the single specimen technique, Δa must be measured with sufficient accuracy. The accuracy of the indirect Δa measurement methods (PU, DCPD, AC, US...) must be better than ± 0.1 mm or $\pm$ 15% Δa, whichever is larger. It is proposed to check the accuracy by comparing the indirectly measured final crack extension with the final crack extension determined directly on the fracture surface.

Crack tip blunting investigations

Experimental

Using the infiltration technique the following quantities were measured, see Fig. 2.

quantity	measured on
$\delta_{45\ Rep}$	Replica
2SZH	Replica
SZH	Frac. surface

Measurements were conducted mainly, during the blunting phase i.e. $J < J_o$, J_o = initiation value.

Materials used:

- X6CrNi1811
- 20MnMoNi55

Specimens used:

CT, W = 50 mm, B = 18-25 mm

a_o/W = 0.5-0.6

Results

From Fig. 3 it can be seen:

$\delta_{45\ Rep.} \approx \delta_{45\ HRR} = d_n \frac{J}{\sigma_o}$, (plane strain), Shih [2]

$2SZH \approx \delta_{45\ Rep.}$

$SZW \approx 0.4 \cdot 2SZH$

according to the determination of d_n and σ_o see ref. [3].

Conclusions

$$SZW = 0.4\, d_n \frac{J}{\sigma_o}$$

if $SZW = \Delta a$

$$\Delta a = 0.4\, d_n \frac{J}{\sigma_o} \qquad \text{blunting line}$$

Application of the blunting line

The blunting line equation $J = \Delta a \cdot \sigma_o / 0.4\, d_n$ was examined by comparison with experimental stretch zone width results measured on the materials shown in table 1, see Fig. 4.

TABLE 1

tested materials	$\sigma_{0.2}$	σ_{UT}	E
X6CrNi1811	24o	622	195 000
20MnMoNi55	478	612	210 000
A 572	400	592	210 000
Al 2024 FC	75	217	71 000
HT 60 [1]	596	667	210 000
HT 80 [1]	765	814	210 000

[N/mm^2]

1) SZW results taken from ref. [4]

It can be seen from the diagrams that the recommended ASTM blunting line $J = 2\, \sigma_f\, \Delta a$ overestimates the stretch zone width whereas the proposed blunting line $J = \Delta a\, \sigma_o / d_n\, 0.4$ gives a good correlation with the experimental results.

REFERENCES

[1] E813-81 Standard Test Method for J_{Ic}, a Measure of Fracture Toughness, Annual Book of ASTM Standards Part. 10, 1983.

[2] Shih, C.F : Relationships between the J-integral and the crack opening displacement for stationary and extending cracks, J. Mech. Phys. Solids 29, 1981, pp. 305-326.

[3] A. Cornec, J. Heerens: Procedure for the determination of a theoretical blunting line, CSNI-Meeting, Workshop on ductile fracture test method, Paris, April 1985.

[4] K. Ohji, A. Otsuka, L. Kobayashi: Evaluation of Several J_{Ic} Testing Procedures Recommended in Japan, ASTM STP 803, pp. 398-419, 1983.

FIGURE CAPTIONS

Fig. 1: Schematic of J_{Ic}-determination procedure being discussed in the german working group "Kennwertermittlung und Anwendung der Bruchmechanik".

Fig. 2: Replica of the crack tip profile showing the definition of stretch zone width (SZW), double stretch zone hight (2SZH) and δ_{45}.

Fig. 3: Stretch zone measurements on crack tip replicas
a) Austenitic steel X6CrNi1811
b) Nuclear reactor pressure vessel steel 20MnMoNi55

Fig. 4: Predicted and measured stretch zone width for all materials of table 1.

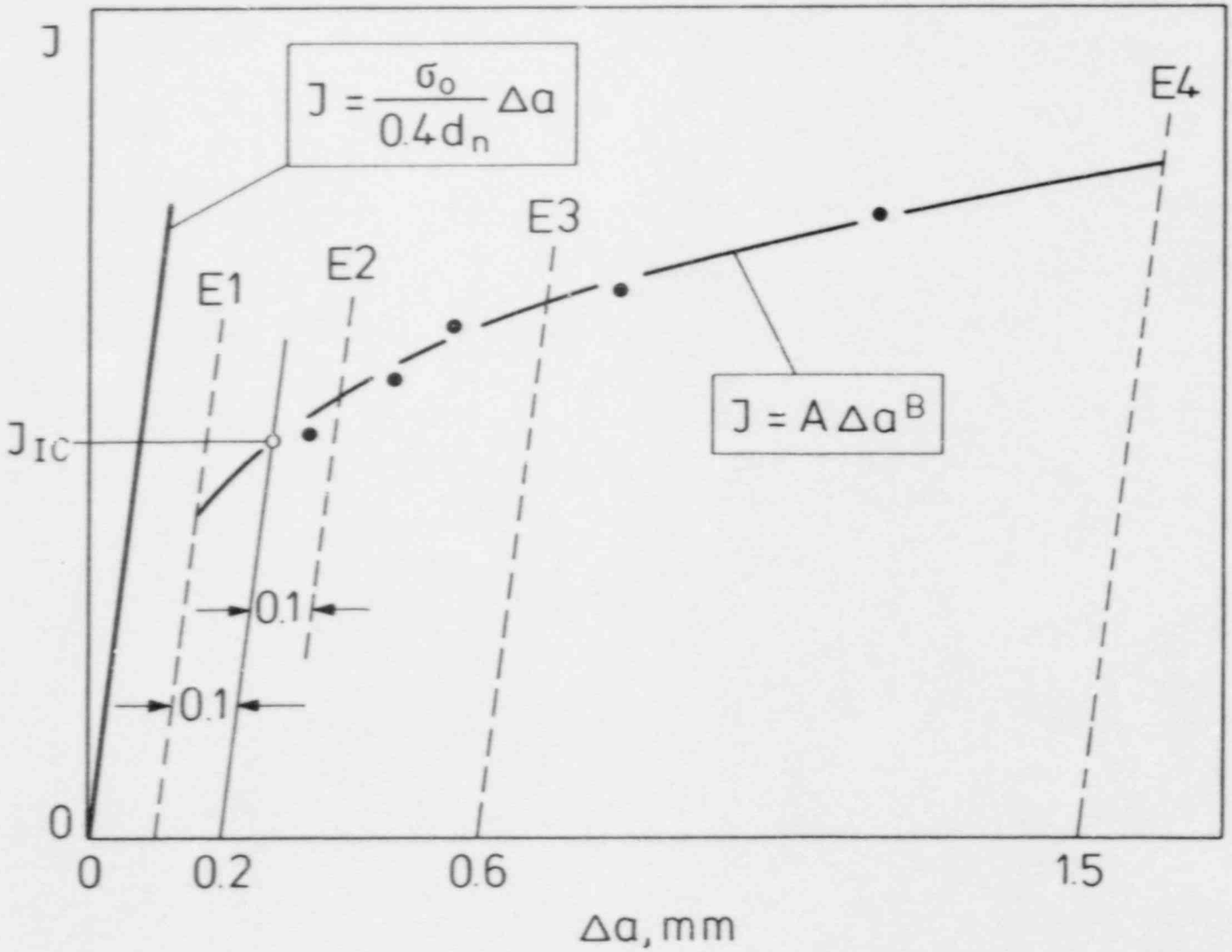
J
$J = \frac{\sigma_o}{0.4 d_n} \Delta a$
E1
E2
E3
E4
J_{IC}
$J = A \Delta a^B$
0.1
0.1
0
0
0.2
0.6
1.5
Δa, mm

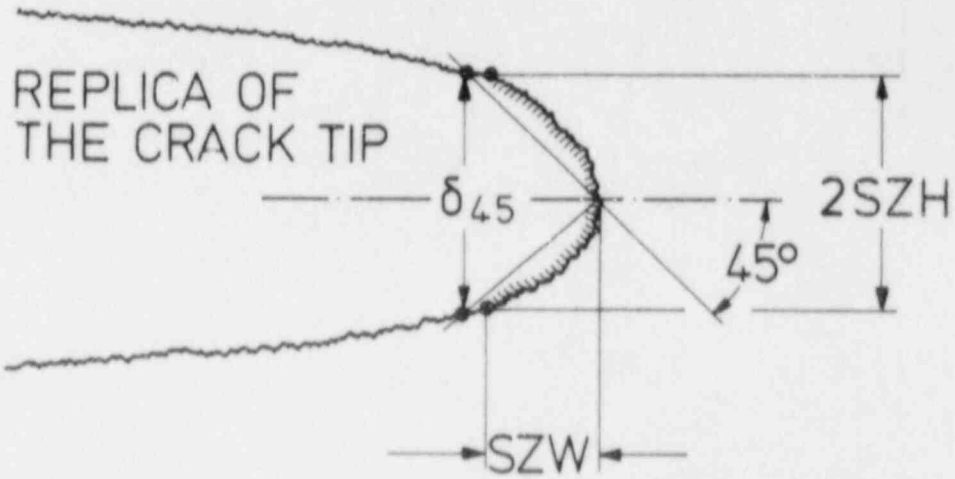
REPLICA OF
THE CRACK TIP
δ45
2SZH
45°
SZW

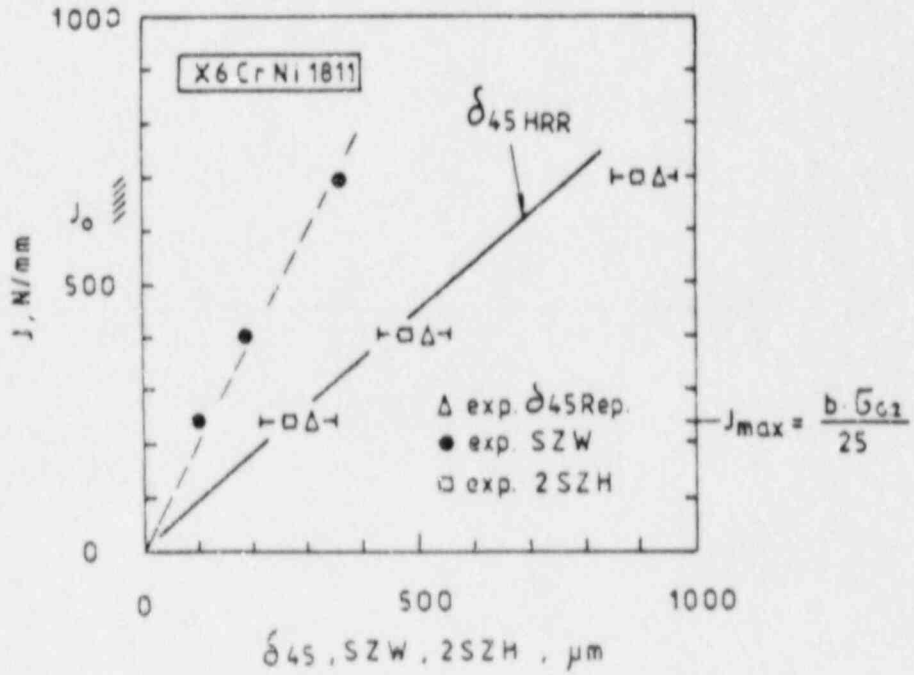
X6CrNi1811
δ_{45} HRR
J_o
J, N/mm
1000
500
0
0
500
1000
δ_{45}, SZW, 2SZH, µm
Δ exp. δ_{45}Rep.
● exp. SZW
□ exp. 2SZH
$J_{max} = \frac{b \cdot \sigma_{02}}{25}$

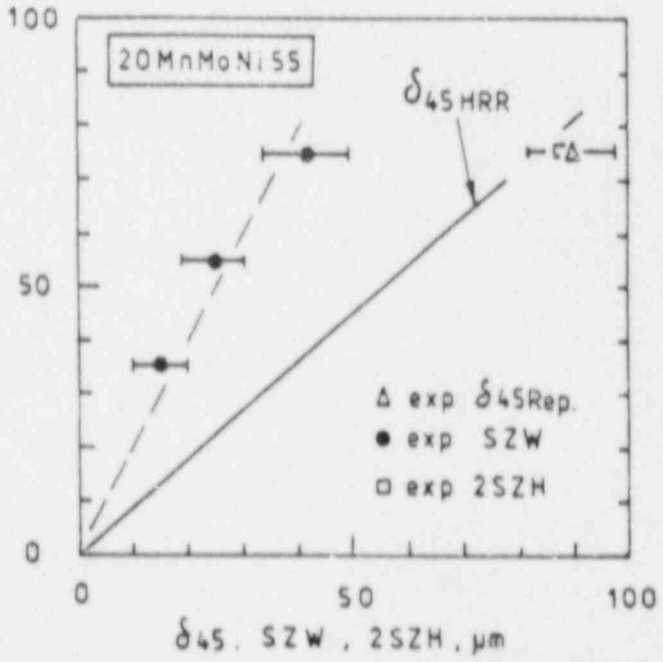
20MnMoNi55
δ_{45} HRR
100
50
0
0
50
100
δ_{45}, SZW, 2SZH, µm
Δ exp δ_{45}Rep.
● exp SZW
□ exp 2SZH

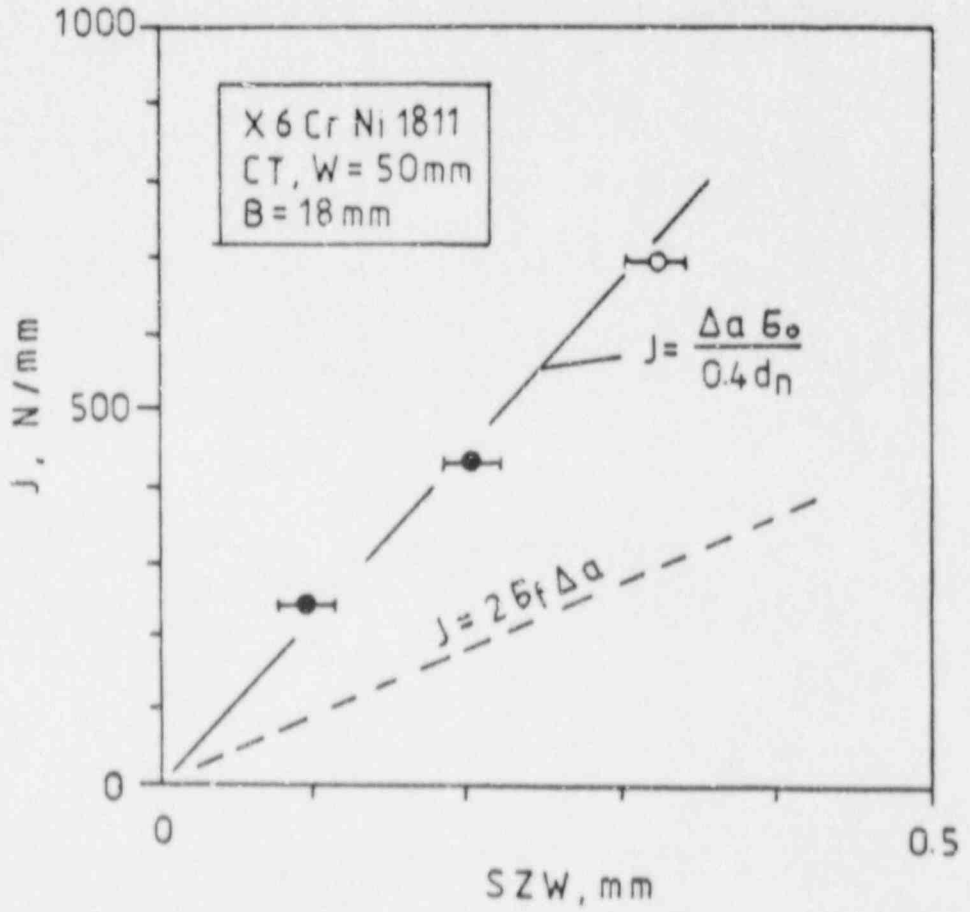
1000
500
0
0
0.5
J, N/mm
SZW, mm
X 6 Cr Ni 1811
CT, W = 50mm
B = 18 mm
J = Δa σ₀ / 0.4 dn
J = 2 σf Δa

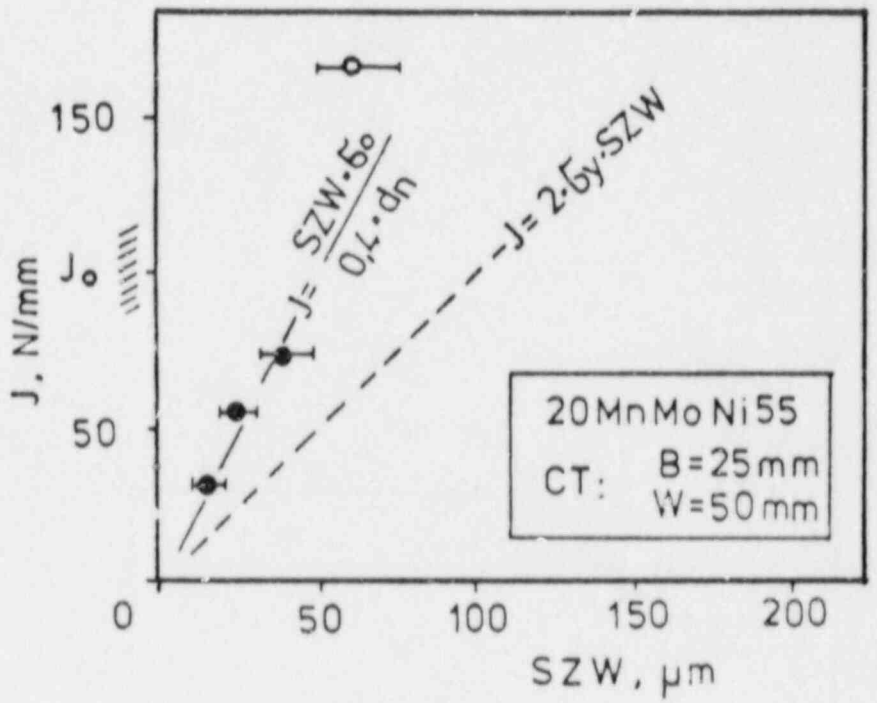
150
J₀
50
0
J, N/mm
J= SZW·σ₀ / 0,4·dn
J= 2·σy·SZW
20MnMoNi55
CT: B=25mm
W=50mm
50
100
150
200
SZW, µm

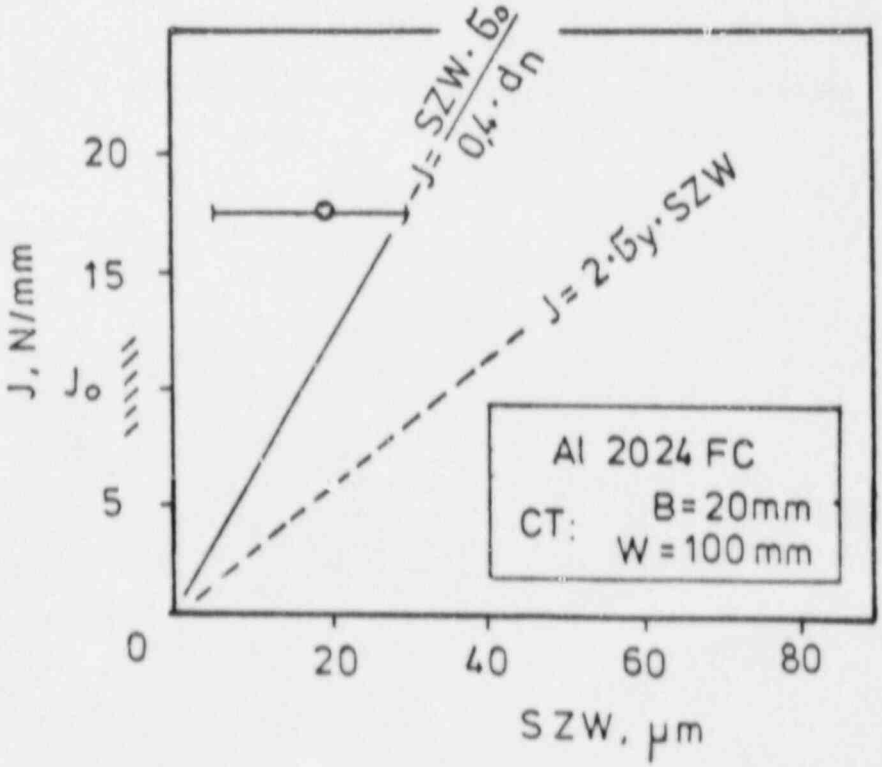
20
15
J₀
5
0
J, N/mm
J= SZW·σ₀ / 0,4·dn
J= 2·σy·SZW
Al 2024 FC
CT: B=20mm
W=100mm
20
40
60
80
SZW, µm

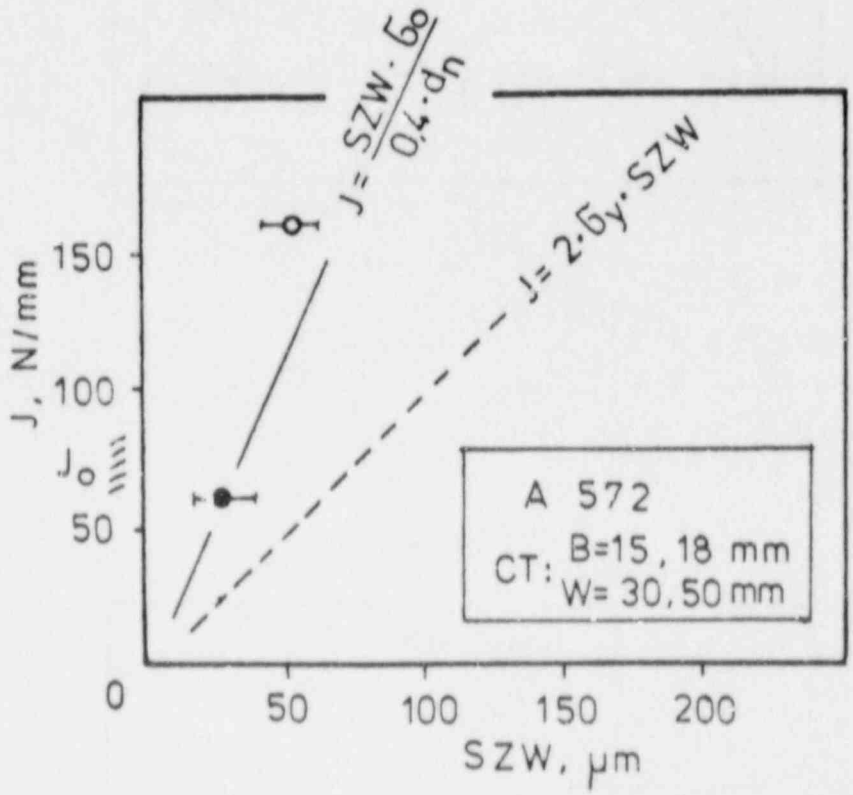
J = SZW · σ0 / 0.4 · σn
J = 2 · σy · SZW
J, N/mm
150
100
J0
50
0
50
100
150
200
SZW, µm
A 572
CT: B=15, 18 mm
W= 30, 50 mm

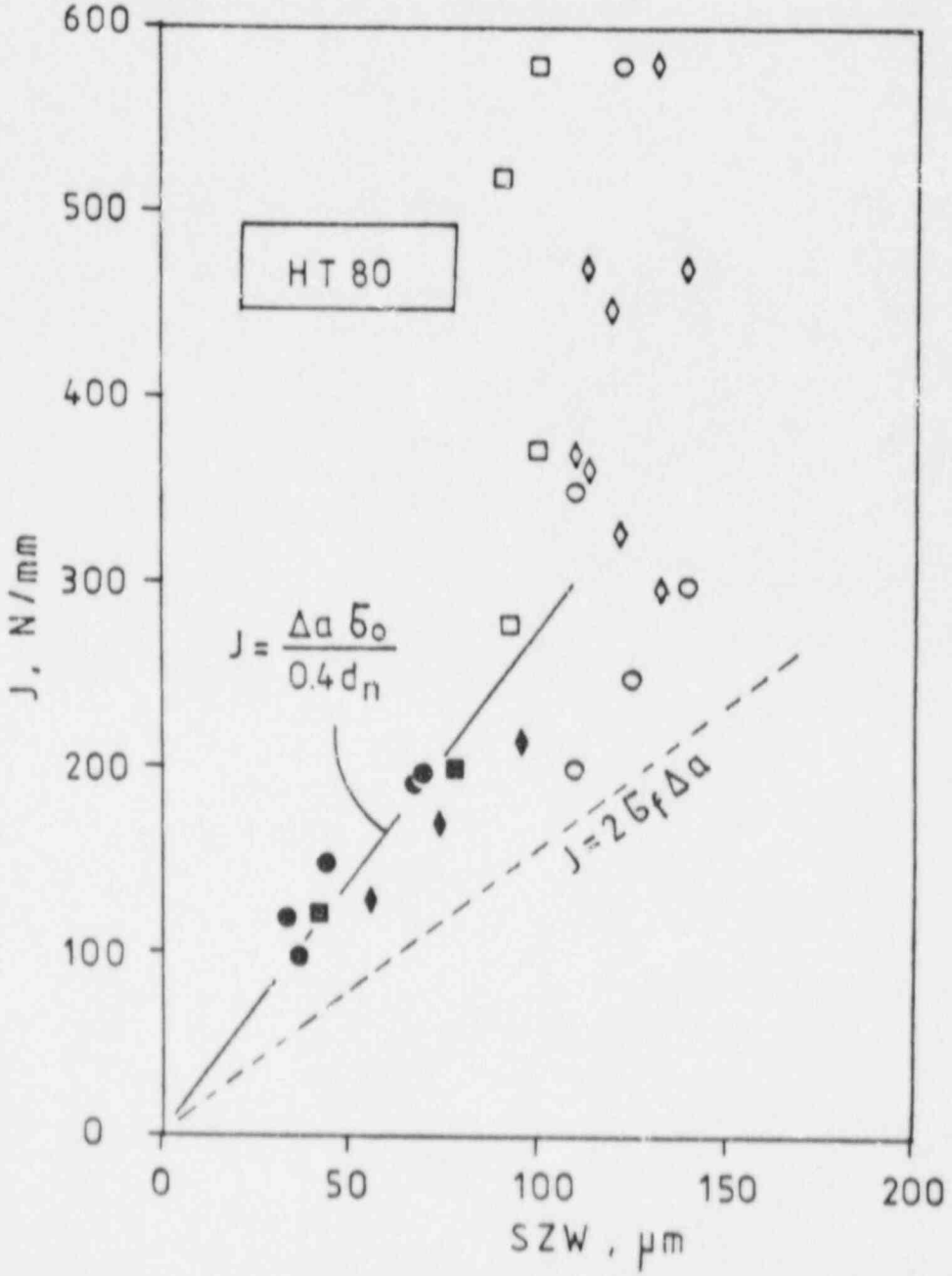
600
500
400
300
200
100
0
J , N/mm
HT 80
$J = \frac{\Delta a \, \bar{\sigma}_0}{0.4 d_n}$
$J = 2 \bar{\sigma}_f \Delta a$
0
50
100
150
200
SZW , µm

SIZE REQUIREMENTS FOR J-R AND δ-R-CURVE TESTING

K.-H. Schwalbe and D. Hellmann

GKSS-Forschungszentrum Geesthacht GmbH
Institut für Werkstofftechnologie
Max-Planck-Str.
D-2054 Geesthacht, FRG.

ABSTRACT

Experimental methods are described which serve to determine size requirements fr J- and δ-controlled crack growth. These methods are:

a) The curve splitting method which takes the points of divergence of the R-curves due to variation of specimen size as the limiting condition for J- or δ-controlled crack growth.

b) A single specimen method exploiting the linear realtionship between J and δ_5. The point of breakdown of this linearity is taken as the limit of J control.

c) A further single specimen method which takes the end of linearity between J and load line displacement as the limit of J control.

All methods result in comparable criteria.

INTRODUCTION

Comprehensive experimental work on relating stable crack growth to the parameters J-integral and crack tip opening displacement (CTOD) has been done at GKSS with the main emphasis on size and geometry effects on the crack growth resistance curve (R-curve). The experimental data can be evaluated such that information on criteria for size and geometry independent R-curves are obtained.

By "J-integral" we mean the deformation J the use of which is now common practice, see for example Refs. [1,2]. The merits of the modified J-integral proposed by Ernst [3] will be investigated in the near future.

The CTOD is measured on the specimen's side surface at the fatigue crack tip over a gage length of 5 mm. This way we free ourselves from the restriction of the standardised CTOD measurement [4] to bend specimens. Our δ_5 can be measured on any specimen geometry of interest.

The first phase of the investigation has concentrated on specimens with thin sections under plane stress conditions; a few cases with plane strain and mixed mode behaviour have been studied as well. Complete reference to experimental procedures and results obtained so far is made in Ref. [5]. The following statements refer to conditions of plane stress.

The J-integral and the CTOD in terms of δ_5 have been determined independently on each specimen tested. Within certain limits which will be discussed below, compatibility between J and δ_5 can be demonstrated, which means that for a given material there is a unique relationship between J and δ_5, independent of size and geometry, Fig. 1 (see also Ref. [6]).

This relationship is linear and can be expressed as

$$\delta_5 = \frac{1}{m}\frac{J}{\sigma_Y} \qquad (1)$$

The data points used for Fig. 1 are within the limits of validity of J for each individual specimen.

It may be noted that net section yielding conditions are present beyond J values of approximately 25kJ/m^2. The question may arise whether there is any relation between our δ_5 and the CTOD determined by the British Standard BS 5762 [4] and by a similar draft ASTM method. It will be shown in a separate paper [7] that both quantities are equal provided that the slight material dependence of the rotation factor, k, in the following equation and a crack growth correction are taken into account. Thus, a modified CTOD according to BS 5762 can be determined as follows:

$$\delta^M_{BS} = \frac{K^2(a)}{2\sigma_{0.2}E} + \frac{v_{pl}}{a+z+\frac{W-a}{k}} \Bigg/ \left(a-a_0+\frac{W-a}{k}\right) \qquad (2)$$

where a_o is the pre-crack length, a the actual crack length, v_{pl} the plastic portion of the front face displacement; for the other symbols see the nomenclature. The rotation factor, k, is affected by the material such that the centre of rotation is the closer to the crack tip the higher the strain hardening of the material is. There is some support of the assumption that the method underlying Eq(2) can be applied to single edge notched bend (SENB) and compact (CT) specimens.

Two interesting features arose from the plane stress work:

- In plane stress, tension type specimens: centre cracked tension (CCT) and double edge notched tension (DENT) exhibit longer valid R-curves than the bend type SENB and CT specimens if the original ligament $W-a_o$ is the same, Fig. 2. This applies for both J- and δ_5-R-curves.
- The δ_5-R-curve is valid for substantially more crack growth than the J-R-curve. The results obtained so far suggest that with tension type specimens almost the whole original ligament can be consumed by crack growth and the resulting δ_5-R-curve is still valid in the sence that the same R-curve is obtained on a specimen with a larger initial ligament.

For an R-curve to be valid certain requirements have to be met which can be expressed as requirements for a minimum size of a specimen to be tested in order to determine a valid R-curve with a required maximum crack extension. The reason for this is that the test capacity of a fracture mechanics specimen depends on its size.

Three criteria for a valid J-R-curve arise from theoretical considerations [8-11]:

- For J to dominate the crack tip field the CTOD should not exceed a certain fraction, $1/\rho$, of the ligament, b,

$$\frac{CTOD}{b} = \frac{J}{\sigma_F b} < \frac{1}{\rho} \qquad (3)$$

  with $\sigma_F = 0.5\ (\sigma_{0.2} + \sigma_u)$.
- The unloading effects of crack growth are believed to be negligible if the increase in external load is sufficiently large. This can be expressed in a minimum slope of the R-curve

$$\frac{(dJ/da)_b}{J} > \omega \qquad (4)$$

- In addition, the amount of crack growth shall not exeed a certain fraction, α, of the original ligament length, b_o

$$\frac{\Delta a^*}{b_o} < \alpha \qquad (5)$$

Estimates for the constants α, ρ, and ω have been obtained for nuclear reactor pressure vessel steel under plane strain conditions [8-11].

Bending	Tension	
$\alpha \approx 0.0.6$	$\alpha \approx 0.01$	(6)
$\rho \approx 25...50$	$\rho \approx 200$	(7)
$\omega \approx 10$	$\omega \approx 80$	(8)

To the knowledge of the authors there is little experimental verification of these criteria; furthermore, similar results for plane stress don't seem to exist at all. This was one of the motivations for our investigations of crack growth in relatively thin sections [5]. Furthermore, size requirements for δ-R-curve testing had not been established at all.

It is the aim of the present report to describe three empirical methods for the determination of size requirements for a "valid" J-R-curve. By "valid" it is meant that the J-R-curve is unique if size and geometry of the specimen are varied. Concerning the δ_5-R-curves, only one method was utilised.

METHODS AND RESULTS

J-R-Curves

The three methods used are depicted in Fig. 3. The first one is a "multiple specimen" method requiring R-curve plots of at least two specimens with different ligament sizes. Starting with the argument that the specimen with the shorter initial ligament, b_0, exhibits the shorter valid R-curve, the event of deviation of this R-curve from that one obtained on the specimen with the longer ligament should be indicative of the limit of validity of the former R-curve. At this point of R-curve splitting the values of α, ρ, and ω have to be evaluated. Ideally, constant values should be obtained for a variety of ligament lengths. Any actual figures for these criteria depend of course on the error accepted for the quantity of interest. In our case, we chose a deviation of 5% in J, see Fig. 4 for an example. The individual values of α, ρ, and ω, henceforth marked with the index "J" to distinguish between J- and δ_5-R-curves, are plotted in Fig. 5.

The second method is a "single specimen" method; it is based on the experience that δ_5 provides a unique description of the specimen behaviour up to substantially,

- higher loads,
- higher deformations, or
- more crack growth.

Since it has been found [5, 6, 12] that there is a unique linear realtionship between J and δ_5 for a given material (see also Fig. 1), the breakdown of this linearity should be a measure of the limit of validity of J, see Fig. 3b. The three examples plotted in Fig. 6 illustrate this. With this method only a few evaluations (2024-FC) were done the results of which are compiled in Fig. 7a.

The third method is also a single specimen method. It relies also on a linear relationship, namely on that one between J and the load line displacement, s, see Fig. 3c, and again the deviation from linearity is taken as the limit of validity of J. However, the method works only for bending configurations (Fig. 8a and b) since there is no distinct linear section in the experimental

J-s-curves obtained on CCT specimens (Fig. 8c). This may be due to the larger contribution of elastic deformations to the total elongation of CCT specimens. The same behaviour has been shown by the theoretical work of Ref. [14]. Fig. 8a shows the evaluation of two SENB specimens with different widths. The slope of the linear curve section is almost exactly equal to the theoretical slope which was determined as follows: for rigid-ideally plastic behaviour one obtains [13]

$$J = 2.912\sigma_Y \frac{s}{5} (W-a_o) \qquad (9)$$

with S being the span width of the bend specimen.

This slope was then corrected for strain hardening according to the difference between the curves for $1/n = 3$ and for perfect plasticity in Fig. 6a of Ref. [14]. It can be shown that the correction of the slope for crack growth (which would result in a non-linear curve as well) doesn't change the situation of the present case very much.

This may not be true in other cases where the deviation of the experimental curve from the non-linear theoretical curve has to be evaluated.

The curve splitting method has been applied to all of our R-curve tests whereas the two single specimen methods have been used in a few cases only. The results of the former method can be summarised as follows:

Bending	Tension, Low Hardening	
$\alpha_J = 0.04\text{-}0.1$	$\alpha_J = 0.1 - 0.2$	(10)
$\rho_J = 30 - 60$	$\rho_J = 10 - 40$	(11)
$\omega_J = 4 - 14$	$\omega_J = 3 - 7$	(12)
	Tension, High Hardening	
	$\alpha_J = 0.25\text{-}0.35$	(13)
	$\rho_J = 10$	(14)
	$\omega_J = 2 - 3$	(15)

The single specimen methods yield larger scatter. Nevertheless, the results of the linearity check of the $J\text{-}\delta_5$ relationship are comparable with those listed above. However, according to Fig. 7b the linearity check of the J-s relationship yields δ_J values which are consistently higher than those of the other two methods, see Fig. 6b.

Thus, it may be concluded that the curve splitting method is the base method since it shows immediately what one is interested in, namely to what extent J correlates crack growth in a unique way. If only one ligament size can be tested the linearity check of the $J\text{-}\delta_5$ relationship seems to be a good substitute whereas the third method - at least in its form used here - yields specimen size requirements which are too optimistic.

δ_5-R-curves

Of the three methods shown in Fig. 3 only the curve splitting method makes sense. The data obtained thereby are compiled in Fig. 9. A rough representation of these data can be given by the following equations:

Bending	Tension	
α_δ = 0.2...0.3	α_δ = 0.7	(16)
ρ_δ = 10 ... 20	ρ_δ = 5	(17)
ω_δ = 2 - 3	ω_δ = 0.5	(18)
in addition:	b > B	(19)

The latter condition has been introduced to avoid constraint effects which may occur when the actual ligament, b, becomes smaller than the thickness, B, and which may shift the state of stress from plane stress towards plane strain.

Similar work for plane strain is at present being done at GKSS to derive size requirements for this regime.

CONCLUSIONS

- In spite of the different approaches to verify the criteria for J-controlled crack growth our data for α_J, ρ_J, and ω_J obtained for CT and SENB specimens are in remarkably good agreement with the data given by Eqs(6-8).
- Various independent methods can be employed to determine size requirements for J-controlled crack growth resulting in comparable results.
- For δ_5-R-curves, only the curve splitting method was used; it ends up with the conclusion that substantially smaller specimens are needed if a valid R-curve of a required extension has to be determined.

NOMENCLATURE

a	actual crack length
a_o	fatigue pre-crack length
Δa	crack length increment
b	actual length of remaining ligament
b_o	value of b for $a = a_o$
B	thickness of specimen
E	Young's modulus
J	J-integral
K	linear elastic stress intensity factor
s	load line displacement
S	span width of bend specimen
W	width of bend and CT specimen, half width of CCT specimen
z	distance of knife edges from specimen's front face
δ_5	crack tip opening displacement measured at the fatigue crack tip with a gage length of 5 mm
σ_F	flow stress, average of $\sigma_{0.2}$ and σ_u
σ_u	ultimate tensile strength
σ_Y	yield strength, general
$\sigma_{0.2}$	0.2 percent proof stress

REFERENCES

1. Landes, J.D., H. Walker, and G.A. Clarke: Evaluation of estimation procedures used in J-integral testing, ASTM STP 668, 1979, pp. 266-287.

2. Standard Test for J_{Ic}, a Measure of Fracture Toughness, E813-81, Annual Book of ASTM Standards, Part 10, 1981.

3. Ernst, H.: The J-resistance curve approach to elastic-plastic fracture evaluation, Meeting of ASTM Subcommittee E24:06, 19 April 1983, Louisville, KY, U.S.A.

4. Methods for crack opening displacement (COD) testing; BS 5762:1979, British Standards Institution, London, 1979.

5. Schwalbe, K-H., and D. Hellmann: Correlation of stable crack growth with the J-integral and the crack tip opening displacement, effects of geometry, size, and material; progress report on an investigation of the elastic-plastic R-curve methodology, GKSS 84/E/37, GKSS Research Centre, Geesthacht, 1984.

6. Schwalbe, K.-H.: Extension of the Engineering Treatment Model (ETM) to bending configurations under plane stress, to be published as a GKSS report.

7. Hellmann, D., and K.-H. Schwalbe: On the experimental determination of CTOD based R-curves, Workshop on the CTOD Methodology, GKSS Geesthacht, 23-25 April 1985.

8. Hutchinson, J.W., and P.C. Paris: Stability analysis of J-controlled crack growth, Elastic-Plastic Fracture, ASTM STP 668, J.D. Landes, J.A. Begley, and G.A. Clarke, Eds., American Society for Testing and Materials, 1979, pp. 37-64.

9. Shih, C.F., H.G. deLorenzi, and W.R. Andrews: Studies on crack initiation and stable crack growth, ibid., pp. 65-120.

10. McMeeking, R.M., and D.M. Parks: On criteria for J-dominance of crack-tip fields in large scale yielding, ibid, pp. 175-194.

11. Shih, C.F.: Relationships between the J-integral and the crack opening displacement for stationary and extending cracks, J. Mech. Phys. Solids 29, 1981, pp. 305-326.

12. Hellmann, D., and K.-H. Schwalbe: Geometry and size effects on J-R and δ-R-curves under plane stress conditions, in: ASTM STP 833, 1984, pp. 577-605.

13. Bucci, R.J., Paris, P.C., Landes, J.D., Rice, J.R.: J-integral Estimation Procedures. ASTM STP 514, 1972, pp. 40-69.

14. Shih, F.C., Hutchinson, J.W.: Fully Plastic Solutions and Large Scale Yielding Estimates for Plane Stress Crack Problems. J. of Engng. Mat. and Technol., 1976, pp. 289-295.

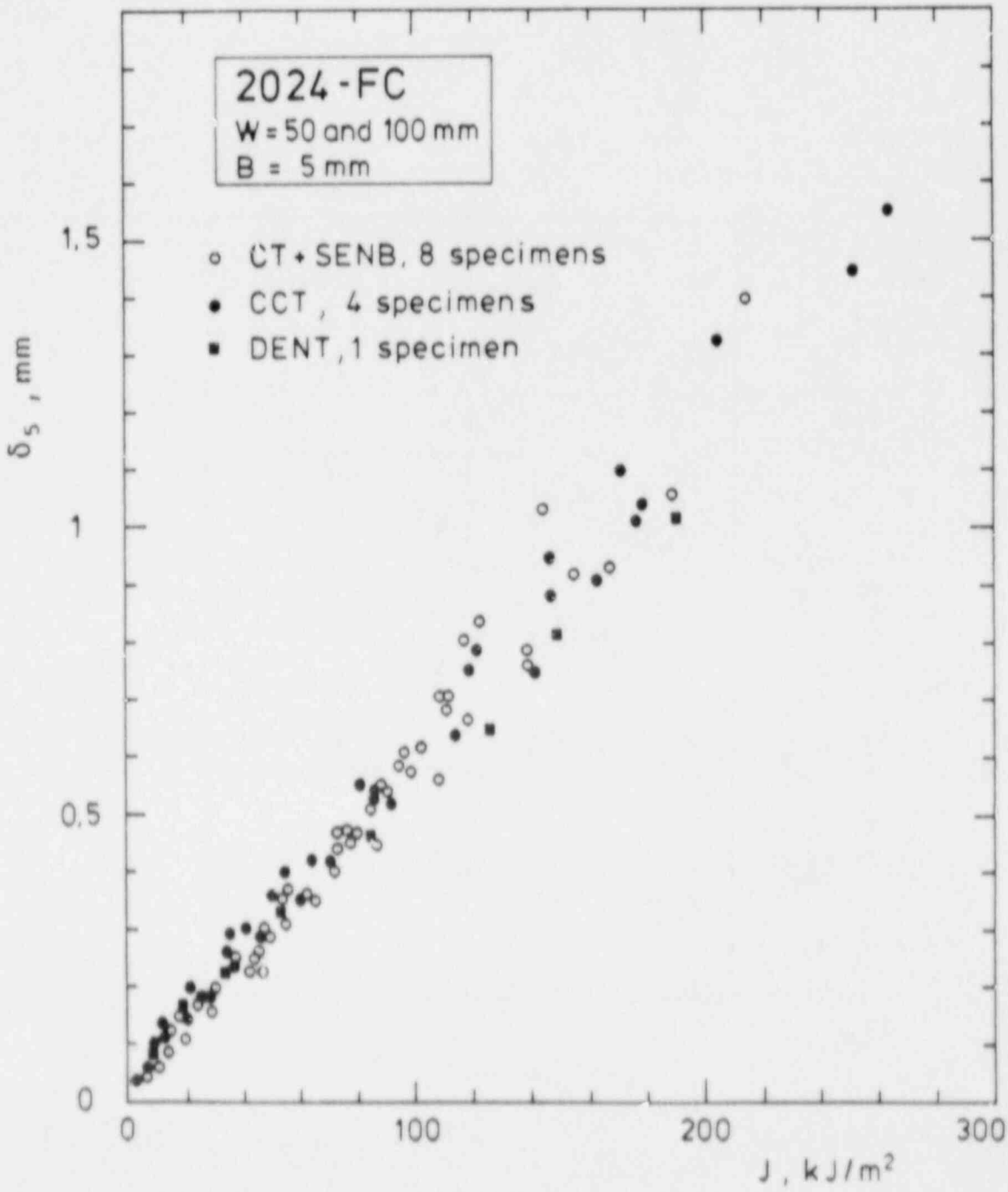

Fig. 1: The crack tip opening displacement in terms of δ_5 as a function of the J-integral showing a linear relationship. The graph is taken from Ref. [6].

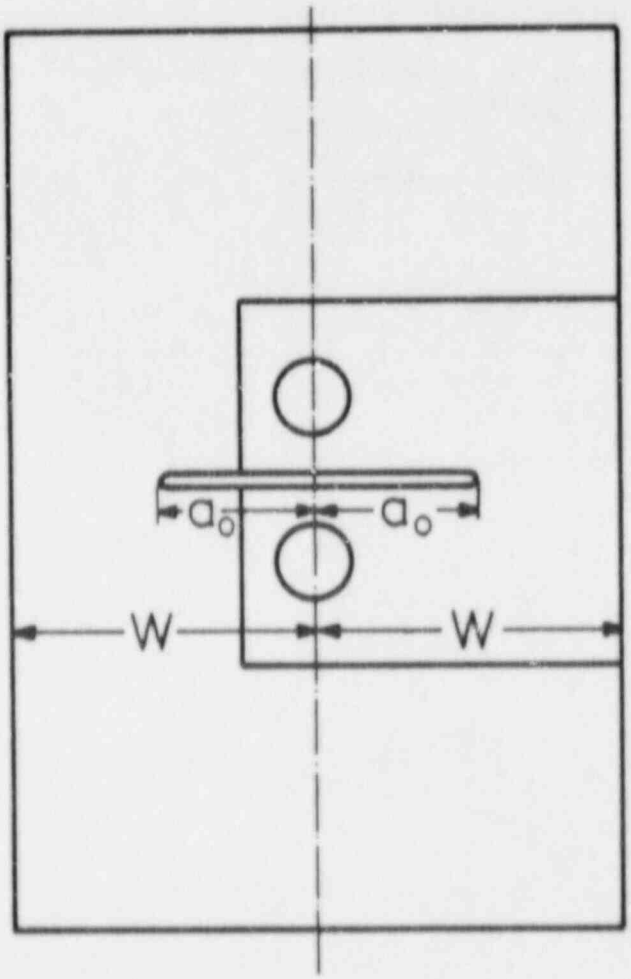

Fig. 2: Schematic showing definition of a_o and W.

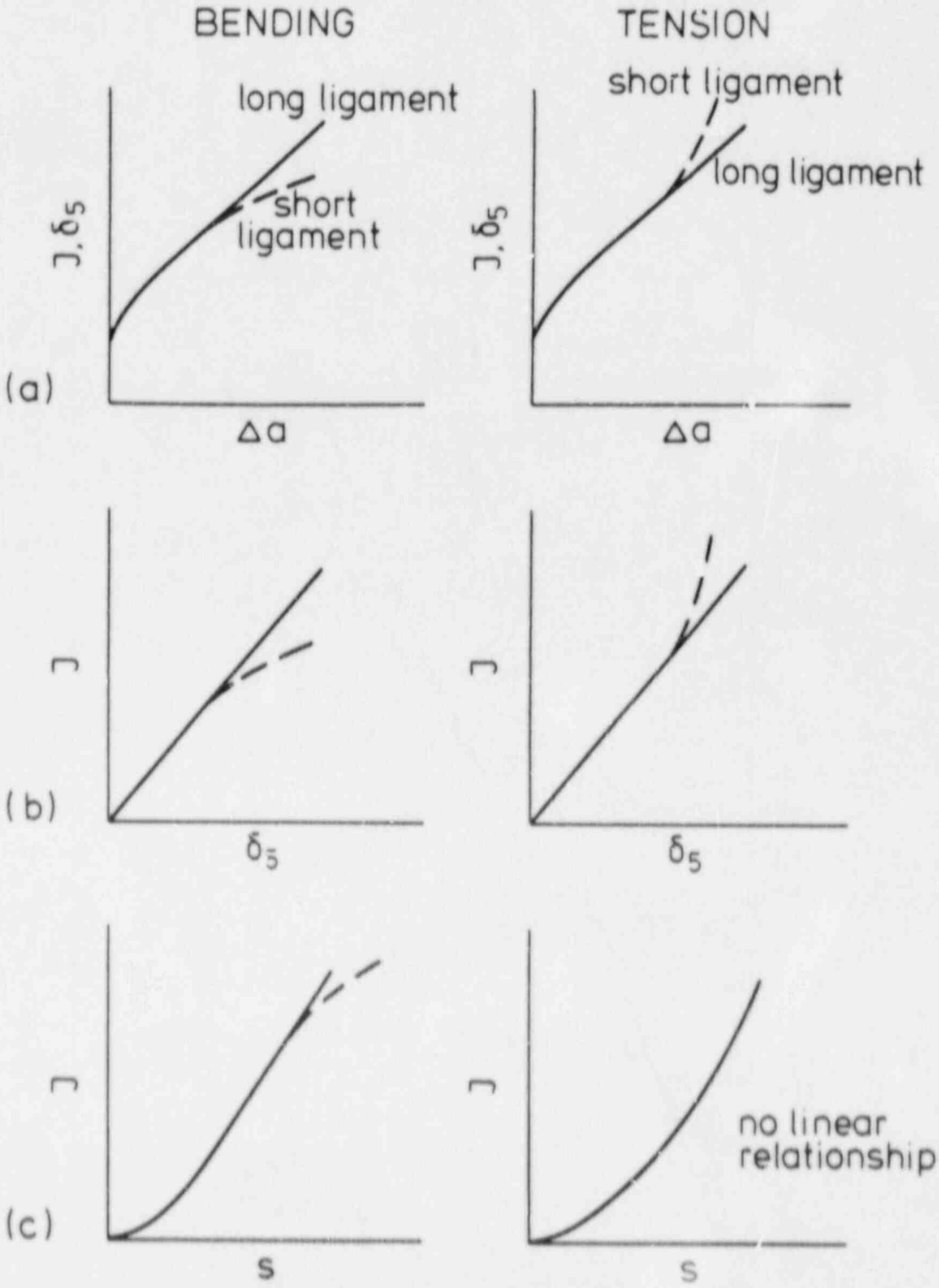

Fig. 3: Schematic showing the three experimental methods used for determining size requirements of valid R-curves:
a) R-curve splitting
b) J-δ_5-relationship
c) J-load line displacement-relationship.

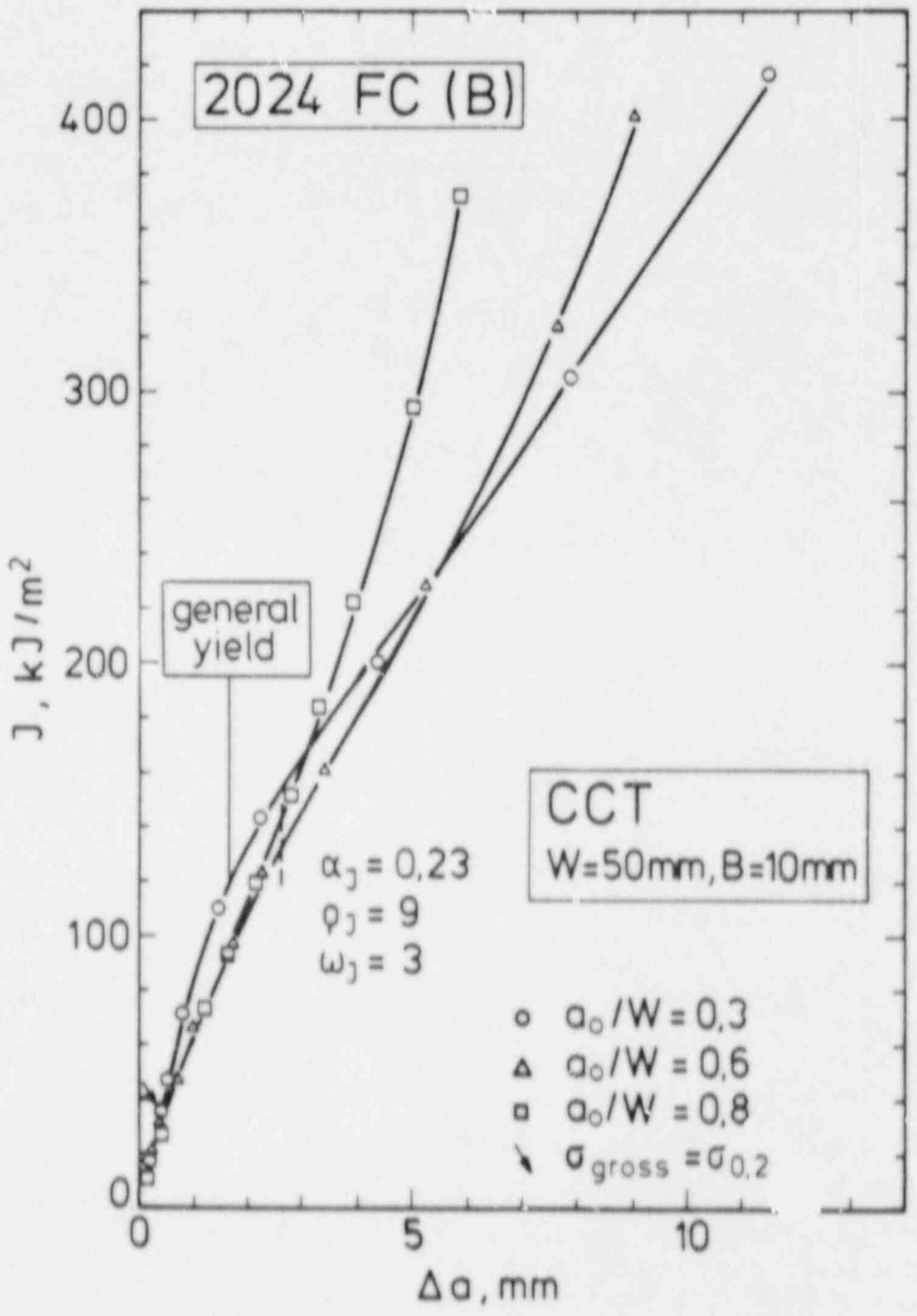

Fig. 4: J-R-curves for CCT specimens of 2024-FC(B).

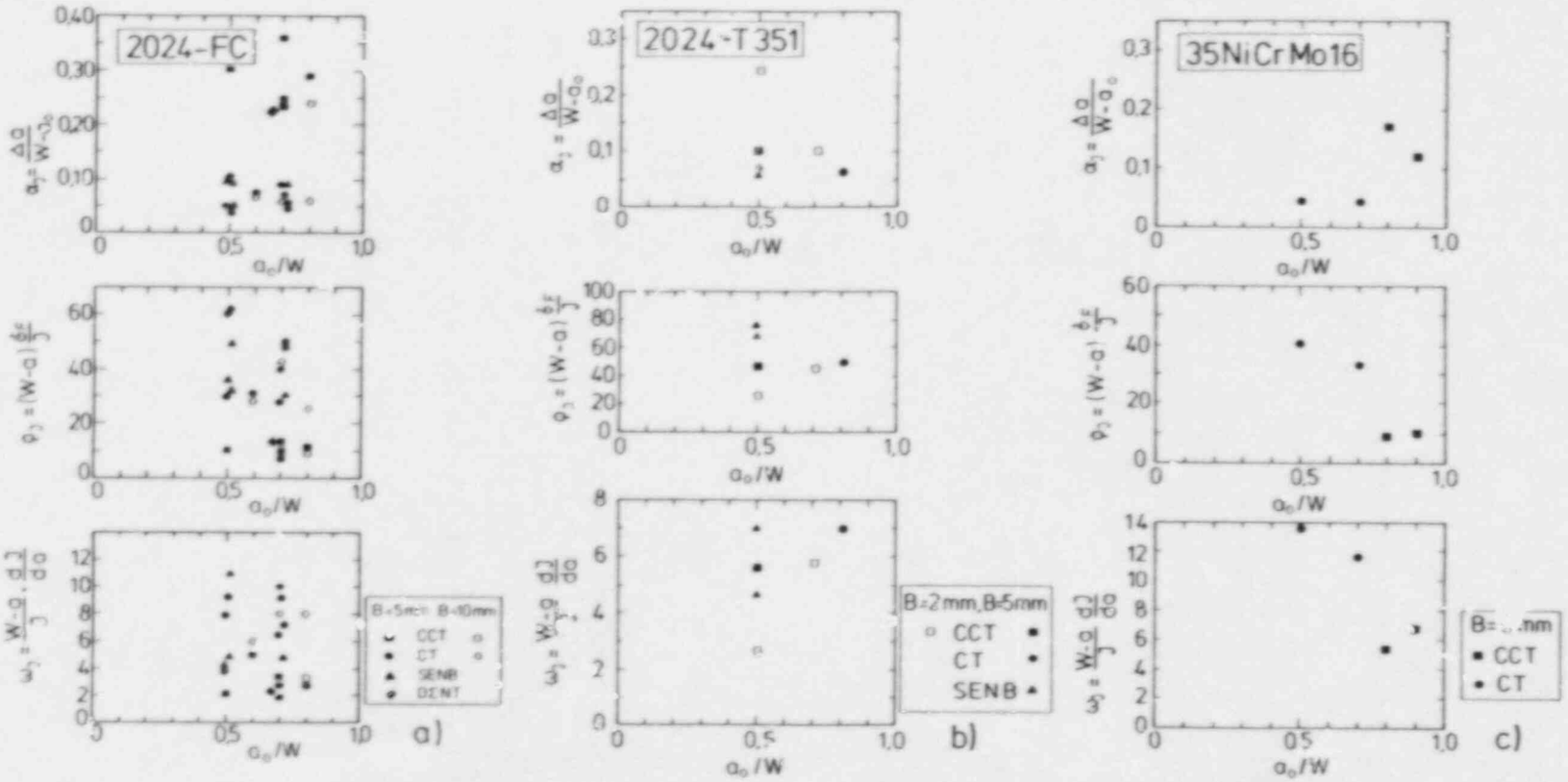

Fig. 5: Values of α_j, ρ_j, and ω_j determined by the curve splitting method; this graph contains results in addition to the compilation reported in Ref. [12].

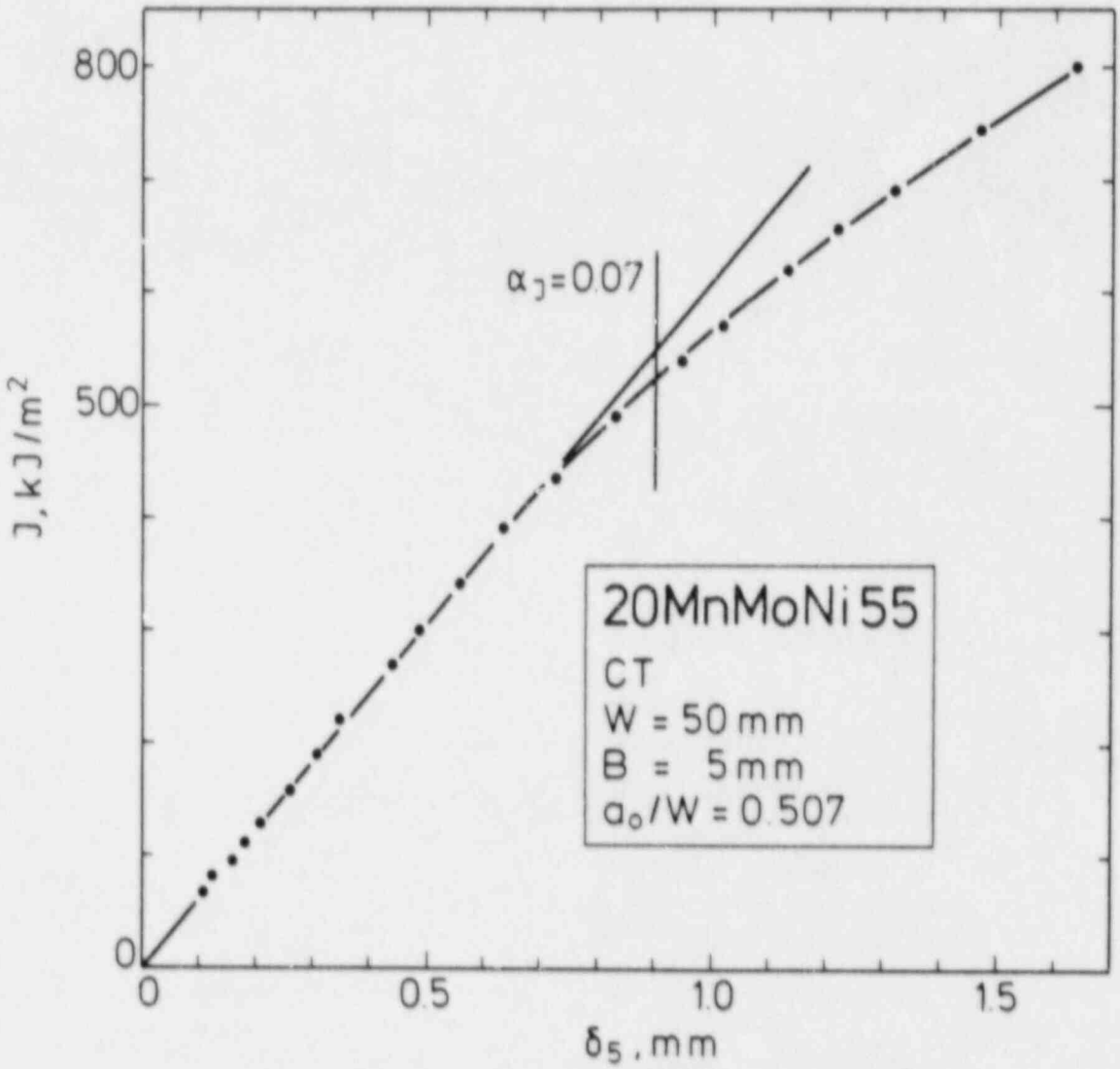

Fig. 6a: Breakdown of linearity in J-δ_5-relationships indicating limit of validity of J-integral:
CT specimen, steel 20MnMoNi55,

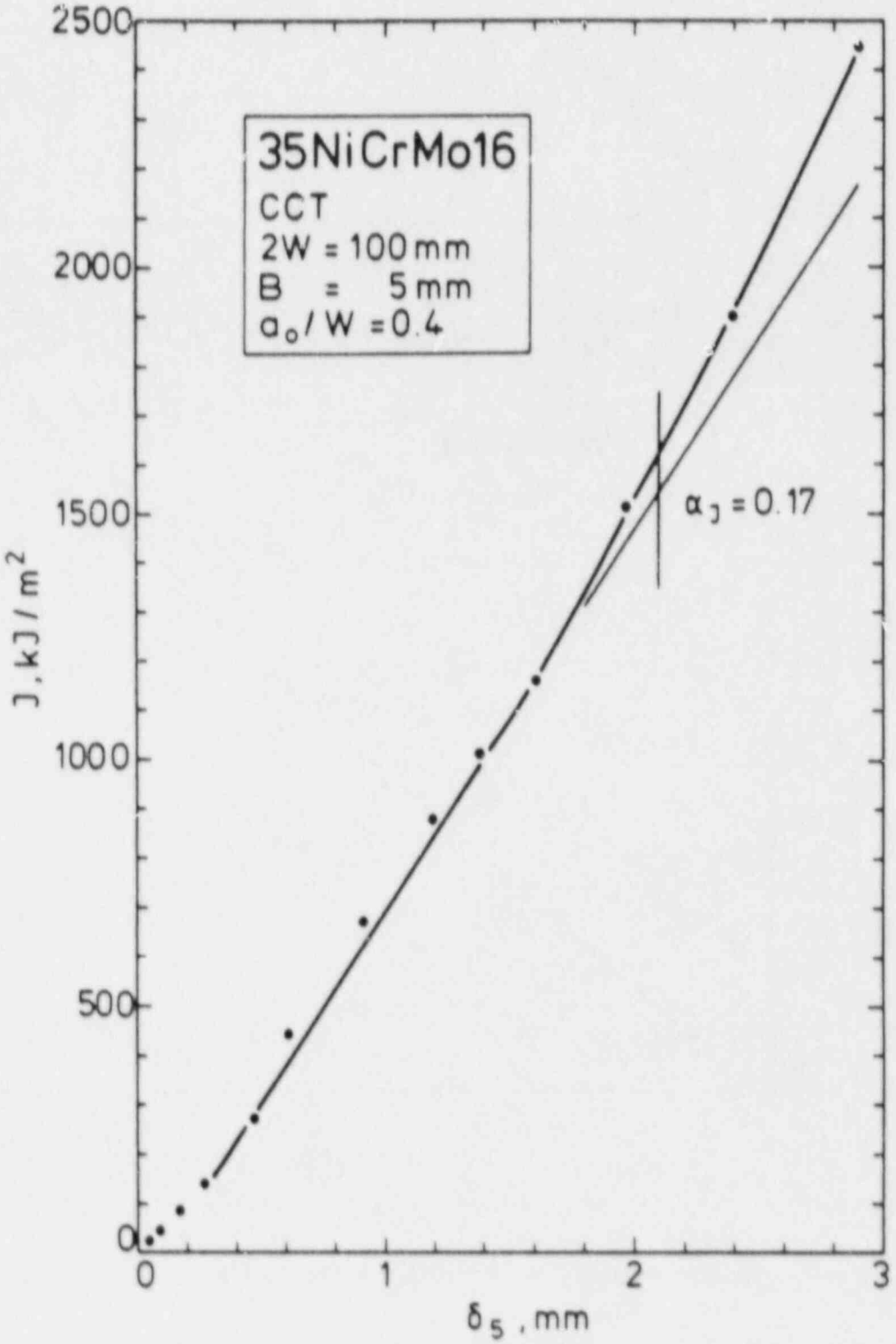

Fig. 6b: Breakdown of linearity in J-δ_5-relationships indicating limit of validity of J-integral:
CCT specimen, steel 35NiCrMo16,

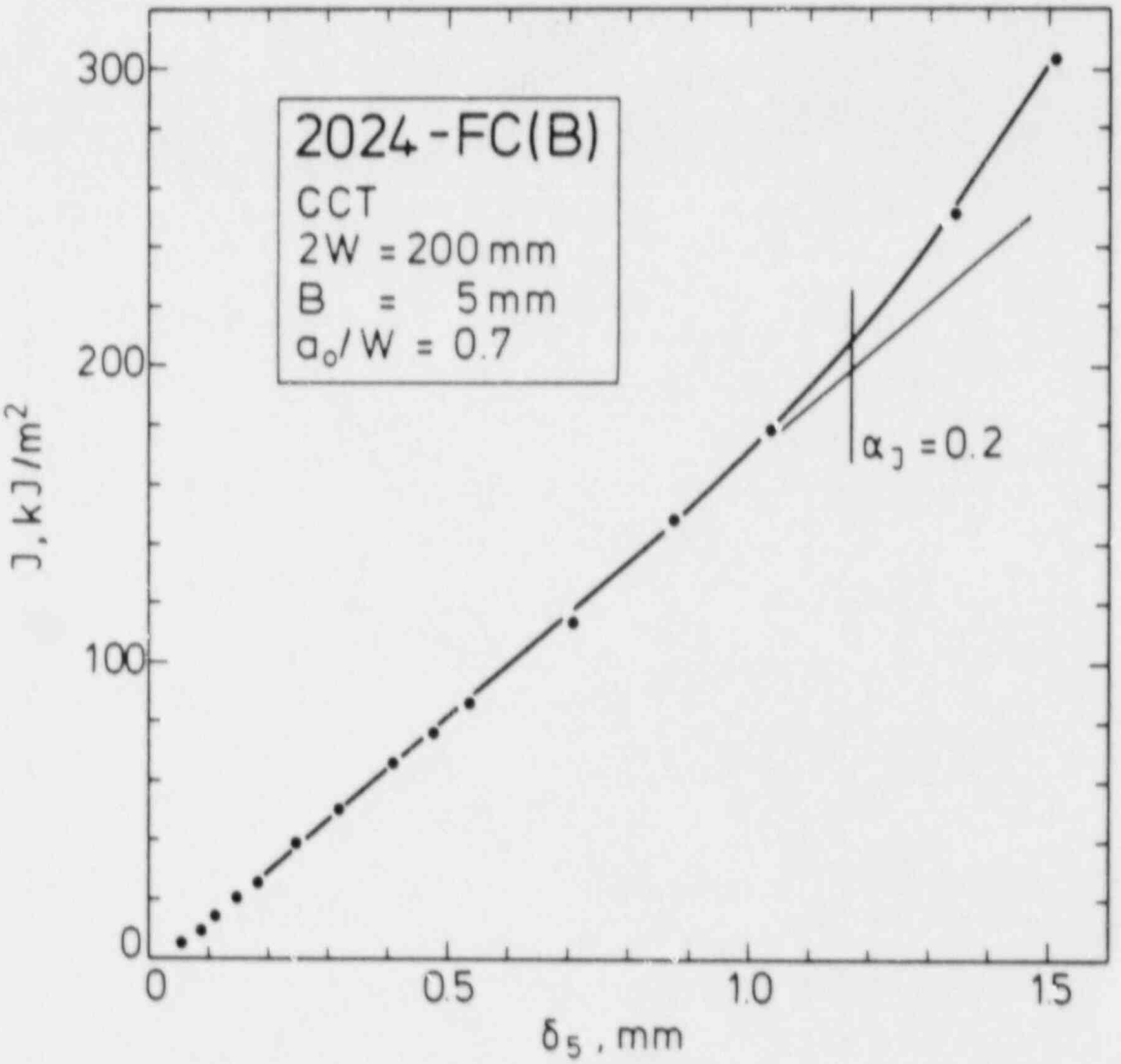

Fig. 6c: Breakdown of linearity in J-δ_5-relationships indicating limit of validity of J-integral:
CCT specimen, aluminium 2024-FC(B).

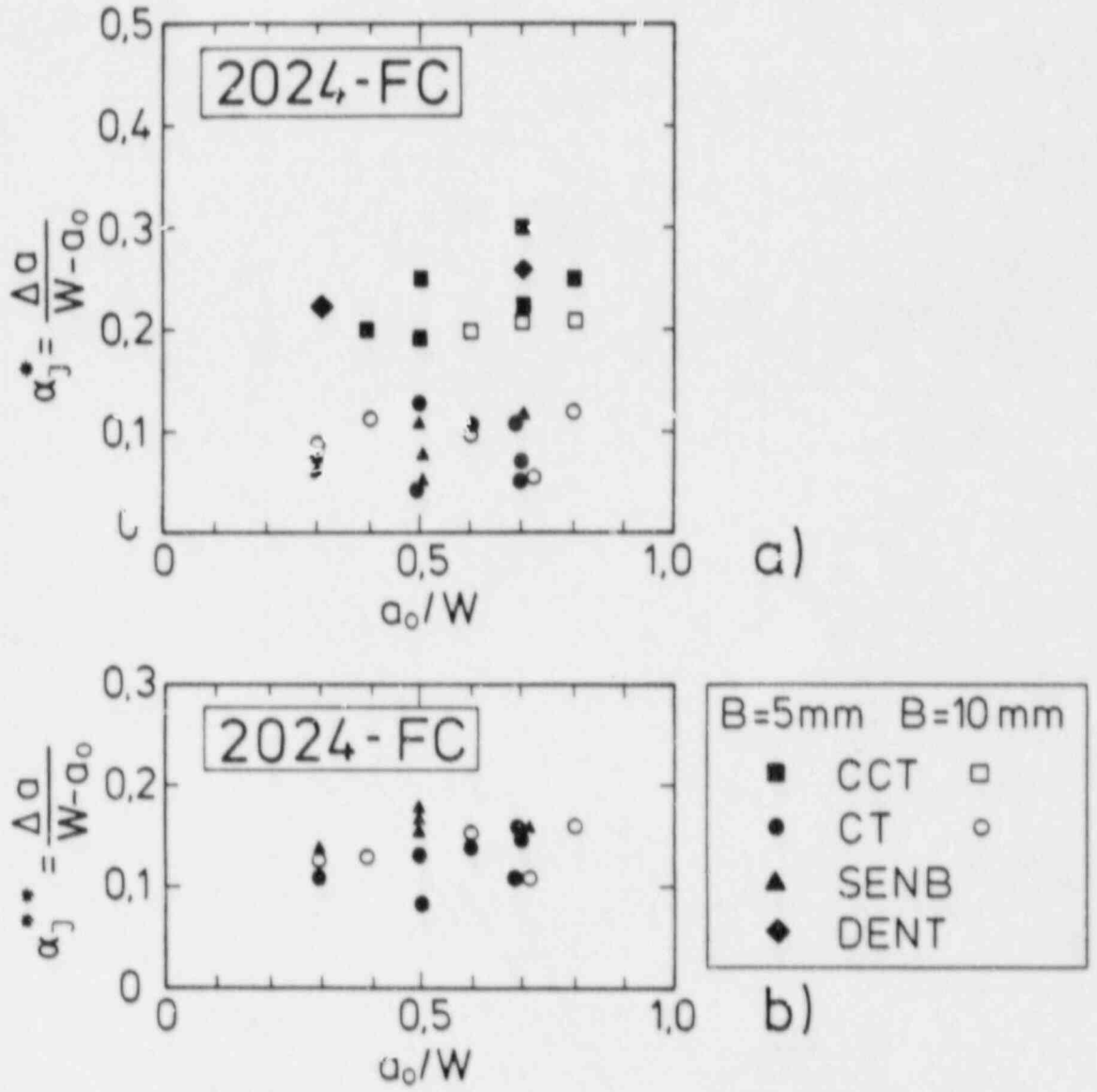

Fig. 7: Values of α_J determined by single specimen methods:
a) J-δ_5-relationship
b) J-load line displacement relationship.

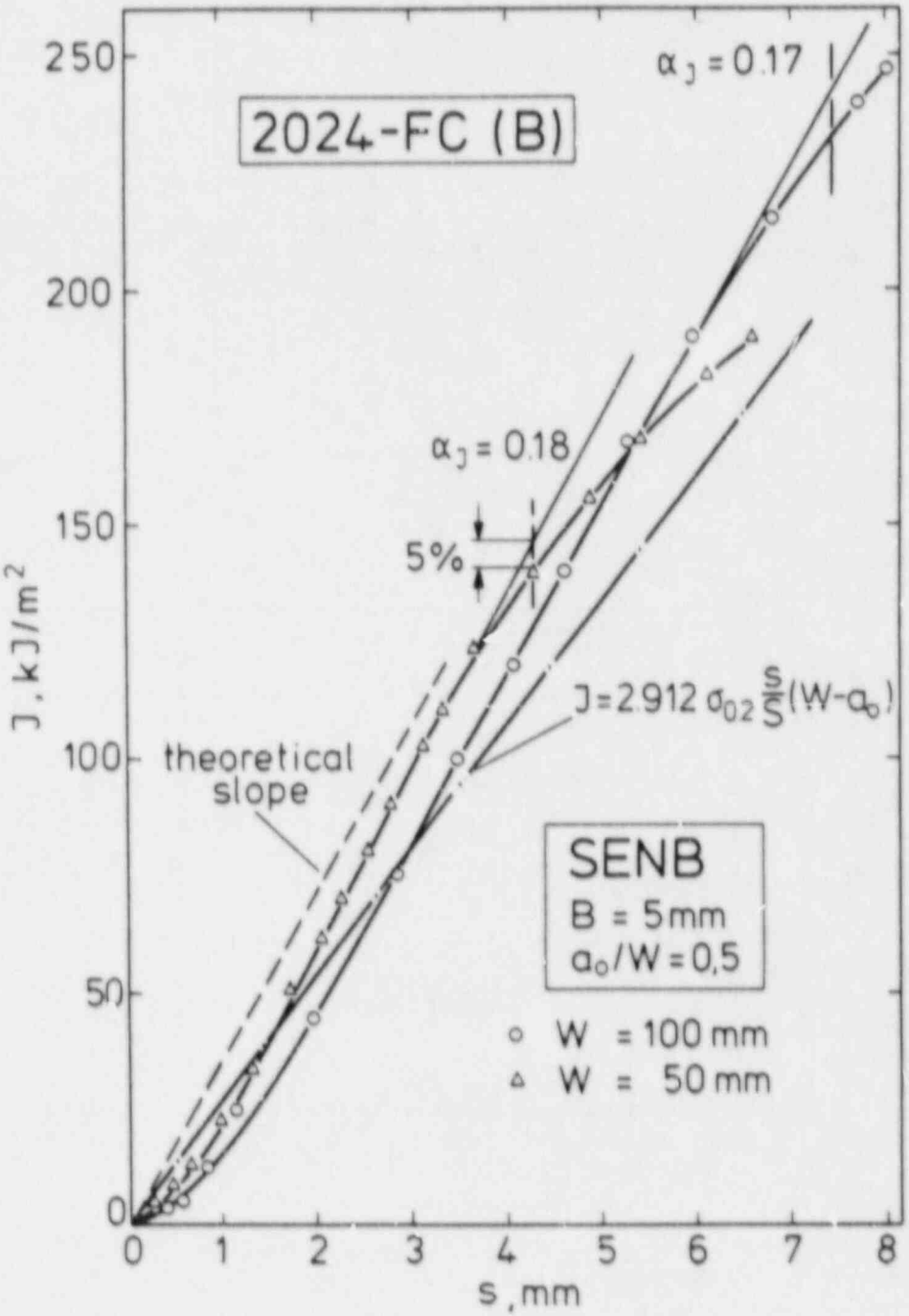

Fig. 8a: Breakdown of linearity in J-s-relationship indicating limit of validity of J-integral:
two bend specimens, aluminium 2024-FC(B),

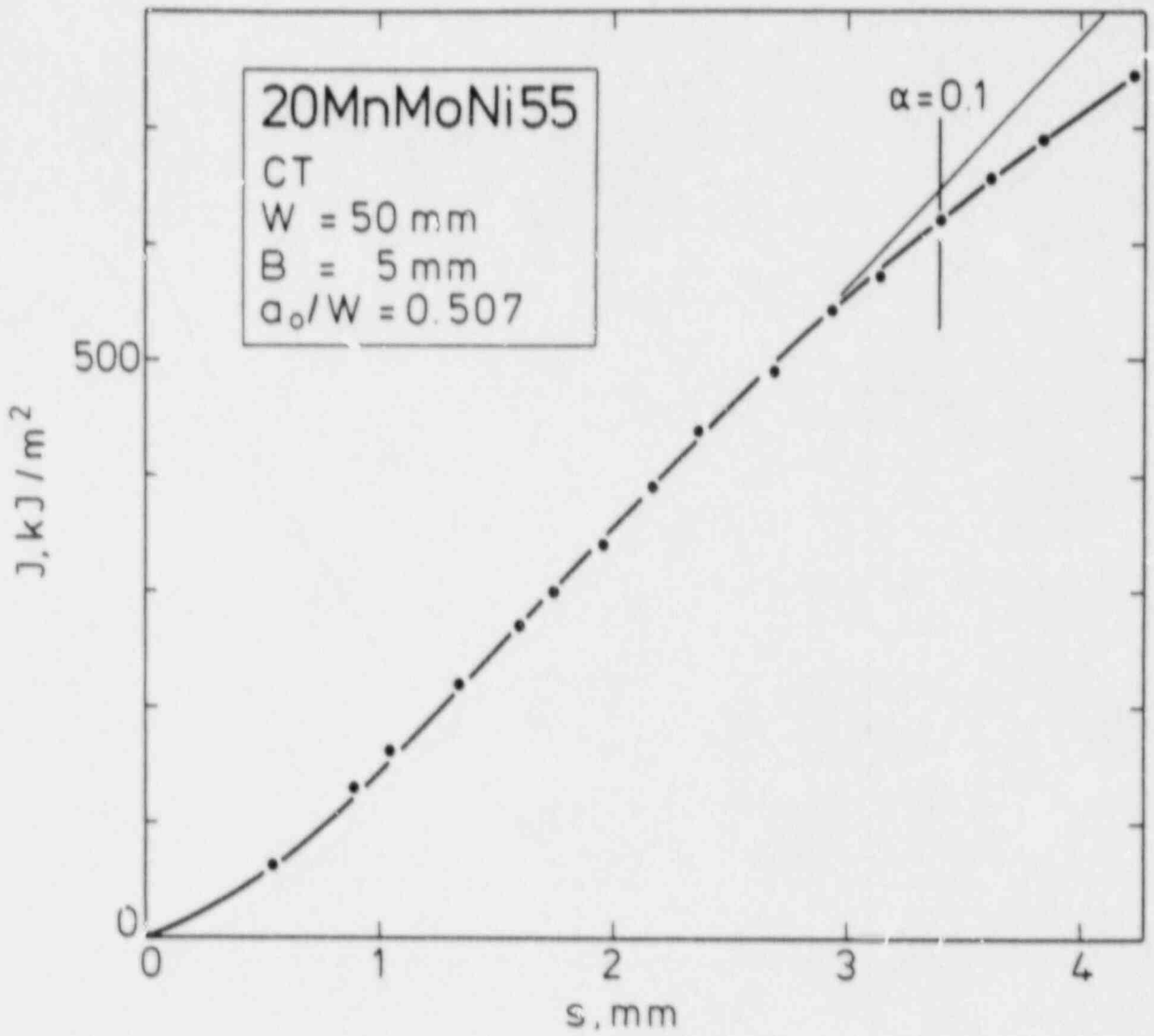

Fig. 8b: Breakdown of linearity in J-s-relationship indicating limit of validity of J-integral:
CT specimen, steel 20MnMoNi55,

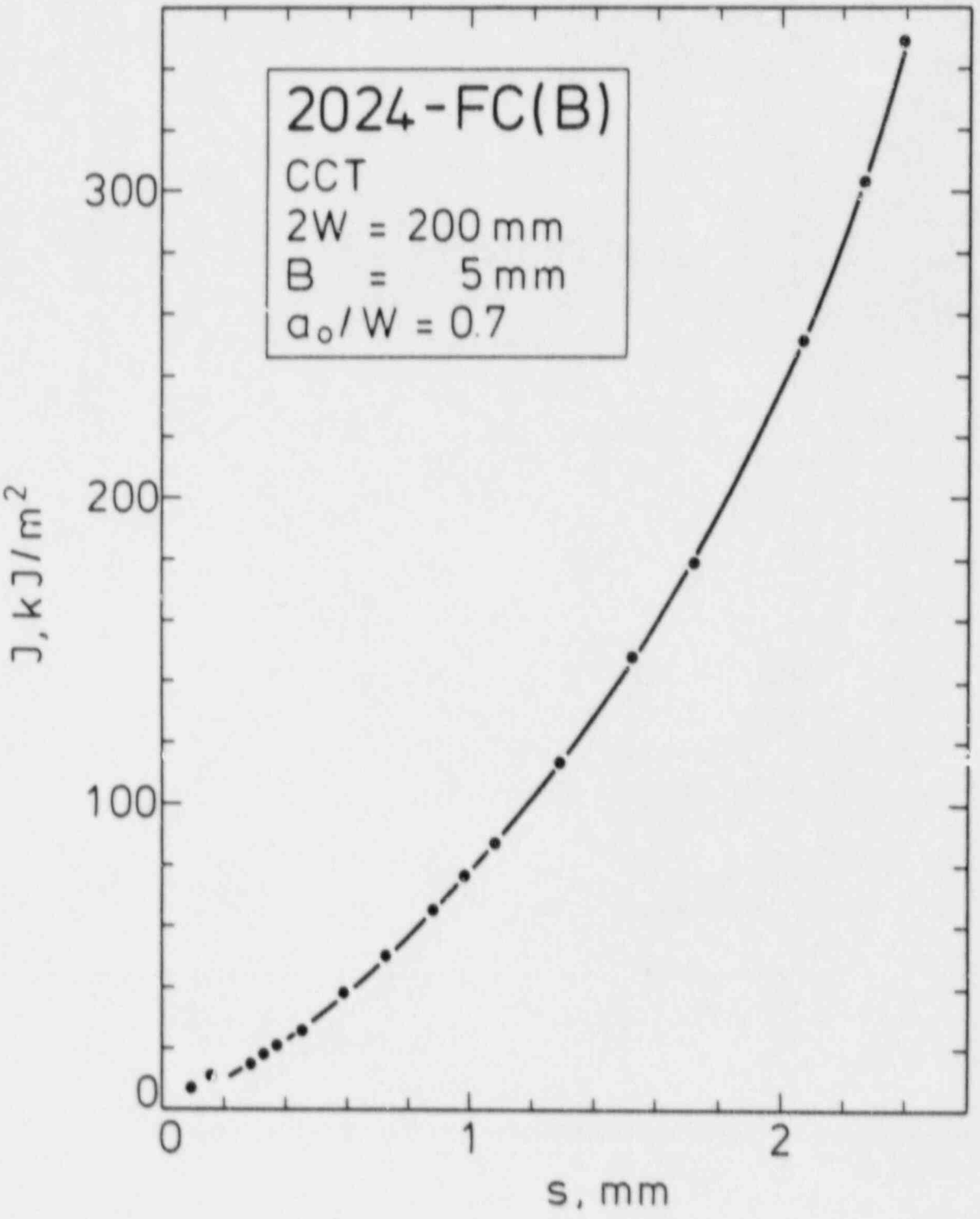

Fig. 8c: Breakdown of linearity in J-s-relationship indicating limit of validity of J-integral:
CCT specimen, aluminium 2024-FC(B).

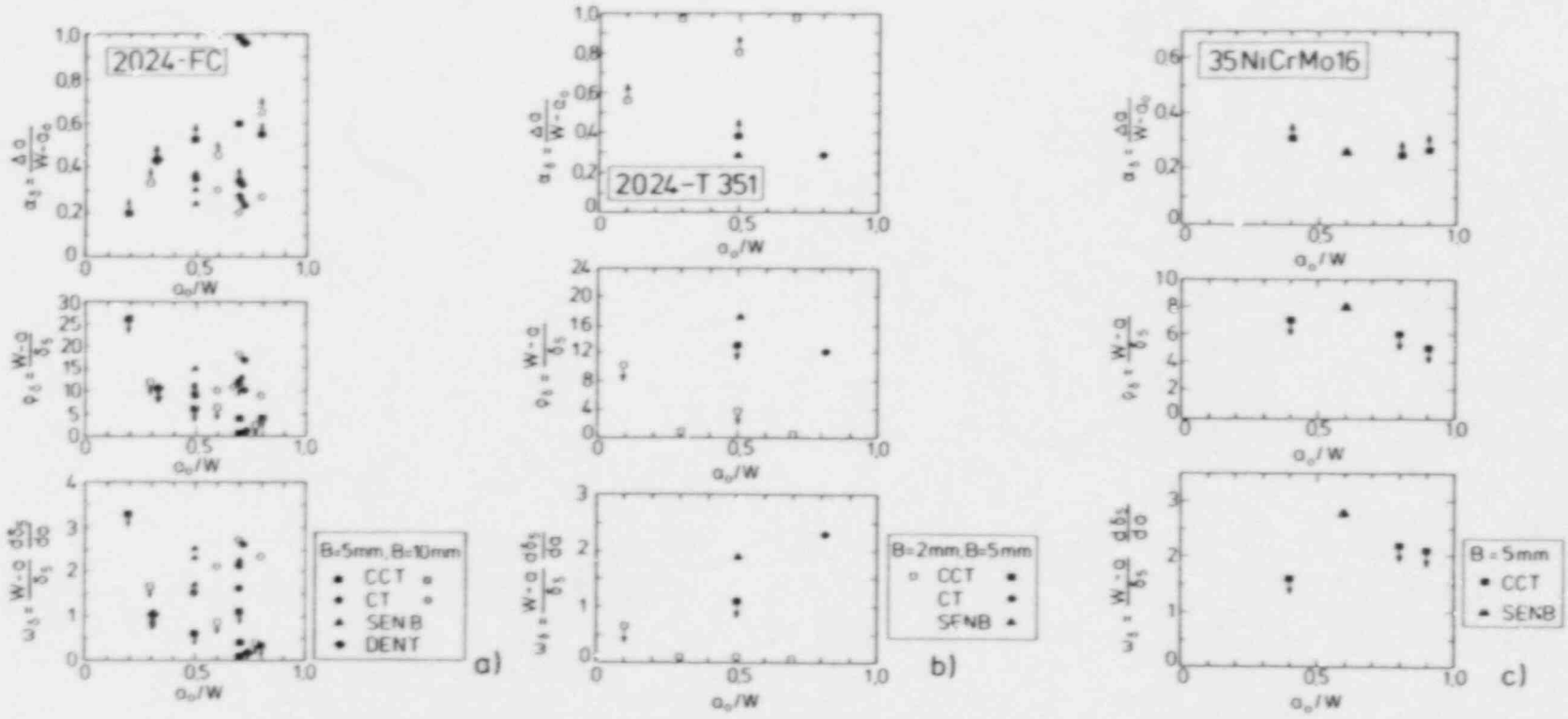

Fig. 9: Values of α_δ, ρ_δ, and ω_δ determined by the curve splitting method.

SUMMARY OF ELASTIC-PLASTIC R-CURVE STUDIES

D. E. McCabe

Westinghouse R&D
1310 Beulah Road
Pittsburgh, PA 15235

INTRODUCTION

A program titled "Elastic-Plastic Methodology to Establish R-Curves and Instability Criteria" had an objective to determine if there are geometry effects in the fracture toughness performance of structural steels. The work has been supported by the Electric Power Research Institute over a period of about six years. (ref. 1) Specifically, the postulate that R-Curve is a material property, independent of geometry variations was under study using a carefully planned pattern of controlled experiments.

For the first part of the presentation, we will show results of testing steam generator A508 tube plate steel (Table I) as compact specimens; investigating thickness and/or starting ligament size effects (ref. 2). These results were used to set up a test practice for reactor vessel surveillance specimens. The second part of the presentation will show an evaluation of loading mode (tension vs bend) on R-Curves. The material was 0.1-inch thick A533B steel. (Table I) Thin section specimens were used in this case to control constraint to that of plane stress throughout.

Compact Specimen Results

The matrix of test specimens is shown in Table II. All specimens were 20% side grooved. There had been some metallurgical inhomogeneity mixed within the matrix and only the results from those specimens that were demonstrated to be equivalent by key curve will be compared here. The diagonal from top left to bottom right represents compact specimens of E399 proportionality from 1/2T to 10T size with $a_o/W = 0.5$. The J_R-Curve data appeared to be independent of specimen size, Fig. 1, with perhaps some subtile deviation for 1T at the largest values of Δa_p. In Fig. 2 we add the 1/2T specimen which clearly shows difficulty with deformation theory J; open points. Note that $\Delta a_p \leq 0.1\ b_o$ seems to be critical to geometry dependence with deformation theory J. Ernst had developed modified J, based on a postulate, originally specialized to a specific problem solution by Rice and Herman in earlier work (ref. 3). See Table III. The new J-like parameter tends to display independence

from crack growth whereas deformation theory J tends to develop inaccuracy due to growth.

Surveillance Specimen Tests

Fracture mechanics specimens had been introduced into reactor surveillance capsules at a time when fracture mechanics was K_{IC} based and brittle fracture behavior was anticipated. Specimens were 1XWOL where the arms were designed to be weaker than the strength of the remaining ligament, and these were unsuitable for R-Curve work. Nevertheless the exposed specimens were irreplaceable from the standpoint of the irradiated metallurgical conditions that they represented and R-Curves were needed. To make R-Curve specimens, the following was done:

i) Back edge was trimmed to H/W = 0.6; the plan view proportionality of compact specimens.

ii) Specimens were side grooved 20%.

iii) Front face displacement was measured and crack growth was determined using differential compliance.

iv) Load line displacement for J calculation was inferred by a procedure of Landes. (ref. 4)

v) Modified J was used.

vi) A special loading jig was built to accommodate large rotation of specimens in a frictionless connection. See Fig. 3.

Since the typical initial remaining ligament was only about 0.45 inches, modified J was necessary to obtain reasonable geometry independent J_R Curve. To verify the method, we tested one 1XWOL specimen as received versus the modified specimen recommended. See Fig. 4. Note the J_R-Curve from the 10T specimen. Both small specimens were taken from one broken half of the 10T specimen.

Loading Mode Effects

The work to study loading mode effects had emphasized tests on single edge notched specimens where bend to tension stress ratio σ_B/σ_T could be varied through changed relative crack size. The test matrix that indicates specimen widths, relative crack size and corresponding bend to tension ratios is given in Table IV. A modified specimen design was made for economy of material. See Fig. 5. The specimen was tested for elastic-compliance calibration and J-calibration. In all cases the material was 0.1-inch thick to maintain plane stress conditions

throughout. Modified J was used throughout. J_M R-Curves were found to be independent of SEN specimen size Fig. 6 (a/W = 0.3) and Fig. 7 (a/W = 0.5). For variable a/W at fixed size (W = 20) Fig. 8 is given. Note that solid data points are from compact specimens.

A second part of this study was to test center cracked and double edge cracked tension panels; Table V. Panel width reduction was measured during the tests using dial gages. The J_M R-Curves for the four center cracked panels is shown in Fig. 9. These data are consistent with traditional R-Curve concepts from the standpoint that there is no crack size, remaining ligament, or specimen width effects in the data set. However, the solid line represents the fit to SEN specimens. The width reduction measurements proved to be enlightening from the standpoint of what they revealed about the deformation mechanism. Figure 10 shows overall panel displacement on the abscissa versus width reduction. The relationship of linearity between the two measurements is suggestive of classical slip line field development depicted schematically in Fig. 11. All four CCT panels displaced exactly the same, with the same angle of slip line, independent of initial ligament size. The development of such a wedge shaped zone can be expected at onset of general yield. However, the unusual aspect here was that onset started at about half of general yield.

It was concluded that the center cracked panel may be unique and not representative of the general tension loading case. To explore this, we tested double edge notched specimens of comparable size. Figure 12 compares J_M R-Curve data at a/W = 0.5 for three specimen designs. The unique slip line character of CCT panels had been eliminated by DEN design R-Curve independence from loading mode was thusly demonstrated. Finally Figs. 13 and 14 show the difference between CCT and DEN plastic deformation visually. To make these photos, the specimens were coated with blue machining dye after the test, and then the test sections were surface ground to clean off those areas unaffected by plastic deformation. The plastic flow regions remain accentuated by the dye.

CONCLUSIONS

Within the compact specimen geometry, J_R-Curve was found to be independent of plan view size and relative crack size. Modified J was calculated to retain geometry independence when crack growth exceeded 10% of initial ligament size.

A test practice incorporating many special modification schemes has been devised for the R-Curve testing of nuclear reactor surveillance specimens.

Loading mode per se does not have an effect on R-Curve behavior of materials. The CCT geometry, however, will yield a different R-Curve than other specimen geometries because of a unique deformation characteristic.

REFERENCES

1. EPRI Contract RP 1238-2.

2. McCabe, D. E., Landes, J. D., and Ernst, H. A., "An Evaluation of the J_R-Curve Method for Fracture Toughness Characterization," STP 803, Vol. 2, pp. 562-581.

3. Herman, L., Rice, J. R., "Comparison of Experiment and Theory for Elastic-Plastic Plane Strain Crack Growth," Brown Univ. Report No. 76, Feb. 1980.

4. Landes, J. D., "J Calculation From Front Face Displacement Measurement on a Compact Specimen," Int. Journal of Fracture, Vol. 16, 1980, pp. 183-186.

Table I
Mechanical Properties

Material	Yield Strength ksi	Yield Strength MPa	Tensile Strength ksi	Tensile Strength MPa	% El	CVN Ft-Lbs	CVN J	FATT F	FATT k
A508 Class 2A	(55)	380	(80)	550	30	(115)	157	(110)	396
A533B	(68)	469	(90)	620		(92)	126		

D49-82

Table II - Test Matrix

Thickness Inches	Ligament Size - Inches				
	1/2	1	2	4	10
1/2	w = 2	w = 2	w = 4		
1	w = 2	w = 2 w = 8	w = 8	w = 8	w = 20
2	w = 4	w = 8	w = 4 w = 8		
4		w = 8		w = 8	
10					w = 20

Table III
Deformation Theory J, Modified J

$$J_{i+1} = \left[J_i + \left(\frac{\eta}{b}\right)_i \frac{A_{i,\,i+1}}{B_N} \right] \left[1 - \left(\frac{\gamma}{b}\right)_i \left(a_{i+1} - a_i \right) \right]$$

$$J_D = J_{i+1}$$

$$J_M = J_D - \int_{a_o}^{a} \frac{\gamma}{b} J_p \, da \qquad \text{(Old)}$$

$$J_M = K^2/E + \int_{o}^{\delta_p} \left(\frac{\eta_p}{b}\right)_i P \, d\delta \qquad \text{(New)}$$

η_p = From Fully Plastic Solutions
= f (a/b, h_1, h_3, n)

Table IV
Single Edge Cracked Specimens

a/w	0.3	0.4	0.5	0.6	0.7
σ_B/σ_T	1.3	2.0	3.0	4.5	7.0
W = 254 mm	X		X		X
508 mm	X	X	X	X	X
762 mm	X		X		X

Table V
Tension Test Specimens

Width (mm)	Type	$2a_o/w$
406	CCT	0.5
406	CCT	0.6
203	CCT	0.5
203	CCT	0.6
406	DEN	0.35
406	DEN	0.50
203	DEN	0.35
203	DEN	0.5

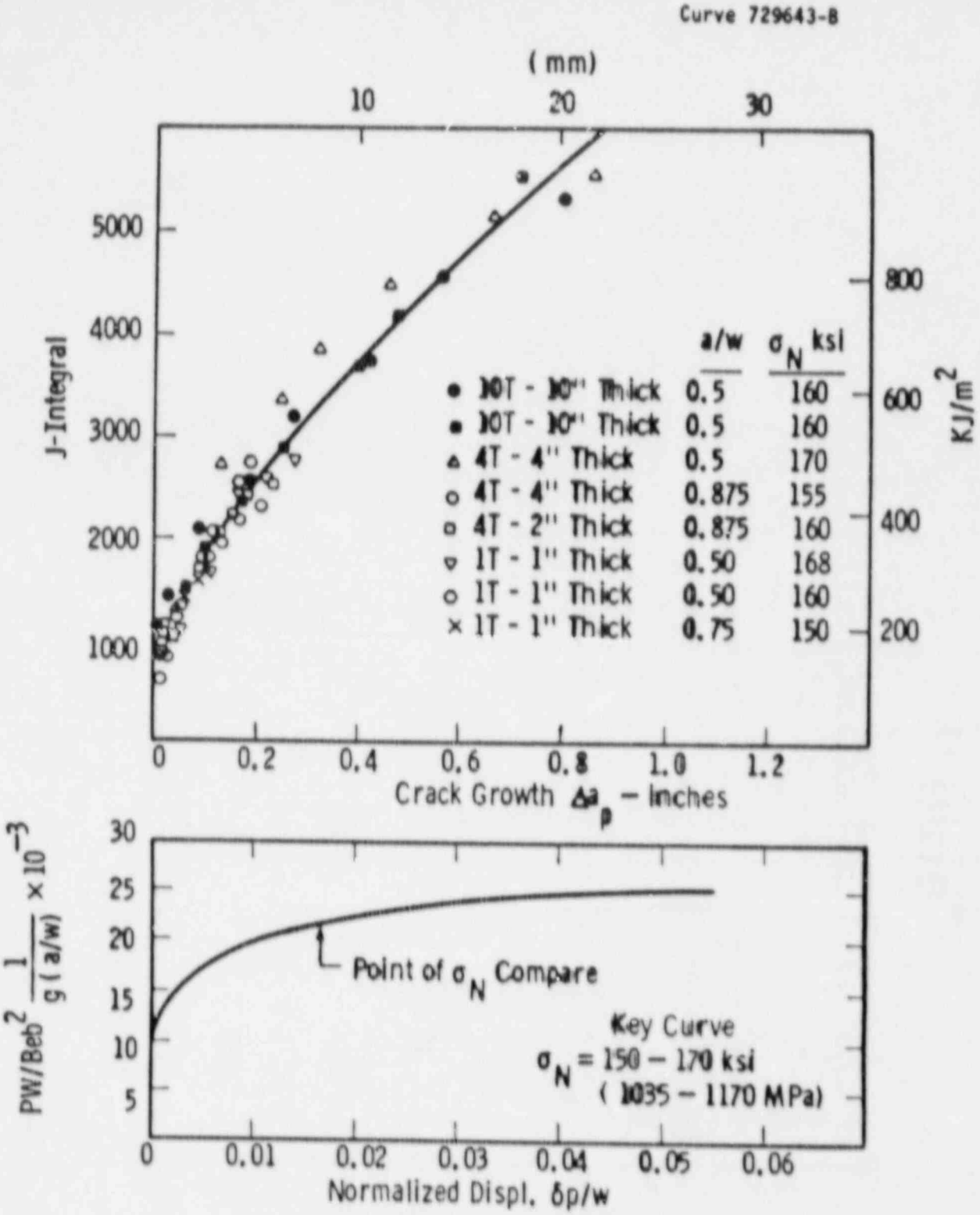

Fig. 1 - J_R-curves for material in the 150-170 ksi nominal strength category.

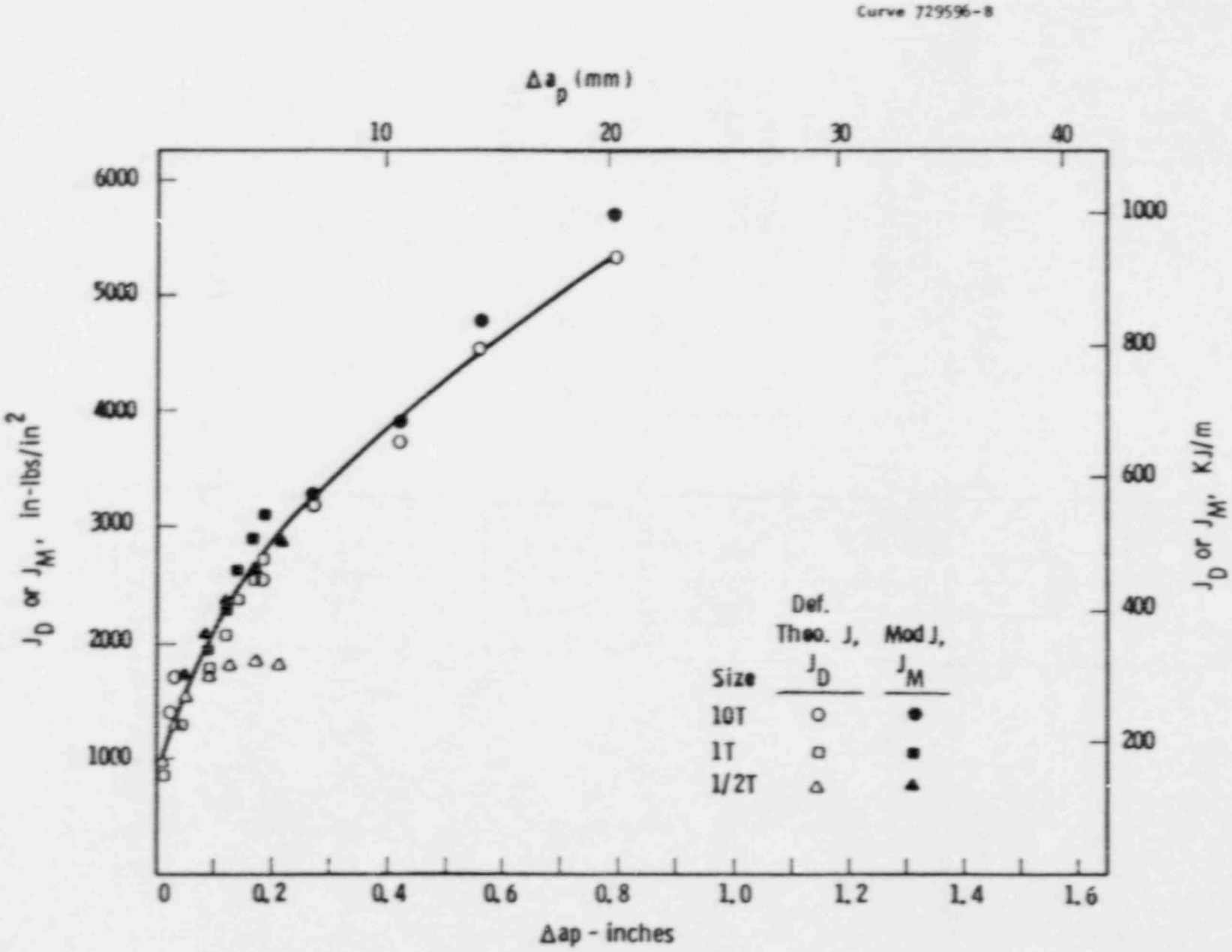

Fig. 2 - J_R-curve data for three sizes of 20% side grooved specimens.

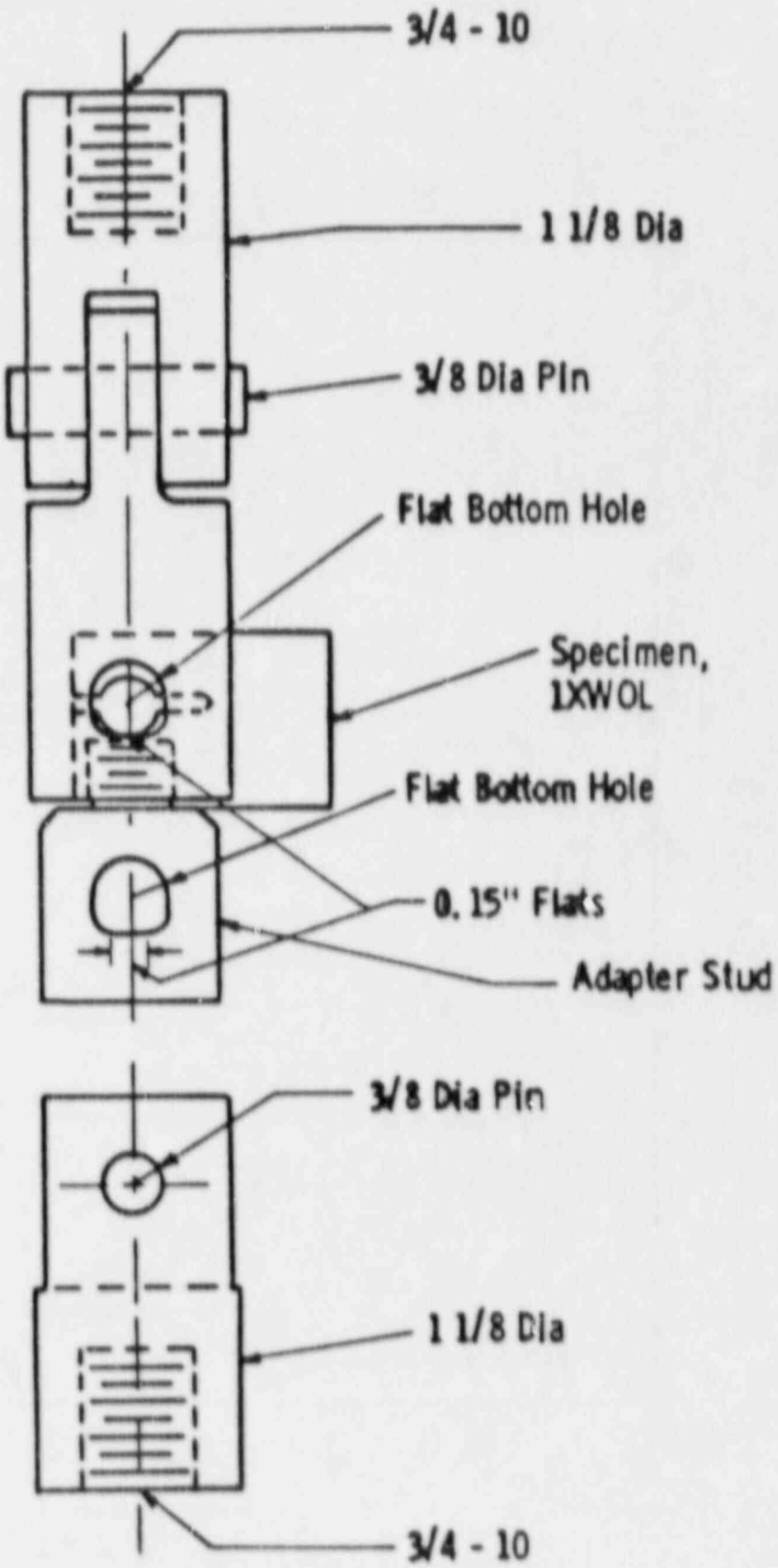

Fig. 3 - Fixtures for 1X-WOL testing.

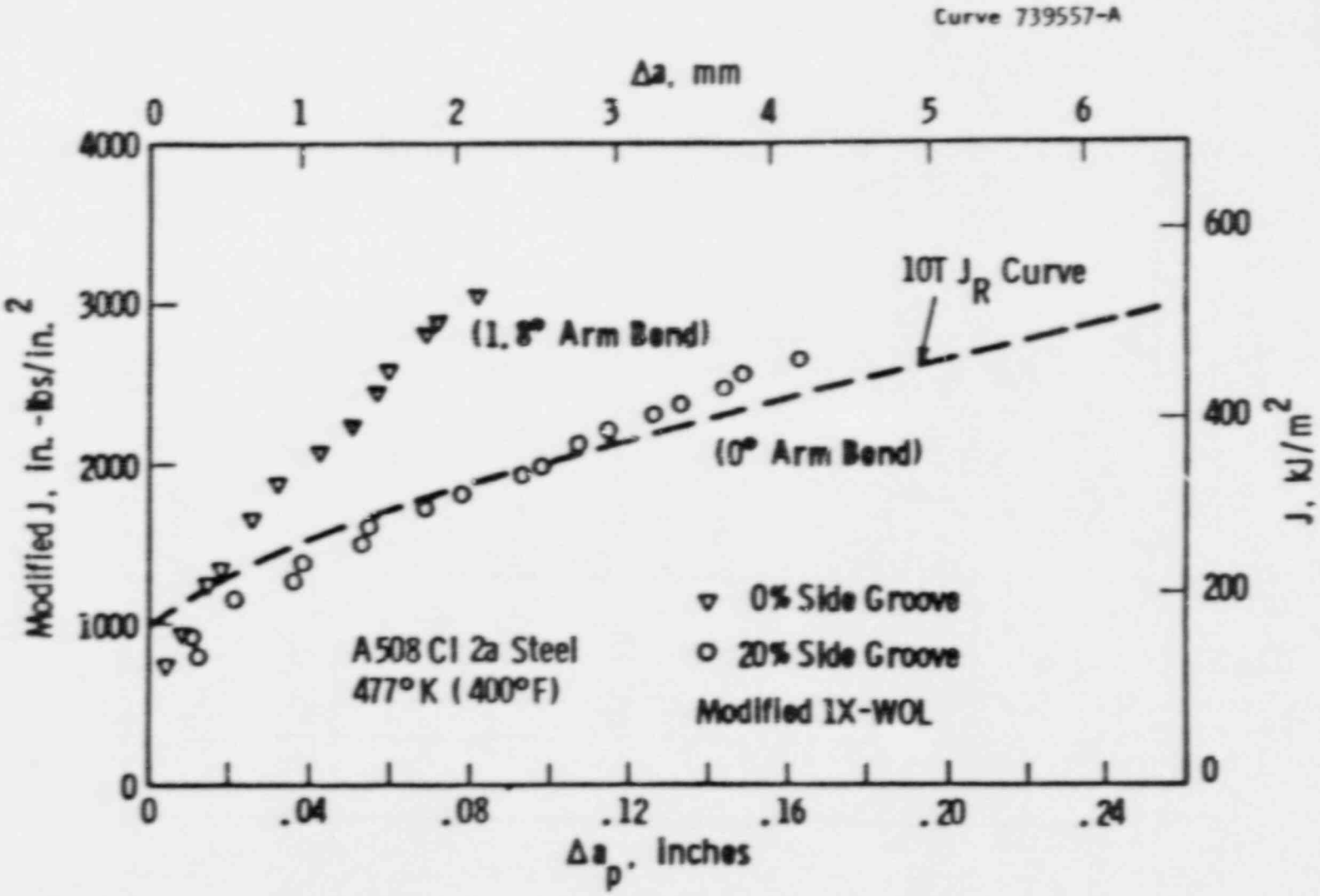

Fig. 4 - Modified 1X-WOL geometry with W = 0.95 inch. A508 Class 2A, test temperature 400^{0}F.

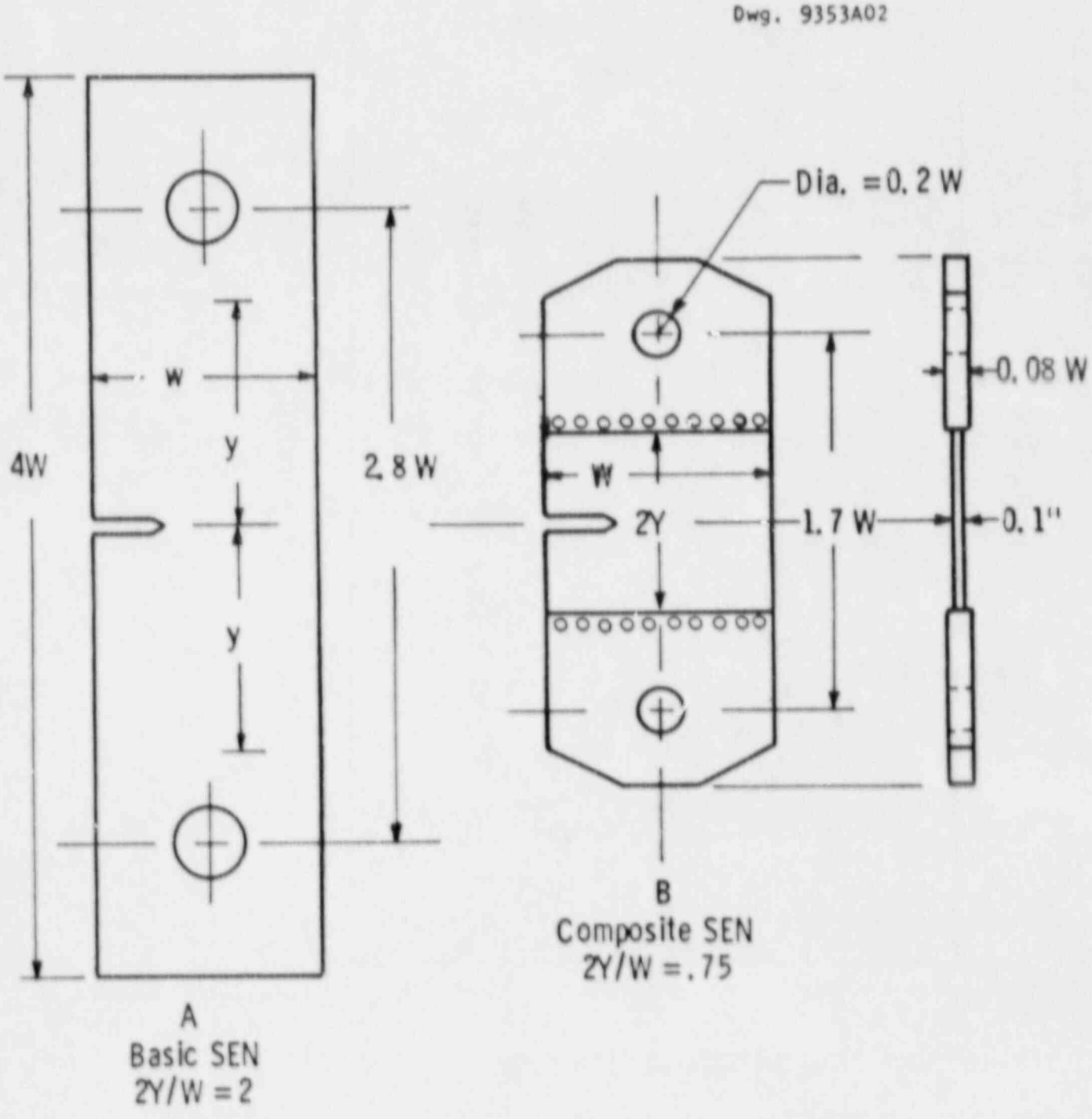

Fig. 5 - SEN and modified SEN specimens.

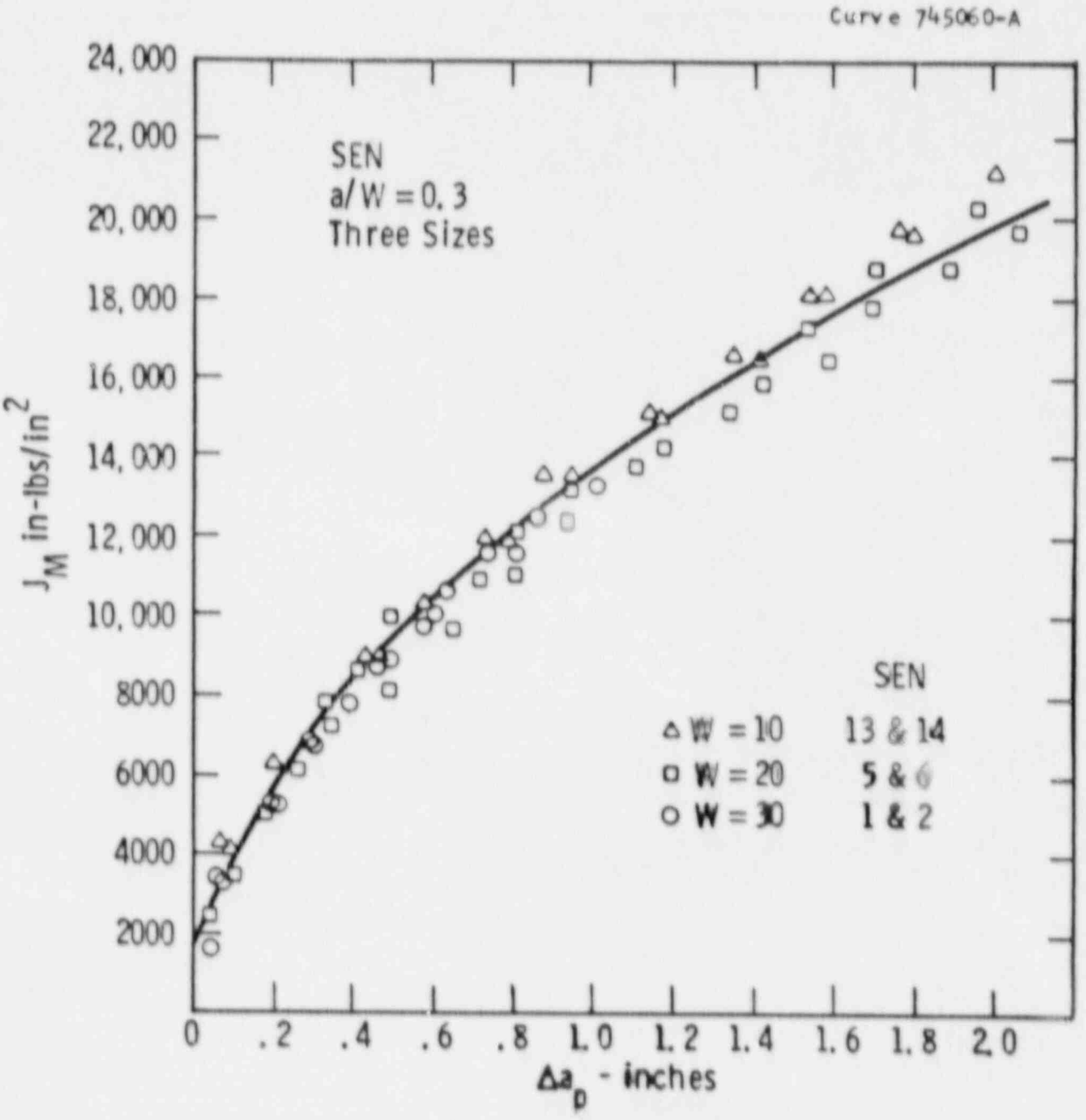

Fig. 6 - J_M-R curve from SEN specimens of a/W = 0.3 and variable width.

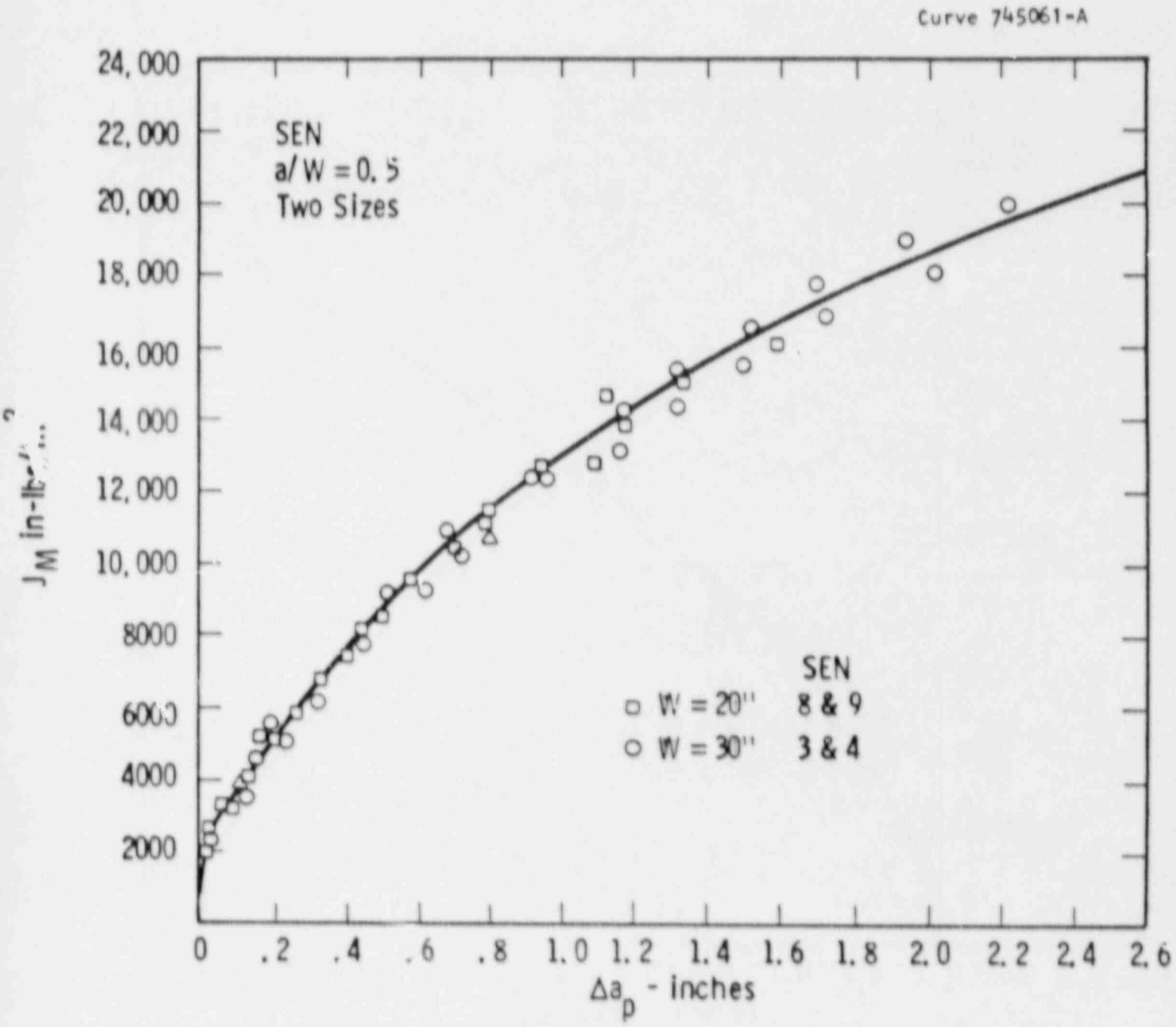

Fig. 7 - J_M-R curve for SEN specimens of a/W = 0.5 and variable width.

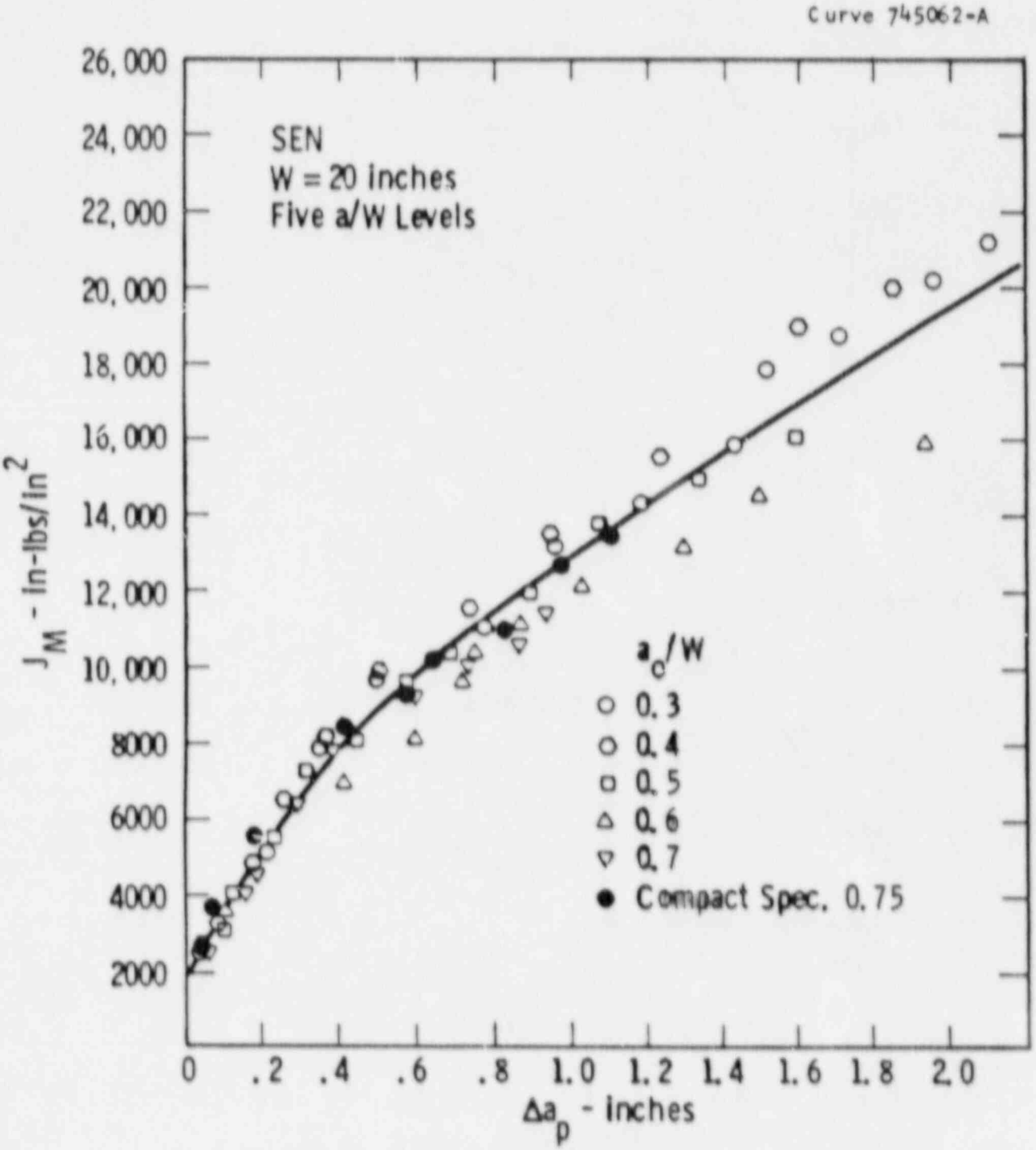

Fig. 8 - J_M-R curve for SEN specimens of fixed width and variable relative crack size.

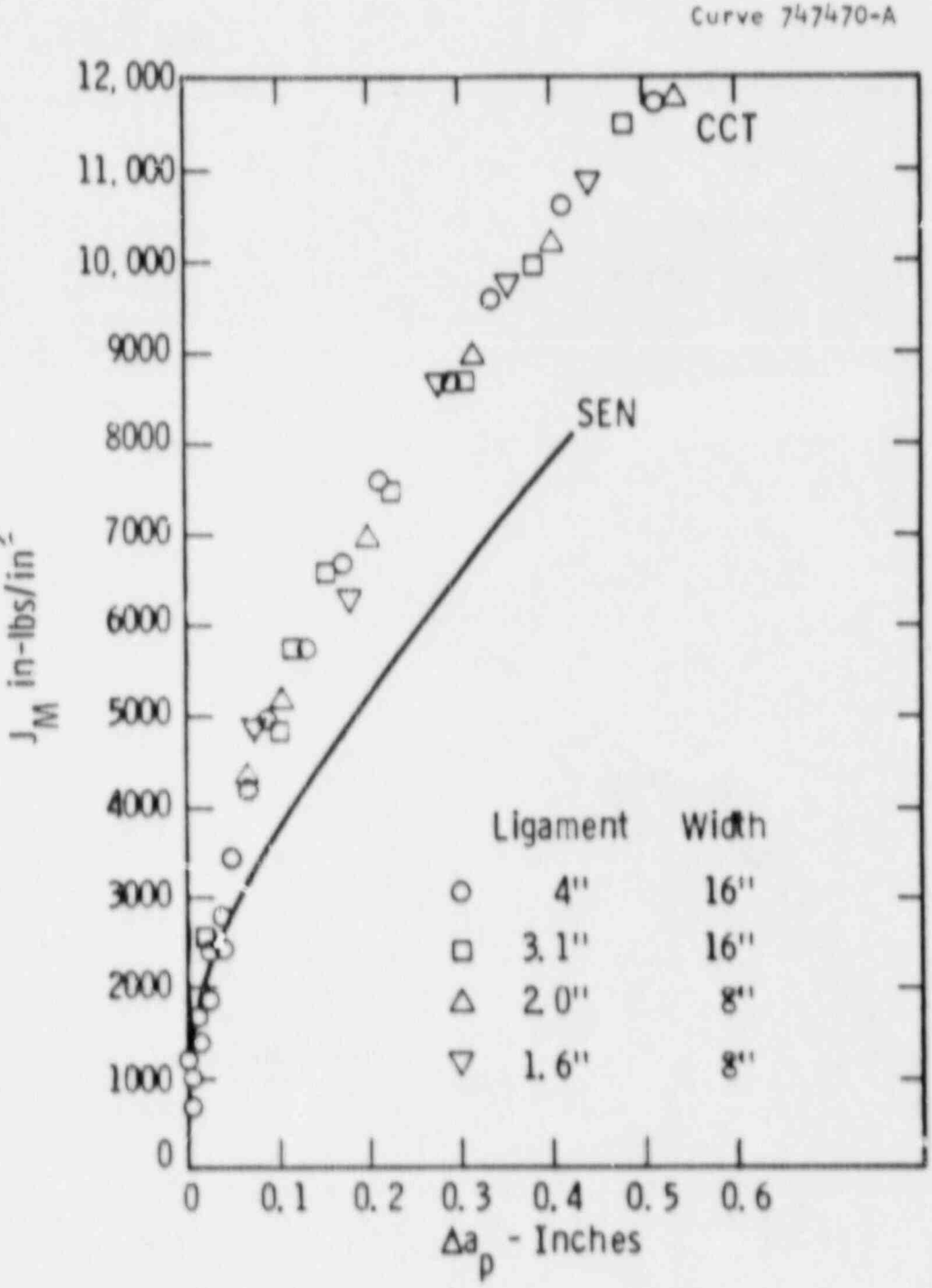

Fig. 9 - J_M-R curve for three CCT dimensions.

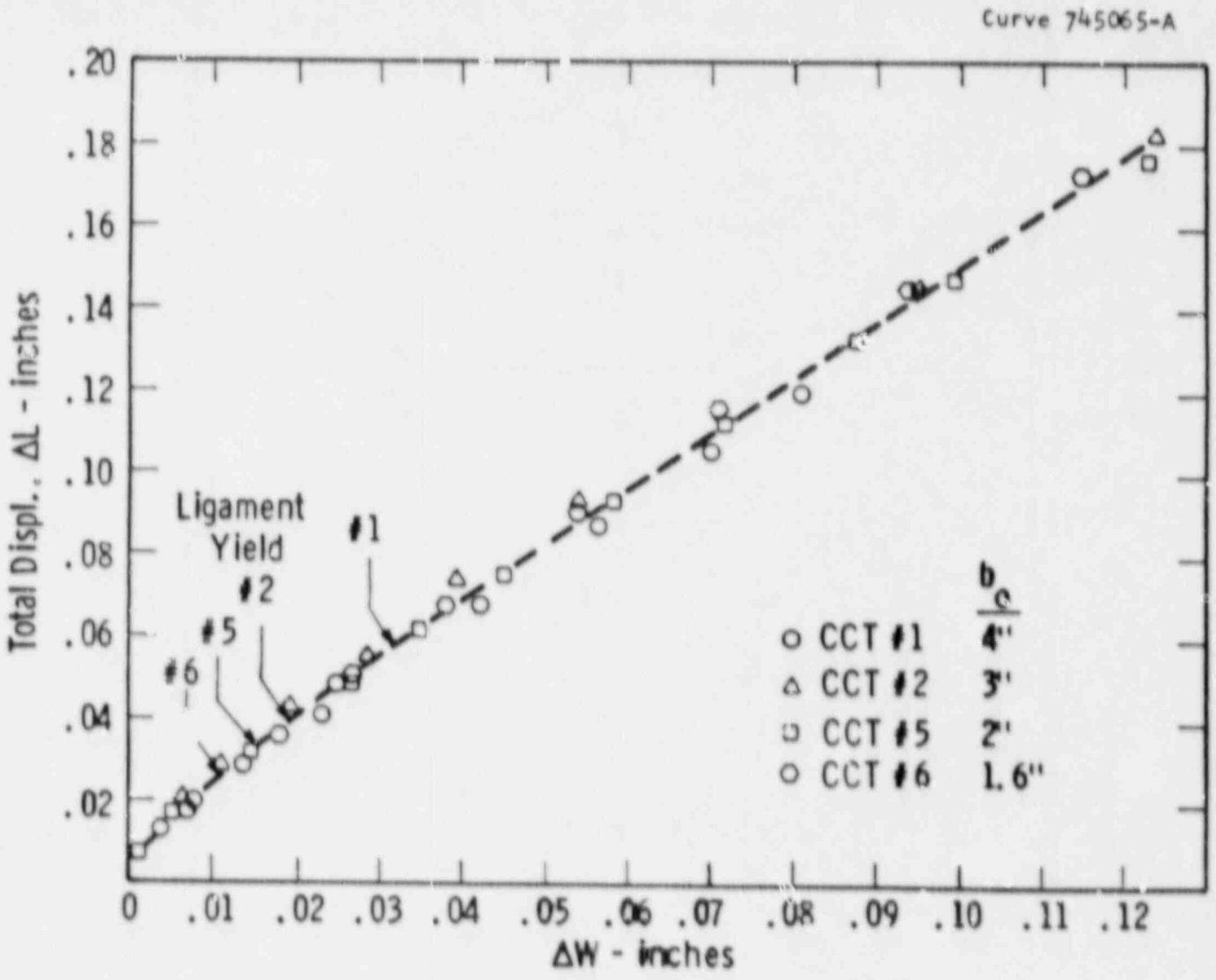

Fig. 10 - CCT panel width reduction versus overall displacement.

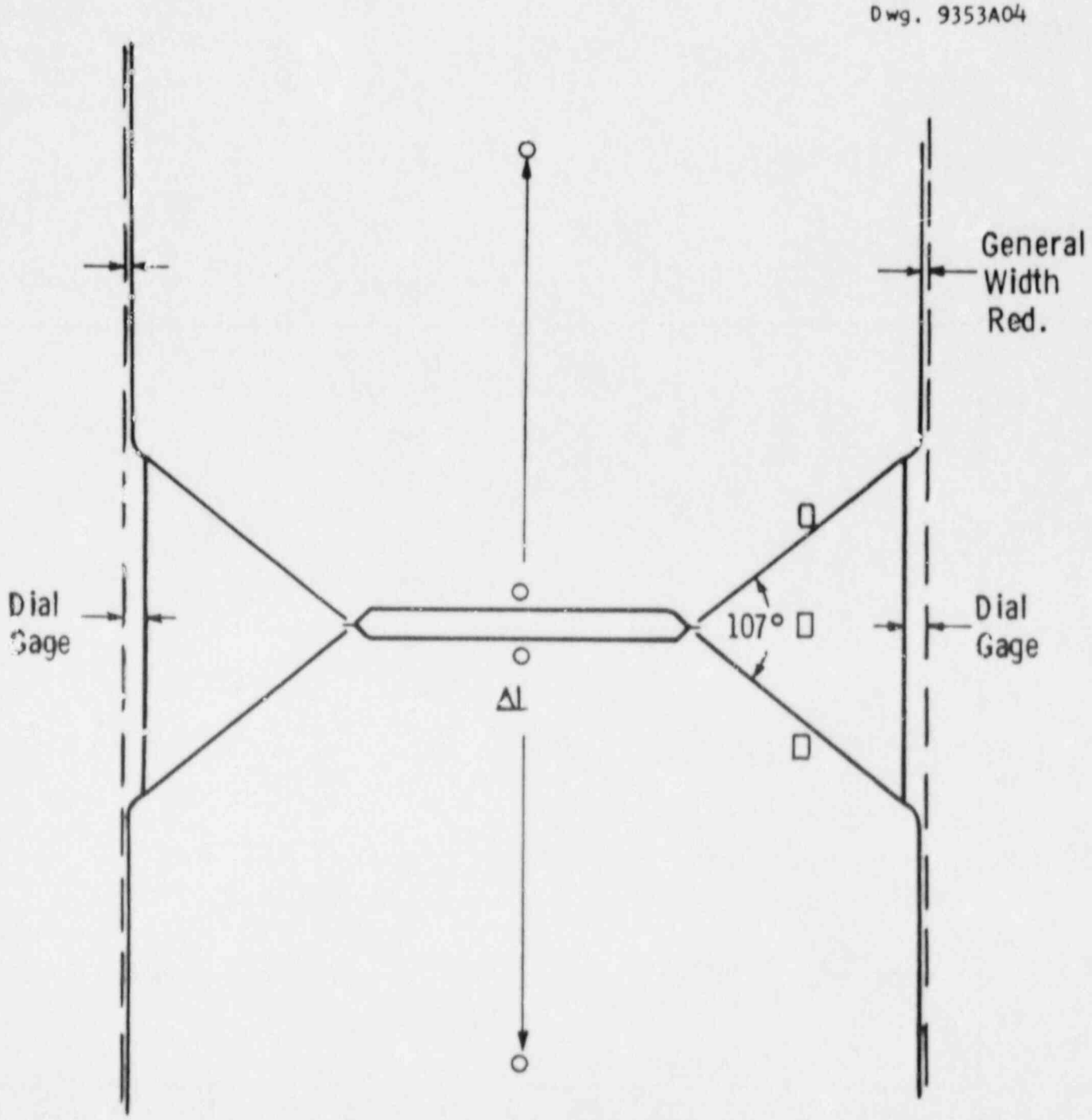

Fig. 11 - Slip line deformation in CCT panels.

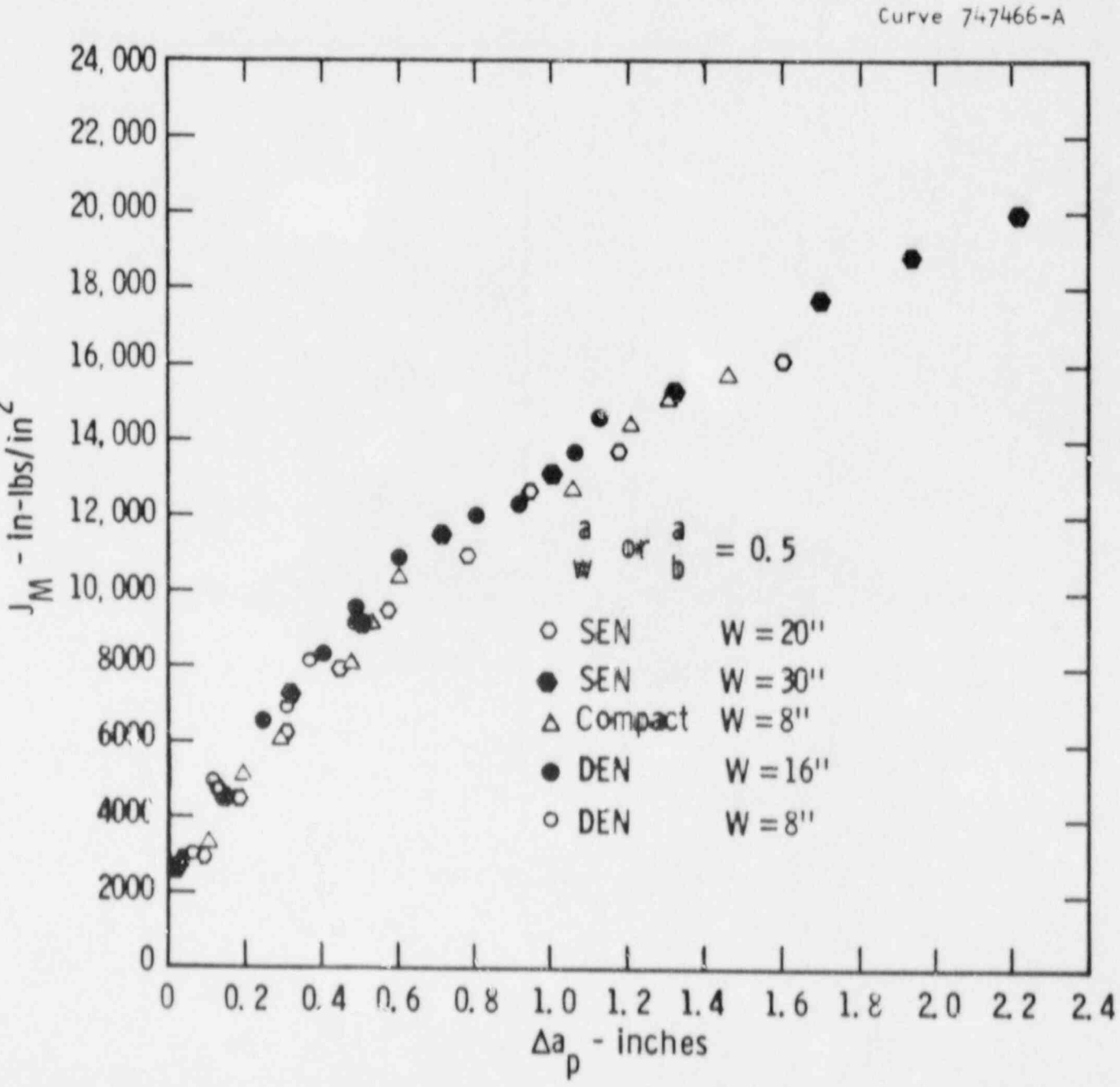

Fig. 12 - J_M-R curve for SEN, DEN, and compact specimens.

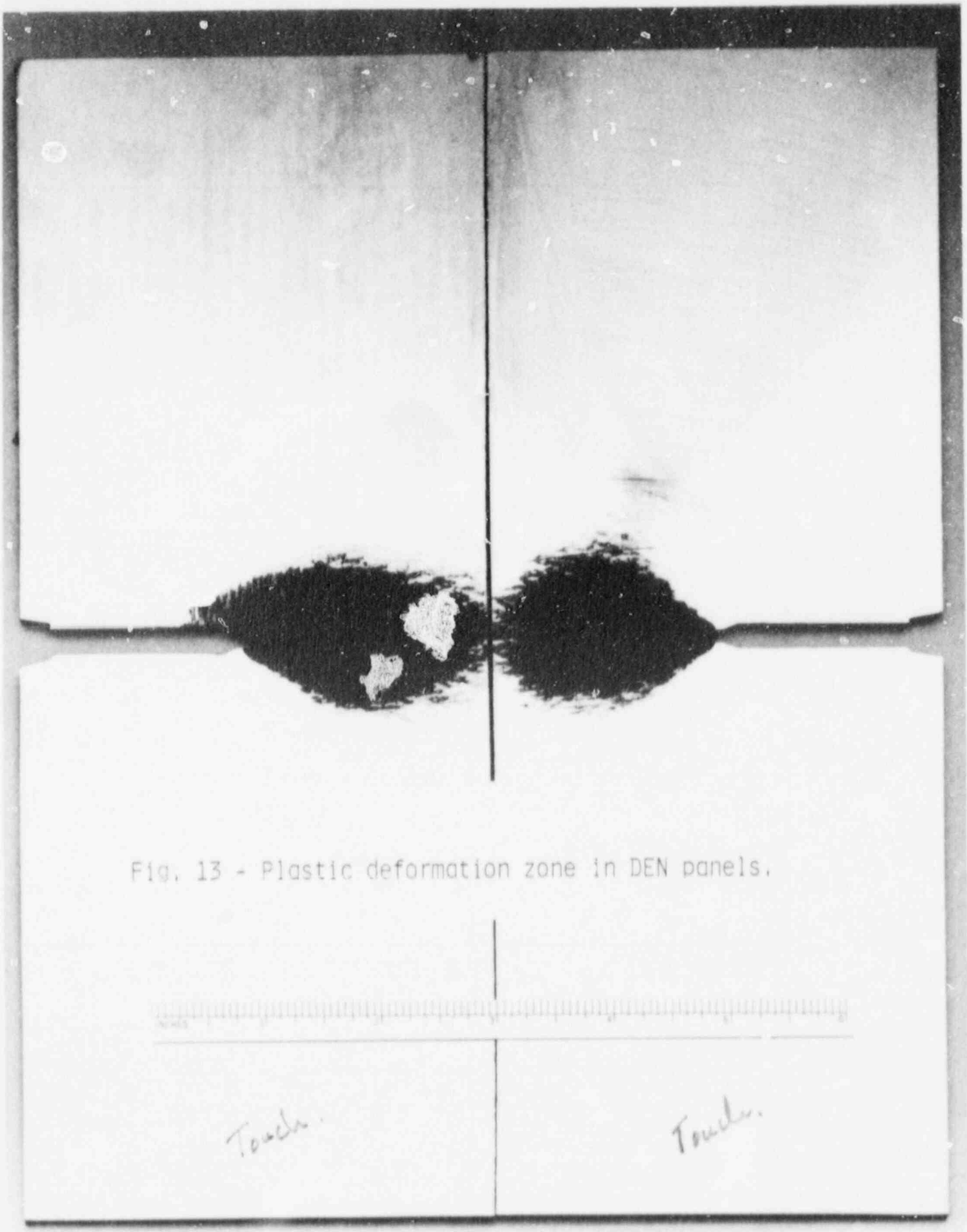

Fig. 13 - Plastic deformation zone in DEN panels.

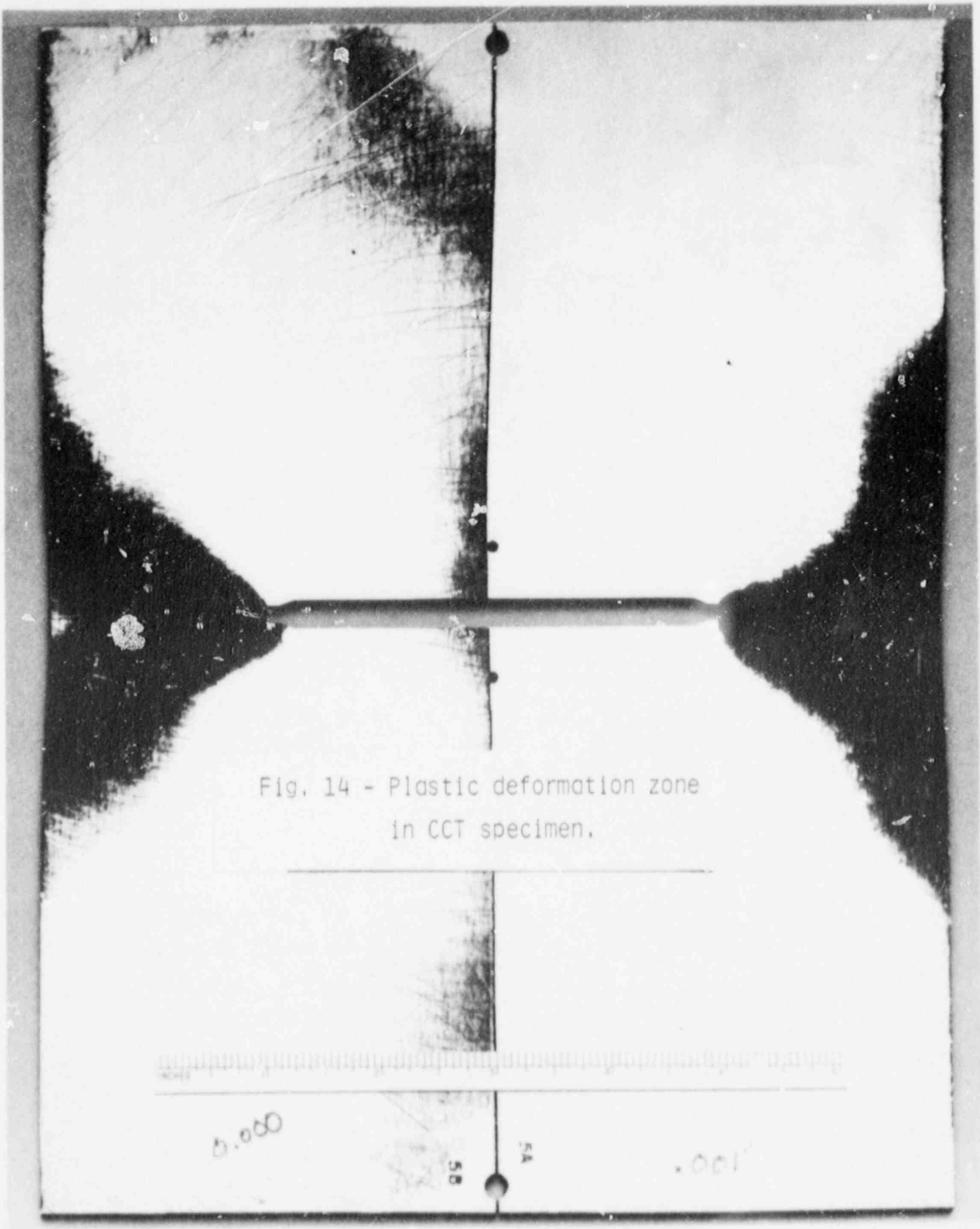

Fig. 14 - Plastic deformation zone in CCT specimen.

THE ANALYSIS OF J-Δa DATA, WITH PARTICULAR REFERENCE TO THE CEGB PROCEDURE

K.N. Akhurst

Technology Planning & Research Division
Central Electricity Generating Board
Central Electricity Research Laboratories
Kelvin Avenue, Leatherhead, Surrey KT22 7SE, England

INTRODUCTION

The CEGB J-testing procedure (Ref. 1), which is described by Neale elsewhere in these proceedings, contains requirements relating to both experimental test methods and data analysis. The purpose of the data analysis is to provide a simple description of the valid J-Δa data for use in ductile-tearing structural-integrity assessments. The present paper illustrates the method of data analysis in the CEGB procedure, with particular discussion of the use of alternative validity limits and the significance of $J_{0.2}$. Possible future extensions of the procedure, to cover austenitic steels and the assessment of material variability, are also considered.

THE METHOD OF DATA ANALYSIS

Figure 1 illustrates the application of the CEGB procedure to unloading compliance data for a C-Mn steel. Validity of the results is ensured by applying exclusion lines to the data, and fulfilling requirements on data numbers, data grouping and the gradient of the line (the 'omega' criterion). To describe the J-Δa behaviour, a line is fitted to the data points within the exclusion box. For simplicity and ease of use a straight-line description is preferred (Fig. 1). However, it is recognized that a straight line would not usually adequately describe J-Δa data over large Δa ranges, and for ranges greater than 2 mm a power law fit is required (Fig. 2).

ALTERNATIVE VALIDITY LIMITS

To ensure that the J-Δa line is valid, data for which J or Δa exceeds certain values are excluded from analysis (Fig. 1). Values of J_{max} and Δa_{max} are recommended in the procedure, but alternative values are allowed if the user can justify their use. An increase in J_{max} and Δa_{max} may for example be of value if there are particular limitations on specimen sizes. Such an increase could probably best be justified if tests on a similar material showed agreement between valid data from large specimens and invalid data from smaller specimens, for example as in Fig. 3. Such an argument relies on a close similarity between the steel to be tested and that used for the justification.

A reduction of the values of J_{max} and Δa_{max} can sometimes be of value, if the J-Δa line is invalidated because of the omega (ω) or data grouping requirements in the CEGB procedure (Fig. 4). Such a

reduction is clearly justified as it is more restrictive than the recommended exclusion lines.

THE SIGNIFICANCE OF $J_{0.2}$

It is not intended that the CEGB procedure should be used to obtain a value for J at the initiation of ductile tearing. While for some steels $J_{0.2}$ may give a good agreement with an initiation toughness derived using a blunting line (e.g. ASTM E813; Fig. 5), in general this is not the case. The difference between $J_{0.2}$ and J_{IC} increases the higher the toughness (cf. Fig. 5 and Fig. 6). In addition there is a potential variability in the value of $J_{0.2}$ for a given steel, depending on the range of Δa analysed. A procedure solely intended to derive $J_{0.2}$ would concentrate on obtaining data near 0.2 mm crack growth. The purpose of the CEGB procedure is to describe simply J-Δa behaviour over a variable range of Δa, and some resultant variability in the value of $J_{0.2}$ is an acceptable consequence. Nevertheless, for many steels $J_{0.2}$ should provide a reasonable engineering estimate of the initiation toughness for integrity assessment purposes.

AUSTENITICS

The procedure is currently limited to ferritic steels. In very high toughness austenitic steels it can be difficult to achieve valid data beyond the initiation of ductile tearing (or indeed any valid data) in specimens of a reasonable size (Fig. 7). Even if the results in Fig. 7 were produced by 100 mm thick CT specimens the valid data for this steel would all correspond to crack blunting. This is not necessarily a problem as an integrity assessment is not concerned intrinsically about the mode of crack advance. The value of J_g in such a situation could be regarded as a lower bound to the J for the initiation of tearing . The possible use of the CEGB procedure may therefore present no major problems for austenitic materials, even though it may be difficult to obtain valid data. Some austenitics have relatively low toughness and for these valid data can be obtained relatively easily (Fig. 8).

MATERIAL VARIABILITY

Mean Fracture Resistance

For steels with a large variation in fracture resistance the CEGB procedure recommends the use of a single specimen test method such as unloading compliance. For such steels a small number of multi-specimen data points do not provide sufficient information to establish a reliable regression line (e.g. Fig. 9). In principle, provided sufficient multispecimen data are obtained a best fit line should provide an accurate prediction of the most likely value of J for a given value of Δa. However, the best fit line in such a situation can be strongly dependent on the method of regression (J on Δa, perpendicular distance, Δa on J, or some intermediate method). The statistically most appropriate line depends on several factors (Ref. 2), including statistical bias introduced by the exclusion lines (Fig. 10).

These problems demonstrate the value of using a single specimen method Not only are more data points collected, but the variations in J due to Δa changes in a given test and those due to material scatter between different tests are separated, providing much more information. If only multispecimen data are available then it may be preferable to describe the fracture resistance in terms of the mean of all the data points (e.g. Fig. 9), or 'mean torn toughness' (Ref. 3). All the straight regression lines pass through this point if equal weighting is used, and it is the position where the statistical confidence in the mean lines is highest.

The CEGB procedure makes no recommendation on the number of single specimen tests necessary to ensure that the range of material variability is properly sampled. This cleary depends on the extent of this variability. For the steel of Fig. 9, Milne and Curry (Ref. 4) suggest that at least six single specimen tests would be necessary.

Lower Bound Fracture Resistance

The determination of a lower bound confidence limit to the J-Δa data is not covered by the CEGB procedure. At first sight its incorporation would appear fairly straightforward. The level of confidence (e.g. 95%) would be chosen according to the degree of conservatism required. Lower confidence limits to $J_{0.2}$ and J_g (or Δa at J_{max}) could then be calculated from single specimen data, and a suitable interpolation used to give a lower bound line (Fig. 11). The problem is that confidence limits can be very sensitive to the nature of the statistical distribution that the data is assumed to follow (the values in Fig. 11 were calculated assuming a normal distribution). If the distribution were known, then three or four single specimen tests would probably be sufficient to define the 95% confidence limit with reasonable accuracy (e.g. Ref. 5). In practice it appears that little is known about the statistical distribution of J-Δa data. To establish this distribution in the region of the confidence level would require a large number of tests (~20 single specimen tests for the 95% confidence level). If it is necessary to fit a distribution to inadequate data then the normal distribution appears to be preferable to a three parameter Weibull fit, as the normal distribution generally results in more conservative lower bounds and the analysis, in particular the allowance for uncertainty in the fitting, is simpler.

The determination of lower bound lines is even more difficult with multispecimen data. There is the same problem of choosing the appropriate distribution and the bands of confidence are wider than for the same number of single specimen tests. There is also usually insufficient information from multispecimen data to establish the variation of scatter with Δa, and a simple assumption has to be made. If uniform scatter is assumed, when the J-Δa curves actually diverge, then the lower bound values of $J_{0.2}$ tend to be too low and those of J_g too high (unless J_{max} limited), as shown in Fig. 12. These factors can result in lower bound values which are negative. Windle (Ref. 6) has proposed a method of avoiding this unrealistic outcome by transposing and scaling the data points and fitting a two parameter Weibull distribution to them, ensuring that negative J values are not allowed.

However, wherever possible, single specimen testing is clearly preferable.

Thus, at present it is apparently not possible to determine lower bound values confidently from relatively few tests. Milne and Curry (Ref. 4) have noted that other conservatisms should normally ensure sufficient pessimism when using mean J-Δa data. The reliable allowance for material variability awaits a theoretical or experimental derivation of the appropriate statistical distributions, unless the user is prepared to perform large numbers of tests.

CONCLUSIONS

1. The CEGB procedure allows the use of alternative J_{max} and Δa_{max} exclusion lines, provided that these are justified. While the justification of larger values of J_{max} and Δa_{max} may require considerable effort, the use of smaller values can clearly be justified. Smaller values of J_{max} or Δa_{max} may allow the use of data which fails the data grouping or omega (ω) requirement when the recommended values are used.

2. $J_{0.2}$ is not in general equivalent to J_{IC}, but for many steels it should provide a reasonable engineering estimate of the initiation toughness for the purposes of structural integrity assessments.

3. There should be no major problems in extending the CEGB procedure to cover austenitic steels, although difficulties in obtaining valid data may be encountered.

4. It may only be possible to obtain reliable results with very variable material if a single specimen test method is used.

5. The outstanding problem in determining lower bound J-Δa behaviour is the difficulty in establishing the appropriate statistical distribution. If this is not known then a large number of tests are necessary. If it is required to fit a distribution to inadequate data, then the normal distribution should be preferred unless it predicts negative J values, in which case a two parameter Weibull fit may be preferable (Ref. 6).

ACKNOWLEDGEMENT

The author would like to acknowledge discussions with colleagues throughout the CEGB, and thank those who have allowed the use of unpublished results. The work was carried out at the Central Electricity Research Laboratories and is published by permission of the Central Electricity Generating Board.

REFERENCES

1. B.K. Neale, D.A. Curry, G. Green, J.R. Haigh and K.N. Akhurst, "A Procedure for the Determination of the Fracture Resistance of Ductile Steels", CEGB Report TPRD/B/0495/R84, Berkeley, UK, October 1984

also: K.N. Akhurst, G. Green, J.R. Haigh and B.K. Neale, "Explanatory Background Notes to 'A Procedure for the Determination of the Fracture Resistance of Ductile Steels'", CEGB Report TPRD/B/0496/N84, Berkeley, UK, October 1984

2. K.N. Akhurst and J.H. Pickles, CEGB Report, to be issued, Leatherhead, UK

3. J.R. Haigh, CEGB North West Region, Wythenshawe, UK, private communication, 1983

4. I. Milne and D.A. Curry, "Fracture Toughness, Tearing Resistance and Specimen Size Effects in Submerged Arc and Manual Metal Arc Welds in A5333B Plate", CEGB Report, to be issued, Leatherhead, UK

5. P. Doig, "Evaluation of Lower Bound Fracture Toughness Values in Using Weibull Analysis of Single Specimen Data", CEGB Report SER/SSD/84/0040/N, Gravesend, UK

6. P.L. Windle, "Statistical Models for the Analysis of Fracture Toughness Test Data", CEGB Report SER/SSD/84/0037/N, Gravesend, UK, June 1984

7. M.R. Jones, CERL, Leatherhead, UK, unpublished work, 1985

8. A.L. Hiser, F.J. Loss and B.H. Menke, "Fracture Toughness Characterization of Irradiated Low Upper Shelf Welds", presented at the ASTM 12th International Symposium on the Effects of Radiation on Materials, Williamsburg, Va., US, June 1984

9. T. Ingham, J.T. Bland and G. Wardle, "The Influence of Specimen Size on the Upper Shelf Toughness of SA533B-1 Steel", in proc. 7th Int. Conf. on Structural Mechanics in Reactor Technology, paper G2/3, Chicago, US, August 1983

10. D.A. Curry and I. Milne, CERL, Leatherhead, UK, unpublished work, 1981

11. S.T. Kimmins, CERL, Leatherhead, UK, unpublished work, 1984

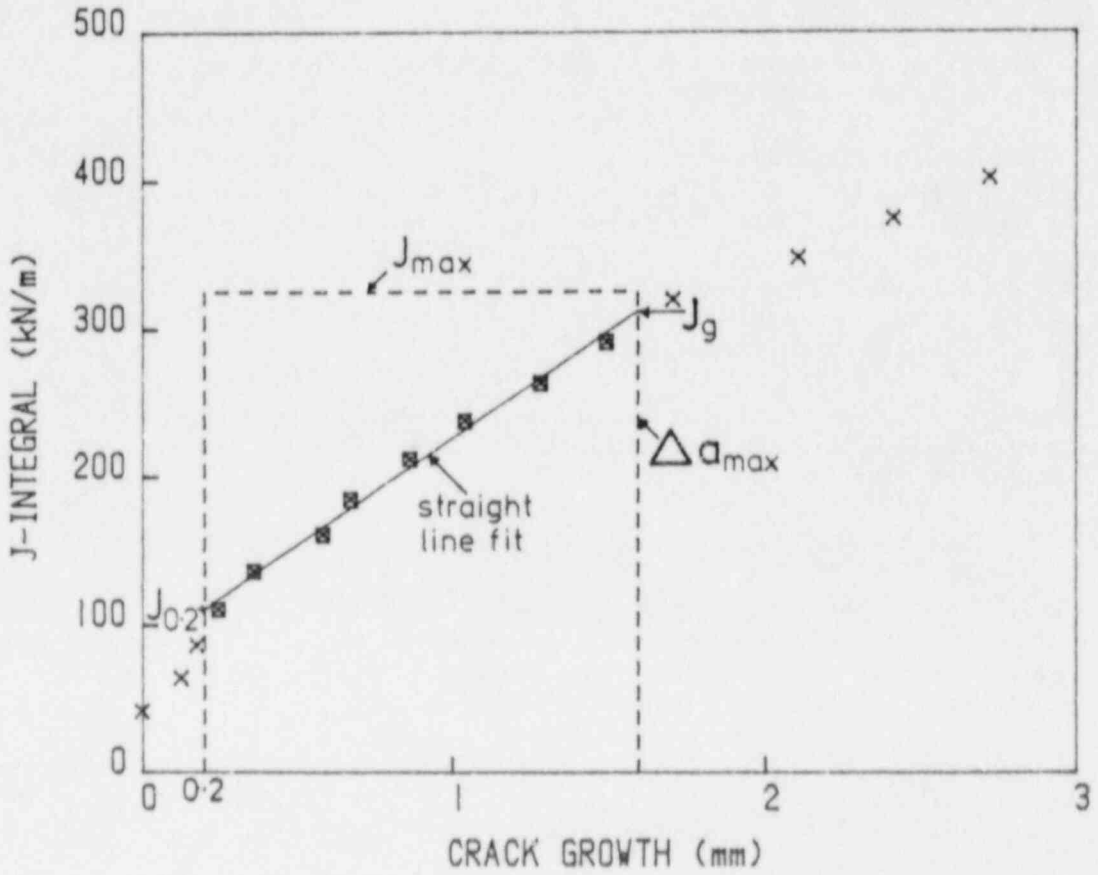

Fig. 1 Application of the CEGB procedure to J-Δa data for a C-Mn steel (from Ref. 7).

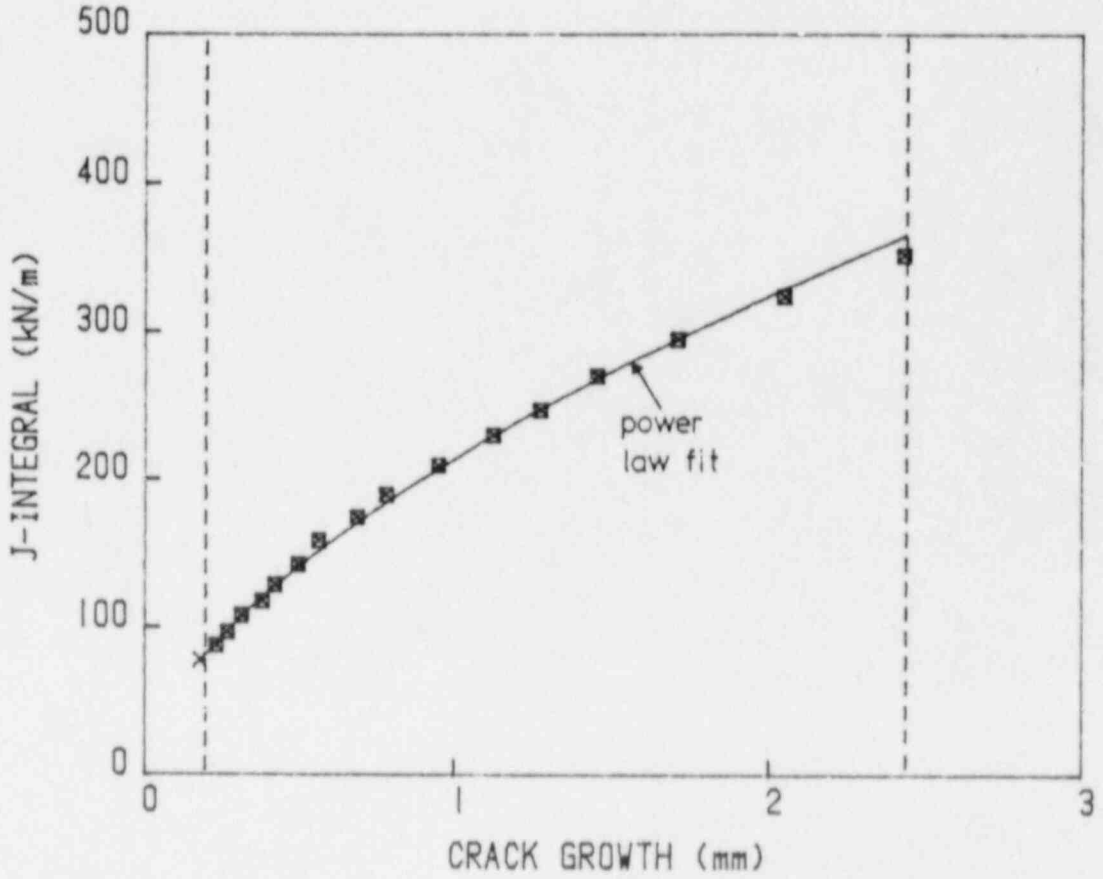

Fig. 2 Analysis of MnNiMo steel weld data (from Ref. 8) illustrating the use of a power law to fit data exceeding 2 mm crack growth.

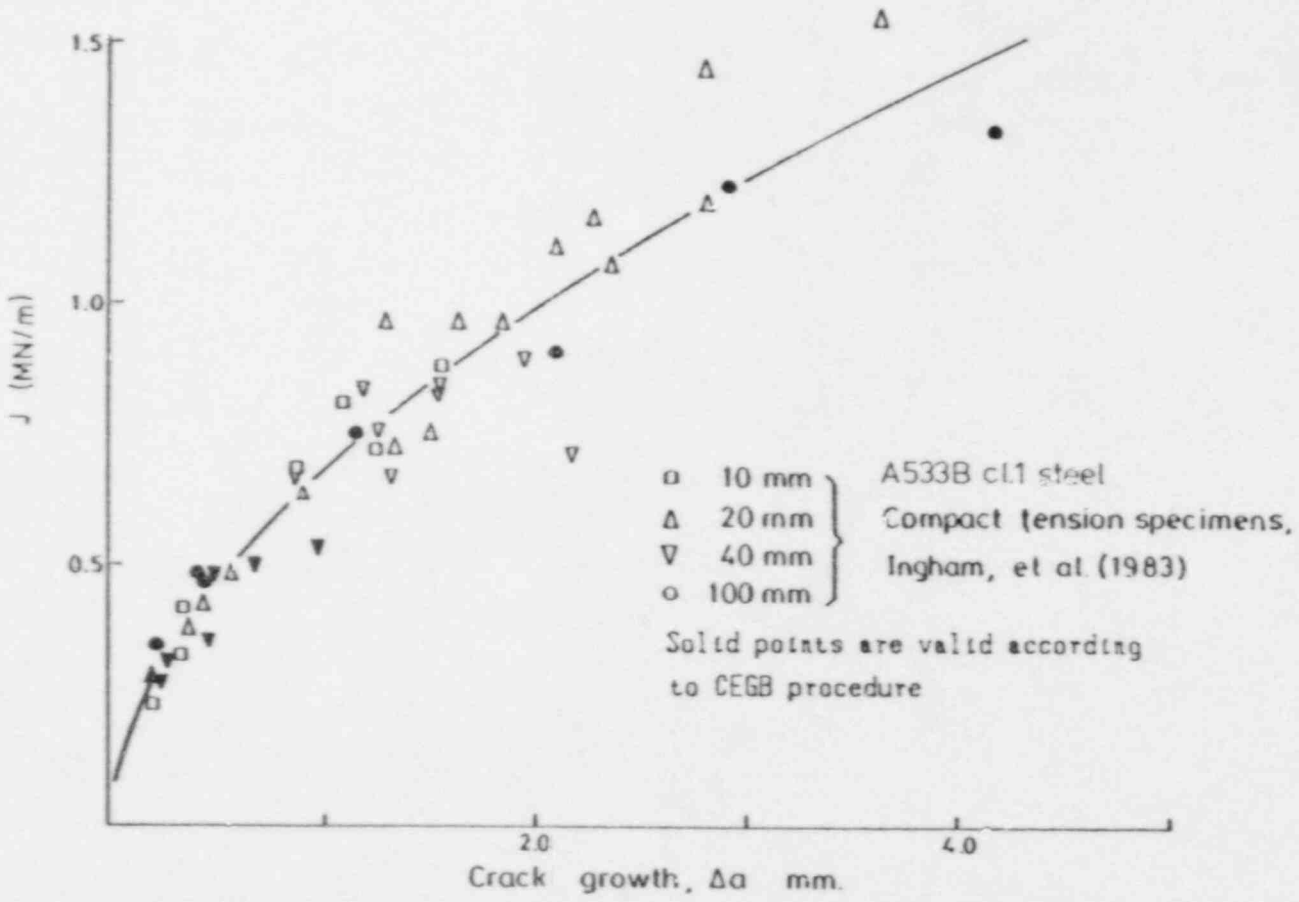

Fig. 3 Data for A533B plate (from Ref. 9) which might be used to justify alternative exclusion lines for similar steels, to allow the analysis of invalid data.

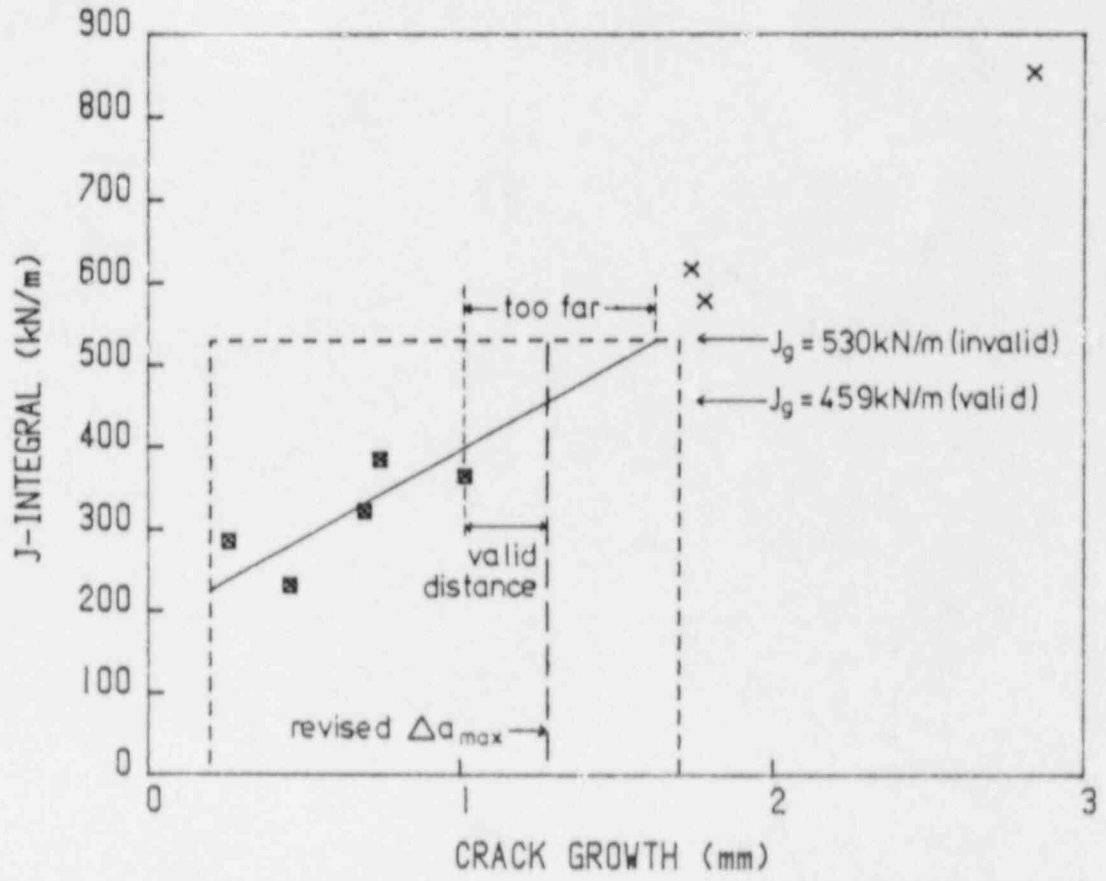

Fig. 4 An illustration of how valid results can sometimes be obtained from data with an invalid grouping by reducing the value of Δa_{max} (data from Ref.4).

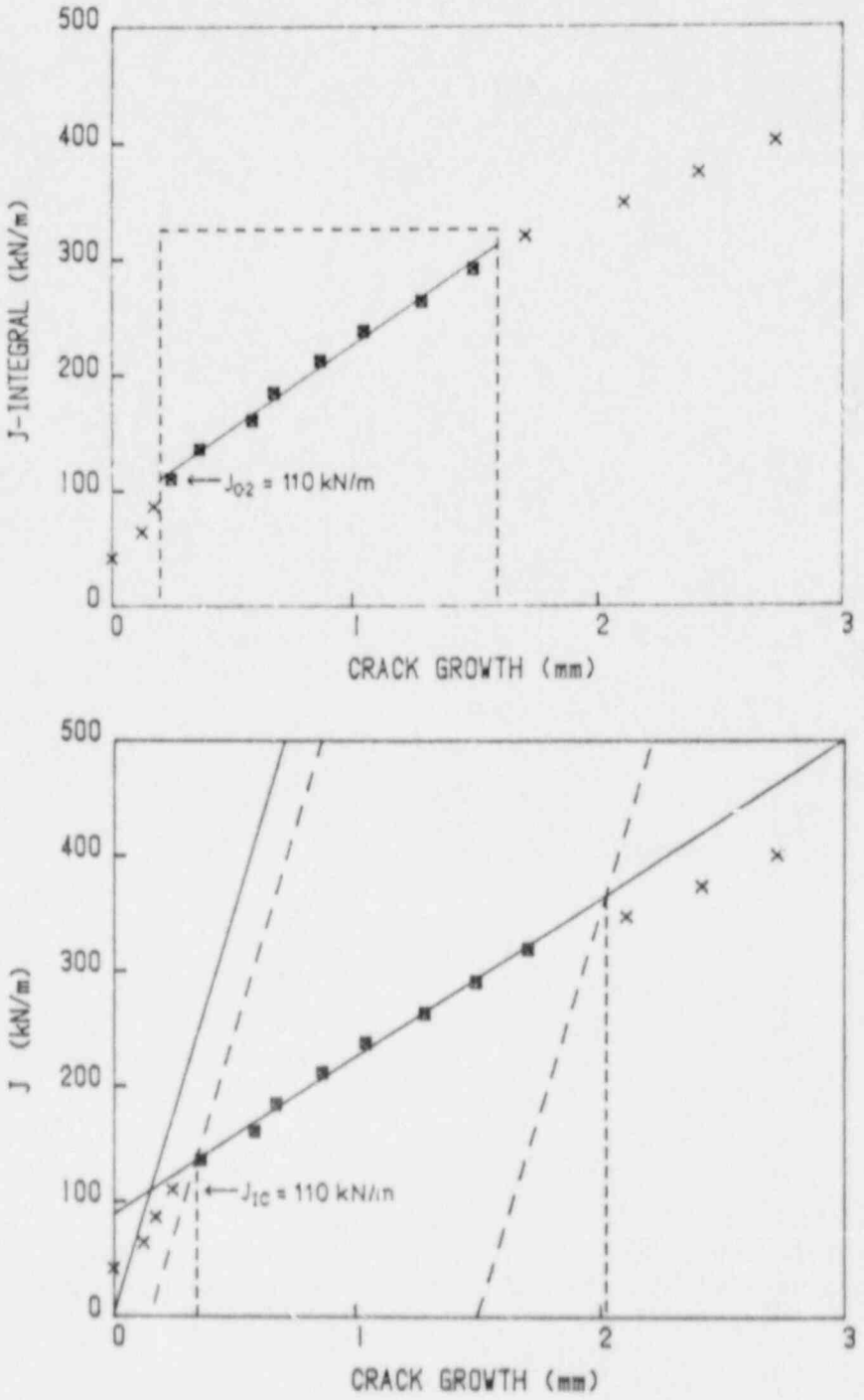

Fig. 5 For steels of relatively low toughness $J_{0.2}$ and J_{IC} can show good agreement (data from Ref. 7).

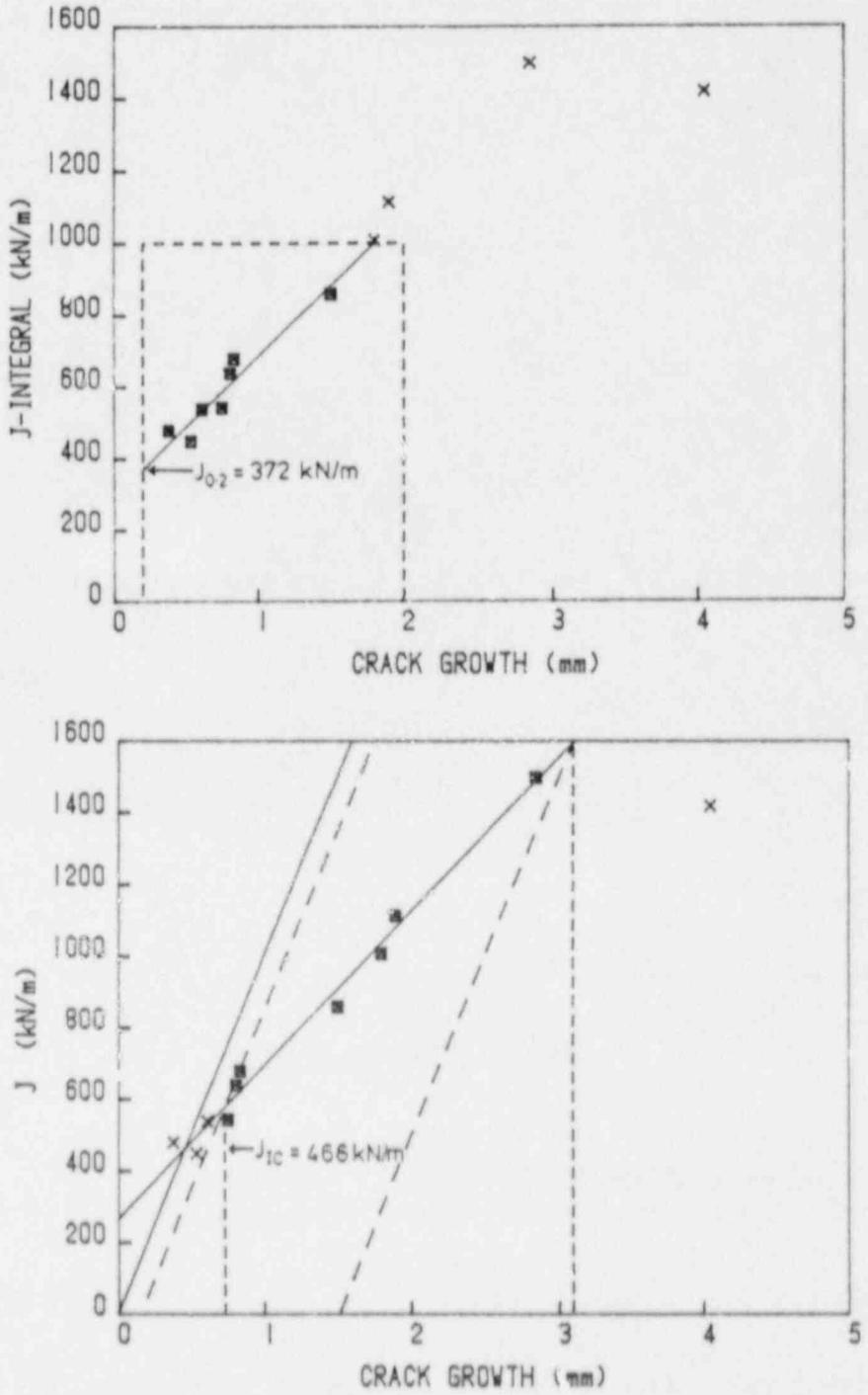

Fig. 6 For high toughness steels $J_{0.2}$ is typically significantly lower than J_{IC} (data from Ref. 10).

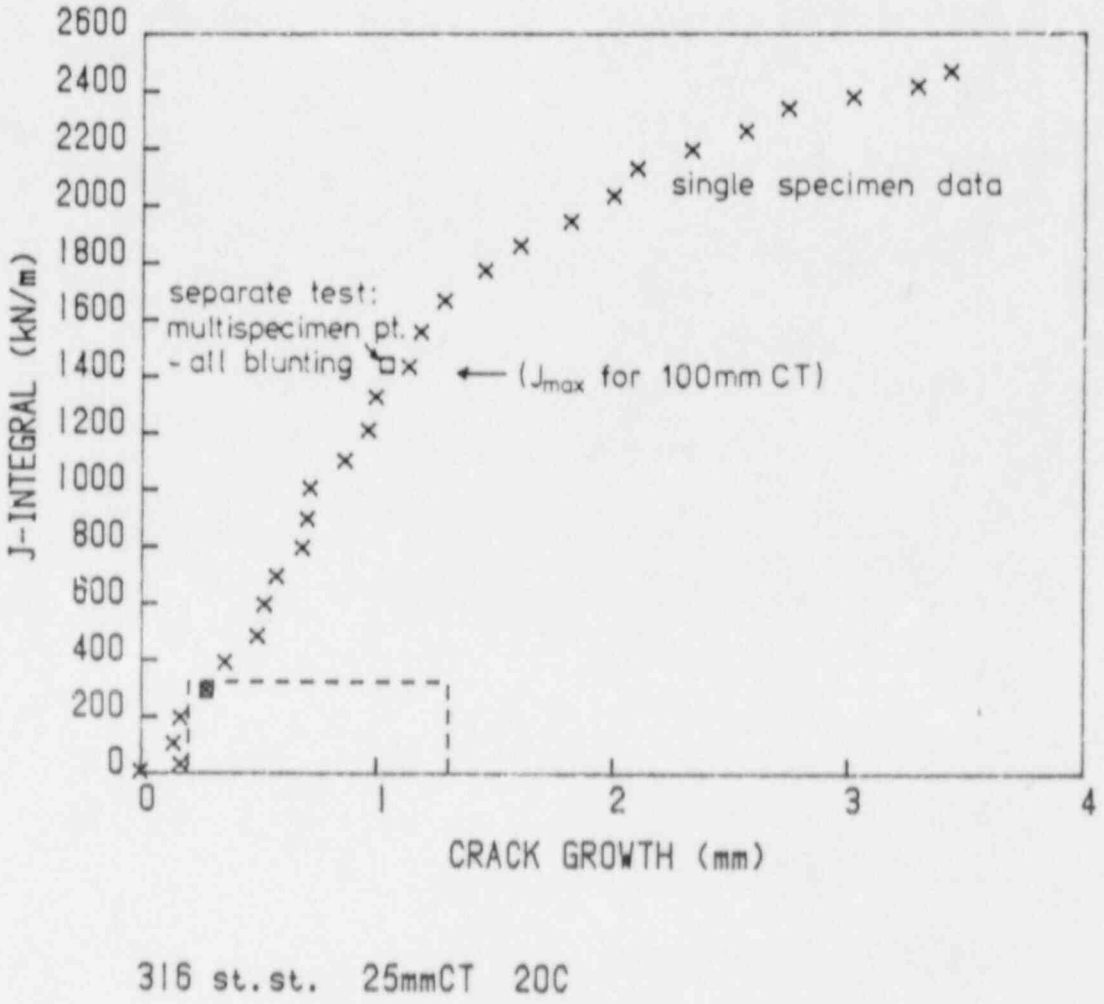

Fig. 7 Data for very tough 316 plate, illustrating the difficulty in achieving valid data beyond the initiation of ductile tearing (or indeed any valid data) in specimens of reasonable size.

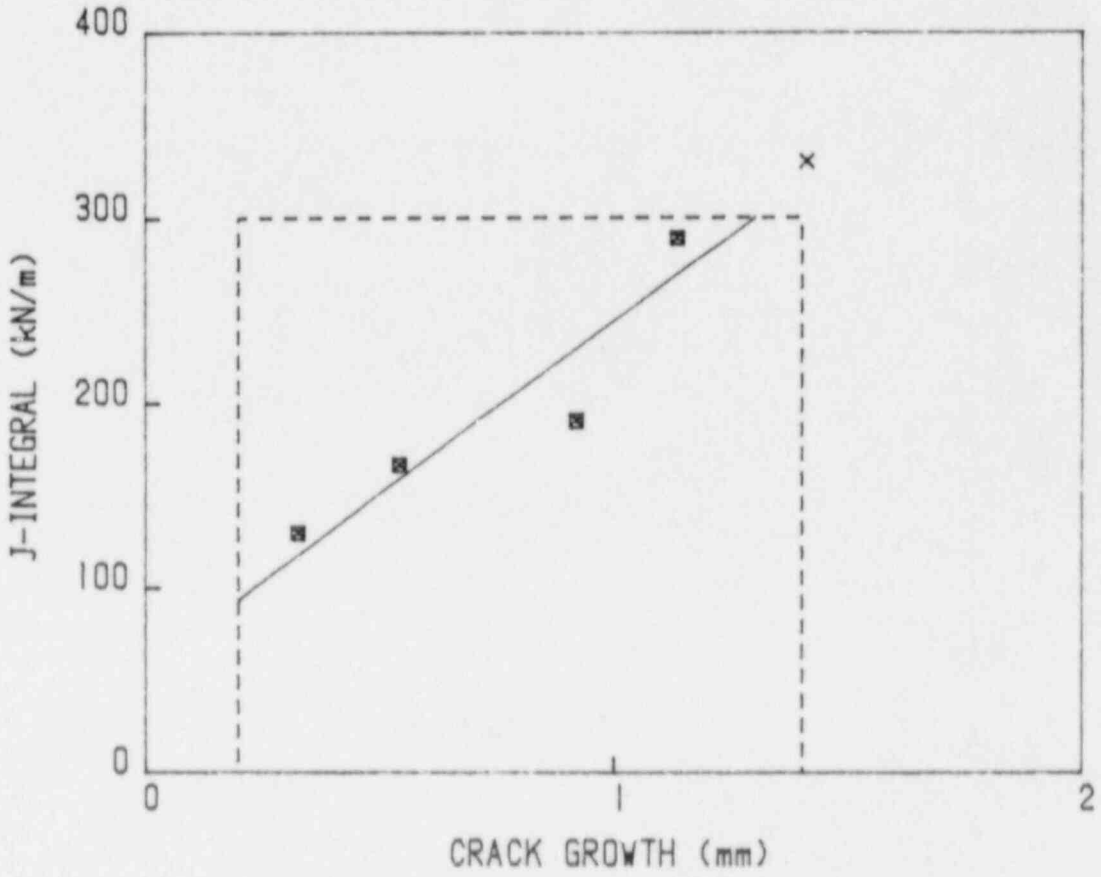

Fig. 8 Data for a low toughness 316 weld (from Ref. 11), for which valid data can be obtained relatively easily (compare J scale with that in Fig. 7).

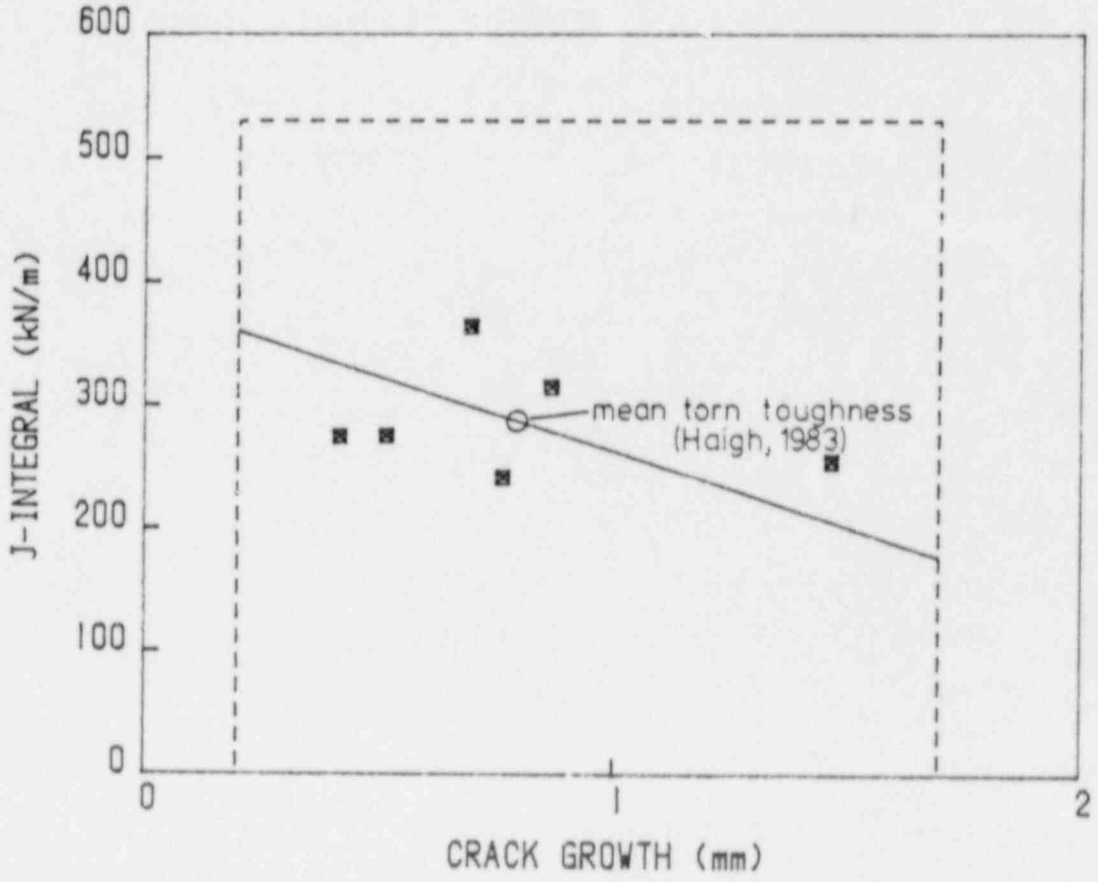

Fig. 9 An illustration of how a few multispecimen data points for a highly variable steel do not provide sufficient information to establish a reliable regression line (data from Ref. 4). This result would be invalidated in the CEGB procedure by the ω requirement. The point on the line which is most reliable is the mean of the data points, indicated in the figure.

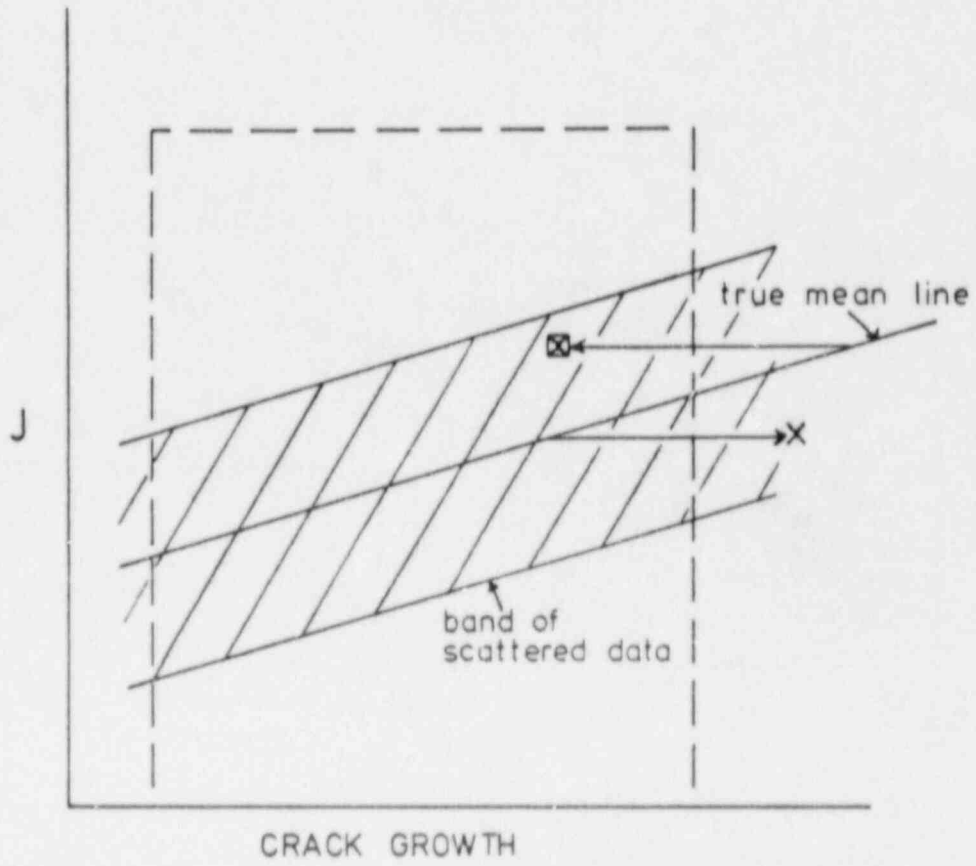

Fig. 10 Statistical bias can be introduced by the application of exclusion lines to scattered data. In the figure, near the Δa_{max} limit, data scattered above the mean line is more likely to be analysed than data below this line (Ref. 2) if any of the scatter results from errors in Δa.

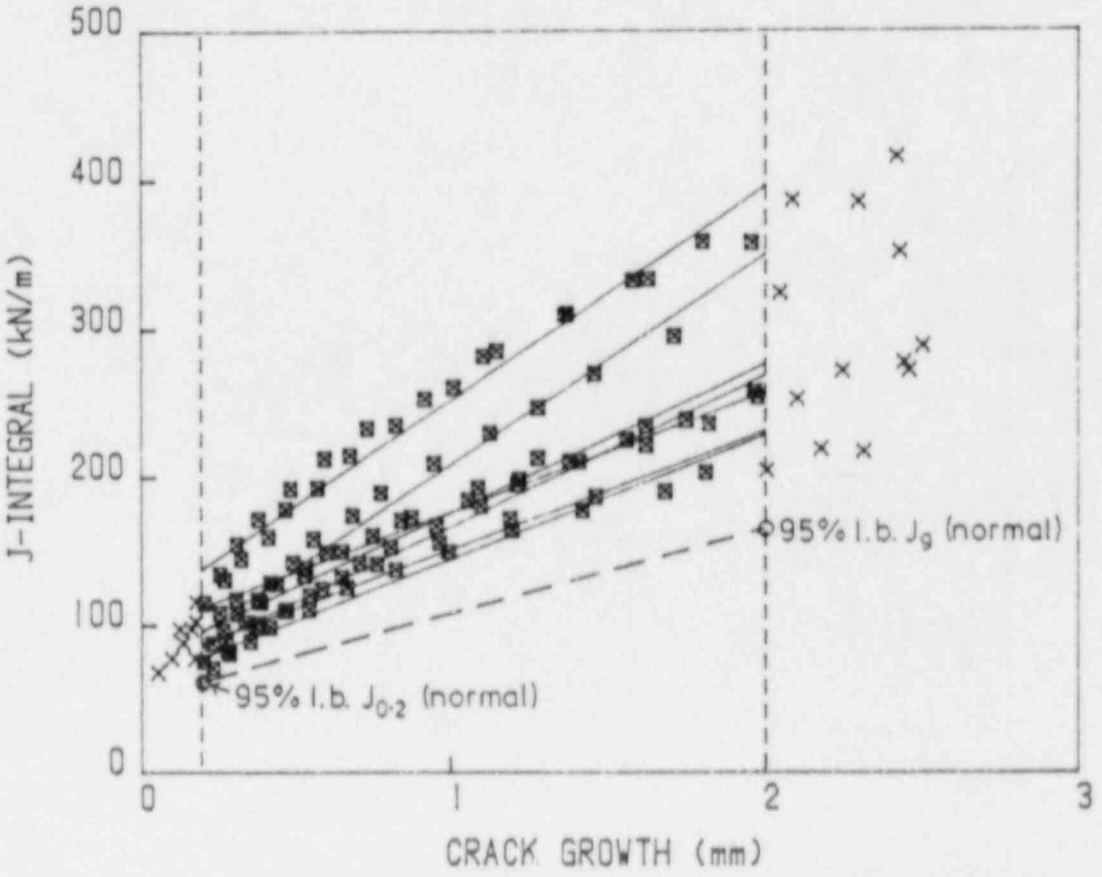

Fig. 11 A possible method of deriving a lower bound line from single specimen data. Data from Ref. 8 was analysed according to the CEGB procedure (limiting Δa_{max} to 2 mm to allow the simplicity of straight line fitting). 95% lower bound confidence limits were calculated from the $J_{0.2}$ and J_g values, assuming a normal distribution, and a straight line taken between the two lower bounds.

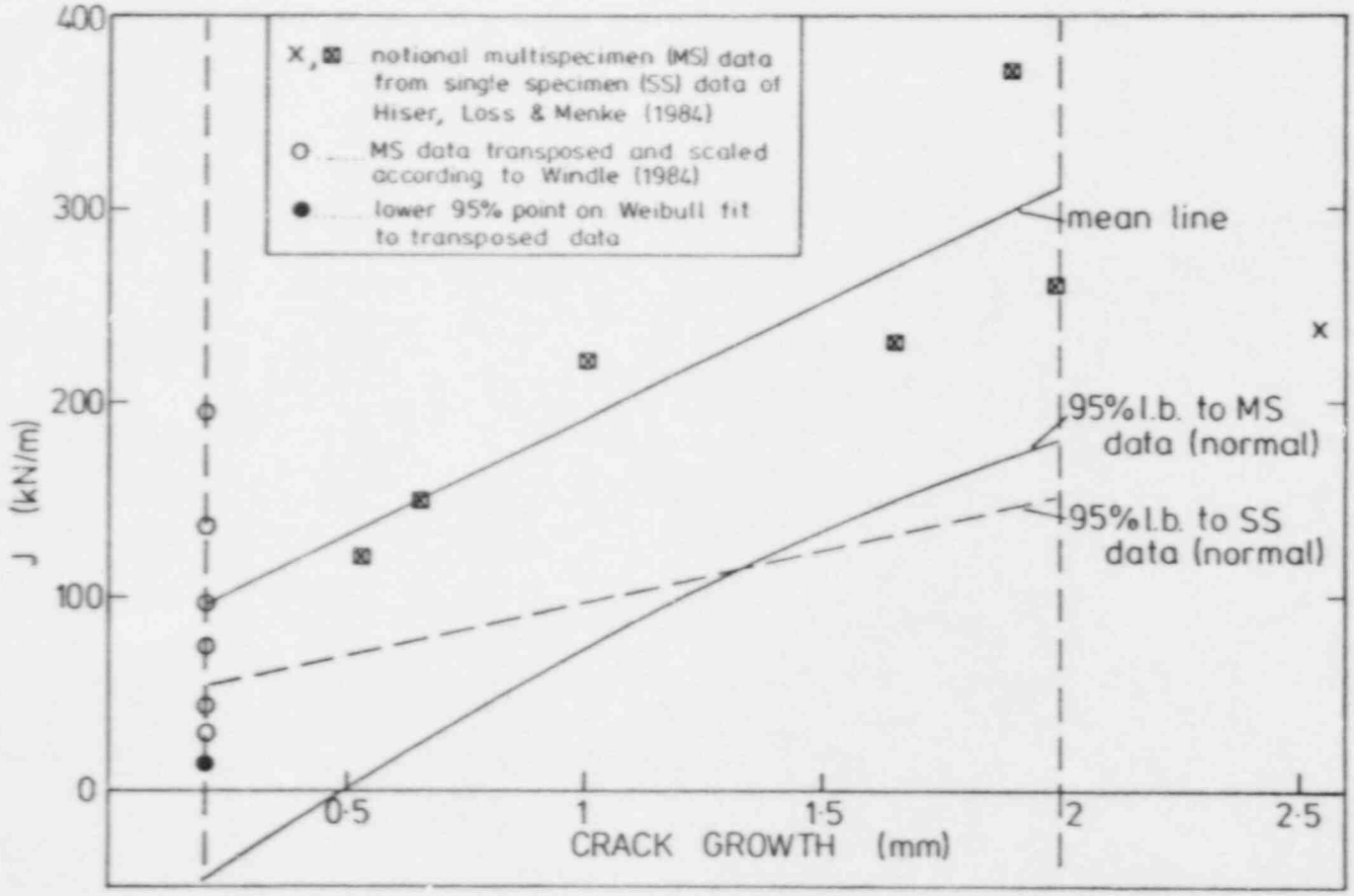

Fig. 12 An illustration of the difficulties in obtaining lower bounds from widely scattered multi-specimen data. Notional multispecimen data points were selectd randomly from the data in Fig. 11, and a 95% lower bound line calculated assuming uniform weighting and a normal distribution. The prediction of negative J values can be avoided by following the method of Windle (Ref. 6) which transposes and scales the data points and fits a two parameter Weibull distribution.

THE INTERPRETATION AND ANALYSIS OF SINGLE SPECIMEN AND MULTI-SPECIMEN J_R DATA

T Ingham, E Morland, G Wardle

UKAEA, RNL

(1) THE VALIDATION OF J_R CURVE DATA GENERATED BY SINGLE SPECIMEN TEST METHODS

Published procedures for interpreting J-Δa data derived using the unloading compliance method base their verification criteria upon agreement between predicted and measured values of absolute initial crack length and final crack growth (Refs 1,2). Under certain circumstances, sole use of these two criteria can lead to anomalous values of "initiation" toughness (Ref 3). Typical examples of situations where problems might arise are shown schematically in Figure 1. The need for additional verification was recognised by Futato et al (Ref 4) and a procedure has subsequently been derived at RNL which is intended to provide a more rigorous validation of J_R data. To date, the procedure has only been developed for and applied to the interpretation of J_R data for ferritic steels.

The procedure involves the two basic checks on initial and final crack length predictions plus three additional checks relating specifically to the initial portion of the J_R curve (the blunting region) and the shape of the J_R curve. The details of the procedure are summarised as follows:-

1) Initial Crack Length:

a_o predicted = a_o measured $\pm$ 3%. (i)

2) Crack Growth:

Δa predicted = Δa measured $\pm$ 15% or 0.3mm whichever is the smaller. (ii)

3) Level of J Associated With a_o:

The purpose of this check is to ensure that no crack growth has occurred at the J,a point defining a_o ie to guard against abnormally high J values arising from either negative crack growth effects or random error associated with the finite resolution in predicted crack length. It is assumed that, for ferritic steels, an upper bound to crack tip blunting is given by $J = 1.5\sigma_f \Delta a$ where $\sigma_f = \sigma_y + \sigma_u/2$. Measuring J values in MJ/m^2 and σ_f values in MPa, permissible J values which can be used to define a_o, are restricted to:-

$$J(a_o) \leq 1.5\ \sigma_f \times 0.15\text{mm} \quad \text{(iii)}$$

4) Crack Tip Blunting:

This test assesses whether the blunting characteristics are within acceptable bounds.

At least 3 data points are required within the crack growth range $0 \leq \Delta a \leq 0.15mm$. These data are used to define the value of J at $\Delta a = 0.1mm$ $(J_{0.1})$ and thence a "blunting coefficient"

$$m = J_{0.1}/0.1mm \times \sigma_f$$

The acceptance condition for ferritic steels is given by:-

$$1.5 \leq m \leq 3.5 \qquad \text{(iv)}$$

5) Shape of the J_R Curve:

Experience with ferritic steels suggests that a simple power law analysis will provide a satisfactory representation of resistance to crack growth. Accordingly, at least 7 J-Δa data points are required for a power law regression analysis on data where $\Delta a \geq 0.2mm$.

The condition for acceptance is:-

$$r^2 \geq 0.9 \qquad \text{(v)}$$

The restrictions on Δa ranges imposed by criteria iv) and v) ensure that no negative Δa data are included in the R curve definition. The procedure is applied iteratively starting with the first recorded J,a data point to define a_o. A predicted value of a_o can be used to construct a J_R curve only when the J-Δa data associated with this reference data point satisfy criteria (i) to (v). On re-defining a_o, all prior data are ignored ie J-values below Ja_o are not included in the analysis. More than one solution can be obtained from an unloading compliance test, therefore the most conservative J_R curve should usually be used when defining fracture toughness values.

The procedure, which is summarised in Figure 2, has proved to be especially useful when interpreting test results where "negative crack growth" was predicted during the initial part of the J_R curve. A schematic analysis is shown in Figure 3.

Typical examples of as computed and verified J_R data are shown in Figures 4-6. The "negative crack growth" seen in Figure 4 was attributable to lack of care in specimen alignment prior to testing. The "maximum" and "minimum" solutions (Figures 5 and 6) were obtained by defining a_o as respectively, the first or minimum value of a which satisfied criteria (i) to (v). There is little difference between these bounding values, most results falling between the 90% confidence limits to the multi-specimen data.

"Initiation" toughness is far more sensitive to the definition of a_o than resistance to crack growth and comparison of estimates of the former provide a more stringent check on the adequacy of the procedure. The results shown in Figuress 4-6 are part of a larger data base involving 30 separate unloading compliance tests. Taking "initiation" as the value of J at 0.2mm crack growth, $J_{0.2}$, the data base produced 45 $J_{0.2}$ solutions. All of the solutions were within the 95% confidence limits to multi-specimen data and 38 solutions were within the 90% confidence limits. Of the seven solutions between the 90% and 95% confidence limits, three were over-estimates and four were under-estimates.

The presence of negative crack growth in unloading compliance data is generally indicative of poor experimental procedure. It does not however, necessarily preclude the use of some of the J-Δa data (usually after a redefinition of a_o), for subsequent R curve construction, eg ref (2). Additionally, the absence of negative crack growth does not, in itself, ensure valid R curve data. In either case, the eventual J-Δa data which are used to construct an R curve must be rigorously examined. The procedure presented above, is designed to perform this function and screen against the interpretation of "low quality" data. Since the method has been developed for ferritic steels the precise limits that have been set for criteria (iii)-(v) will probably need to be amended to cover different materials and could be more rigorously formalised. It is suggested that inclusion of additional criteria of the type described will provide a more rigorous, test-system independent interpretation of unloading compliance data.

(2) SPECIMEN SIZE EFFECTS

A large number of multi-specimen tests on an A533B-1 steel have been used to demonstrate no significant size effects on J_R when testing standard (W = 2B) compact specimens of thickness 10 to 100mm(5). Further tests on compact and bend specimens within the thickness range 10 to 20mm have been made to provide additional data on specimen sizes suitable for surveillance testing. Equivalence between multi-specimen data from 20mm thick standard (W = 2B) bend and compact specimens is shown in Figure 7. Results for all 20-25% side-grooved specimens tested at ambient temperature are shown in Figure 8. (The J-Δa data points lying close to or below the ~95% confidence limit to all data were obtained from 12.5mm-15mm thick compact specimens and Charpy sized specimens which were extracted from plate mid-thickness). The data-base suggests that for these specimen geometries the size requirements for providing "valid" J_R data for A533B-1 steel could be relaxed considerably. For example, providing shear lip formation is minimised by side-grooving, J-Δa data from small specimens can be realistically taken for up to 20% of the ligament without influencing the J_R curve. Indeed, equivalence between small scale Charpy sized bend specimens and large specimen J-Δa data was obtained for crack growths of approximately 40% of the ligament of the Charpy-sized specimen. Figure 9 compares unloading compliance data from these Charpy size specimens with the 95% confidence limits to data for compact specimens.

Values of initiation toughness, defined as $J_{0.2}$, and tearing moduli at 1.0mm and 2.0mm crack growth from power law analyses for each specimen size are compared in Figure 10. Within experimental limits, the 20-25% side-grooved specimens provide size independent J_R data for all thicknesses examined. Thus, specimens which would be considered useful for surveillance purposes (typically B = 10 or 12.5mm) should provide meaningful J_R data for A533B-1 (and similar) steel, even though the size requirements for J-controlled growth are grossly violated.

All of the J_R data shown in Figs 8-10 were defined using the expression:

$$J = Jo \left(1 - \frac{\left[0.75f \left({}^{a}o/W \right) - 1 \right] \Delta a}{b_o} \right)$$

Unloading compliance data for the Charpy-sized specimens were obtained using experimentally derived relationships between load-line displacement corrected for extraneous displacements (Δ_{corr}) and the knife-edge

displacement (Vg) measured from an initial opening of 4mm, using a conventional clip gauge located at a knife-edge height of 2.5mm from the front face.

$$\Delta_{corr} = a + m\ Vg \ : \ a \to 0.$$

Values of m which were determined at both 20°C and 288°C for 20% side-grooved specimens are m = 0.96 for a/W = 0.5 and m = 0.94 for a/W = 0.6.

Compliance values were then determined using:

$$C(a/W) = E\ Be \left(\frac{m\ Vg}{P}\right)$$

$$\text{where } C(a/W) = \sum_{i=o}^{5} Ai\ C\ (a/W)^i$$

$$A_o = 0.072,\ A_1 = 1.251 \times 10^{-2},\ A_2 = -1.103 \times 10^{-4}$$

$$A_3 = 5.281 \times 10^{-7},\ A_4 = -1.266 \times 10^{-9},\ A_5 = 1.189 \times 10^{-12}$$

$$\text{and}\quad Be = B - \left[\frac{(B-BN)^2}{B}\right]$$

References

1. Albrecht P, Andrews W R, Gudas J P, Joyce J A, Loss F J, McCabe D E, Schmidt D W and Van der Sluys W A. "Tentative test procedures for determining the plane strain J_{I-R} curve". Jnl of Testing and Evaluation Vol 10, No 6, Nov 1982.

2. Neale B K, Curry D A, Green G, Haigh J R and Akhurst K N. "A procedure for the determination of the fracture resistance of ductile steels". CEGB Report TPRD/B/0495/R84.

3. Morland E and Ingham T "The influence on initiation toughness and J-R of variability in initial crack length prediction from unloading compliance measurements" Proceedings of a CSNI workshop on ductile fracture test methods, OECD Paris, 1983, pp 199-205.

4. Futato et al. "A sensitivity study of the unloading compliance single specimen J-test technique" Presented at ASTM symposium on Users Experience with Elastic Plastic Fracture Toughness Test Methods, Louisville, Kentucky, April 1983.

5. Ingham T, Bland J T and Wardle G. "Influence of specimen size on the upper shelf toughness of SA A533B-1 steel". Paper G2/3 7th Int Conf on Structural Mechanics in Reactor Technology, Chicago 1983.

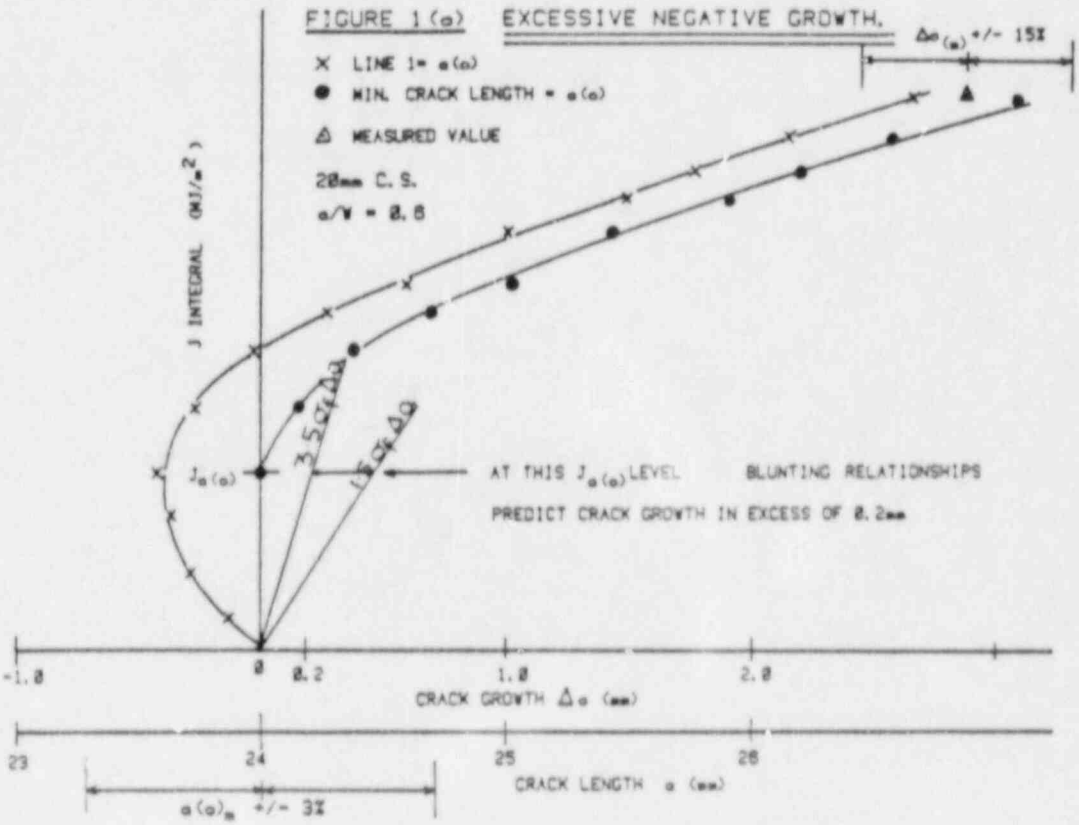

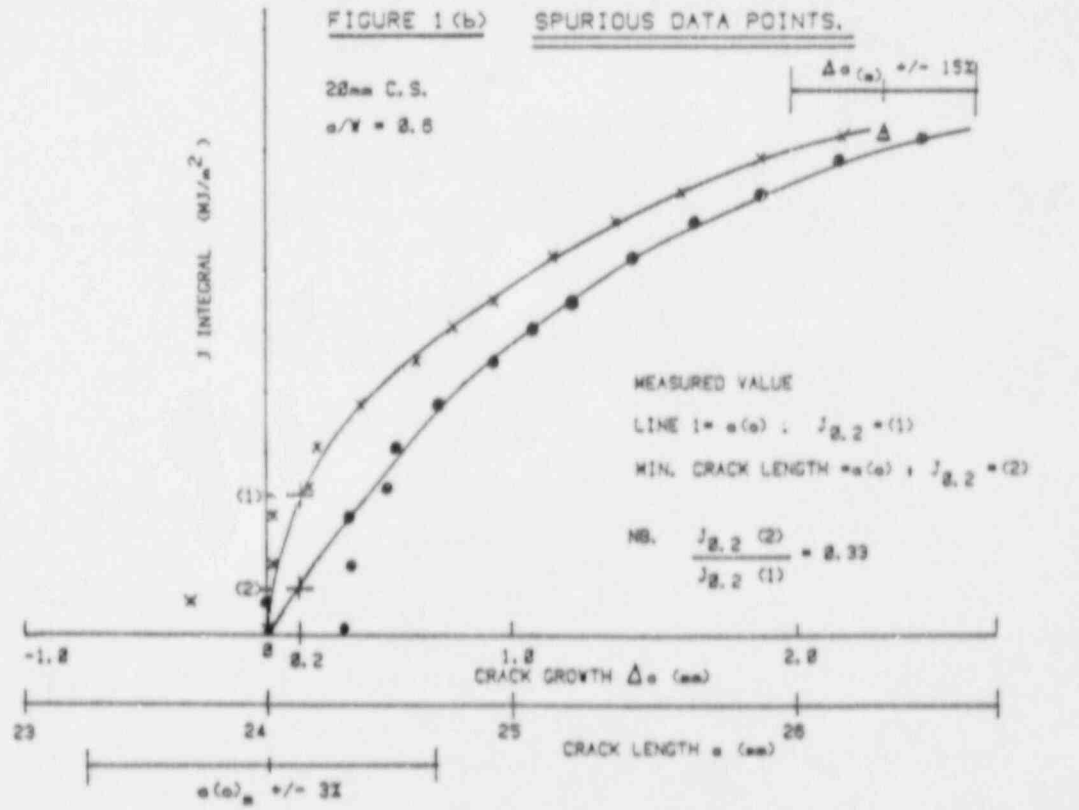

Fig.1 POTENTIAL DIFFICULTIES IN INTERPRETATION OF LOW QUALITY UNLOADING COMPLIANCE DATA.

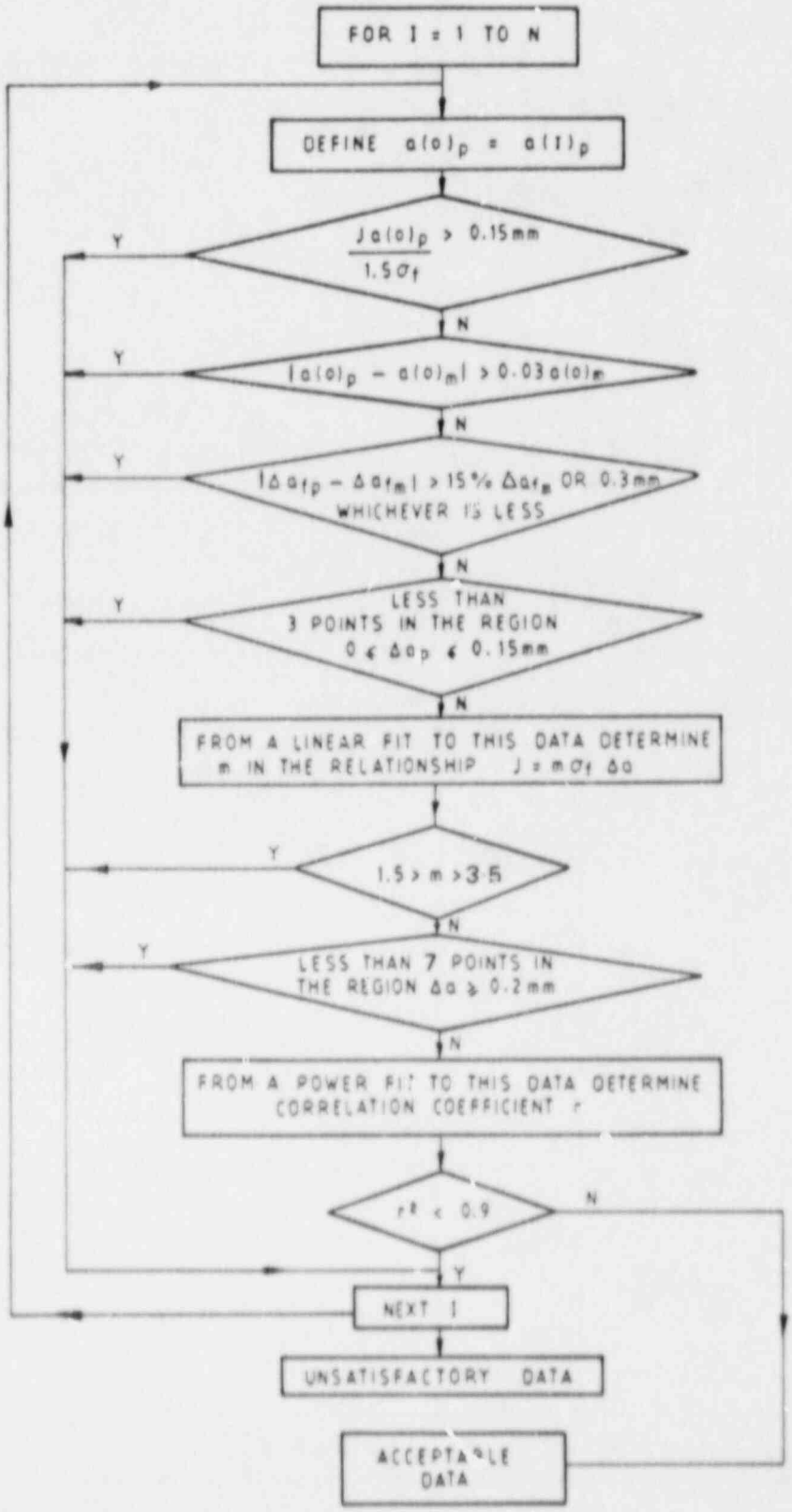

Fig 2 VALIDATION ALGORITHM FOR UNLOADING COMPLIANCE DATA

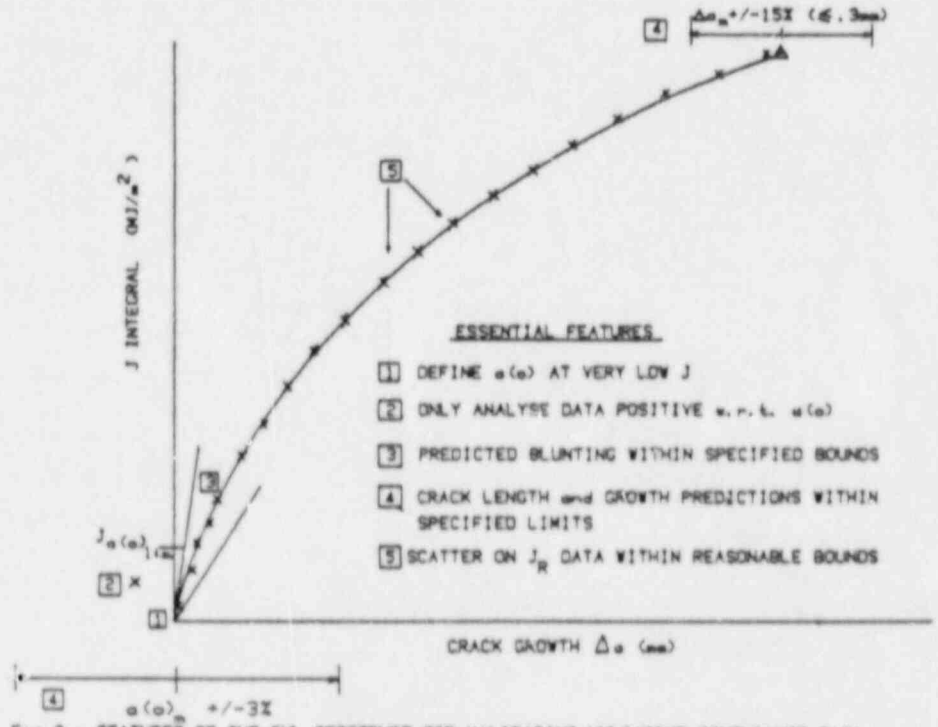

Fig. 3 : FEATURES OF THE RNE PROCEDURE FOR VALIDATING UNLOADING COMPLIANCE DATA.

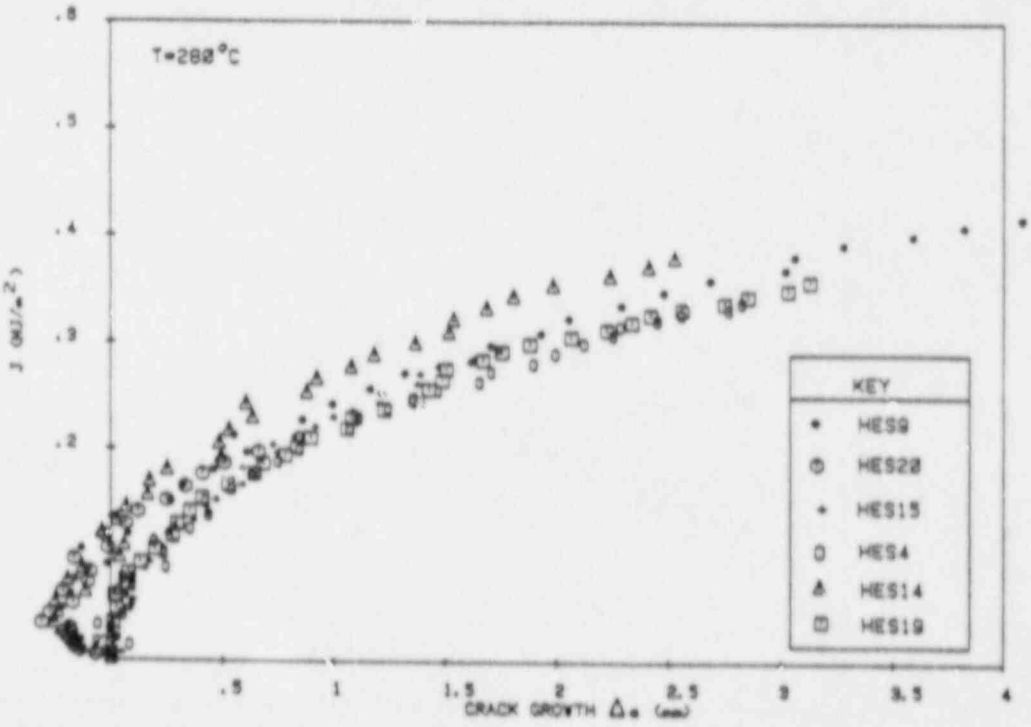

Fig. 4 ORIGINAL UNLOADING COMPLIANCE DATA FOR 25mm CS TESTS ON E/S WELD HEAT AFFECTED ZONE.

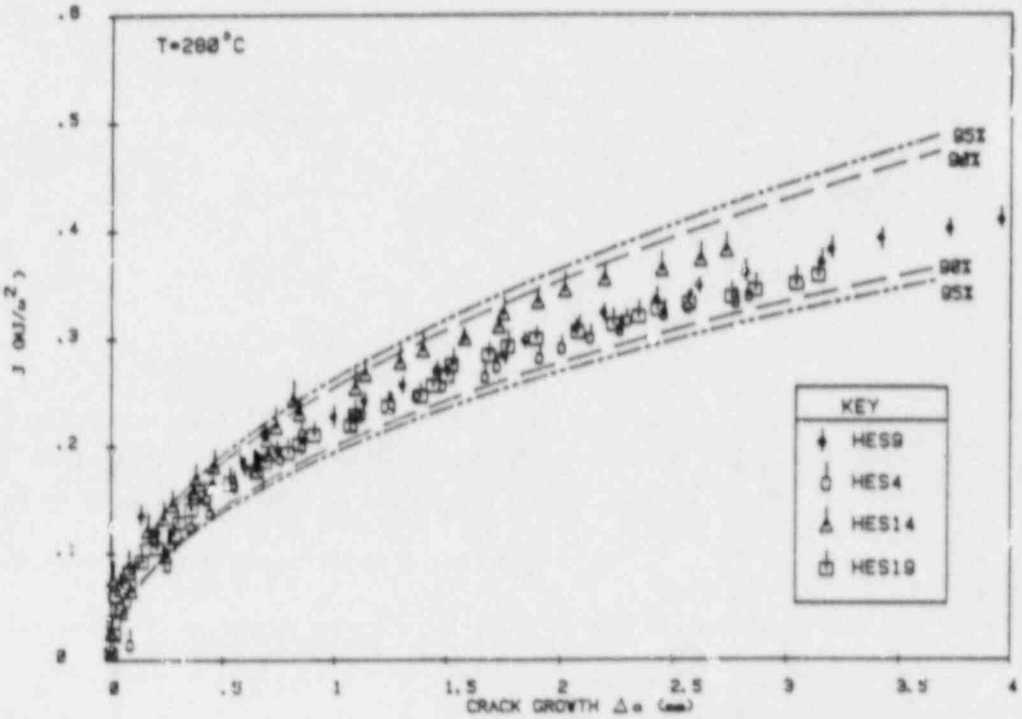

Fig 5. MAXIMUM ALGORITHM SOLUTIONS FOR E/S WELD H.A.Z. UNLOADING COMPLIANCE DATA COMPARED WITH MULTI-SPECIMEN CONFIDENCE LEVELS.

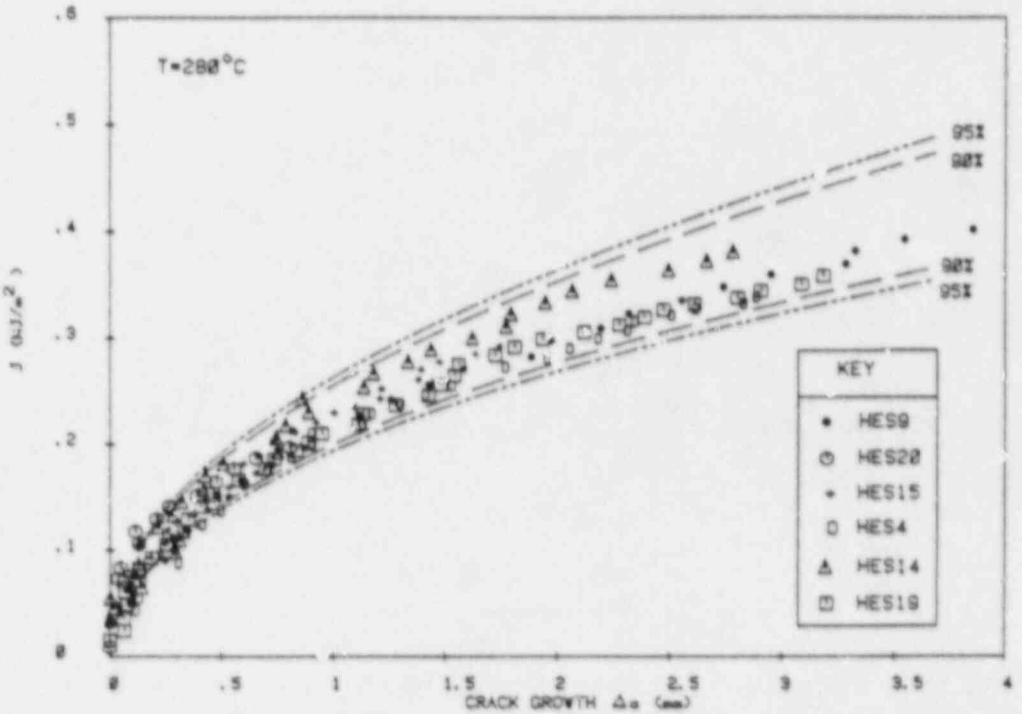

Fig 6. MINIMUM ALGORITHM SOLUTIONS FOR E/S WELD H.A.Z. UNLOADING COMPLIANCE DATA COMPARED WITH MULTI-SPECIMEN CONFIDENCE LEVELS.

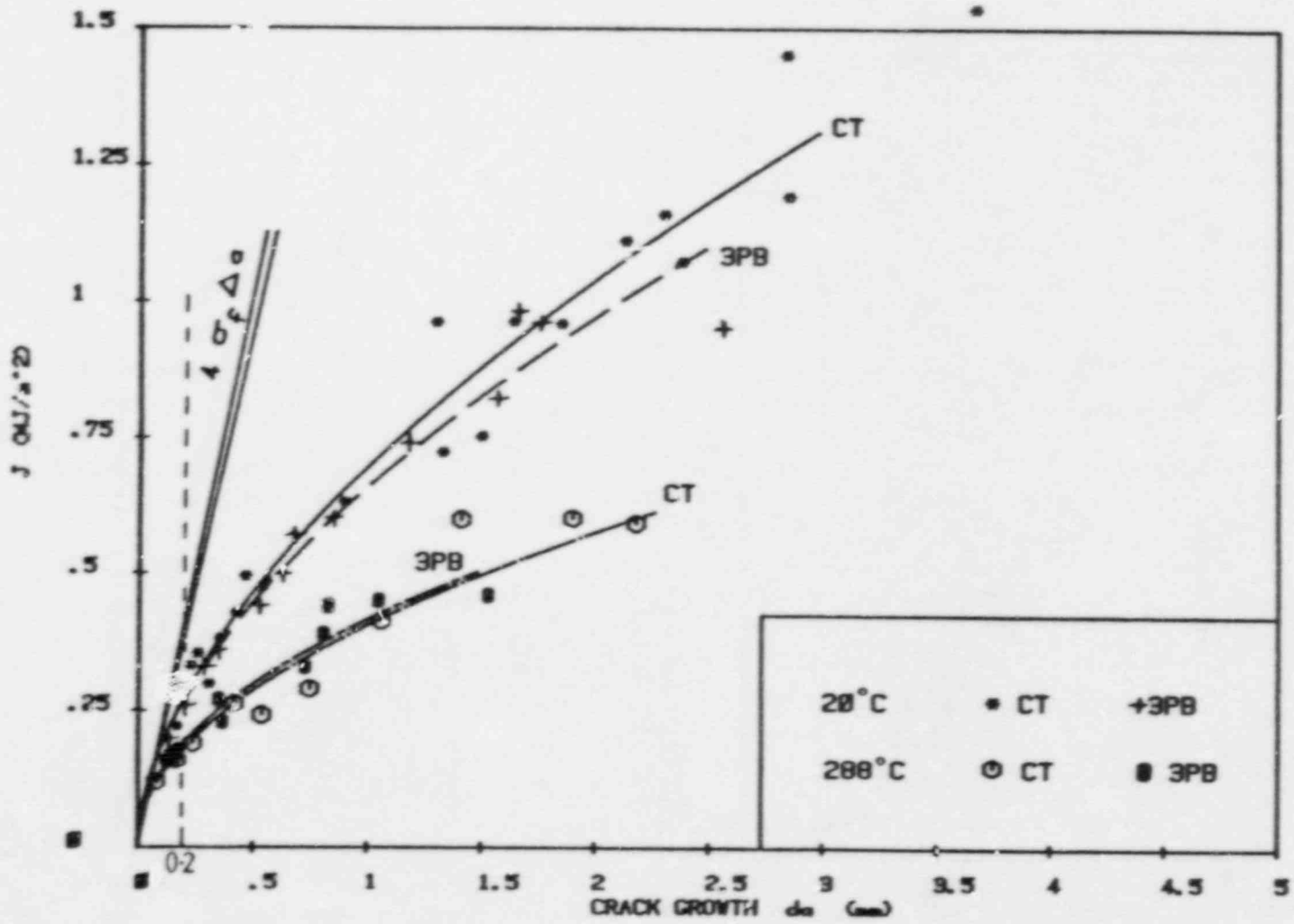

Fig 7. COMPARISON OF CT AND 3PB DATA FOR 20mm THICK NSG SPECIMENS (a/W = 0.6)

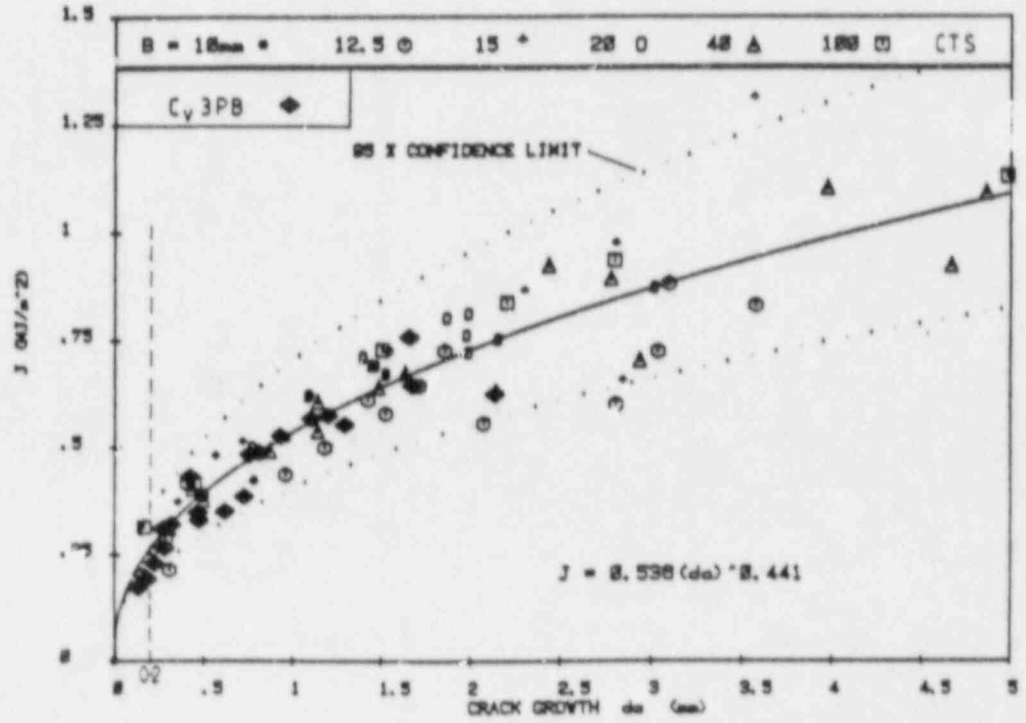

Fig.8 J- Δ a DATA FOR 20-25% SIDE GROOVED SPECIMENS, A533B-1, T=20 C.

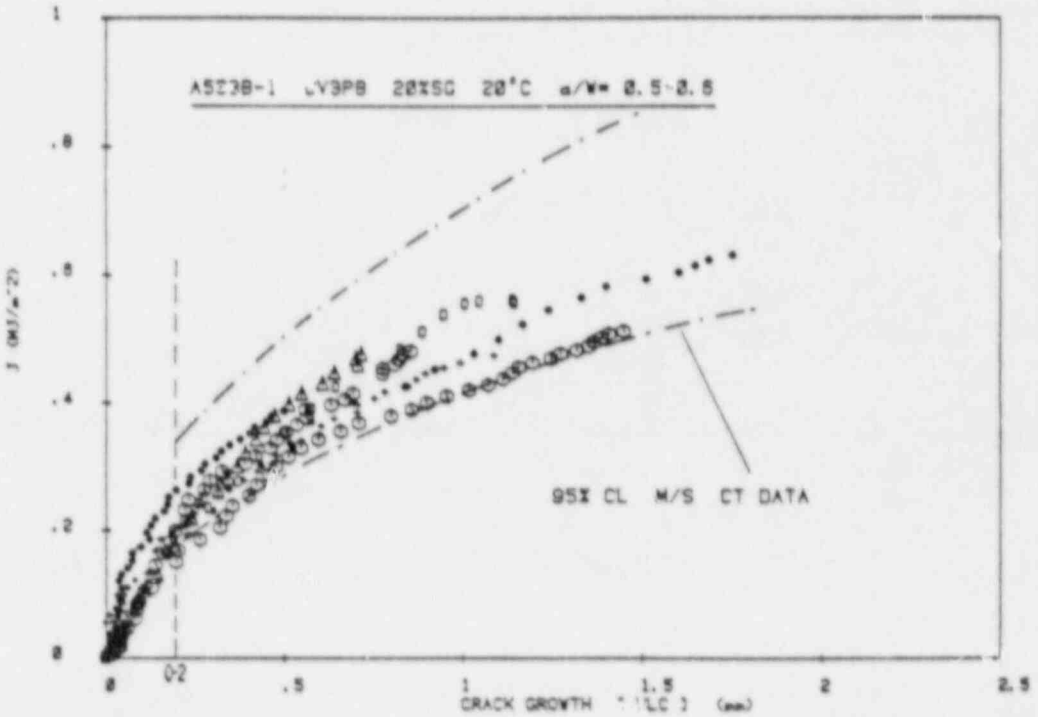

Fig.9 : COMPARISON OF UNLOADING COMPLIANCE DATA FROM CH, PY SIZED BEND SPECIMENS WITH MULTI-SPECIMEN SCATTER BAND FOR COMPACT SPECIMENS (B=10 - 100mm).

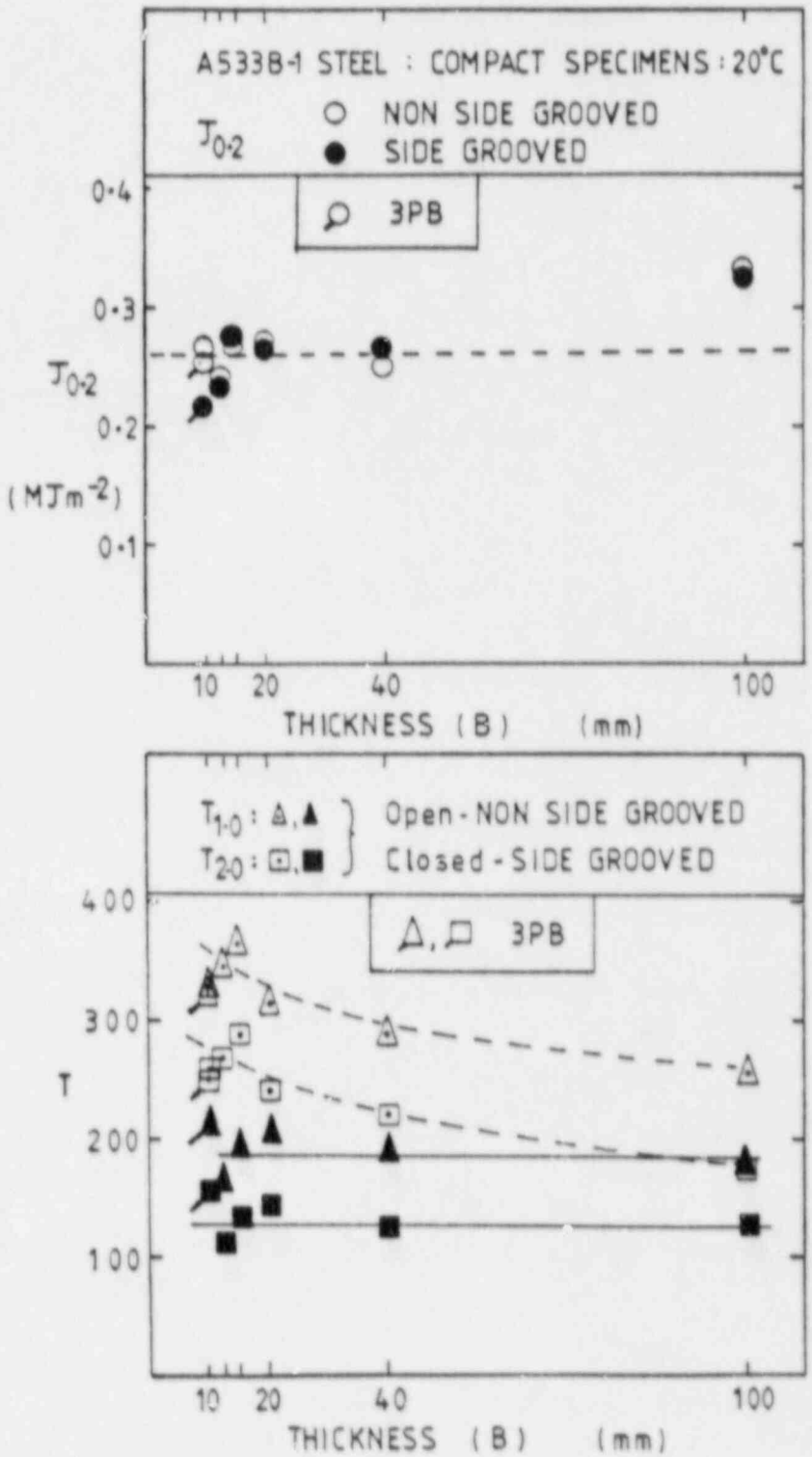

Fig. 18 : EFFECT OF THICKNESS ON $J_{0.2}$ AND TEARING MODULUS A533B-1 STEEL.

APPLICATION OF ELASTIC-PLASTIC FRACTURE TEST METHODS TO NUCLEAR PIPING MATERIALS

G. S. Kramer and G. M. Wilkowski

Battelle's Columbus Laboratories, Columbus, Ohio USA

INTRODUCTION

Over the past several years, Battelle has had great success in applying the direct current potential drop (dc-PD) technique to elastic-plastic fracture testing. While much of this work concentrated on small-scale laboratory specimens, numerous experiments have been conducted on full-scale piping and pressure-vessel components. Recently, Battelle has undertaken a multiyear research program to conduct elastic-plastic fracture experiments on degraded nuclear piping. Both laboratory and full-scale experiments are being conducted at 288 C (550 F). This paper describes the application of the dc-PD technique to several of these full-scale pipe-fracture experiments along with benefits and problems encountered.

ELASTIC-PLASTIC FRACTURE EXPERIMENTS USING dc-PD

Past experimental work has shown the dc-PD technique to be a fairly inexpensive and flexible method of determining crack initiation and crack growth in structures. It has been applied to fatigue cracks, stress corrosion cracks, dynamic crack growth, and elevated-temperature crack growth. The dc-PD method can account for crack tunneling and is an extremely sensitive method if used properly. The method also can be used in pipe-fracture experiments in which the compliance of the pipe changes due to ovalization as well as crack propagation.

Behavior of the dc-PD signal is similar in both laboratory and full-scale fracture experiments. Three distinct stages are observed if the dc-PD signal is plotted against the crack mouth opening displacement as in Figure 1. The first stage is a linear region that corresponds to plastic deformations that occur as the crack tip blunts. Deviation of the dc-DP record from this blunting line determines the point of crack initiation. This has been documented by comparing crack mouth opening versus dc-PD results to multiple specimen testing[1-3] and unloading compliance data[3]. The second stage corresponds to a nonlinear region that is due to crack tunneling in through-wall cracked specimens. The third and final stage corresponds to crack growth occurring with a constant crack-opening angle. This region usually occurs after maximum load has been reached.

TRANSITION FROM LABORATORY TO FULL-SCALE EXPERIMENTS

In general, basic data requirements are similar between laboratory and full-scale pipe-fracture experiments. Load, load-line displacement, and crack growth are the most important parameters. The dc-PD method can

be used to detect crack initiation and propagation in both cases. This requires that the specimen be electrically isolated, that the dc-PD signal be stable, and that the dc-PD data be calibrated to crack growth.

There are also certain problems that are similar due to high-temperature testing. Some of these are:

- Determining a method of heating the specimen to elevated temperature
- Maintaining temperature of the specimen at a constant level
- Electrical noise and drift due to heating method
- Electrical isolation is more difficult
- Time element due to specimen heat-up and cool-down.

The elevated temperature also effects the resistivity of the specimen and, hence, the dc-PD. In addition, thermal electromotive force voltages can effect the dc-PD if the problem wires have a different composition from that of the specimen or if the probe junctions are at different temperatures. Fortunately, this temperature differential is usually negligible with larger specimens.

The greatest difference between laboratory and full-scale pipe-fracture experiments is complexity. In a full-scale environment, the complexity of the instrumentation is increased (more instrumentation, more data, more data storage), complexity of the test facility is increased (higher applied loads, larger displacement, larger energy releases), and complexity of the high-temperature equipment is increased (larger heating elements, more power requirements, longer heat-up times).

Often, the full-scale experiments are conducted outside in a field-like environment due to size or energy release considerations. Thus, natural environmental problems arise. One must contend with moisture and condensation and their effect on instrumentation. Ambient temperature, wind, and precipitation all cause delays and complications.

FULL-SCALE PIPE EXPERIMENTS WITH THROUGH-WALL CRACKS

From past experiments conducted on various diameter pipes at room temperature, a through-wall crack calibration curve has been constructed.[4] This is presented in Figure 2 and plots normalized dc-PD against normalized crack growth. This curve shows close agreement with the theoretical Johnson calibration curve for center-cracked panel tests.

The basic flaw geometry and instrumentation locations used in these full-scale pipe experiments are depicted in Figure 3. These are compared against those of the complex crack pipe experiments that will be described in the following section. Experiments with this flaw geometry were conducted at 288 C (550 F) under 4-point bending loads.

Figure 4 is a post-test photograph of a 711-mm (280-inch) diameter, 22-mm (0.875-inch) wall, through-wall crack pipe experiment. The overall specimen length of this carbon steel pipe was approximately 15.2 m (50 feet). In this experiment, the crack initiated and quickly turned at a 35- to 40-degree angle from the original crack plane. Figure 5 shows the fracture behavior at one of the crack tips. Figure 6 is a post-test photograph of similar crack-propagation behavior in a 102-mm (4-inch) diameter carbon steel pipe experiment and in a 1T compact tension specimen machined from the same pipe specimen.

The dc-PD technique was used in each of these experiments to measure crack initiation and growth. Figure 7 is a typical dc-PD versus crack-opening displacement record from the 102-mm (4-inch) diameter experiment showing data from potential drop probes at each crack tip. Clearly, in this experiment, crack initiation at each crack tip occurred at different points. Once initiation was determined using the probes at the crack tips, average crack propagation was determined using the centerline dc-PD probe.

Figure 8 presents the results of the load versus load-line displacement record from the 102-mm (4-inch) pipe experiment. Once past maximum load in the experiment, the specimen was unloaded several times in order to mark the extent of crack growth. Due to the out-of-plane behavior of the crack propagation, these unloading profile markings were quite useful. They were used to calibrate the dc-PD signal to the total out-of-plane crack extension. The crack growth also was projected back to the plane of the original crack for comparison purposes. These crack-growth results also are presented in Figure 8. Construction of a J-resistance curve from this experiment is continuing at this time.

FULL-SCALE PIPE EXPERIMENTS WITH COMPLEX CRACKS

As defined in this paper, a complex crack is one in which a long internal surface crack (up to 360 degrees) has propagated through the wall of the pipe at some point creating a short through-wall crack. The crack geometry for this type of specimen was shown in Figure 2. From past experimental work[5], we have seen that the constraint imposed on the propagating crack front by the existing internal surface crack greatly lowers the J-resistance curve. This is shown in Figure 9 for a Type 304 stainless steel pipe. Current experiments have been conducted on 152-mm (6-inch) diameter carbon steel, Type 304 stainless steel, and Inconel 600 pipe.

Crack initiation and propagation were again determined using the dc-PD technique. Unloading cycles also were used to mark crack growth once past maximum load. Figure 10 compares the load versus load-line displacement curves from the Type 304 stainless steel and carbon steel pipe experiments.

The effect of the unloading cycles on crack arrest and reinitiation was examined more closely in these experiments. It was found that the unloading cycles did not significantly lower the applied load at which the crack would reinitiate. This can be seen in Figure 11 which is a

blown-up portion of a test record from a Type 304 stainless steel pipe experiment. Reinitiation appears to occur once the load-line displacement has exceeded its previous maximum value at the unloading point.

Figure 12 is a post-test photograph of the fracture surface from the Type 304 stainless steel pipe experiment. Also evident are the crack front unloading marks along each side of the specimen. As seen in the photograph, crack propagation along the inside pipe surface greatly precedes crack propagation along the outside surface. Figure 13 details these unloading profiles and relates each to the corresponding total applied load at the unloadings. Crack-growth measurements were made using the inside surface, outside surface, and 9-point averages from each of the profiles. A continuous record of crack growth versus load-line displacement was then calculated by calibrating the centerline dc-PD data to the measured crack-growth data from the unloadings. This is presented in Figure 14 for the inside, outside, and average crack growth.

Based on the results of five complex crack-pipe experiments, a normalized dc-PD versus average crack-growth calibration curve was generated. This is presented in Figure 15 and is compared against the calibration curves previously presented in Figure 2. Although the complex crack pipe data fall somewhat below the first two curves, the overall agreement is quite good.

CONCLUSIONS

Successful results have been obtained using the dc-PD technique on both laboratory specimens and full-scale piping. In both cases, the general behavior of the dc-PD signal is quite similar.

In addition, the dc-PD technique has been quite useful in conducting full-scale nuclear pipe fracture experiments at 288 C (550 F). It has been successful in experiments where (1) crack initiation occurs at two crack tips, (2) the pipe specimen ovalizes, (3) crack propagation is out of plane, and (4) crack propagation is nonuniform through the thickness.

REFERENCES

(1) Lowes, J. M and Fearnehough, G. D., "The Detection of Slow Crack Growth in Crack Opening Displacement Specimens Using an Electrical Potential Method", Eng. Fract. Mech., Vol. 3, pp 103-108 (1971).

(2) Wilkowski, G. M., Wambaugh, J. D., and Prabhat, K., "Single Specimen J-Resistance Curve Evaluations Using the dc Electric Potential Method and a Computerized Data Acquisition System", Presented at Fracture Mechanics: Fifteenth National Symposium.

(3) Vassilaros, M. G. and Hacket, E. M., "J-Integral R-Curve Testing of High Strength Steels Utilizing the dc Potential Drop Method", Presented at the ASTM 15th National Symposium on Fracture Mechanics (July 8, 1982).

(4) Wilkowski, G. M. and Maxey, W. A., "Review and Application of the Electric Potential Method for Measuring Crack Growth in Specimens, Flawed Pipe and Pressure Vessels", Presented at the ASTM 14th National Symposium on Fracture Mechanics, Los Angeles, California (June 30-July 2, 1981).

(5) Kanninen, M. F., Zahoor, A., Wilkowski, G. M., Abou-Sayed, I., Marschall, C., Broek, D., Sampath, S., Rhee, C., and Ahmad, J., "Instability Predictions for Circumferentially Cracked Type 304 Stainless Steel Pipes Under Dynamic Loading", EPRI Report NP2347 on Project T118-2, April, 1982.

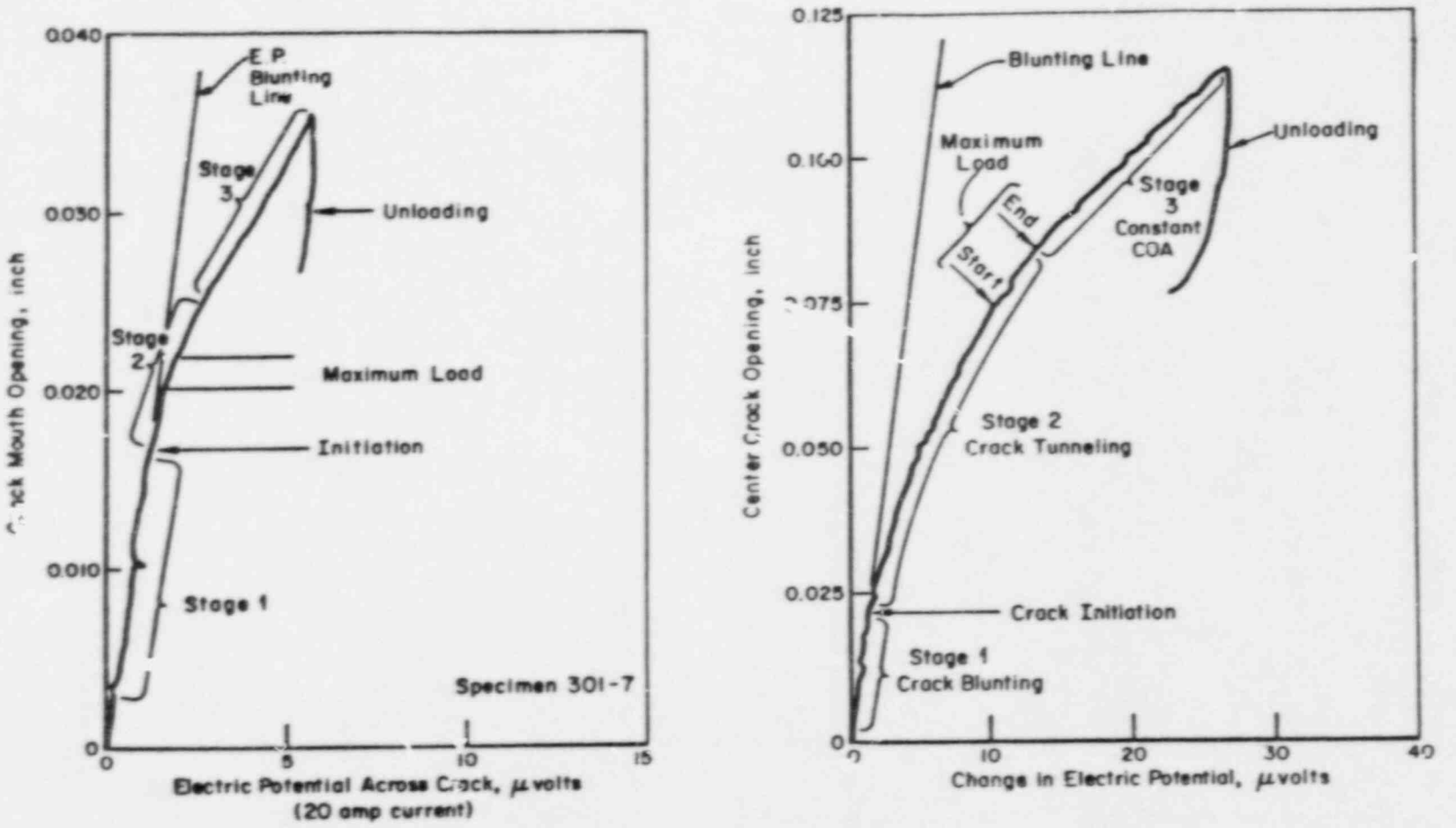

(a) Three Point Bend Bar Specimen

(b) Circumferential Through-Wall Cracked Pipe in Bending

FIGURE 1. COMPARISON OF DCPD DATA FROM CARBON-STEEL THREE-POINT BEND SPECIMEN AND CIRCUMFERENTIAL THROUGH-WALL-CRACK PIPE-BEND EXPERIMENT

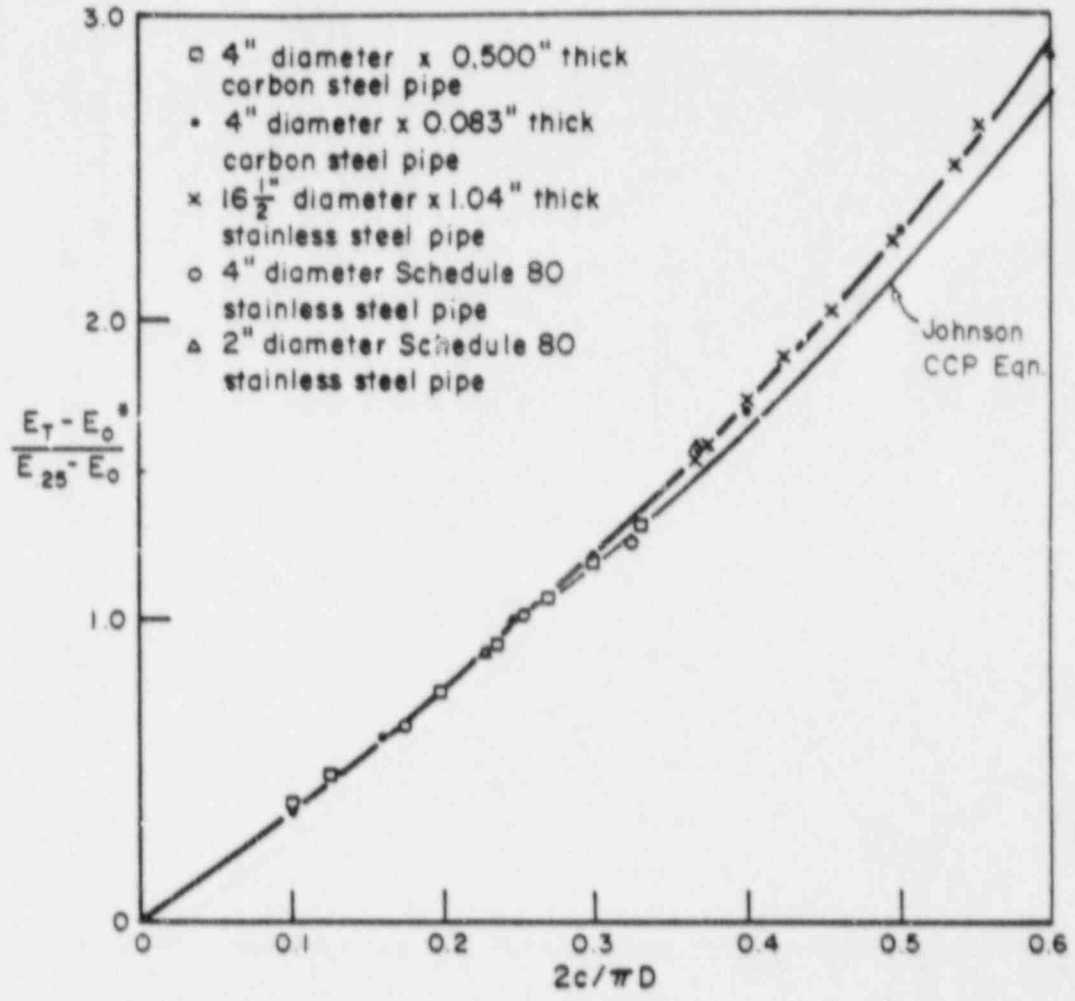

FIGURE 2. COMPARISON OF CALIBRATION CURVES FROM JOHNSON CENTER CRACKED PANEL EQUATION AND THROUGH-WALL CRACKED PIPE EXPERIMENT DATA

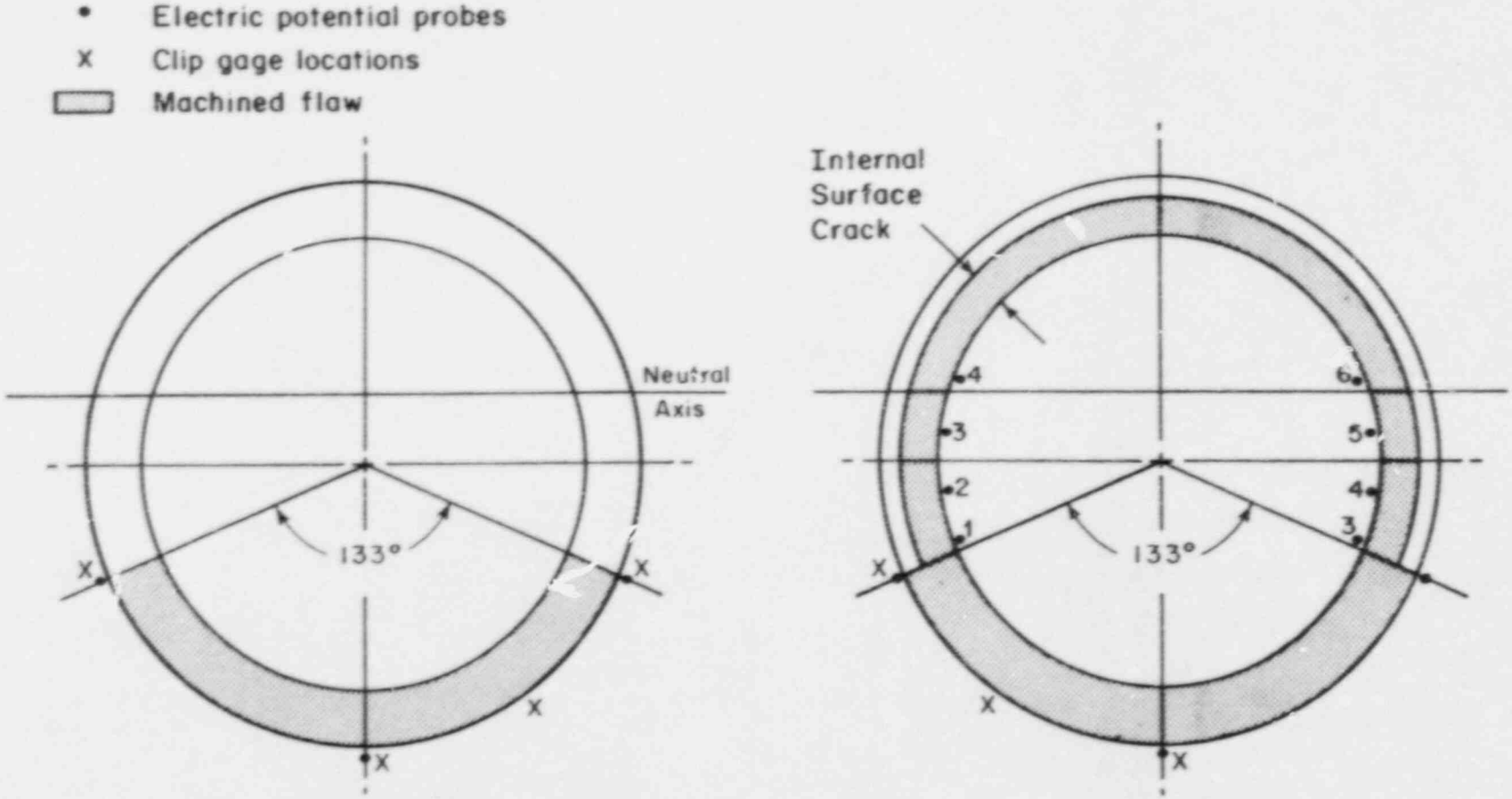

FIGURE 3. COMPARISON OF BASIC FLAW GEOMETRIES AND INSTRUMENTATION LOCATIONS IN THROUGH-WALL CRACK AND COMPLEX CRACKED PIPE-BEND EXPERIMENTS

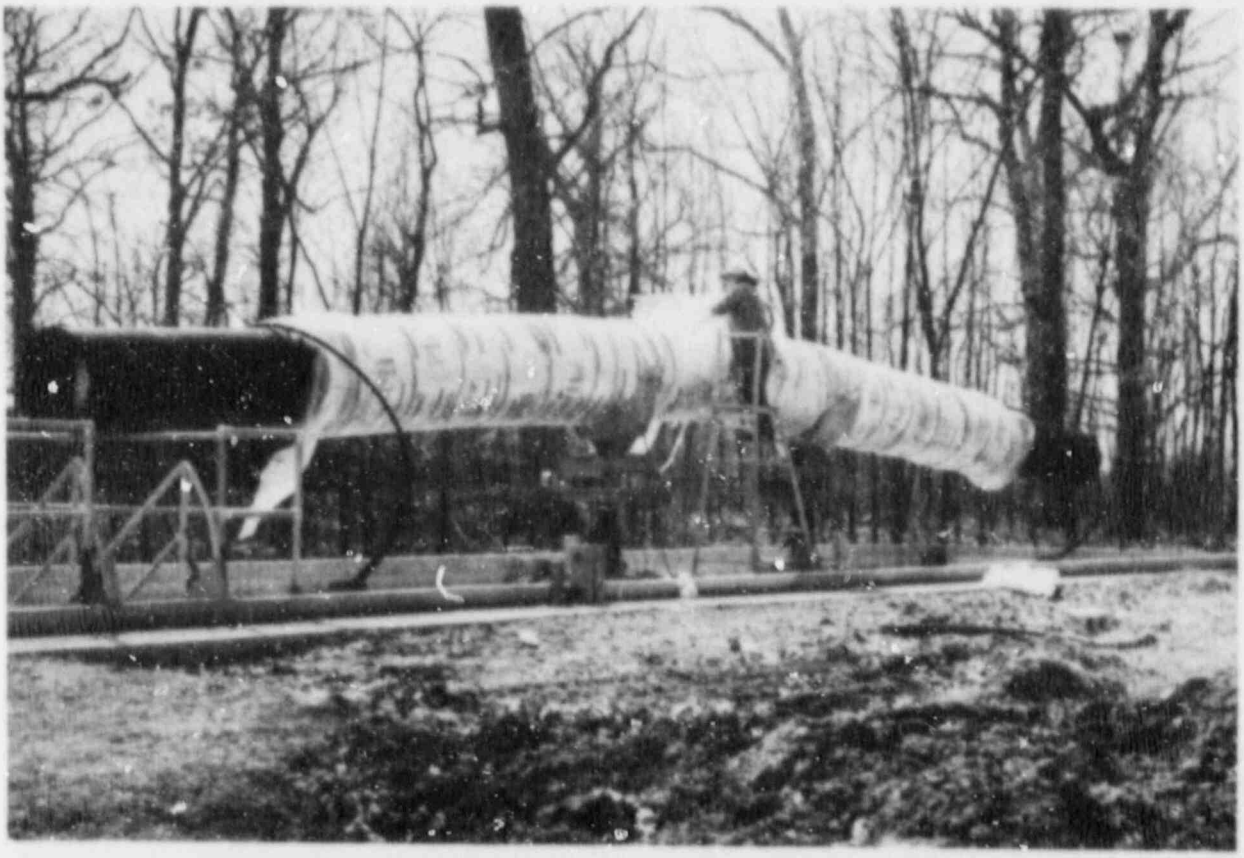

FIGURE 4. POST-TEST RESULTS OF 711 MM (28 INCH) DIAMETER PIPE-BEND EXPERIMENT CONDUCTED AT 288 C (550 F). THIS CARBON-STEEL PIPE SPECIMEN CONTAINED A THROUGH-WALL CRACK 37 PERCENT OF THE CIRCUMFERENCE.

FIGURE 5. CLOSE-UP OF FRACTURE PROPAGATION AT ONE CRACK TIP IN 711 MM (28 INCH) DIAMETER PIPE-BEND EXPERIMENT

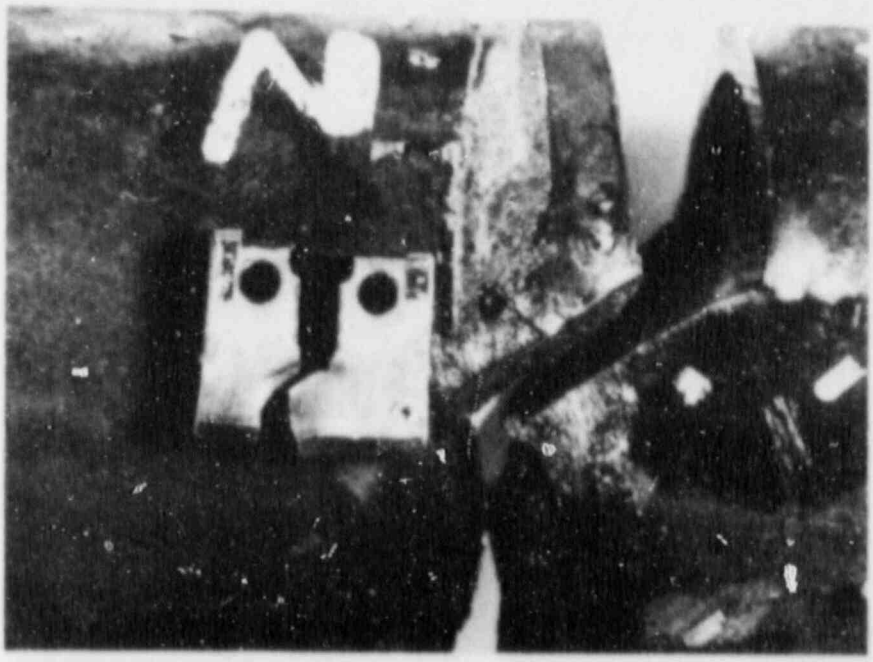

FIGURE 6. COMPARISON OF CRACK GROWTH IN A 102 MM (4 INCH) DIAMETER CARBON-STEEL PIPE WITH A CT SPECIMEN MACHINED FROM THE PIPE SPECIMEN (UNFLATTENED)

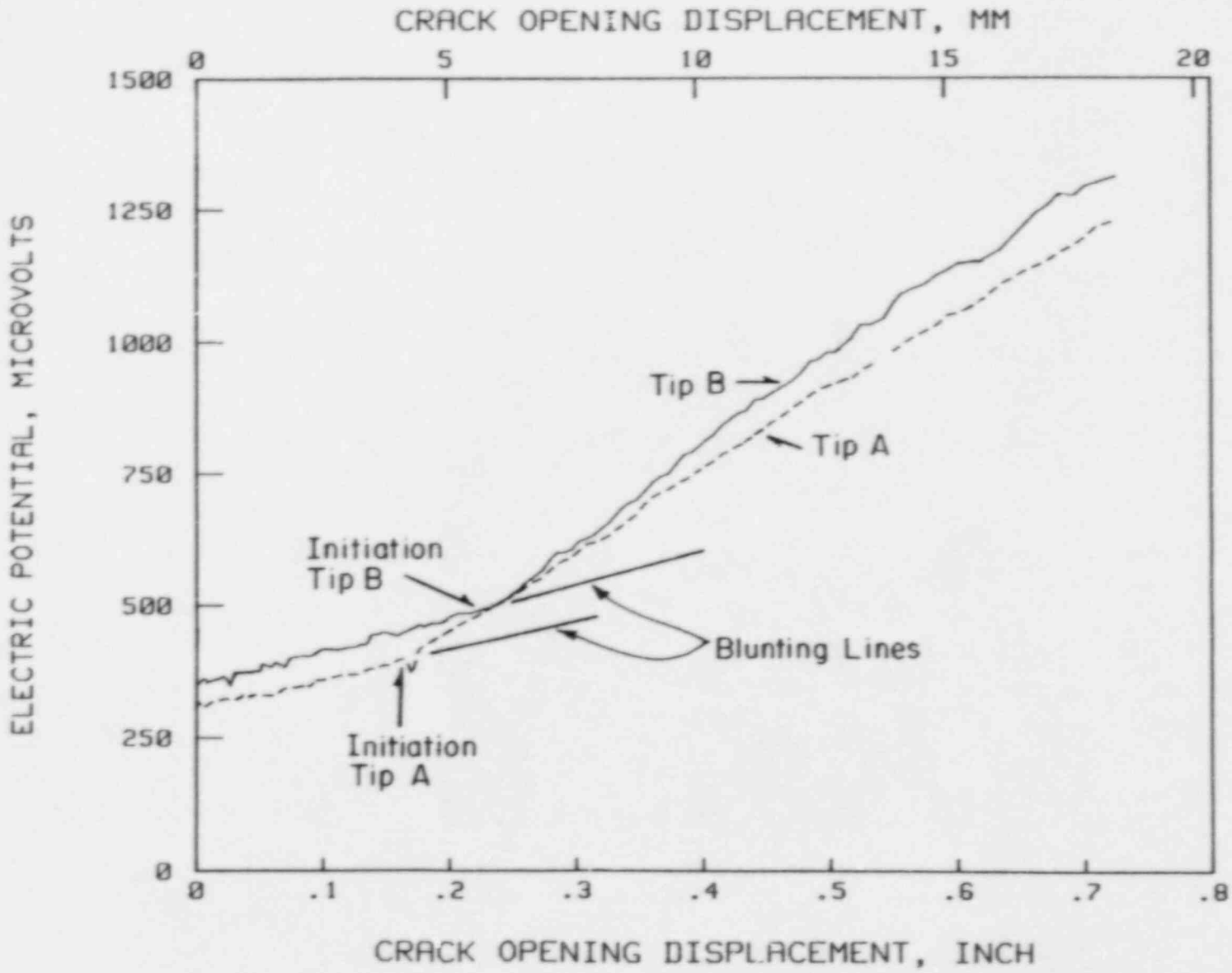

FIGURE 7. COMPARISON OF CRACK INITIATION FOR EACH CRACK TIP FROM 102-MM (4-INCH) DIAMETER THROUGH-WALL CRACK PIPE-BEND EXPERIMENT

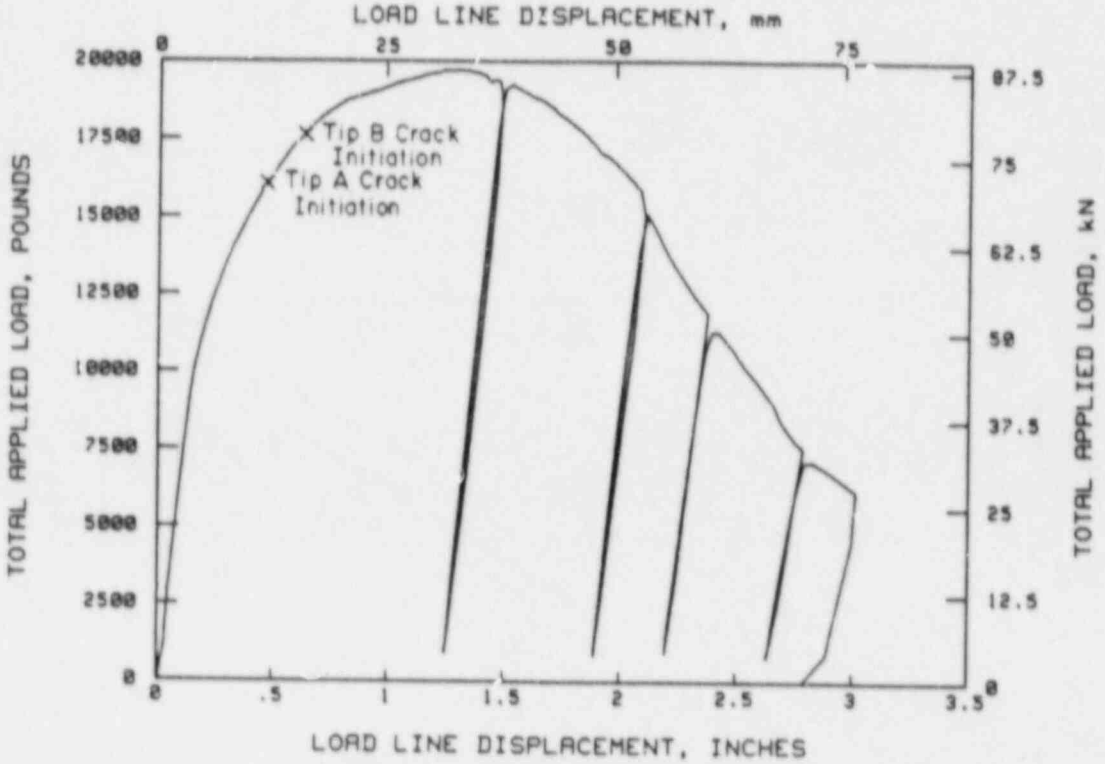

a. Load versus load-line displacement record

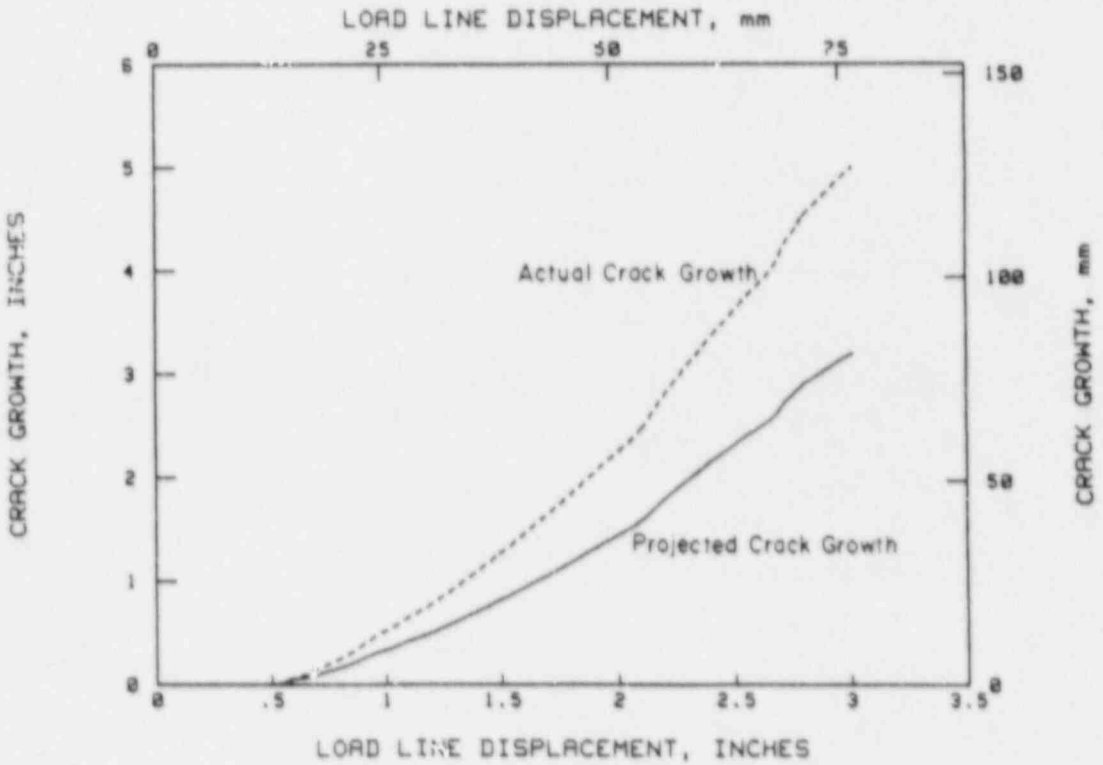

b. Crack growth generated from dc-PD data and unloading profiles

FIGURE 8. RESULTS OF 102-MM (4-INCH) DIAMETER THROUGH-WALL CRACK PIPE EXPERIMENT SHOWING UNLOADING CYCLES AND ACTUAL AND PROJECTED CRACK-GROWTH DATA

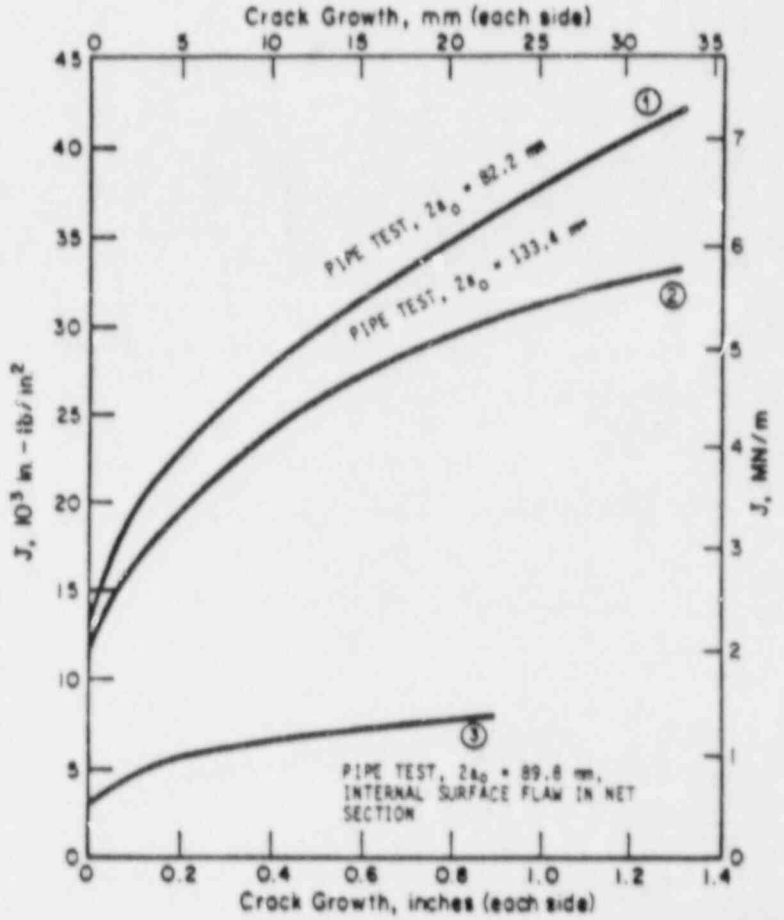

FIGURE 9. COMPARISON OF J-RESISTANCE CURVES FROM THROUGH-WALL CRACK PIPE EXPERIMENTS (CURVES 1 AND 2) WITH COMPLEX CRACK PIPE EXPERIMENT (CURVE 3) CONDUCTED UNDER FOUR-POINT BENDING

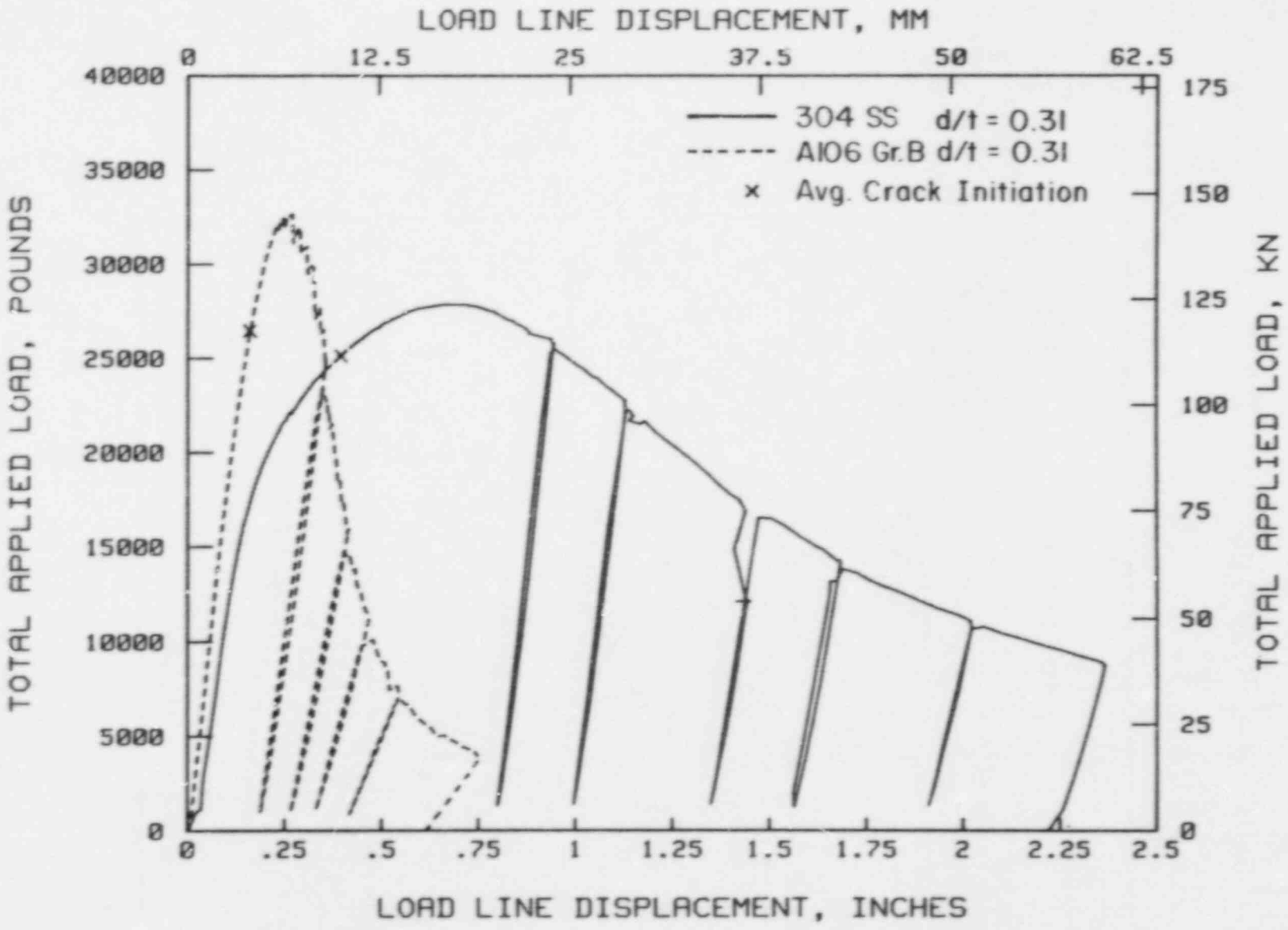

FIGURE 10. COMPARISON OF LOAD VERSUS LOAD-LINE DISPLACEMENT RECORDS FROM TWO COMPLEX CRACK PIPE EXPERIMENTS CONDUCTED AT 288 C (550 F)

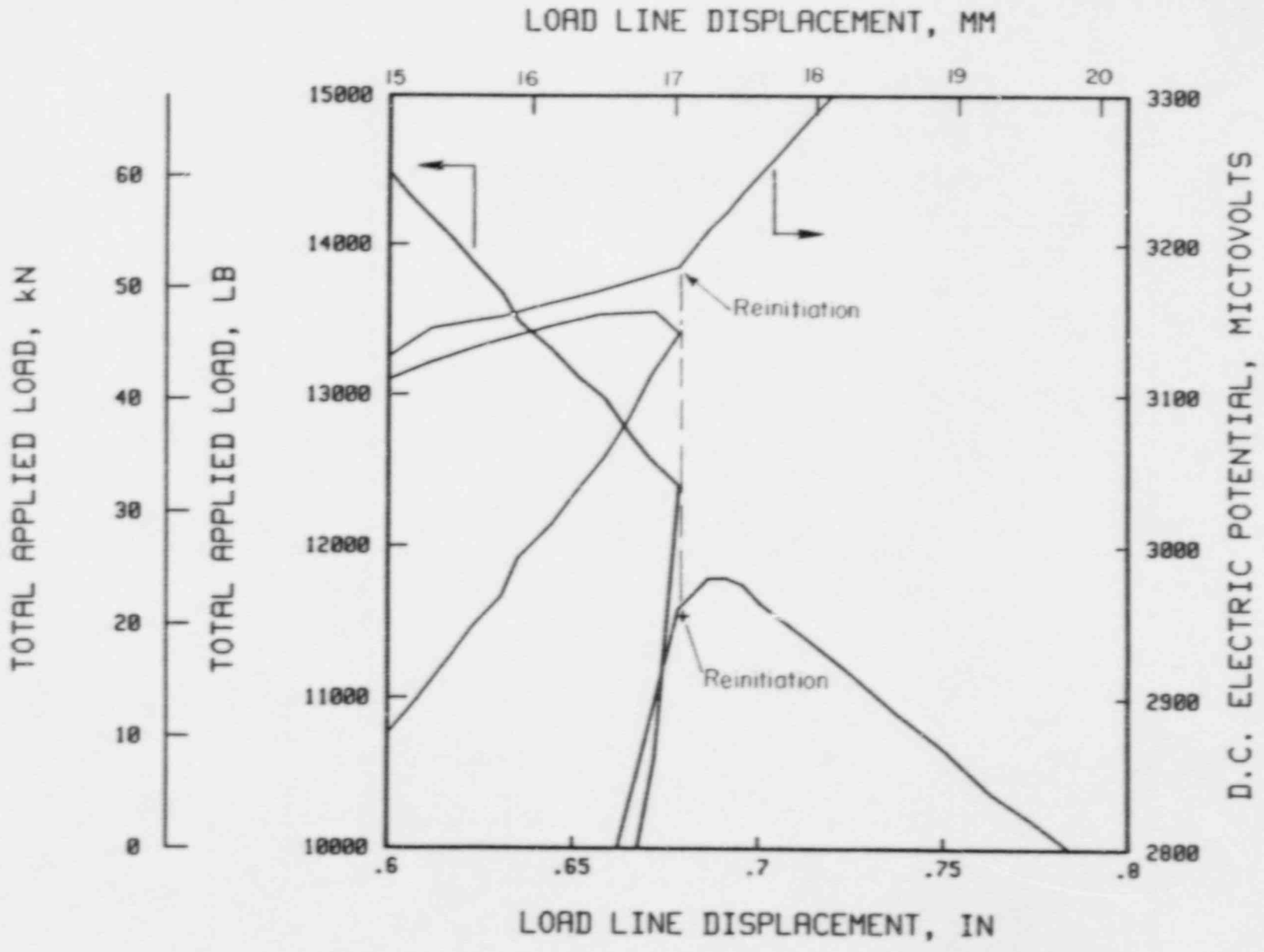

FIGURE 11. EFFECTS OF UNLOADING-RELOADING CYCLES ON CRACK REINITIATION IN A TYPE 304 STAINLESS STEEL COMPLEX CRACKED PIPE EXPERIMENT

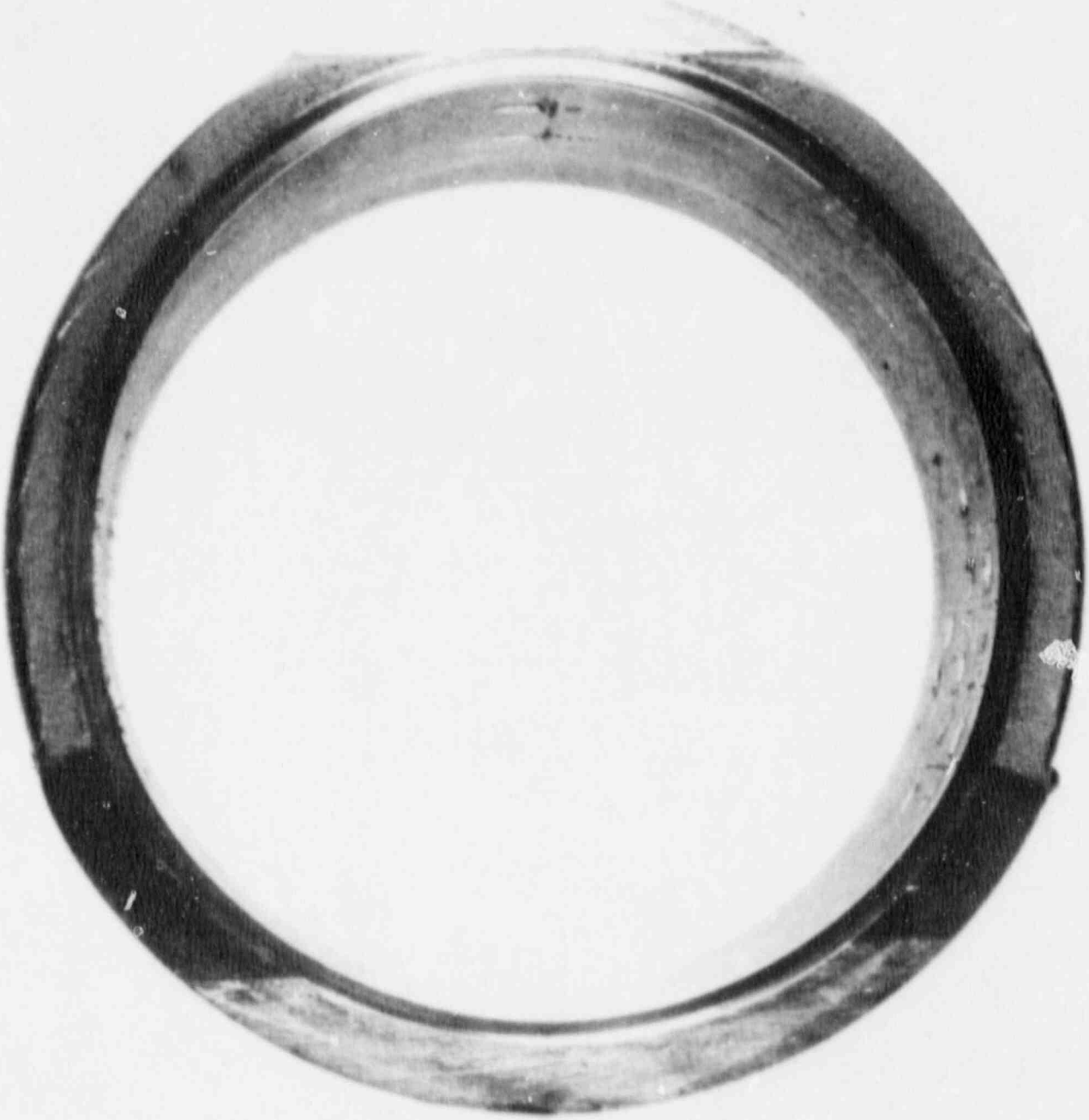

FIGURE 12. FRACTURE SURFACE FROM A TYPE 304 STAINLESS STEEL COMPLEX CRACK PIPE EXPERIMENT SHOWING INITIAL FLAW GEOMETRY AND UNLOADING CRACK MARKS

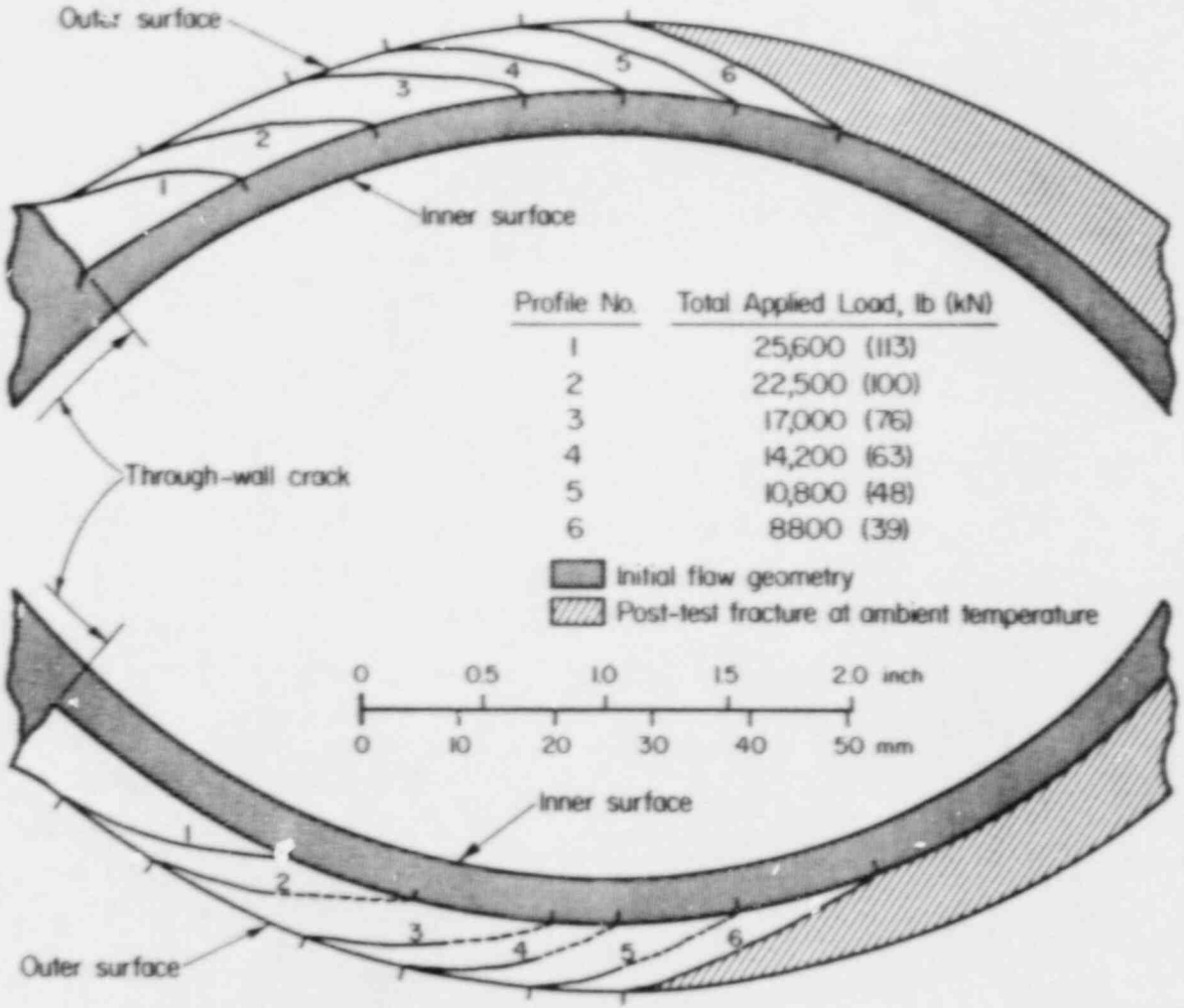

FIGURE 13. DETAILS OF CRACK PROFILES OBSERVED FROM THE PIPE FRACTURE SURFACE SHOWN IN FIGURE 12

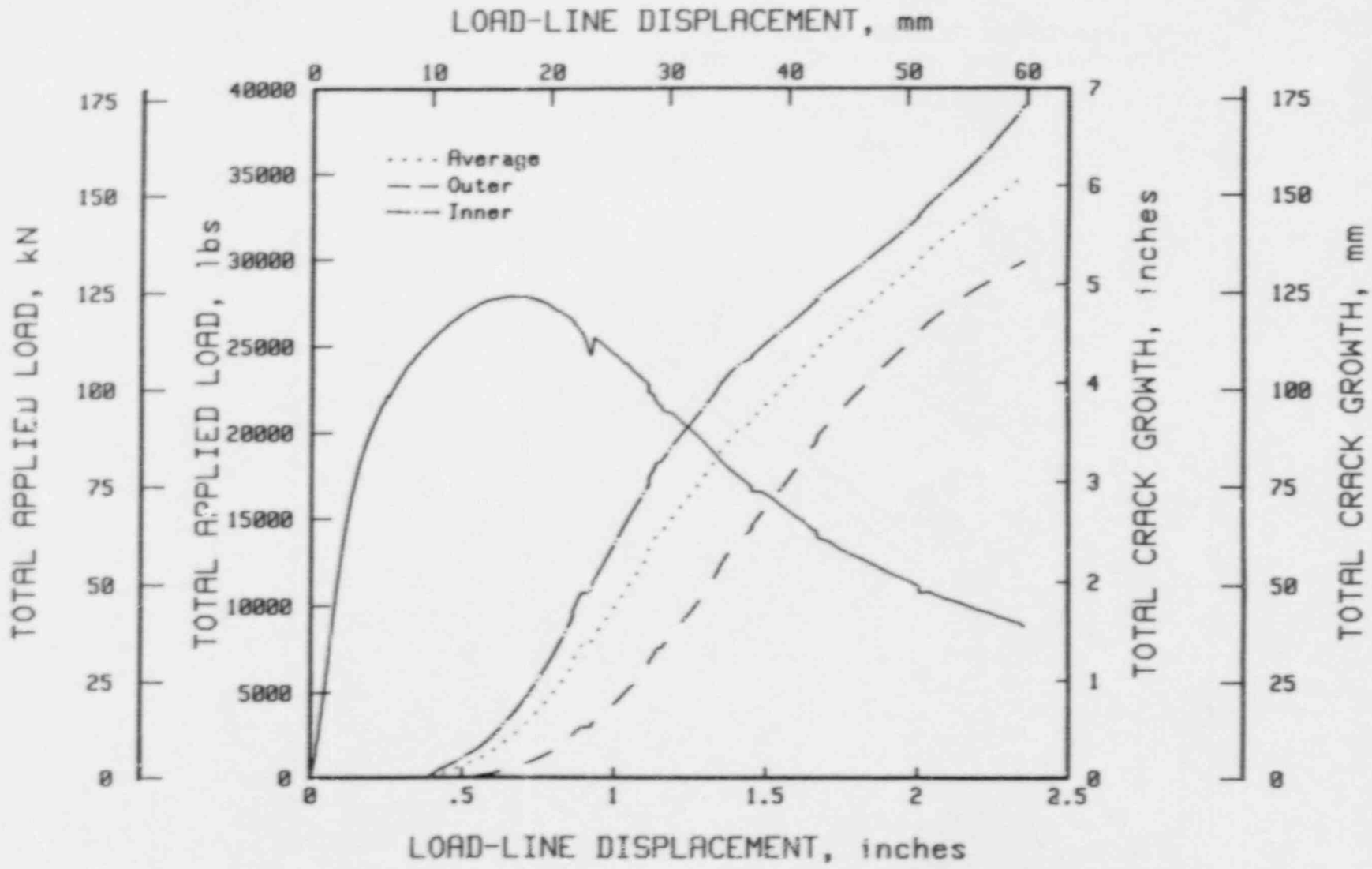

FIGURE 14. COMPARISON OF CRACK-GROWTH DATA IN TYPE 304 STAINLESS STEEL PIPE EXPERIMENT ON THE INNER SURFACE, OUTER SURFACE, AND 9 POINT AVERAGE

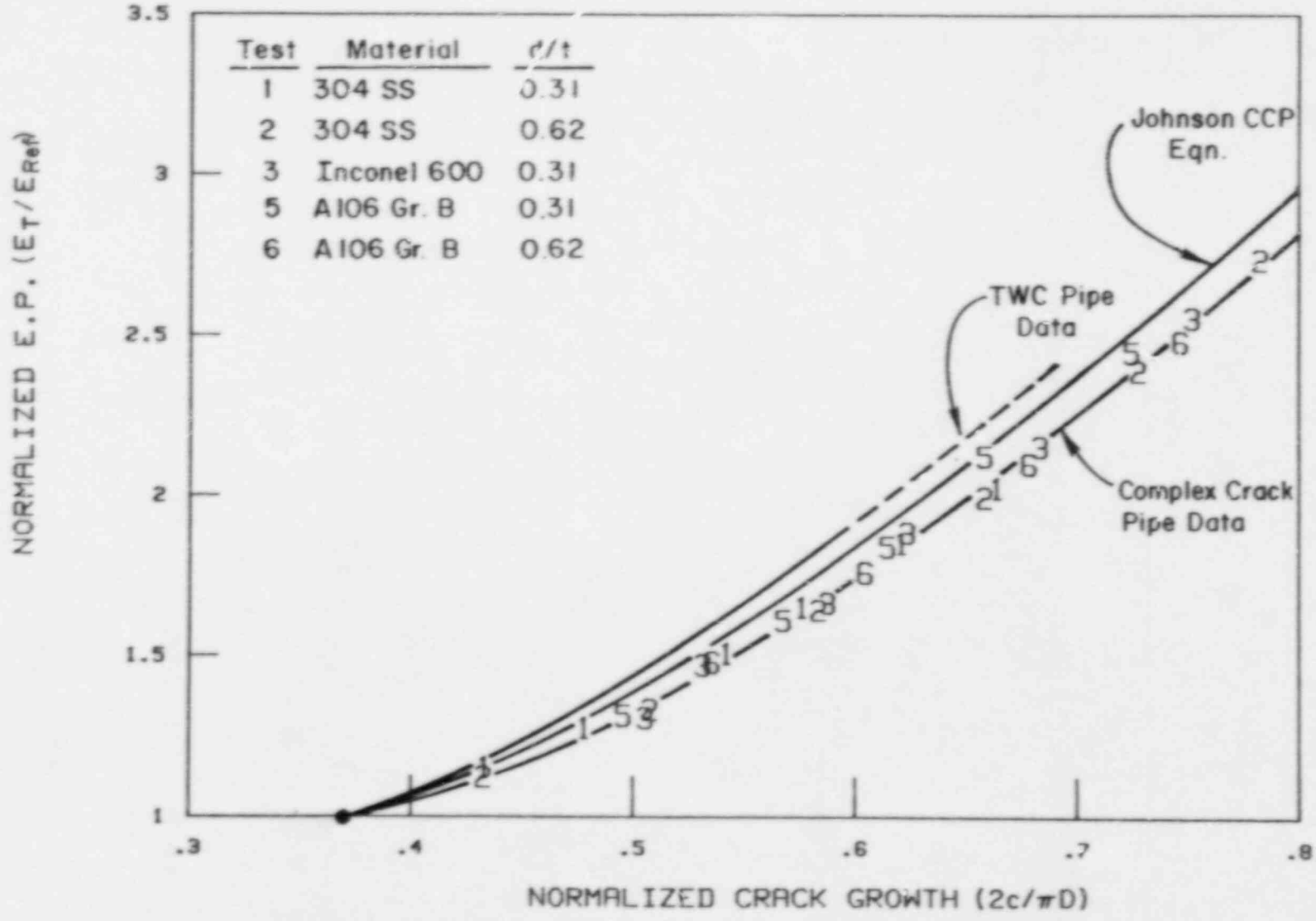

FIGURE 15. COMPARISON OF CALIBRATION CURVES FROM RECENT COMPLEX CRACK-PIPE EXPERIMENTS TO PAST THROUGH-WALL CRACK-PIPE EXPERIMENTS AND THEORETICAL JOHNSON CENTER CRACKED PANEL EQUATION

DETERMINATION OF FRACTURE MECHANICS PARAMETERS OF SMALL AND LARGE SCALE SPECIMENS

E. ROOS

STAATLICHE MATERIALPRÜFUNGSANSTALT

UNIVERSITY OF STUTTGART

DIRECTOR: PROF.DR.-ING.K.KUSSMAUL

1. Introduction

A material characteristic describing the crack initiation behaviour of a specimen or component independent of size, geometry and loading condition is necessary for the calculation of the crack initiation load of notched or cracked components. This paper describes a method utilizing the fracture toughness parameter J-integral to determine a physical and transferable crack initiation value.

2. Determination of Material Characteristics on Small Scale Specimens

Generally, the crack initiation value on the basis of the J-integral is determined by the crack resistance curve (J_R-curve) of CT-25 specimens. The known methods provide the value J_{Ic} according to ASTM E-813 /1/ and the value $J_{0,15}$ according to Loss /2/. These values represent a qualifying evaluation of the material but not the physical crack initiation value. At the MPA, the points measured experimentally by means of single or multiple specimen techniques are approximated within the entire range by the power law fit described by Loss or by a polynominal. The physical crack initiation value J_i can be determined by measuring

the stretch zone width (SZW) Δa_{st} on the specimen surface and intersecting the J_R-curve with a line running parallel to the ordinate with a distance of Δa_{st}, Fig. 1 /3/. A summary of three values (J_{Ic}, $J_{0,15}$, J_i) measured on a fine-grained structural steel is given in Fig. 2. The dimensions of the SZW measured by a scanning electron microscope on specimens of various thickness show the size independence for specimens up to CT 100, made of the same material, Fig. 3. However, the SZW varies across the specimen thickness on large and small double edge notched tensile specimens (DENT, DECT) and CT-specimens without side grooves, but the average SZW value varies only insignificantly with specimen size and geometry, Fig. 4, /6/.

A wide range of material toughnesses was investigated within the research programme "Integrity of Compont" (FKS), Fig. 5. The J_R curves for these materials are plotted in Fig. 6. The difference between J_{Ic}, $J_{0,15}$ and J_i-values increases with increasing material toughness, Fig. 7. These differences in the crack initiation parameters influence directly the results of the computed initiation load for structures and provide values on the unsafe side.

3. Determination of Material Characteristics on Large Scale Specimen

Tests were performed within the toughness spectrum in Fig. 5 on a number of specimens with component-like dimensions, Fig. 8, which can be calculated easily /7,8/. J-integral load curves as well as crack resistance curves with help of the partial unloading method have been recorded on large scale specimens by means of extensive instrumentation and a computer code system PROMEON /9/, Fig. 9. It was possible to show that two large DENT-specimens made of various tough materials tested in the upper shelf energy level had attained the physical crack initiation value J_i at instability load, however, no stable crack extension could be detected. The values $J_{0,15}$ and J_{Ic} are

distinctly above the experimentally measured instability load, Figs. 10 and 11. A J_R-curve could be determined for another large DENT-specimen that exhibited stable crack extension. The J_i-value agreed well with the value from CT-specimen, Fig. 12. The CT-specimen has been examined with the same notch configuration as the DENT specimen. The good agreement of the physical values J_i determined according to this method compared with a CT-25 specimen, can also be found for a large SENT and DENT-specimen, Fig. 13. Here it is worth mentioning that the CT-25 specimen with 20 percent side grooves has the lowest tearing resistance /10/. A further proof of the size and geometry independence of the J_i-value on the notched round tensile specimens up to a diameter of D = 143 mm, is shown in Fig. 14.

4. Transferability to a Large Scale Specimen under Pressurized Thermal Shock Conditions

The examination of the transferability of the physical crack initiation value could also be performed under the complex conditions of pressurized thermal shock (PTS). A 200 mm thick hollow cylinder with an internal circumferential crack was subjected to cold water injection, internal pressure and a high axial tensile load. The stress state is similar to that in a real vessel with an axial flaw, Fig. 15. The first test of a whole series with different material toughness levels was completed recently. The upper shelf energy (USE) for this cylinder was in the range of 200 J, and its crack resistance curve is shown in Fig. 16. The driving force for the specific PTS condition was computed in terms of J-Integral in the elastic-plastic regime for an artificial 50 mm deep circumferential crack and compared with the material resistance curve, Fig. 16. From this investigation a stable crack extension of approximately 1 mm was predicted for the experiment. Nondestructive testing and subsequent fractographical examination confirmed an average crack extension of about 1 mm, Fig. 17. This result is in good agreement with the analytical treatment of this complex situation. Further investigations will show if this good agreement can also be established for the other specimens with lower shelf energy /11/.

5. Numerical Investigations to Explain the stable Crack Extension Beyond to Initiation.

The examples of large scale specimens (Figs. 10, 11 and 12) proved a trend towards a more stable crack growth for smaller crack depths of geometrically similar specimens /8/. To explain this effect, the J-integral and the state of stress were examined for CT and DENT specimens, as well as for a pressure vessel.

To determine the stress state in front of a crack tip, the values of the principal stresses or the invariants of the stress tensor have to be known. In so far, a single parameter like the J-integral or the crack opening displacement (COD) cannot adequately describe the behaviour of the crack tip stress field, especially if larger amounts of plastic strain occur. Considering this, it is proposed to quantify the stress state by a second parameter called the constraint factor. This factor is a measure for the reduction in plastic flow due to the three dimensional stress state. The constraint factor is defined:

$$\pi = \frac{\sigma_v}{\sigma_1} = \frac{1}{\sqrt{2}\,\sigma_1}\sqrt{(\sigma_1-\sigma_2)^2+(\sigma_2-\sigma_3)^2+(\sigma_3-\sigma_1)^2}$$

For several loading steps with increasing nominal stress levels, the various values of the constraint factor π in front of the crack tip are shown in Fig. 18 for a DENT specimen. All calculations show a minimum π in front of the crack tip. The value of this minimum increases with growing plastic deformation which means that the constraint effect decreases with increasing plastic flow.

A plot of these minimum values for each loading step versus the J-integral is shown in Fig. 19. In addition π -values for axial cracks of different depths for a pressure vessel have been plotted. As expected, the vessel containing deeper cracks had more constraint than the one with shallow cracks, and the CT-25 specimen reached the highest constraint over the entire loading range.

The experimental results show crack initiation and stable crack growth at the CT-25 and DENT specimen at locations marked with arrows in Fig. 19. However, no stable crack extension could be detected in a test made on a pressure vessel with a crack depth ratio of a/W = 0,75 /12/. Consequently, the assumption is that a critical value of the J-integral and of constraint is necessary for the onset of stable crack growth /13/. The distances of the location of maximum constraint from the crack tip are plotted in a micrograph of the DENT specimen, Fig. 20, so that the effect of maximum constraint on crack initiation can be seen. Void nucleation has been observed to originate at the location of maximum constraint. It is not obvious whether the crack starts growing first from the crack tip or from the voids.

6. Conclusions

The physical crack initiation value J_i can be determined from CT-specimens with the method presented. The methods generally used for determining J_{I_c} or $J_{0,15}$ provide values which are evidently higher than those compared with the ones from the physical initiation value. The development of a method to determine the J-integral and crack resistance curve in the test also on large scale specimens confirm the transferability of the J_i value even to the complex conditions of pressurized thermal shock. The additional dependence of the stable crack extension on constraint as well as the J-integral could be proved by means of finite element analyses.

References

/1/ Standard Test for J_{Ic}, A Measure of Fracture Toughness ASTM E 813-81

/2/ Loss, F.J. (Editor):
Structural Integrity of Water Reactor Pressure Boundary Components. Quarterly Progress Rep. Apr.-June 1980, NUREG/CR 1783

/3/ Kussmaul, K., Roos, E.:
Statistische Ermittlung von zähbruchmechanischen Kennwerten auf der Grundlage des Kerbschlagbiegeversuches 10. MPA-Seminar, Universität Stuttgart, 1984

/4/ Roos, E., Eisele, U.:
Anmerkung zur Problematik der Kennwertbestimmung in der elastisch-plastischen Bruchmechanik bei J-Integral Rißwiderstandskurven. To be published

/5/ Kussmaul, K.:
Aufgaben, Ziele und erste Ergebnisse des Forschungsprogrammes Komponentensicherheit. VGB Kraftwerkstechnik, Juni 1980

/6/ Roos, E., Kockelmann, H.:
A Survey of Different Experimental Methods for the Determination of Crack Initiation Parameters of Small and Large Scale Specimens Ductile Fracture Test Methods, Proc. of a CSNI Workshop, Dec. 1982, Paris

/7/ Issler, L., Birk, R., Hund, R.:
Anwendung eines neuen Näherungsverfahrens aus den USA zur Zähbruchanalyse. 6. MPA Seminar, Staatliche Materialprüfungsanstalt Stuttgart (1980)

/8/ Kussmaul, K., Issler, L.:
Evaluation on the Elastic-Plastic Fracture Mechanics Methodology on the Basis of Large-Scale Specimens, ASTM STP 803 (1983) pp. 11-41

/9/ Roos, E., Kiessling, D.J., Silcher, H., Eisele. U.:
PROMEON: Program for Acquisitation of Measurement Data for the ON-line Determination of Fracture Mechanics Parameters on Large Specimens, to be published

/10/ Roos, E., Eisele, U., Silcher, H., Beyer, H.:
Experimental Determination of Ductile Fracture Mechanics Parameter on Large Scale Specimens
Trans. of 8th SMIRT (1985), Brussels

/11/ Kussmaul, K., Sauter, A.:
Anlagensimulation zur Behandlung der Notkühlproblematik beim Leichtwasserreaktor-Druckbehälter
10. MPA-Seminar, Sicherheit und Verfügbarkeit in der Anlagentechnik, 10. - 13. Okt. 1984, Stuttgart Germany,F.R.

/12/ Kussmaul et al:
Experimental Investigations on the Crack Opening Behaviour of Cylindrical Vessels under Light Water Reactor Service Conditions, in "Reliability and Safety of Pressure Components - PVP.82" ed.by C. Sundaravajan, Am. Soc. of Mech. Eng.. pp. 97

/13/ Roos, E., Schwantes, S.:
Problems of Transferring Fracture Mechanics Parameters to Components.Trans. of 8th SMIRT (1985), Brussels

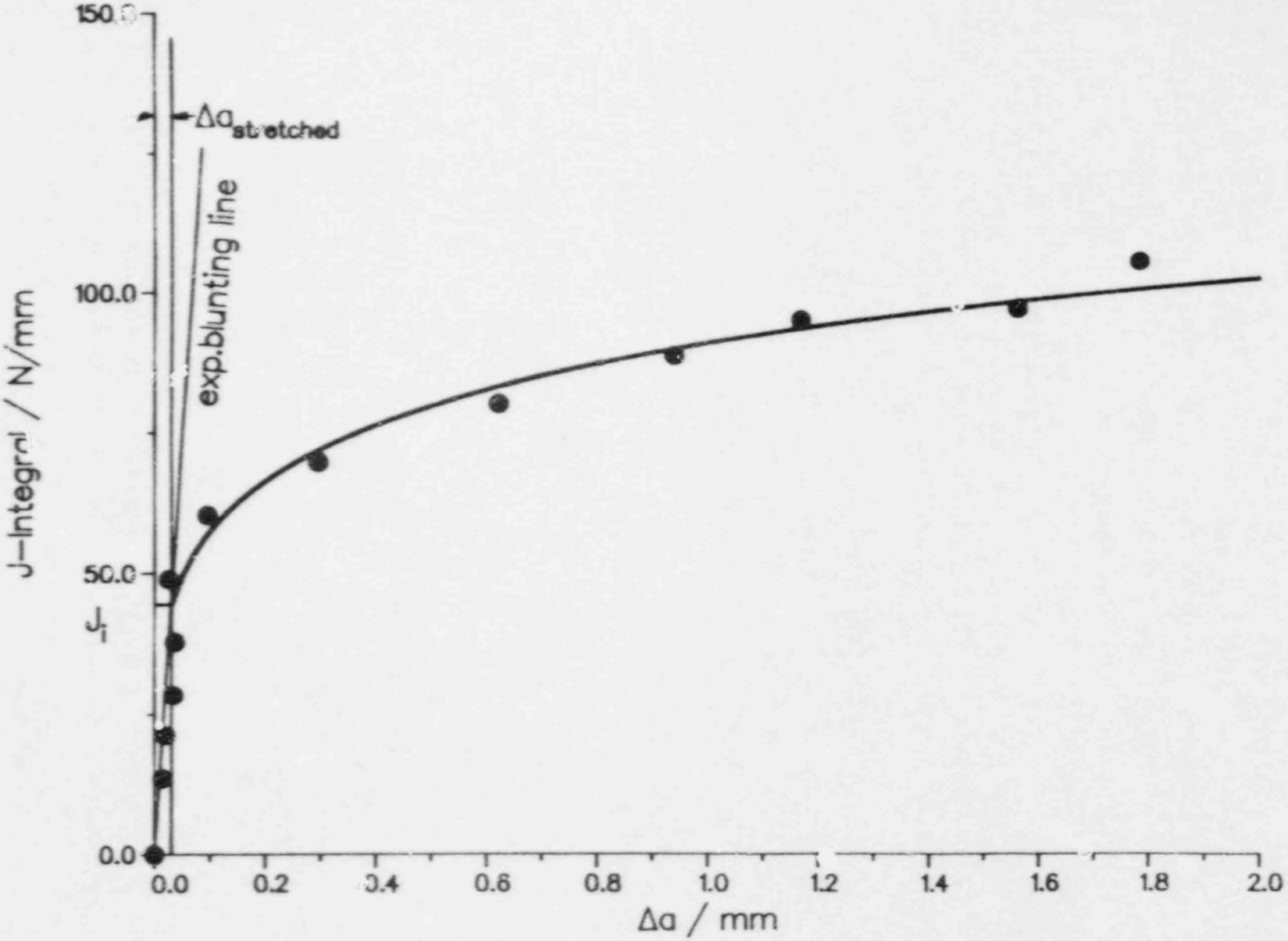

Fig. 1: Determination of the crack initiation parameter J_i from the stretched zone

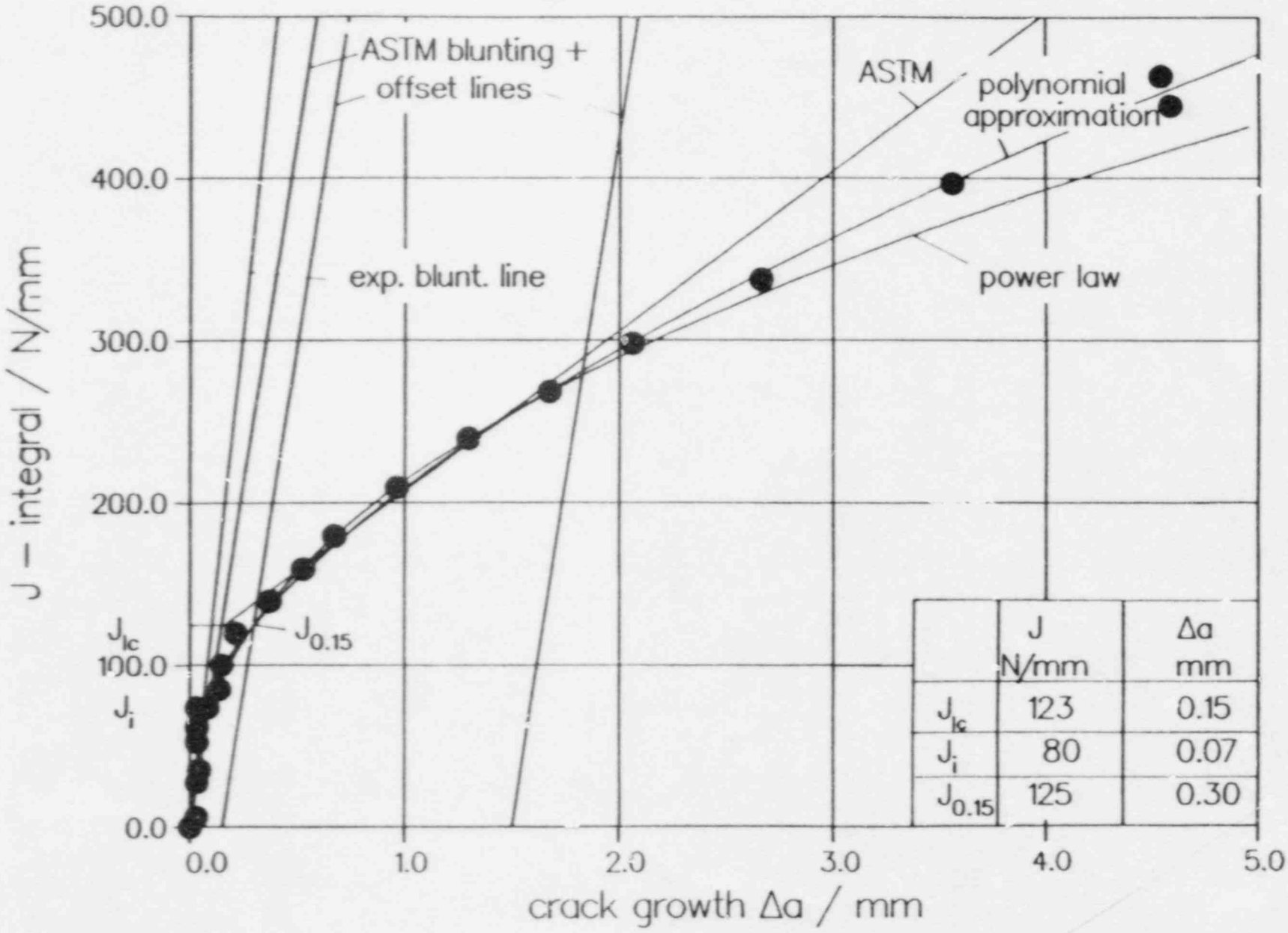

Fig. 2: J_R-curve of fine-grained structural steel tested at USE with J_i, J_{Ic} and $J_{0.15}$ values

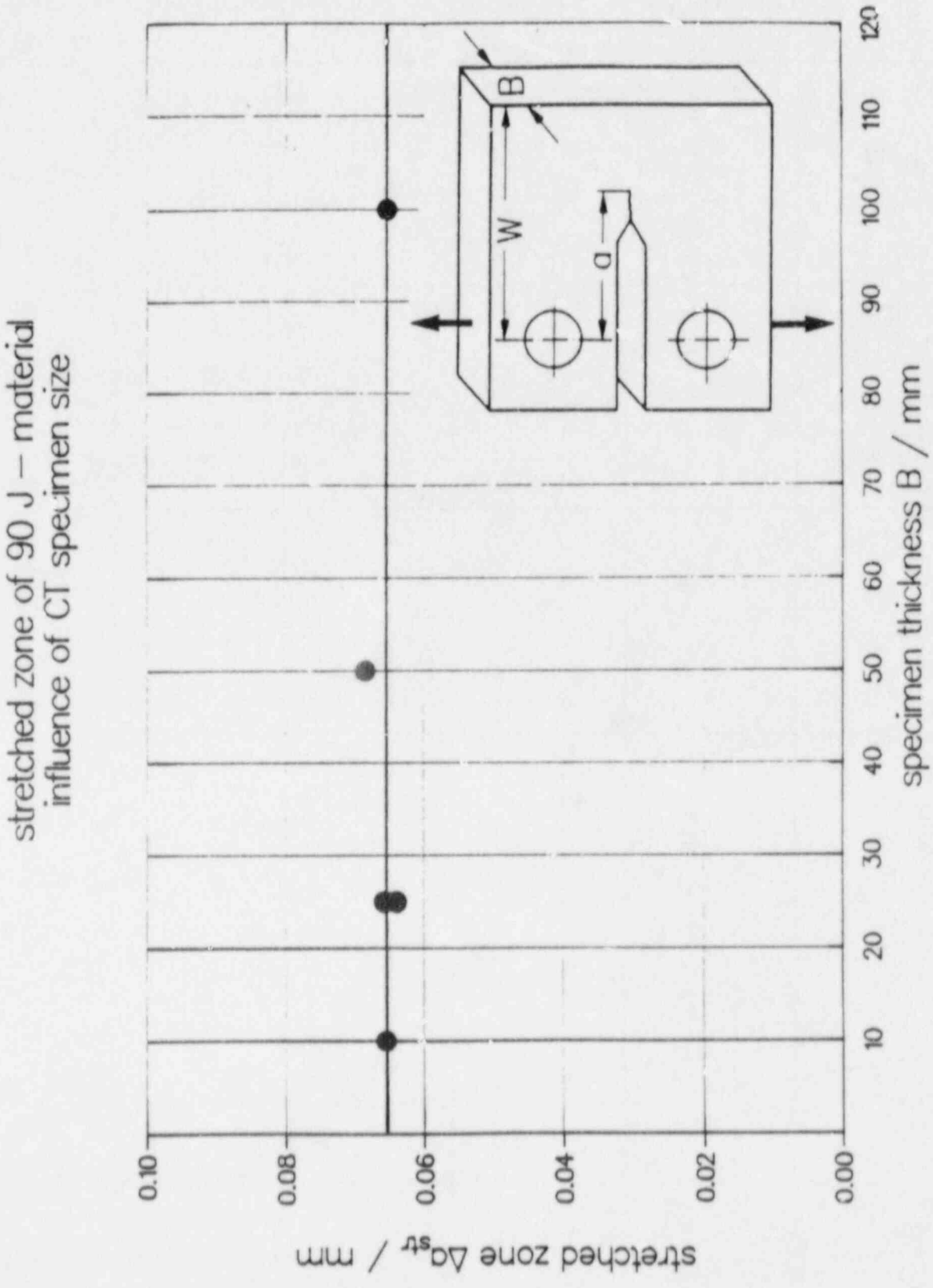

Fig. 3: Influence of CT-specimen size on stretched zone of fine grained structural steel (USE = 90 J)

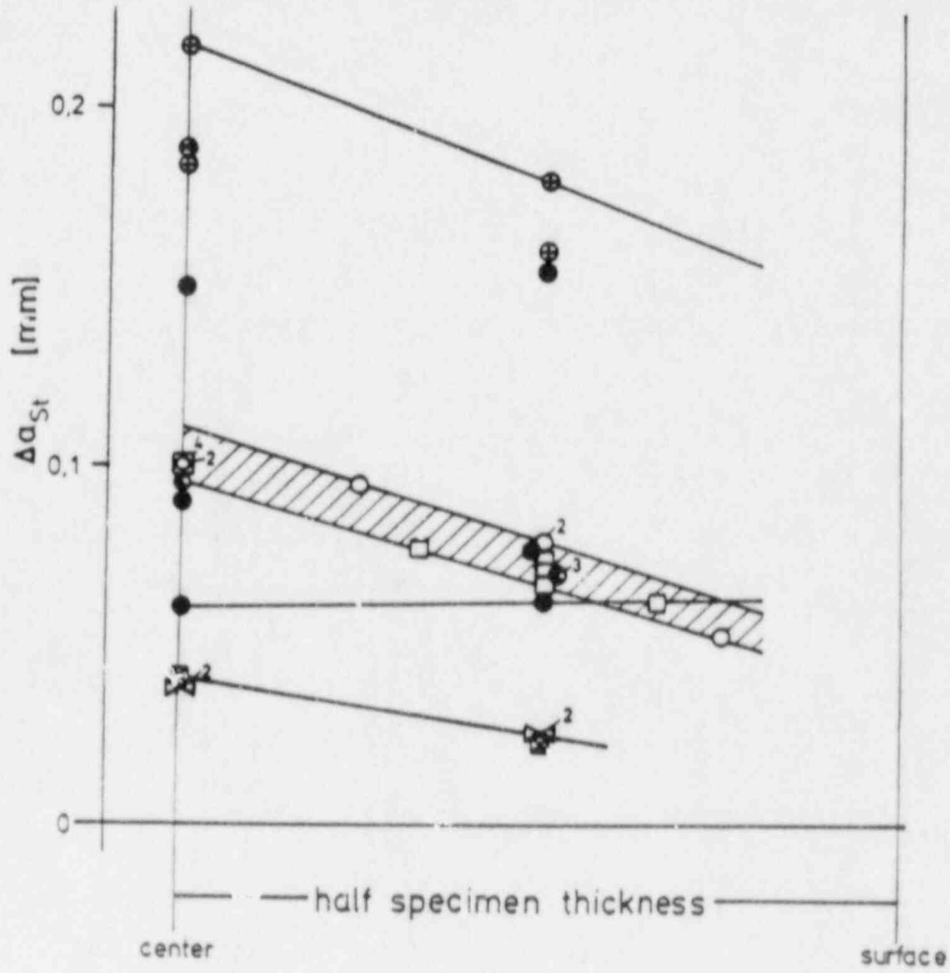

specimen	symbol	flaw	specimen thickness (mm)	testing temperature (°C)
DECT	●	fatigue crack	12,2 31,6 252	+ 80
CT 25	□		25	
CT 50	○		50	
DECT	⋈		12,4	- 20
CT 25	⊠		25	- 20
DENT	●	notch	4 12 14	+ 80
	●		253	
CT 50	◕		50	

Fig. 4: Stretched zone width across the thickness of various specimens

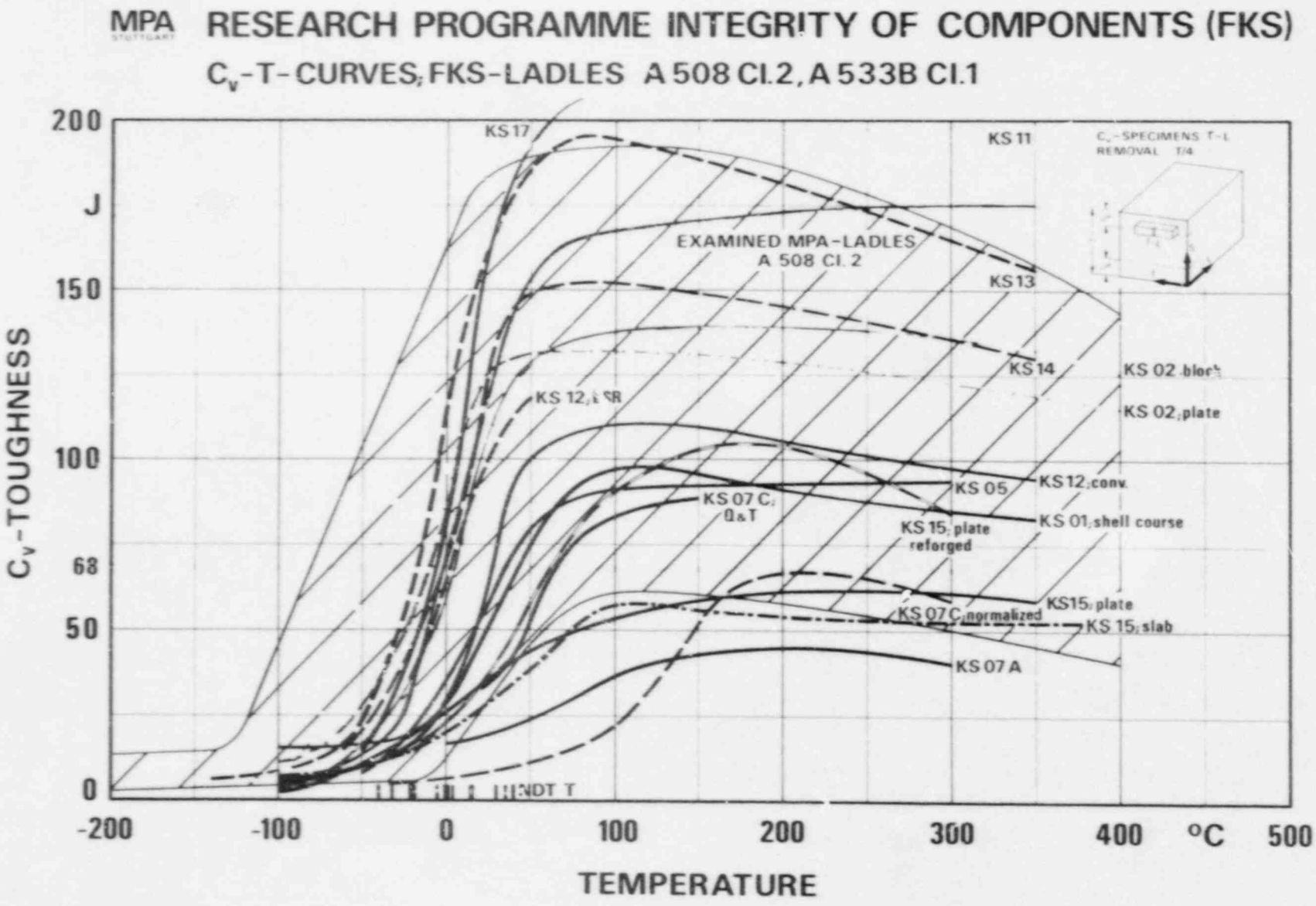

Fig. 5: Scatterband of notch impact energy - temperature curves of tested materials

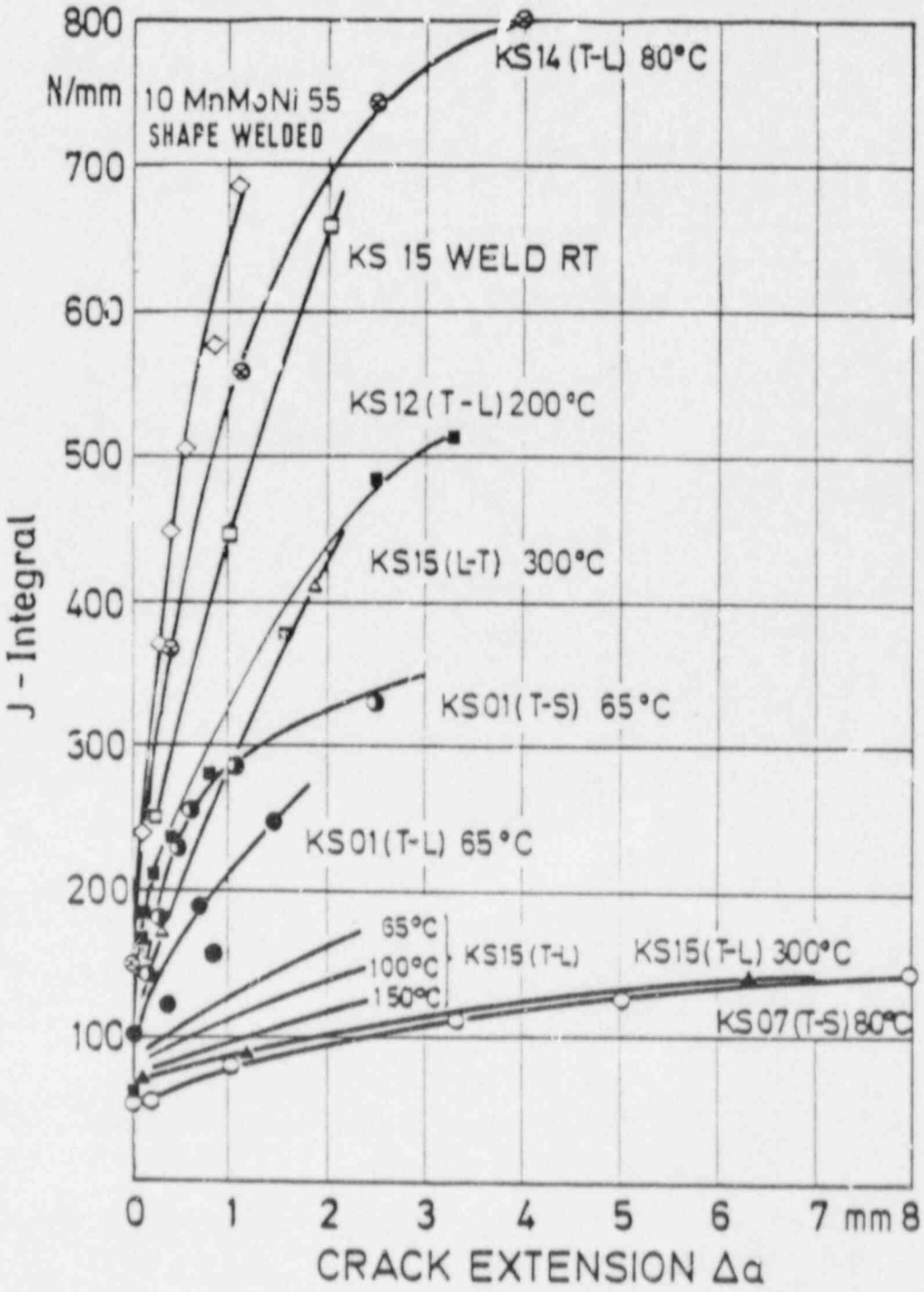

Fig. 6: J_R-curves of fine grained structural steels with different upper shelf energy levels

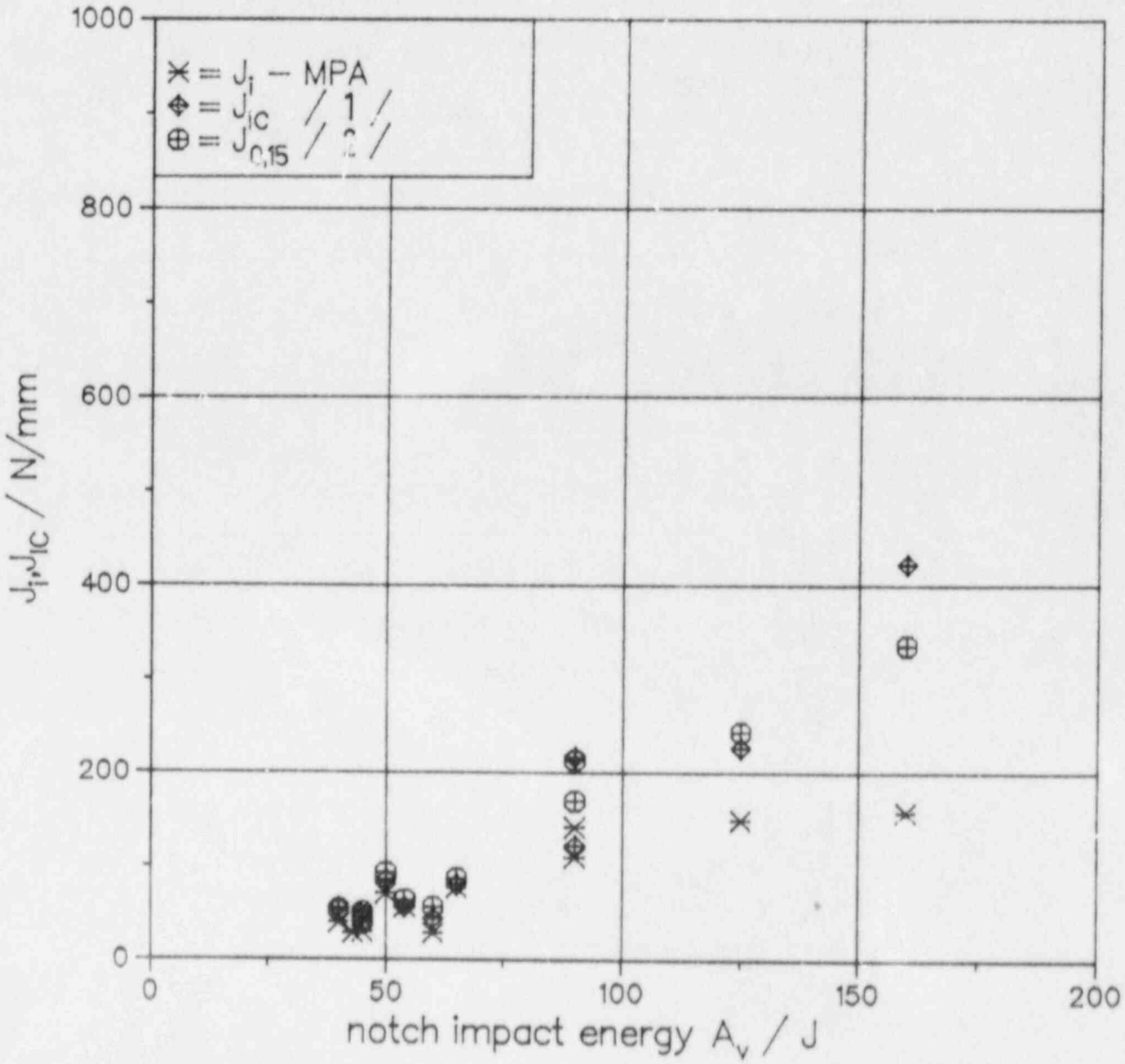

Fig. 7: Comparison of J_i (J_{Ic}, $J_{0,15}$) - values according to various methods. The values are plotted as a function of the upper shelf of the notch impact energy

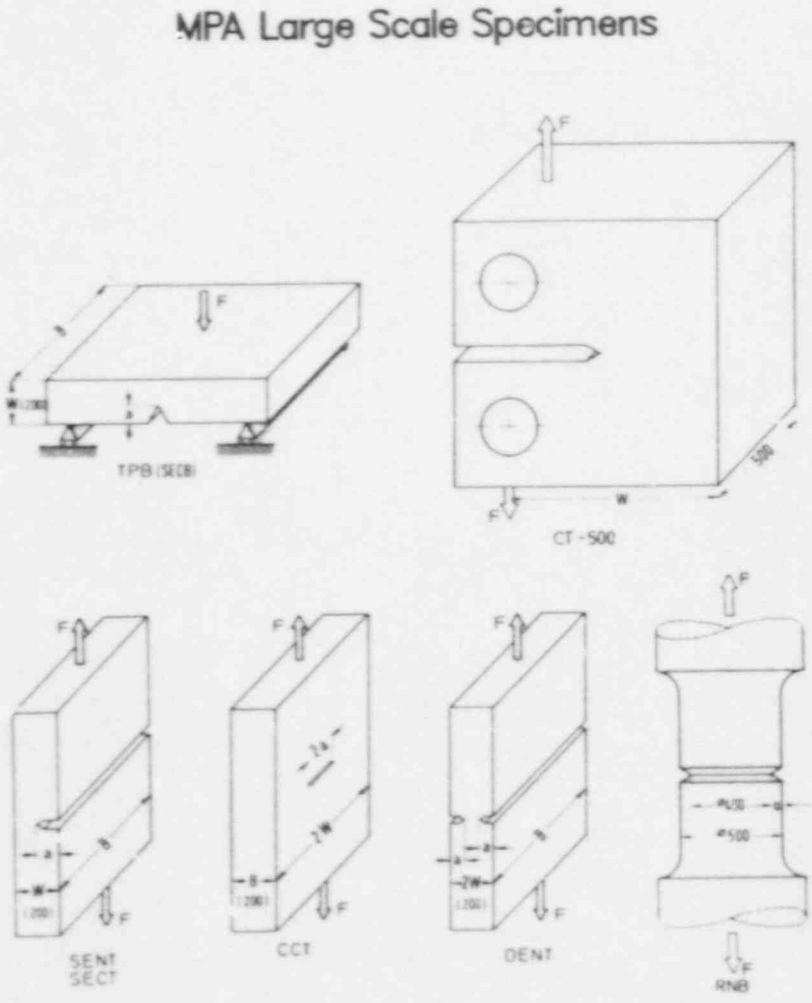

Fig. 8: Summary of MPA large scale specimens

Computer Controlled Large Scale Specimen Test

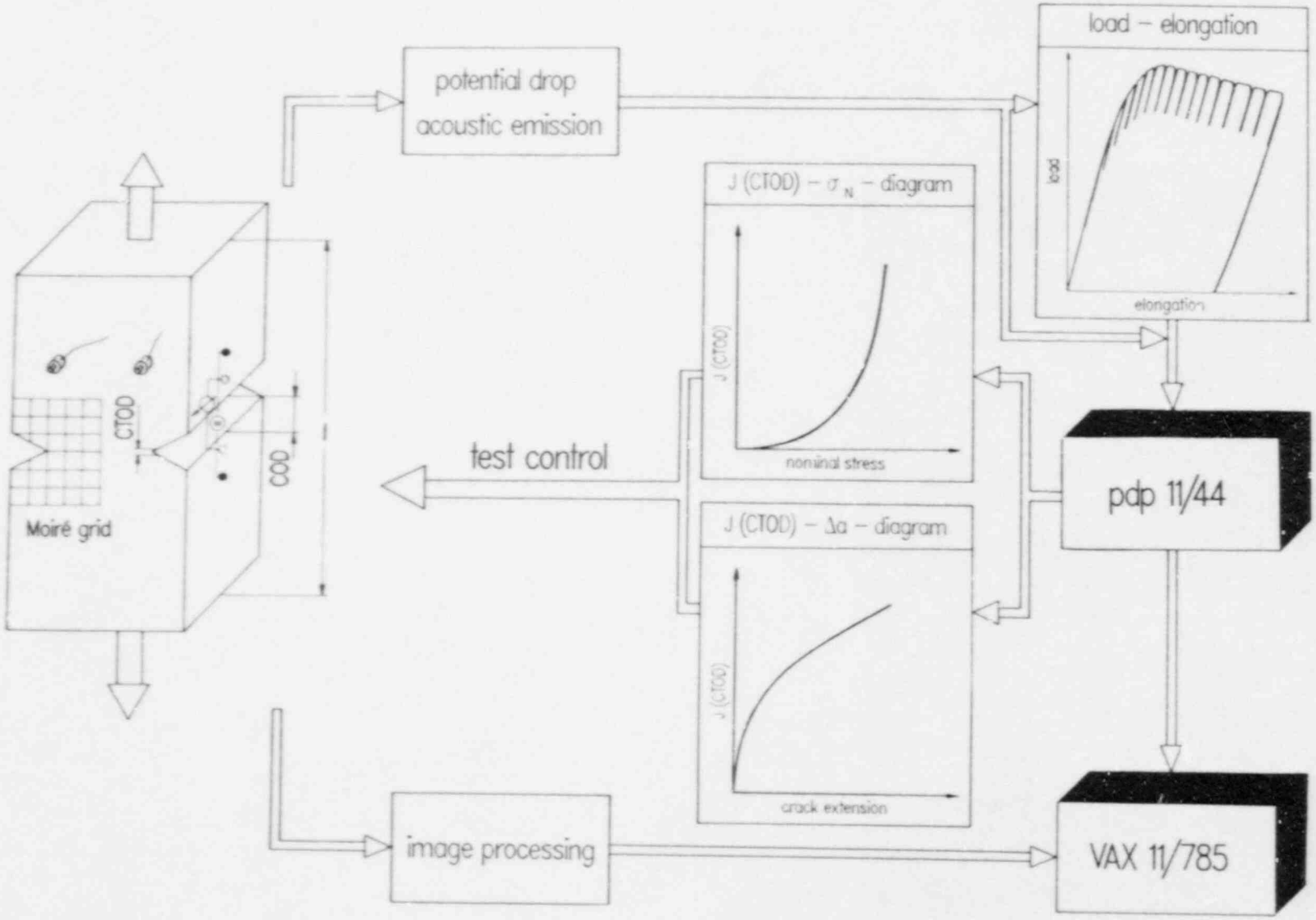

Fig. 9: Program System PROMEON for the on-line evaluation of crack resistance curves on the large specimens of Fig. 8 and for controlling the test

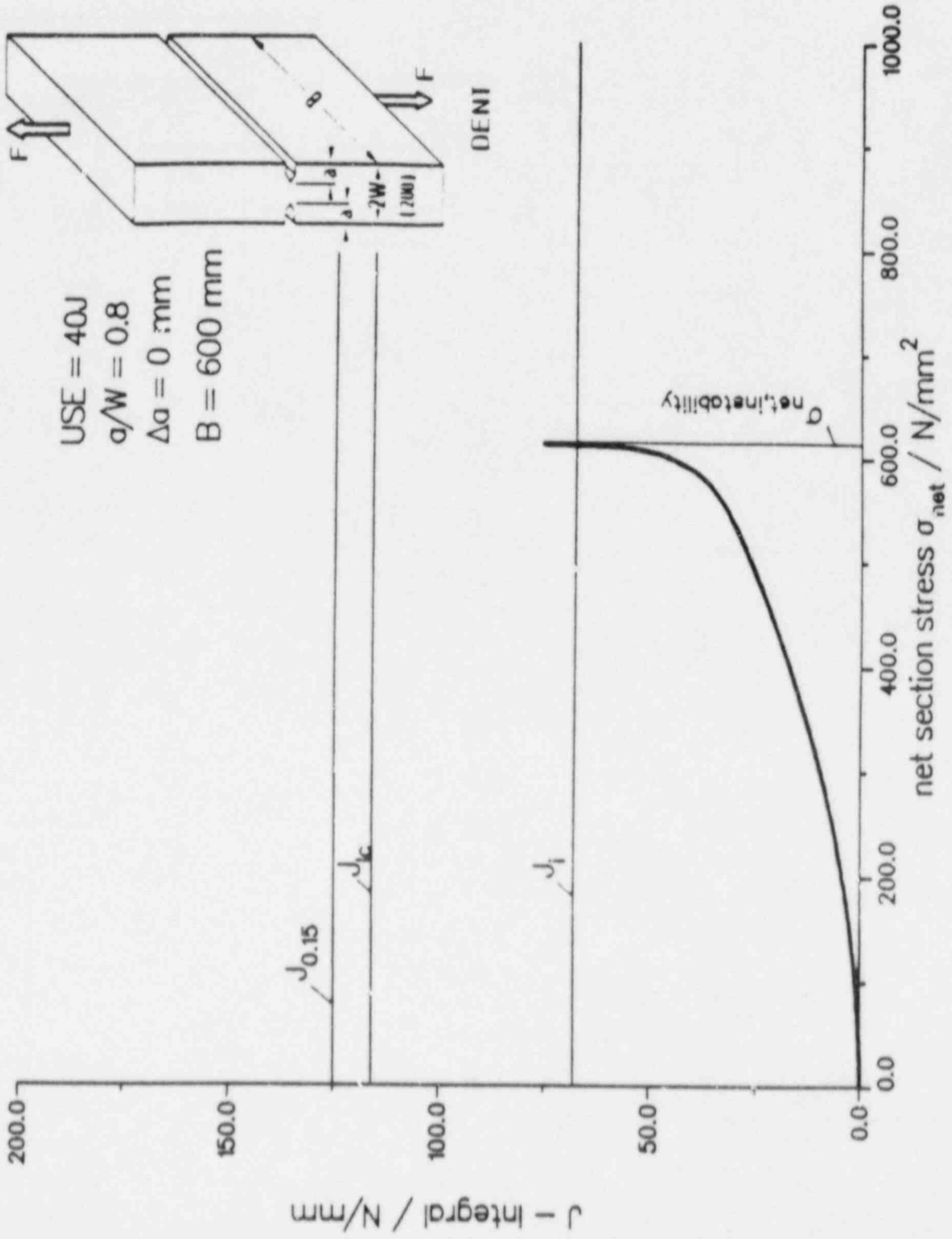

Fig. 10: Experimentally determined J-integral as a function of net nominal stress of a DENT-specimen made of modified fine-grained structural steel (22 NiMoCr 3 7) with USE of 40 J

Fig. 11: Experimentally determined J-integral as a function of net nominal stress of a DENT-specimen made of 20 MnMoNi 5 5 with USE of 160 J

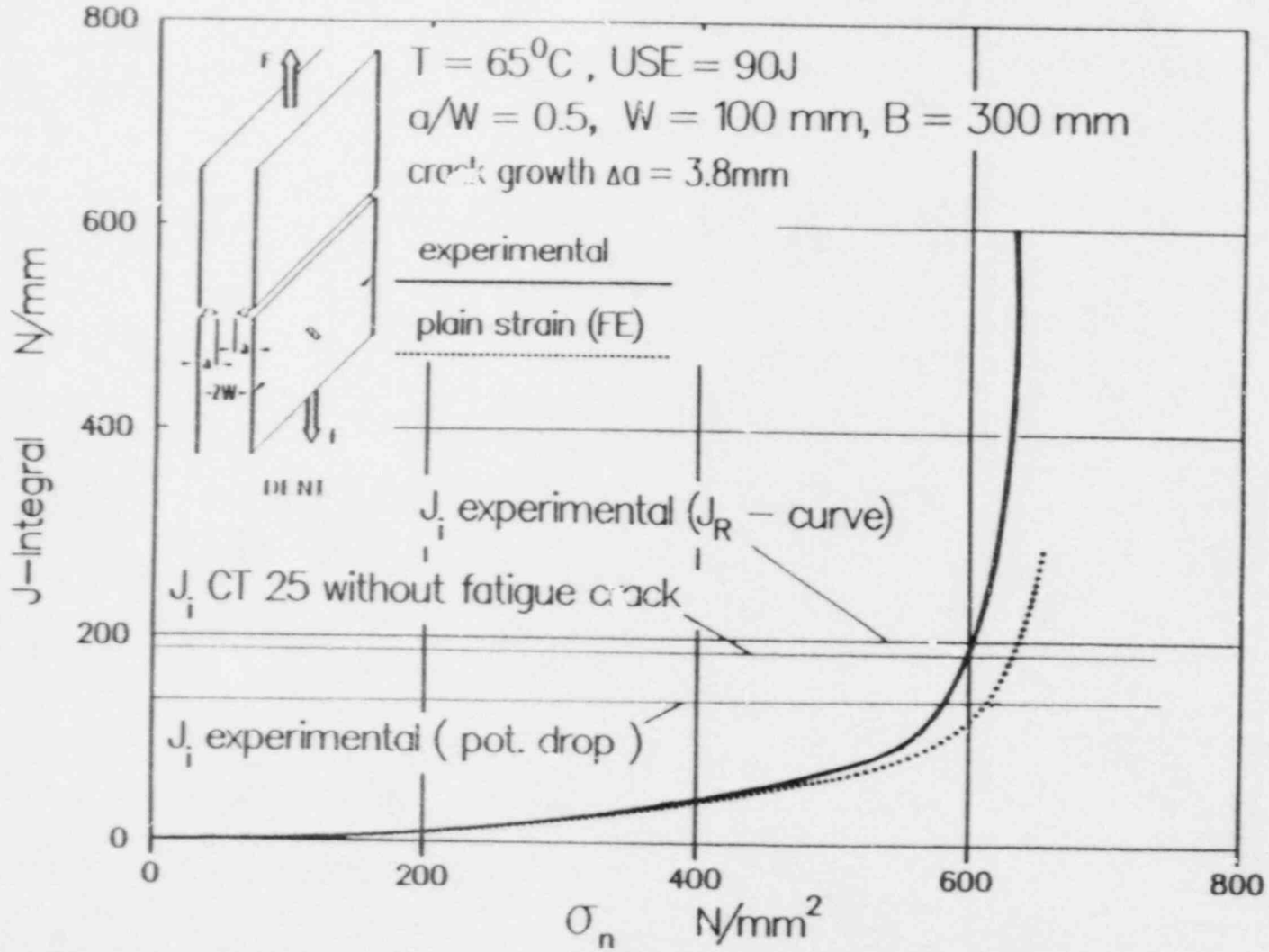

Fig. 12: J-integral determined by means of FE-calculation and experiment on a DENT-specimen made of 22 NiMoCr 3 7 (USE = 90 J). Comparison of J_i-values evaluated from J_R-curves

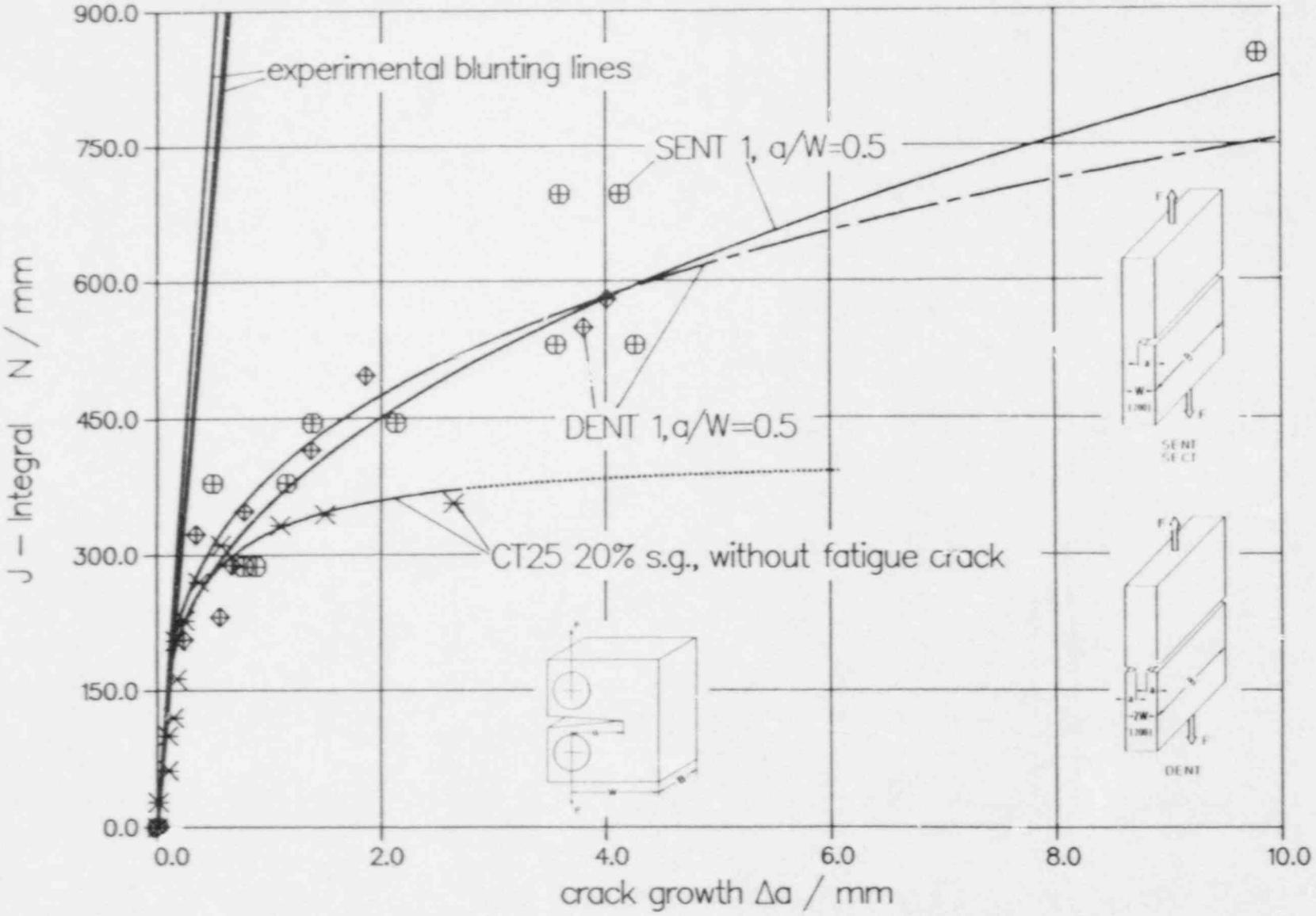

Fig. 13: J_R-curves of large DENT and SENT specimens compared with a J_R-curve of a CT-specimen with 20% side grooving

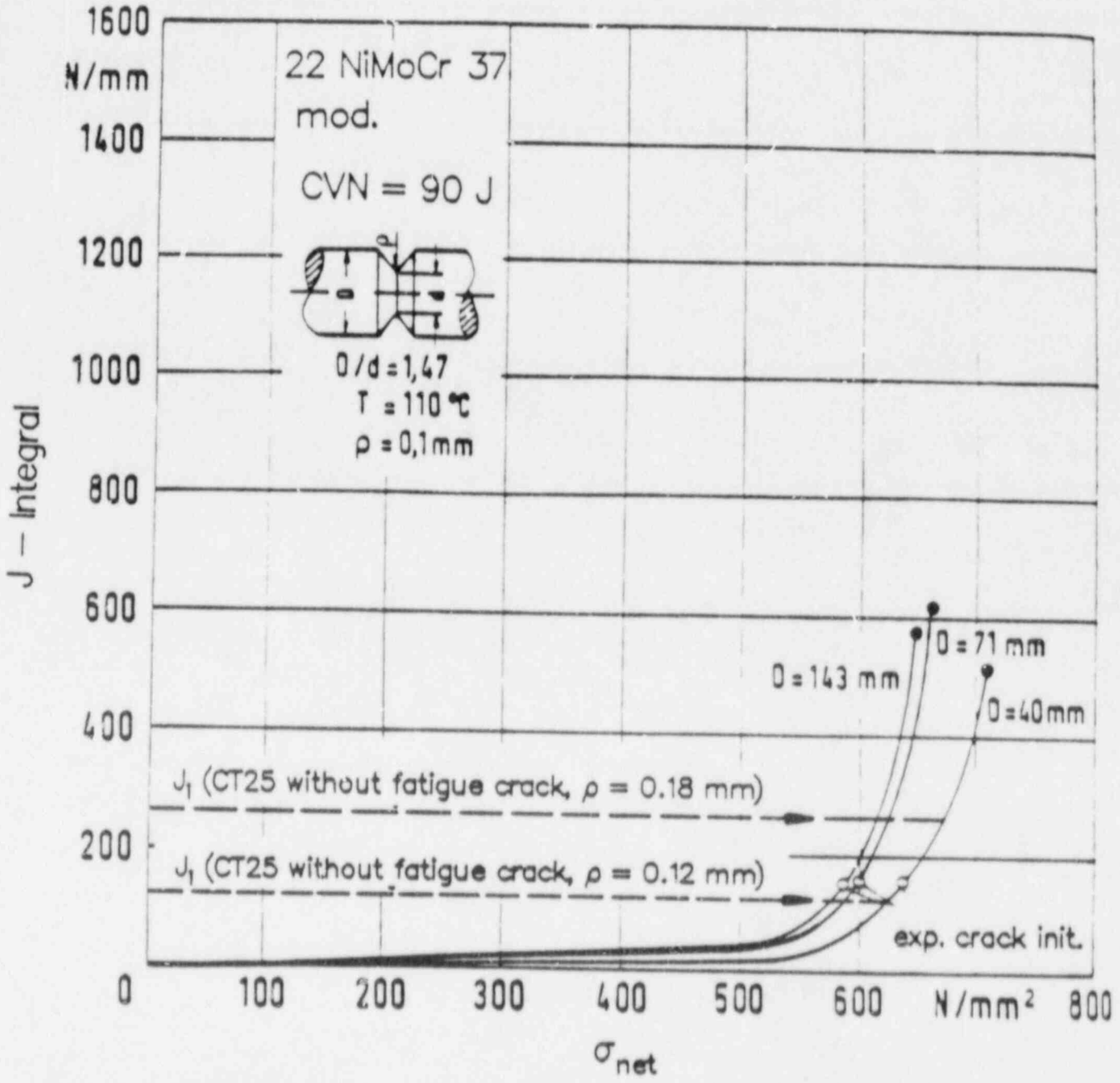

Fig. 14: Comparison of J_i-values of round notched bars and CT-specimens

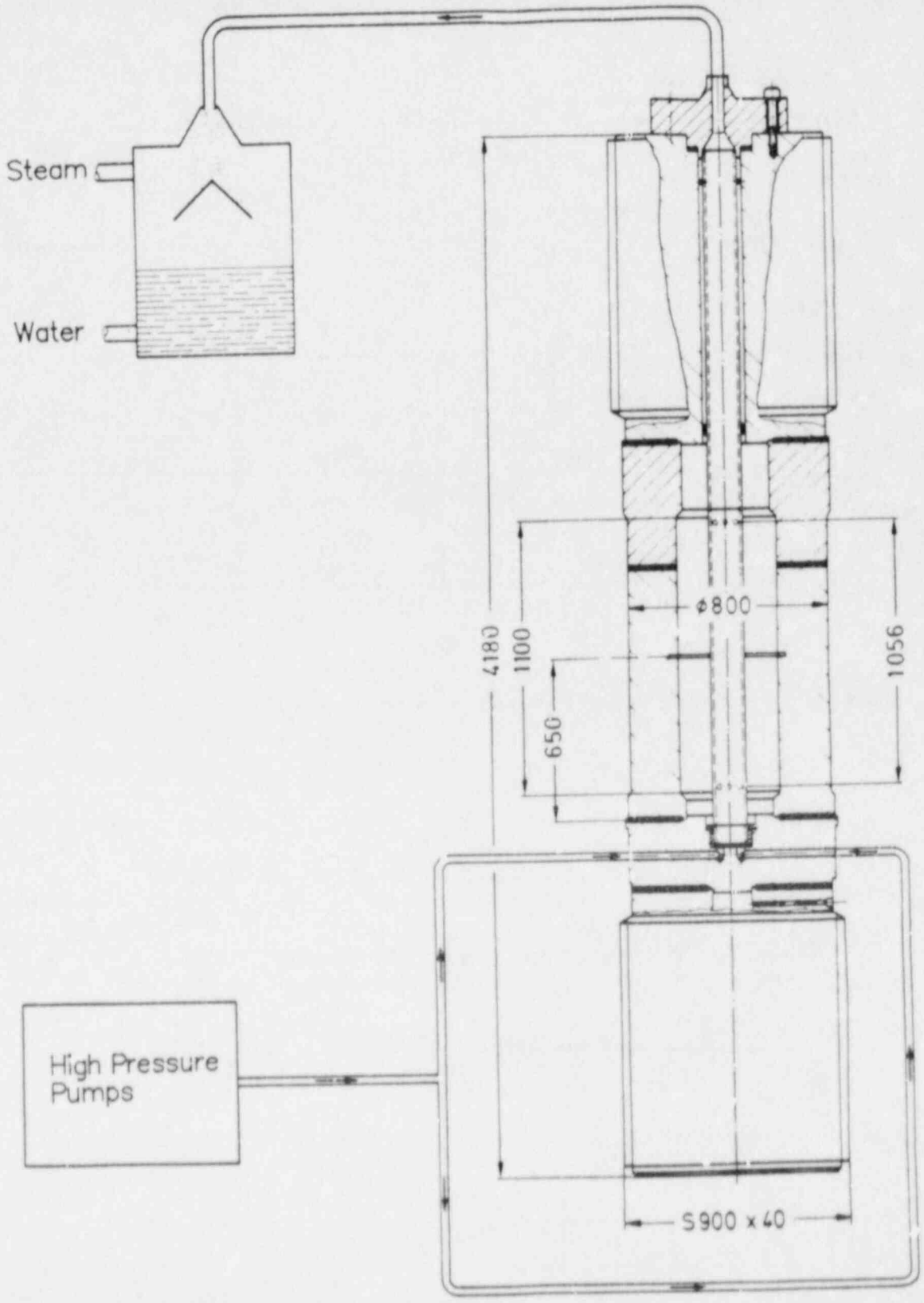

Fig. 15: Large scale hollow cylinder specimen for pressurized thermal shock experiment

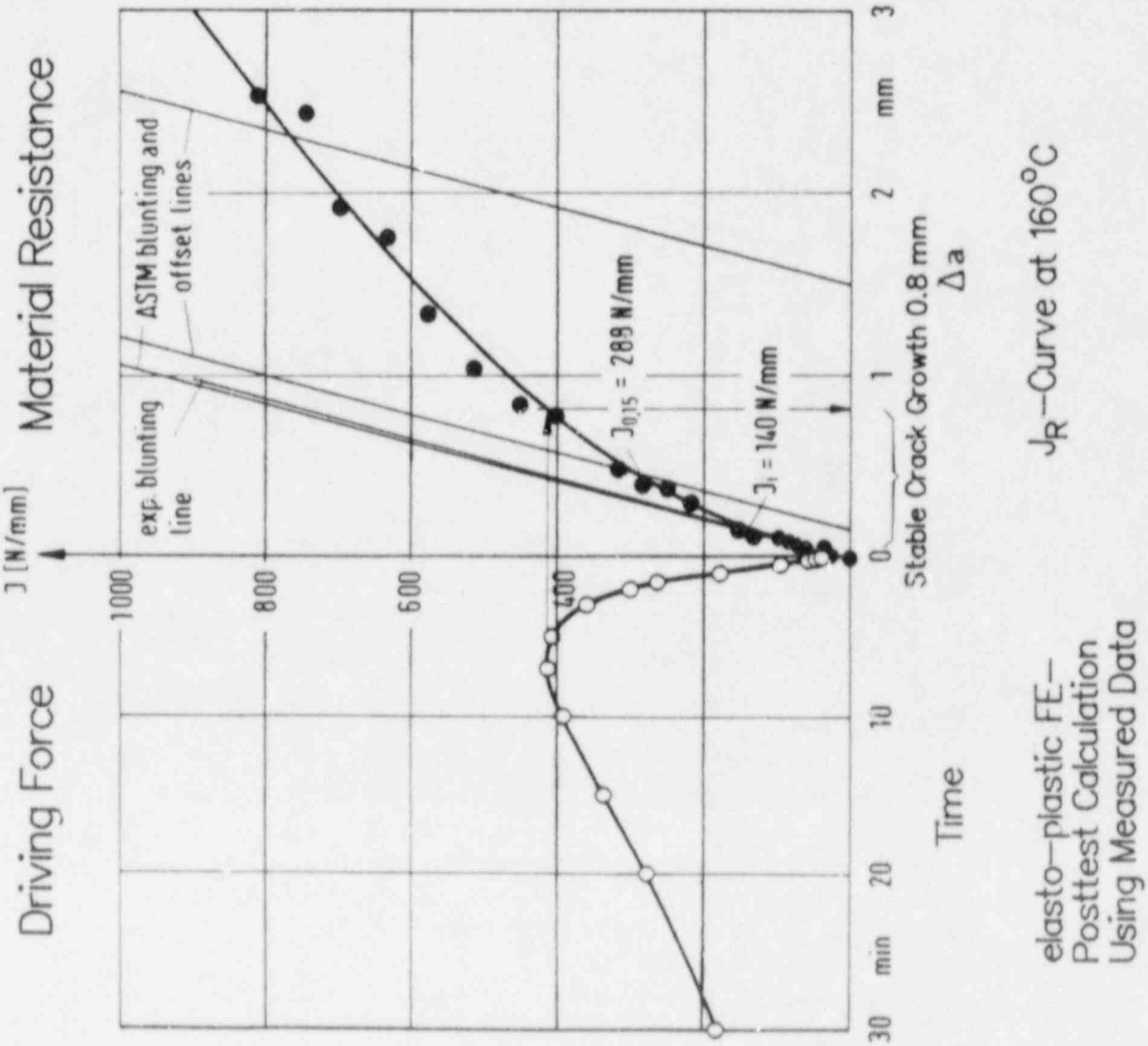

Fig. 16: J-integral evaluation of the thermal shock specimen (see Fig. 19) and material resistance curve J_R to determine stable crack growth and failure behaviour, upper shelf Charpy energy 200 J

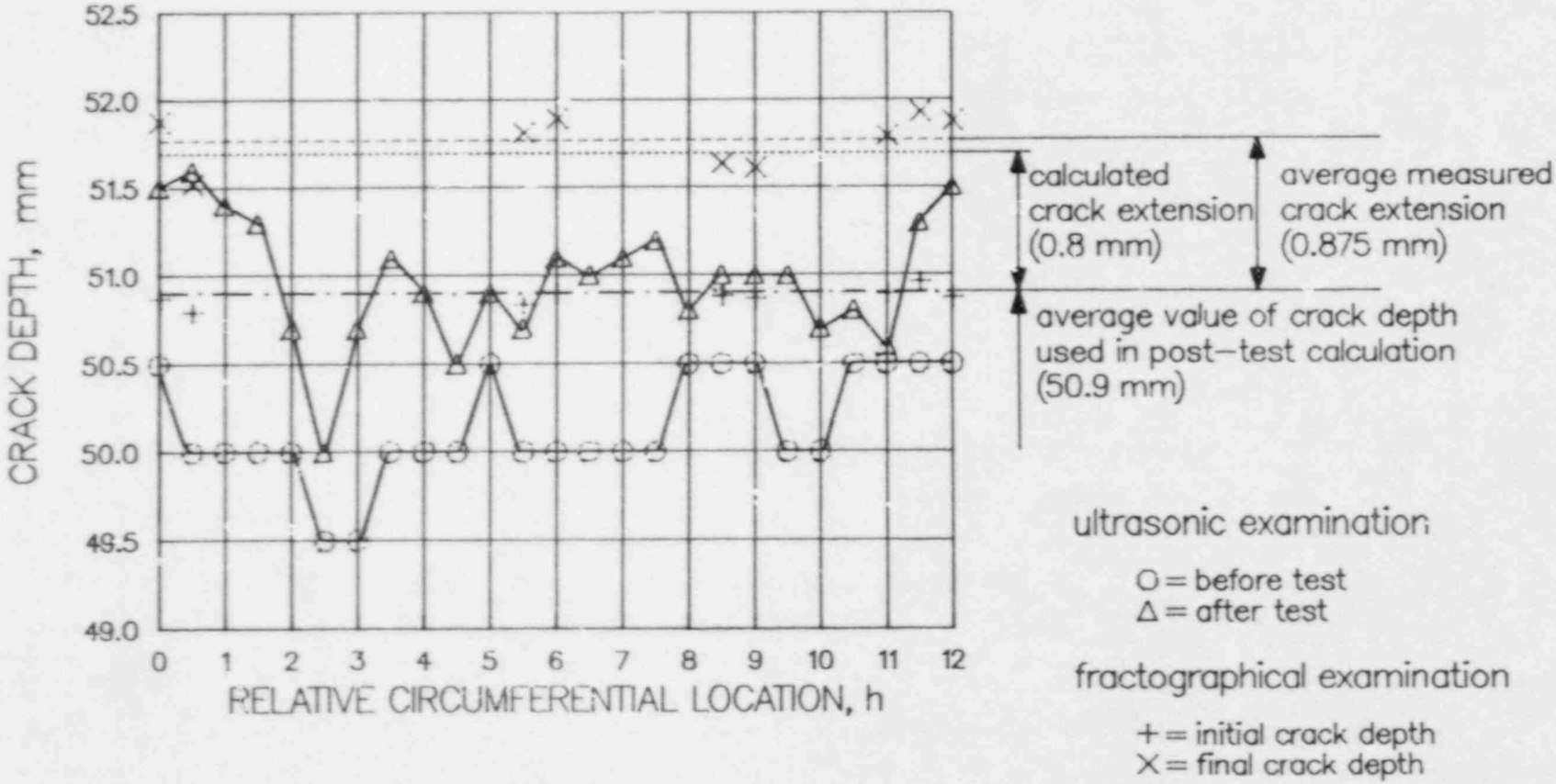

Fig. 17: Stable crack growth caused by pressurized thermal shock in the specimen with 200 J upper shelf Charpy energy

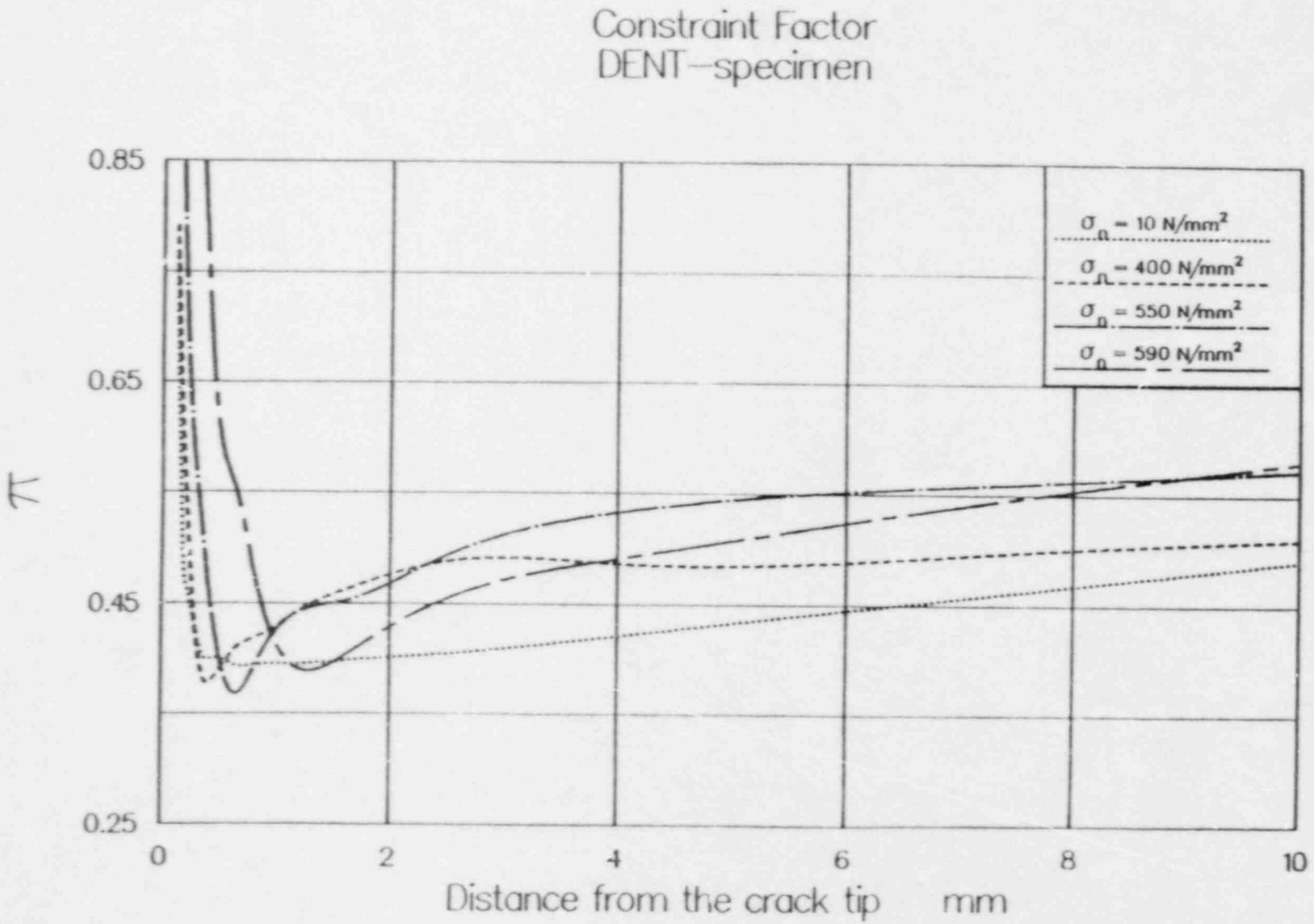

Fig. 18: Constraint factor along ligament of a DENT-specimen at different load steps

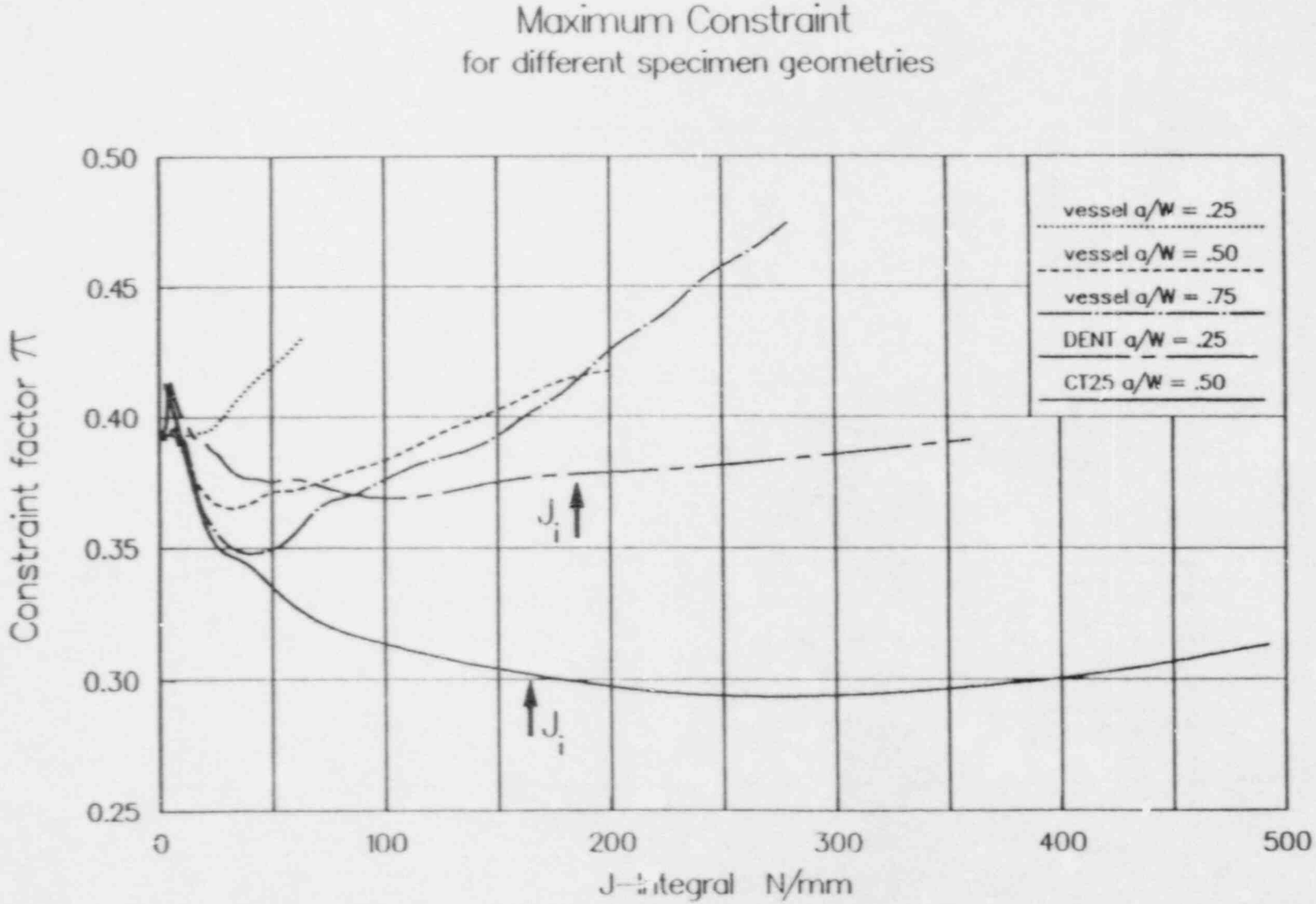

Fig. 19: Variation of the minimum of the constraint factor as a function of the J-integral

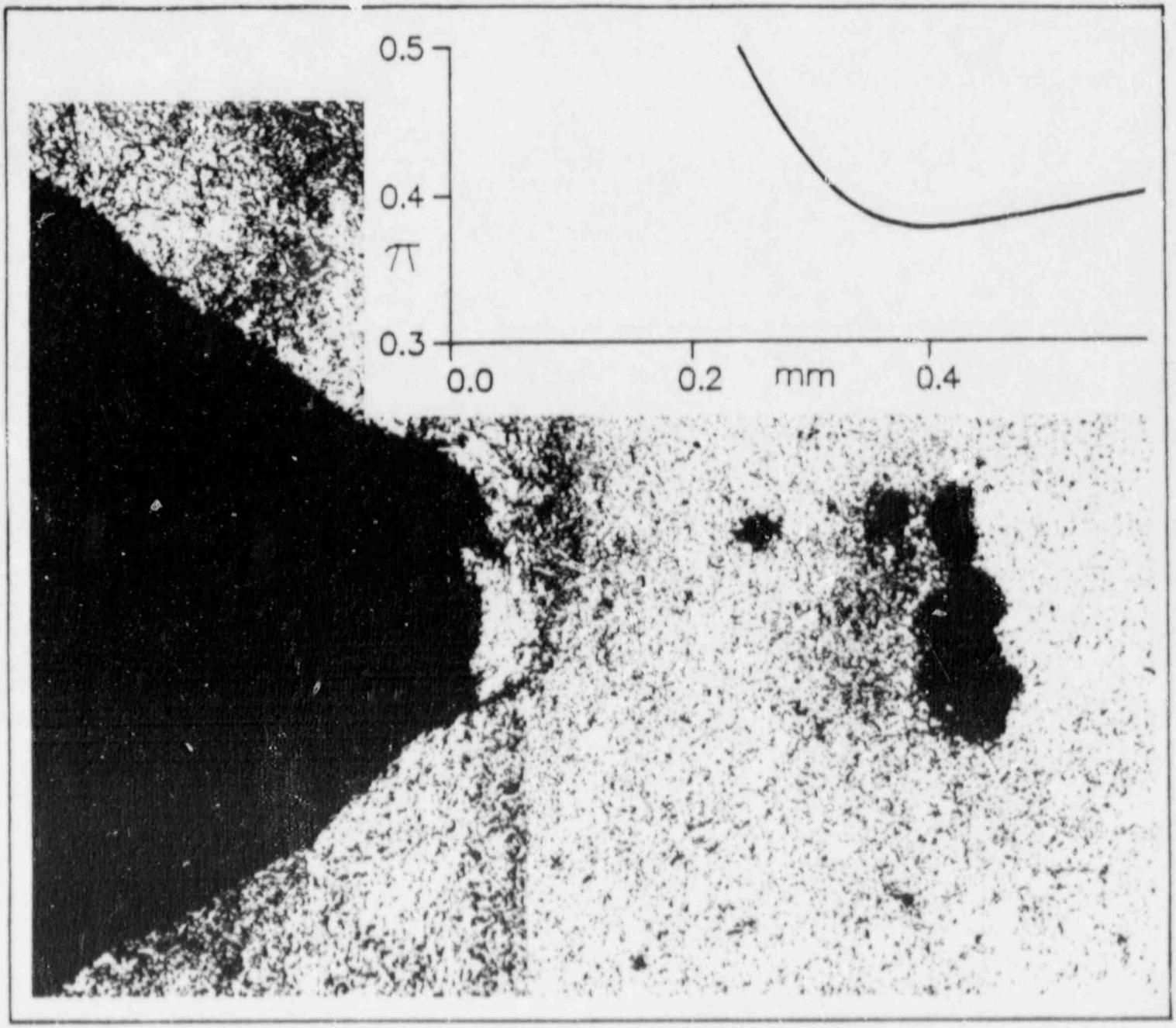

Fig. 20: Comparison of the location of voids in a DENT specimen with the minimum of the constraint factor

SECOND CSNI WORKSHOP ON DUCTILE FRACTURE TEST METHODS

OCED Headquarters
Paris, France
April 17-19, 1985

List of Attendees

P. Van Asbroeck
CEN/SCK
Boeretang 200
B-2400 Mol
BELGIUM

K. Wallin
VTT
Metals Laboratory
Vuorimiehentie 5
SF-02150 Espoo 15
FINLAND

P. Balladon
UNIREC
Centre de Recherches d'Unieux
B. P. 34
42701 Firminy
FRANCE

M. Bethmont
EDF-Department Etude des Materiaux
Les Renardieres
77250 Moret-sur-Loing
FRANCE

B. Houssin
Framatome - Materials Department
Tour Fiat - CEDEX 16
92054 Paris la Defense
FRANCE

G. Rousselier
EDF - Department Etude des Materiaux
Les Renardieres
77250 Moret-sur-Long
FRANCE

Miss H. Tibi
DAS/SASCEL
DEA-DSN
CEN/FAR
B. P. no. 6
92260 Fontenay-aux-Roses
FRANCE

D. Azodi
Gesellschaft fur Reaktorsicherheit
Glockengasse 2
D-5000 Koln 1
FEDERAL REPUBLIC OF GERMANY

K. Bruninghaus
Technical University Aachen
Intzestr. 1
5100 Achen
FEDERAL REPUBLIC OF GERMANY

A. Cornec
GKSS
Max Planck Str.
2054 Geesthacht
FEDERAL REPUBLIC OF GERMANY

J. Heerens
GKSS
Max Planck Str.
2054 Geesthacht
FEDERAL REPUBLIC OF GERMANY

E. Roos
MPA
Universitat Stuttgart
Pfaffenwaldring 32
D-7000 Stuttgart 80
FEDERAL REPUBLIC OF GERMANY

K.- H. Schwalbe
GKSS
Max Planck Str.
2054 Geesthacht
FEDERAL REPUBLIC OF GERMANY

B. Voss
Fraunhofer-Institut fur
Werkstoffmechanik
Wohlerstr. 11
7800 Freiburg
FEDERAL REPUBLIC OF GERMANY

C. Fossati
ENEL
Via Rubattino 54
21034 Milano
ITALY

S. Ragazzonni
ENEL
Via Rubattino 54
20134 Milano
ITALY

P. A. J. M. Steenkamp
Delft University of Technology
Laboratory for Thermal Power
Engineering
P. O. Box 5055
2600 GB Delft
NETHERLANDS

Mr. G. L. Tjoa
Chemistry and Materials Development
ECN
1755 ZG Petten
NETHERLANDS

A. Tamarro Aparicio
TECNATOM S. A.
Km. 19 C. N. I. Madrid - Irun
San Sebastian de los Reyes
Madrid
SPAIN

T. Varga
HSK
CH - 5303 Wurenlingen
SWITZERLAND

K. N. Akhurst
CEGB Central Electricity Research
Laboratories
Kelvin Ave.
Leatherhead
Surrey KT22 7SE
UNITED KINGDOM

S. L. Creswell
H.M. Nuclear Installations
Inspectorate
Thames House North
Millbank
London SW1P 4QS
UNITED KINGDOM

S. J. Garwood
The Welding Institute
Abington
Cambridge CB1 6AL
UNITED KINGDOM

G. Gibson
UKAEA
AERE Harwell
Oxon OX11 ORA
UNITED KINGDOM

T. Ingham
UKAEA
Risley Nuclear Power Development
Laboratories
Risley
Warrington WA3 6AT
UNITED KINGDOM

B. K. Neale
CEGB Berkeley Nuclear Laboratories
Berkeley, Glos. GL13 9BP
UNITED KINGDOM

W. R. Andrews
General Electric Co.
Bldg. 55 Room 163
Schenectady, NY 12345
USA

G. Kramer
Battelle Columbus Labs
Room 11-4133
505 King Ave.
Columbus OH 43201
USA

F. J. Loss
Materials Engineering Associates
9700-B M.L.King Jr. Highway
Lanham, MD 20706
USA

H. A. Ernst
School of Mechanical Engineering
Georgia Institute of Technology
Atlanta, GA 30332
USA

D. E. McCabe
Materials Engineering Associates
9700-B M.L. King Jr. Highway
Lanham, MD 20706

H. A. Maurer
Division of Safety of Nuclear Installations
DG XII/D/3
Commission of the European Communitites
200 rue de la Loi
1049 Brussels
BELGIUM

J. Bernard
CEC Joint Research Center
Ispra Establishment
Ispra, Varese
I-21020 ITALY

A. Lucia
CEC Joint Research Center
Ispra Establishment
Ispra, Varese
I-21020 ITALY

M. Stephens
Nuclear Safety Division
OECD/NEA
38 Boulevard Suchet
F-75016 Paris
FRANCE

NRC FORM 335 (11-81)

U.S. NUCLEAR REGULATORY COMMISSION

BIBLIOGRAPHIC DATA SHEET

1. REPORT NUMBER (Assigned by DDC)
NUREG/CP-0064
CSNI Report No. 105
MEA-2313

4. TITLE AND SUBTITLE (Add Volume No., if appropriate)
SECOND CSNI WORKSHOP ON DUCTILE FRACTURE TEST METHODS

2. (Leave blank)

3. RECIPIENT'S ACCESSION NO.

7. AUTHOR(S)
Edited by F. J. Loss

5. DATE REPORT COMPLETED
MONTH August | YEAR 1988

9. PERFORMING ORGANIZATION NAME AND MAILING ADDRESS (Include Zip Code)
Materials Engineering Associates, Inc.
9700-B Martin Luther King, Jr., Highway
Lanham, Maryland 20706-1837

DATE REPORT ISSUED
MONTH August | YEAR 1988

6. (Leave blank)

8. (Leave blank)

12. SPONSORING ORGANIZATION NAME AND MAILING ADDRESS (Include Zip Code)
Division of Engineering
Office of Nuclear Regulatory Research
U. S. Nuclear Regulatory Commission
Washington, D.C. 20555

10. PROJECT TASK/WORK UNIT NO.

11. FIN NO.
B8900

13. TYPE OF REPORT
Conference Proceedings

PERIOD COVERED (Inclusive dates)

15. SUPPLEMENTARY NOTES

14. (Leave blank)

16. ABSTRACT (200 words or less)

This report is a compilation of papers presented at the Second CSNI Workshop on Ductile Fracture Test Methods, held at OECD Headquarters, Paris, France, on April 17-19, 1985. The contributors addressed advances in test methods to characterize the fracture toughness of structural steels. Sessions were held on new and improved test techniques, standardized J-R curve test procedures, experience and problems with existing techniques, and use of fracture mechanics by the nuclear industry. Summaries of the individual sessions have been prepared by the session chairmen.

The meeting identified progress in test methods since the first workshop was held in 1982. A clear movement to standardize J-R curve tests is now apparent. However, there exists a continuing need to improve elastic-plastic fracture test methods.

17. KEY WORDS AND DOCUMENT ANALYSIS

17a. DESCRIPTORS

Fracture Test Methods; Ductile Fracture Toughness; J-R Curve; CTOD; Experimental Test Methods; Structural Steels; Irradiated Steels; Notched Tensile Test; Standardized J-R Test Procedure; DCPD Test Procedure; Key Curve; Charpy Test; Elastic Plastic Fracture Mechanics; Dynamic J-R Test

17b. IDENTIFIERS/OPEN-ENDED TERMS

18. AVAILABILITY STATEMENT
Unlimited

19. SECURITY CLASS (This report)
Unclassified

21. NO. OF PAGES

20. SECURITY CLASS (This page)
Unclassified

22. PRICE
$

NRC FORM 335 (11-81)

UNITED STATES
NUCLEAR REGULATORY COMMISSION
WASHINGTON, D.C. 20555

OFFICIAL BUSINESS
PENALTY FOR PRIVATE USE, $300

SPECIAL FOURTH-CLASS RATE
POSTAGE & FEES PAID
USNRC
PERMIT No. G-67

120555139217 1 1AN1RF1R5
US NRC-OARM-ADM
DIV FOIA & PUBLICATIONS SVCS
RRES-PDR NUREG
P-210
WASHINGTON DC 20555